Harnessing antibody-dependent cellular cytotoxicity against HIV-1-infected cells

Sai Priya Anand

Department of Microbiology and Immunology

Faculty of Medicine

McGill University, Montréal, Québec, Canada

March 2022

A thesis submitted to McGill University in partial fulfillment

of the requirements of the degree of

Doctor of Philosophy

To my loving Sai Maa, Bhagavan Sri Sathya Sai Baba,
This work is a humble offering at your divine lotus feet.

ॐ साईं राम

ABSTRACT

In the absence of an efficient vaccine and with current antiretroviral therapies unable to eradicate the virus, HIV/AIDS remains a serious global public health concern. The successful elimination of the long-lived latent cellular reservoir poses a significant hurdle for cure strategies. Novel therapeutic interventions currently being explored include antibody-based immunotherapy. The HIV-1 envelope glycoproteins (Env) represent the only antigen exposed at the surface of infected cells and thus, represent a unique target for intervention. Env of most clinical HIV-1 isolates assumes a 'closed' conformation, preventing the binding of non-neutralizing antibodies (nNAbs), which preferentially bind when Env is 'open'. While nNAbs are naturally present in sera from infected individuals, broadly neutralizing antibodies (bNAbs) that recognize the 'closed' conformation are elicited only in a small proportion of infected individuals. Nevertheless, anti-Env antibodies can mediate Fc-effector functions via interactions between their Fc domains and IgG Fc receptors (FcγR), including antibody-dependent cellular cytotoxicity (ADCC). The passive administration of bNAbs can control disease progression *in vivo* and their capacity to eliminate infected cells is currently being investigated in ongoing human clinical trials. Another strategy to eliminate infected cells includes the use of small CD4 mimetics (CD4mc) to 'open' the Env and facilitate the recognition by nNAbs. In this thesis, we studied three different strategies to harness Fc-effector activities of both bNAbs and nNAbs to eliminate HIV-1-infected cells.

Two families of nNAbs predominant in HIV+ sera were shown to exert ADCC activity in the presence of CD4mc. Our first objective was to understand how these two classes of nNAbs cooperate for Fc-effector functionality and we observed that both their Fc regions act in concert to engage FcγRIIIa and mediate ADCC.

HIV-1 is a master of immune evasion and increasing evidence indicates that it has developed several mechanisms to avoid the premature recognition of its Env. In this thesis, we uncover a new evasion mechanism, wherein Env is internalized upon the binding by antibodies recognizing its 'closed' conformation. This new understanding led us to test the hypothesis that blocking antibody-induced Env internalization could enhance Fc-effector responses. We found that blocking dynamin function translates into a higher susceptibility of infected cells to ADCC, exploiting another approach to target the viral reservoir.

Lastly, to take advantage of the transient formation of antibody-Env immune complexes on the cell surface, we explored the impact of enhancing Fc functionality by glycan modifications. Using *Nicotiana benthamiana* to generate Fc-glycovariants of a clinically relevant bNAb, we found that afucosylated antibodies, independent of their galactosylation status, demonstrated augmented FcγRIIIa interaction and ADCC activity. Our results with plant-produced antibodies confirms the growing interest in affordable biologic production platforms for antibody-based treatments against infected cells.

Altogether, findings from this thesis highlight important ways that Fc-mediated effector functions of both bNAbs and nnAbs are modulated and can inform the design of immunotherapies against HIV-1-infected cells. With additional studies to evaluate the potential of these factors in controlling HIV-1 replication *in vivo*, these results could potentially be applied towards strategies targeting latently infected cells to decrease the viral reservoir.

RÉSUMÉ

En l'absence d'un vaccin efficace et avec les thérapies antirétrovirales actuelles incapables d'éradiquer le virus, le VIH/SIDA reste un grave problème de santé publique au niveau mondial. L'élimination du réservoir cellulaire latent à longue durée de vie constitue le plus grand obstacle pour les stratégies de guérison. Parmi les nouvelles interventions thérapeutiques actuellement à l'étude figurent les immunothérapies à base d'anticorps. Les glycoprotéines de l'enveloppe du VIH-1 (Env) représentent le seul antigène exposé à la surface des cellules infectées et constituent donc une cible unique pour une intervention. L'Env de la plupart des isolats cliniques du VIH-1 adopte une conformation ‘fermée’, empêchant la liaison des anticorps non neutralisants (nNAbs), qui se fixent de préférence lorsque l'Env est ‘ouverte’. Alors que les nNAbs sont naturellement présents dans le sérum des personnes infectées, les anticorps neutralisants à large spectre (bNAbs) qui reconnaissent la conformation ‘fermée’ ne sont produits que chez une très faible proportion de personnes infectées. Néanmoins, les anticorps anti-Env peuvent médier des fonctions effectrices via des interactions entre leurs domaines Fc et les récepteurs Fc (FcγR), y compris la cytotoxicité cellulaire dépendante des anticorps (ADCC). L'administration passive de bNAbs peut contrôler la progression de la maladie *in vivo* et leur capacité à éliminer les cellules infectées est actuellement étudiée dans des essais cliniques humains en cours. Une autre stratégie pour éliminer les cellules infectées inclut l'utilisation de mimétiques moléculaires de CD4 (CD4mc) pour 'ouvrir' l'Env et faciliter sa reconnaissance par les nNAbs. Dans cette thèse, nous avons étudié trois stratégies différentes pour exploiter les activités effectrices des bNAbs et des nNAbs afin d'éliminer les cellules infectées par le VIH-1.

Deux familles de nNAbs prédominantes dans les sérums VIH+, ont été montrées comme exerçant une activité ADCC en présence de CD4mc. Notre premier objectif était de comprendre comment ces deux classes de nNAbs coopèrent pour la fonctionnalité effectrice et nous avons observé que leurs deux régions Fc agissent de concert pour engager le récepteur FcγRIIIa et médier ADCC.

Le VIH-1 est un maître de l'évasion immunitaire et il y a de plus en plus de preuves montrant qu'il a développé plusieurs mécanismes pour éviter la reconnaissance prématurée d’Env. Dans cette thèse, nous avons identifié un nouveau mécanisme d'évasion, dans lequel Env est

internalisé lors de la liaison par des anticorps reconnaissant sa conformation ‘fermée’. Cette nouvelle compréhension nous a conduit à tester l'hypothèse selon laquelle le blocage de l'internalisation de l'Env induite par les anticorps pourrait améliorer les réponses effectrices. Nous avons constaté que le blocage de la fonction de la dynamine se traduit par une plus grande susceptibilité des cellules infectées à l'ADCC, exploitant ainsi une autre approche pour cibler le réservoir.

Enfin, pour prendre avantage de la formation transitoire de complexes immuns anticorps-Env à la surface des cellules, nous avons exploré l'impact de l'amélioration de la fonctionnalité des domaines Fc par des modifications de glycans. En utilisant *Nicotiana benthamiana* pour générer des glycovariants d'un bNAb ayant un potentiel clinique, nous avons découvert que les anticorps afucosylés, indépendamment de leur statut de galactosylation, démontraient une interaction avec le FcγRIIIa et une activité ADCC accrues. Nos résultats avec les anticorps produits par des plantes confirment l'intérêt croissant pour les plateformes de production biologique abordables pour les traitements à base d'anticorps contre les cellules infectées.

Dans l'ensemble, les résultats de cette thèse mettent en évidence des façons importantes de moduler les fonctions effectrices médiées par le Fc des bNAbs et des nnAbs et peuvent informer la conception d'immunothérapies contre les cellules infectées par le VIH-1. Avec des études supplémentaires pour évaluer le potentiel de ces facteurs dans le contrôle de la réplication du VIH-1 *in vivo*, ces résultats pourraient potentiellement être appliqués à des stratégies ciblant les cellules infectées de façon latente pour diminuer le réservoir viral.

ACKNOWLEDGMENTS

I would like to begin by expressing my deepest appreciation to my supervisor, Dr. Andrés Finzi: for your guidance on science and life and for always being there with your never-ending energy. Your discipline in life and way of performing science has been the greatest school. I am indebted to have joined your laboratory and for the invaluable opportunities that you provided to present and publish my research. Moreover, your care, understanding, and patience towards my physical and mental health will always be remembered. You are a true mentor, and it has been an honour to learn from you – Thank you!!!

I am very grateful to my co-supervisor, Dr. Martin Olivier, and my advisory committee members, Dr. Chen Liang and Dr. Nicole Bernard, for their kind encouragement, support, and advice not only towards my projects, but my training as a whole! I am also sincerely appreciative to the Department of Microbiology and Immunology and the Faculty of Medicine at McGill University as well the Canadian Institutes of Health Research (CIHR) and National Institute of Health (NIH) for supporting my studies with financial awards and for their administrative support. I will take this opportunity to thank all the collaborators who contributed to my research with assay developments, reagents, and discussions (including the articles not presented herein) and to the professors that supported me during my graduate training, in particular the members of my comprehensive exam committee, Dr. Jacques Archambault, Dr. Selena Sagan, and Dr. Guy Lemay. In this regard, a heartfelt thank you to all the scientists over the years that taught me and helped shape the scientist I am today, including Dr. Marceline Côté, my undergraduate mentor, for her kindness and for helping spark my interest towards the academic field of virology.

I would also like to extend my gratitude to all past and current members of the Finzi laboratory, for their technical help/support and for making the lab such a comfortable and enjoyable work environment! Very special thank you: to Dr. Jonathan Richard for your constant solid input on all my projects, sharing your experiences/helpful advice, and for always encouraging me throughout my training; to Dr. Shilei Ding, Dr. Nirmin Alsahafi, and Dr. Halima Medjahed,

for your companionship & for supporting me since my arrival in the lab; to Sophie Baril for helping me with the projects herein.

Further thanking all the scientists and students at the CRCHUM for their support and aiding significantly to my scientific training; as well as the cytometry, BSL-3, and cellular imaging facilities for providing vital training. Shout out to my dear friends Dr. Julia Nießl & (soon-to-be Drs.) Elsa Brunet-Ratnasingham, Myriam Verly, and Gérémy Sannier – I am very thankful for sharing the grad school experience with you and making many wonderful memories! Thank you to Simone Loo, Kavita Raniga, and Gowthami S. for your warmth and being there for me during the first years of my graduate training.

Importantly, a huge thank you from the bottom of my heart to all my family and friends near and far – I am very fortunate to receive your nurturing love! The beautiful parts of my life Sathya Anand, Noémie Bucourt, and Émil Anand for filling me with joy; my parents, Sanjay Anand and Dr. Poonam Anand, for your unfaltering belief in me and sacrificing so much to allow me the chance for a rich schooling – my education is a gift from your unconditional love. To my new parents, Jacinthe Thibodeau and Benoît Prévost, for your love, care, and giving me happiness!

Finally, I would like to express loving gratitude to my co-scientist, lab partner, and husband (pretty much already a Dr.) Jérémie Prévost. You have always stood by me – your loving support means everything, and words fall short to thank you. I look forward to forever sharing the love of science and life with you!

PREFACE

This thesis was written in accordance with the guidelines provided for a "Manuscript-based (Article-based) thesis" format from McGill University's Graduate and Postdoctoral Studies "Guidelines for Preparation of a Thesis":

"As an alternative to the traditional format, a thesis may be presented as a collection of scholarly papers of which the student is the first author or co-first author. A manuscript-based doctoral thesis must include the text of a minimum of two manuscripts published, submitted or to be submitted for publication. Manuscripts for publication in journals are frequently very concise documents. A thesis, however, is expected to consist of more detailed, scholarly work. A manuscript-based thesis will be evaluated by the examiners as a unified, logically coherent document in the same way a traditional thesis is evaluated."

The thesis consists of 6 chapters. Chapter 1 is a comprehensive literature review of the topics central to this thesis and outlines the objectives of the research presented in this thesis. Chapters 2, 3, 4, and 5 are four respective manuscripts that are published in scientific journals; the candidate is the first or co-first author of all these manuscripts. The contributions of all authors on these manuscripts are listed in following 'Contribution of Authors' section. These chapters are composed of their own introduction, methods, results, discussion, and references. The results presented in this thesis represents a significant contribution to knowledge that is the result of independent scholarship and is summarised and discussed in Chapter 6. The references for Chapters 1 and 6 are listed at the end of the thesis. The candidate's supervisor, Dr. Andrés Finzi, provided editorial support in the preparation of this thesis.

Manuscripts which the candidate has included in this thesis are the following publications:

1. **Anand SP** and Finzi A. **Understudied Factors Influencing Fc-Mediated Immune Responses against Viral Infections.** *Vaccines.* (2019 August)

2. **Anand SP**, Prévost J, Baril S, Richard J, Medjahed H, Chapleau JP, Tolbert WD, Kirk S, Smith III AB, Wines BD, Kent SJ, Hogarth PM, Parsons MS, Pazgier M, Finzi A. **Two families of Env antibodies efficiently engage Fc-gamma receptors and eliminate HIV-1-infected cells**. *Journal of Virology*. (2019 January)

3. **Anand SP**, Grover JR, Tolbert WD, Prévost J, Richard J, Ding S, Baril S, Medjahed H, Evans DT, Pazgier M, Mothes W, Finzi A. **Antibody-induced internalization of HIV-1 Env proteins limits surface expression of the closed conformation of Env.** *Journal of Virology.* (2019 May)

4. **Anand SP**, Prévost J, Descôteaux-Dinelle J, Richard J, Nguyen DN, Medjahed H, Chen HC, Smith AB, Pazgier M, Finzi A. **HIV-1 Envelope Glycoprotein Cell Surface Localization Is Associated with Antibody-Induced Internalization**. *Viruses.* (2021 October)

5. **Anand SP*,** Ding S*, Tolbert WD, Prévost J, Richard J, Gil HM, Gendron-Lepage G, Cheung WF, Wang H, Pastora R, Saxena H, Wakarchuk W, Medjahed H, Wines BD, Hogarth PM, Shaw GM, Martin MA, Burton DR, Hangartner, L, Evans DT, Pazgier M, Cossar D, McLean MD, Finzi A. **Enhanced Ability of Plant-Derived PGT121 Glycovariants to Eliminate HIV-1-Infected Cells**. *Journal of Virology.* (2021 August) ***contributed equally**

Manuscripts not included in this thesis, for which the candidate made significant contributions during her PhD training, include the following publications:

1. Prévost J, **Anand SP**, Rajashekar JK, Richard J, Goyette G, Medjahed H, Gendron-Lepage G, Chen H-C, Chen Y, Horwitz JA, Grunst MW, Zolla-Pazner S, Haynes BF, Burton DR, Flavell RA, Kirchhoff F, Hahn BH, Smith AB, Pazgier M, Nussenzweig MC, Kumar P, Finzi A. **HIV-1 Vpu restricts Fc-mediated effector functions in vivo.** *bioRxiv* (2022 March)

2. Tauzin A, Gendron-Lepage G, Nayrac M, **Anand SP**, Bourassa C, Medjahed H, Goyette G, Dubé M, Bazin R, Kaufmann D, Finzi A. **Evolution of anti-RBD IgG avidity following SARS-CoV-2 infection.** *Viruses*. (2022 March)

3. Ding S, Adam D, Beaudoin-Bussières G, Tauzin A, Gong SY, Gasser R, Laumaea A, **Anand SP**, Privé A, Bourassa C, Medjahed H, Prévost J, Charest H, Richard J, Brochiero E, Finzi A. **SARS-CoV-2 Spike Expression at the Surface of Infected Primary Human Airway Epithelial Cells**. *Viruses.* (2022 January)

4. Chen Y, Sun L, Ullah I, Beaudoin-Bussieres G, **Anand SP**, Hederman AP, Tolbert WD, Sherburn R, Nguyen DN, Marchitto L, Ding S, Wu D, Luo Y, Gottumukkala S, Moran S, Kumar P, Piszczek G, Mothes W, Ackerman ME, Finzi A, Uchil PD, Gonzalez FJ, Pazgier M. **Engineered ACE2-Fc counters murine lethal SARS-CoV-2 infection through direct neutralization and Fc-effector activities**. *bioRxiv.* (2021 November)

5. Li W, Chen Y, Prévost J, Ullah I, Lu M, Gong SY, Tauzin A, Gasser R, Vézina D, **Anand SP**, Goyette G, Chaterjee D, Ding S, Tolbert WD, Grunst MW, Bo Y, Zhang S, Richard J, Zhou F, Huang RK, Esser L, Zeher A, Côté M, Kumar P, Sodroski J, Xia D, Uchil PD, Pazgier M, Finzi A, Mothes W. **Structural Basis and Mode of Action for Two Broadly Neutralizing Antibodies Against SARS-CoV-2 Emerging Variants of Concern**. *Cell Reports.* (2021 November)

6. Brunet-Ratnasingham E*, **Anand SP***, Gantner P*, Dyachenko A*, Moquin-Beaudry G, Brassard N, Beaudoin-Bussieres G, Pagliuzza A, Gasser R, Benlarbi M, Point F, Prevost J, Laumaea A, Niessl J, Nayrac M, Sannier G, Orban C, Messier-Peet M, Butler-Laporte G, Morrison DR, Zhou S, Nakanishi T, Boutin M, Descoteaux-Dinelle J, Gendron-Lepage G, Goyette G, Bourassa C, Medjahed H, Laurent L, Rebillard RM, Richard J, Dube M, Fromentin R, Arbour N, Prat A, Larochelle C, Durand M, Richards JB, Chasse M, Tetreault M, Chomont N, Finzi A, Kaufmann DE. **Integrated immunovirological profiling validates plasma SARS-CoV-2 RNA as an early predictor of COVID-19 mortality.** *Science Advances*. (2021 November) ***contributed equally**

7. Valcourt EJ, Manguiat K, Robinson A, Lin YC, Abe KT, Mubareka S, Shigayeva A, Zhong Z, Girardin RC, DuPuis A, Payne A, McDonough K, Wang Z, Gasser R, Laumaea A, Benlarbi M, Richard J, Prévost J, **Anand SP**, Dimitrova K, Phillipson C, McGeer A, Gingras A-C, Liang C, Petric M, Sekirov I, Morshed M, Finzi A, Drebot M, and Wood H. **Evaluating Humoral Immunity against SARS-CoV-2: Validation of a Plaque-Reduction Neutralization Test and a Multilaboratory Comparison of Conventional and Surrogate Neutralization Assays**. *Microbiology Spectrum*. (2021 November)

8. **REMAP-CAP Investigators**; Writing Committee: Estcourt LJ, Turgeon AF, McQuilten ZK, McVerry BJ, Al-Beidh F, Annane D, Arabi YM, Arnold DM, Beane A, Bégin P, van Bentum-Puijk W, Berry LR, Bhimani Z, Birchall JE, Bonten MJM, Bradbury CA, Brunkhorst FM, Buxton M, Callum JL, Chassé M, Cheng AC, Cove ME, Daly J, Derde L, Detry MA, De Jong M, Evans A, Fergusson DA, Fish M, Fitzgerald M, Foley C, Goossens H, Gordon AC, Gosbell IB, Green C, Haniffa R, Harvala H, Higgins AM, Hills TE, Hoad VC, Horvat C, Huang DT, Hudson CL, Ichihara N, Laing E, Lamikanra AA, Lamontagne F, Lawler PR, Linstrum K, Litton E, Lorenzi E, MacLennan S, Marshall J, McAuley DF, McDyer JF, McGlothlin A, McGuinness S, Miflin G, Montgomery S, Mouncey PR, Murthy S, Nichol A, Parke R, Parker JC, Priddee N, Purcell DFJ, Reyes LF, Richardson P, Robitaille N, Rowan KM, Rynne J, Saito H, Santos M, Saunders CT, Serpa Neto A, Seymour CW, Silversides JA, Tinmouth AA, Triulzi DJ, Turner AM, van de Veerdonk F, Walsh TS, Wood EM, Berry S, Lewis RJ, Menon DK, McArthur C, Zarychanski R, Angus DC, Webb SA, Roberts DJ, Shankar-Hari M. **Effect of**

Convalescent Plasma on Organ Support-Free Days in Critically Ill Patients With COVID-19: A Randomized Clinical Trial. *JAMA.* (2021 October).

9. **CONCOR-1 Study Group**; Writing Committee: Bégin P, Callum J, Jamula E, Cook R, Heddle NM, Tinmouth A, Zeller MP, Beaudoin-Bussières G, Amorim L, Bazin R, Loftsgard KC, Carl R, Chassé M, Cushing MM, Daneman N, Devine DV, Dumaresq J, Fergusson DA, Gabe C, Glesby MJ, Li N, Liu Y, McGeer A, Robitaille N, Sachais BS, Scales DC, Schwartz L, Shehata N, Turgeon AF, Wood H, Zarychanski R, Finzi A, Arnold DM. **Convalescent plasma for hospitalized patients with COVID-19: an open-label, randomized controlled trial.** *Nature Medicine*. (2021 September).

10. Prévost J, Richard J, Gasser R, Ding S, Fage C, **Anand SP**, Adam D, Gupta Vergara N, Tauzin A, Benlarbi M, Gong SY, Goyette G, Privé A, Moreira S, Charest H, Roger M, Mothes W, Pazgier M, Brochiero E, Boivin G, Abrams CF, Schön A, Finzi A. **Impact of temperature on the affinity of SARS-CoV-2 Spike glycoprotein for host ACE2.** *Journal of Biological Chemistry.* (2021 August)

11. Ullah I, Prévost J, Ladinsky MS, Stone H, Lu M, **Anand SP**, Beaudoin-Bussières G, Symmes K, Benlarbi M, Ding S, Gasser R, Fink C, Chen Y, Tauzin A, Goyette G, Bourassa C, Medjahed H, Mack M, Chung K, Wilen CB, Dekaban GA, Dikeakos JD, Bruce EA, Kaufmann DE, Stamatatos L, McGuire AT, Richard J, Pazgier M, Bjorkman PJ, Mothes W, Finzi A, Kumar P, Uchil PD. **Live imaging of SARS-CoV-2 infection in mice reveals that neutralizing antibodies require Fc function for optimal efficacy.** *Immunity.* (2021 September)

12. Tauzin A, Nayrac M, Benlarbi M, Gong SY, Gasser R, Beaudoin-Bussières G, Brassard N, Laumaea A, Vézina D, Prévost J, **Anand SP**, Bourassa C, Gendron-Lepage G, Medjahed H, Goyette G, Niessl J, Tastet O, Gokool L, Morrisseau C, Arlotto P, Stamatatos L, McGuire AT, Larochelle C, Uchil P, Lu M, Mothes W, De Serres G, Moreira S, Roger M, Richard J, Martel-Laferrière V, Duerr R, Tremblay C, Kaufmann DE, Finzi A. **A single dose of the SARS-CoV-2 vaccine BNT162b2 elicits Fc-mediated antibody effector functions and T cell responses.** *Cell Host & Microbe*. (2021 July)

13. Rajashekar JK, Richard J, Beloor J, Prévost J, **Anand SP**, Beaudoin-Bussières G, Shan L, Herndler-Brandstetter D, Gendron-Lepage G, Medjahed H, Bourassa C, Gaudette F, Ullah I, Symmes K, Peric A, Lindemuth E, Bibollet-Ruche F, Park J, Chen HC, Kaufmann DE, Hahn BH, Sodroski J, Pazgier M, Flavell RA, Smith AB 3rd, Finzi A, Kumar P. **Modulating HIV-1 envelope glycoprotein conformation to decrease the HIV-1 reservoir.** *Cell Host & Microbe.* (2021 June)

14. **Anand SP***, Prévost J*, Nayrac M*, Beaudoin-Bussières G*, Benlarbi M, Gasser R, Brassard N, Laumaea A, Gong SY, Bourassa C, Brunet-Ratnasingham E, Medjahed H, Gendron-Lepage G, Goyette G, Gokool L, Morrisseau C, Bégin P, Martel-Laferrière V, Tremblay C, Richard J, Bazin R, Duerr R, Kaufmann DE, Finzi A. **Longitudinal analysis of humoral immunity against SARS-CoV-2 Spike in convalescent individuals up to 8 months post-symptom onset.** *Cell Reports Medicine.* (2021 June) ***contributed equally**

15. Rébillard RM, Charabati M, Grasmuck C, Filali-Mouhim A, Tastet O, Brassard N, Daigneault A, Bourbonnière L, **Anand SP**, Balthazard R, Beaudoin-Bussières G, Gasser R, Benlarbi M, Moratalla AC, Solorio YC, Boutin M, Farzam-Kia N, Descôteaux-Dinelle J, Fournier AP, Gowing E, Laumaea A, Jamann H, Lahav B, Goyette G, Lemaître F, Mamane VH, Prévost J, Richard J, Thai K, Cailhier JF, Chomont N, Finzi A, Chassé M, Durand M, Arbour N, Kaufmann DE, Prat A, Larochelle C. **Identification of SARS-CoV-2-specific immune alterations in acutely ill patients.** *Journal of Clinical Investigation* (2021 April)

16. **Anand SP***, Prévost J*, Richard J*, Perreault J, Tremblay T, Drouin M, Fournier MJ, Lewin A, Bazin R, Finzi A. **High-throughput detection of antibodies targeting the SARS-CoV-2 Spike in longitudinal convalescent plasma samples.** *Transfusion*. (2021 May) ***contributed equally**

17. Lu M, Uchil PD, Li W, Zheng D, Terry DS, Gorman J, Shi W, Zhang B, Zhou T, Ding S, Gasser R, Prévost J, Beaudoin-Bussières G, **Anand SP**, Laumaea A, Grover JR, Liu L, Ho DD, Mascola JR, Finzi A, Kwong PD, Blanchard SC, Mothes W. **Real-Time Conformational Dynamics of SARS-CoV-2 Spikes on Virus Particles.** *Cell Host & Microbe.* (2020 December)

18. Beaudoin-Bussières G*, Laumaea A*, **Anand SP***, Prévost J*, Gasser R*, Goyette G, Medjahed H, Perreault J, Tremblay T, Lewin A, Gokool L, Morrisseau C, Bégin P, Tremblay C, Martel-Laferrière V, Kaufmann DE, Richard J, Bazin R, Finzi A. **Decline of Humoral Responses against SARS-CoV-2 Spike in Convalescent Individuals.** *mBio.* (2020 October) ***contributed equally**

19. Prévost J, Gasser R, Beaudoin-Bussières G, Richard J, Duerr R, Laumaea A, Anand SP, Goyette G, Benlarbi M, Ding S, Medjahed H, Lewin A, Perreault J, Tremblay T, Gendron-Lepage G, Gauthier N, Carrier M, Marcoux D, Piché A, Lavoie M, Benoit A, Loungnarath V, Brochu G, Haddad E, Stacey HD, Miller MS, Desforges M, Talbot PJ, Maule GTG, Côté M, Therrien C, Serhir B, Bazin R, Roger M, Finzi A. **Cross-Sectional Evaluation of Humoral Responses against SARS-CoV-2 Spike.** *Cell Reports Medicine*. (2020 October)

20. **Anand SP**, Chen Y, Prévost J, Gasser R, Beaudoin-Bussières G, Abrams CF, Pazgier M, Finzi A. **Interaction of Human ACE2 to Membrane-Bound SARS-CoV-1 and SARS-CoV-2 S Glycoproteins.** *Viruses.* (2020 September)

21. Alsahafi N, Bakouche N, Kazemi M, Richard J, Ding S, Bhattacharyya S, Das D, **Anand SP**, Prévost J, Tolbert WD, Lu H, Medjahed H, Gendron-Lepage G, Ortega Delgado GG, Kirk S, Melillo B, Mothes W, Sodroski J, Smith AB 3rd, Kaufmann DE, Wu X, Pazgier M, Rouiller I, Finzi A, Munro JB. **An Asymmetric Opening of HIV-1 Envelope Mediates Antibody-Dependent Cellular Cytotoxicity.** *Cell Host & Microbe.* (2019 April)

22. Alsahafi N, **Anand SP**, Castillo-Menendez L, Verly MM, Medjahed H, Prévost J, Herschhorn A, Richard J, Schön A, Melillo B, Freire E, Smith AB 3rd, Sodroski J, Finzi A. **SOSIP Changes Affect Human Immunodeficiency Virus Type 1 Envelope Glycoprotein Conformation and CD4 Engagement.** *Journal of Virology*. (2018 September)

CONTRIBUTION OF AUTHORS

Chapter I (Introduction) and Chapter VI (Discussion):

'Understudied Factors Influencing Fc-Mediated Immune Responses against Viral Infections.'

Sai Priya Anand and Andrés Finzi**.**

Published in *Vaccines* (August 2019)

Parts of this review manuscript were used in Chapters 1 and 6. S.P.A. and A.F. performed the literature review and wrote the paper.

Chapter II:

'Two Families of Env Antibodies Efficiently Engage Fc-Gamma Receptors and Eliminate HIV-1-Infected Cells.'

Sai Priya Anand, Jérémie Prévost, Sophie Baril, Jonathan Richard, Halima Medjahed, Jean-Philippe Chapleau, William D. Tolbert, Sharon Kirk, Amos B. Smith III, Bruce D. Wines, Stephen J. Kent, P. Mark Hogarth, Matthew S. Parsons, Marzena Pazgier, and Andrés Finzi.

Published in *Journal of Virology* (January 2019)

S.P.A. and A.F. conceived the study; S.P.A., J.P., and A.F. designed experimental approaches; S.P.A., J.P., and S.B., performed the experiments; S.P.A., J.P., S.B., J.R., and A.F. analyzed and interpreted the experiments; W.D.T. and M.P. provided the modeling; H.M. and J.-P.C. provided technical help; S.K., A.B.S.III, B.D.W., S.J.K., P.M.H., and M.S.P. contributed unique reagents; S.P.A. and A.F. wrote the paper. Every author has read, edited, and approved the published version of the manuscript.

Chapter III:

'Antibody-Induced Internalization of HIV-1 Env Proteins Limits Surface Expression of the Closed Conformation of Env.'

Sai Priya Anand, Jonathan R. Grover, William D. Tolbert, Jérémie Prévost, Jonathan Richard, Shilei Ding, Sophie Baril, Halima Medjahed, David T. Evans, Marzena Pazgier, Walther Mothes, and Andrés Finzi.

Published in *Journal of Virology* (May 2019)

S.P.A. and A.F. conceived the study; S.P.A., J.R.G., W.M., and A.F. designed experimental approaches; S.P.A. and J.R.G. performed the experiments; S.P.A., J.R.G., J.P., J.R., W.M., and A.F. analyzed and interpreted the experiments; S.D. and S.B. provided technical help; W.D.T., H.M., D.T.E., and M.P. contributed unique reagents; S.P.A., W.M., and A.F. wrote the paper. Every author has read, edited, and approved the published version of the manuscript.

Chapter IV:

'HIV-1 Envelope Glycoprotein Cell Surface Localization Is Associated with Antibody-Induced Internalization.'

Sai Priya Anand, Jérémie Prévost, Jade Descôteaux-Dinelle, Jonathan Richard, Dung N. Nguyen, Halima Medjahed, Hung-Ching Chen, Amos B. Smith III, Marzena Pazgier, and Andrés Finzi.

Published in *Viruses* (September 2021)

S.P.A. and A.F. conceived the study; S.P.A., J.P., and A.F. designed experimental approaches; S.P.A. performed the experiments; S.P.A., J.P., and A.F. analyzed and interpreted the experiments; J.D.-D. and J.R. provided technical help; D.N.N., H.M., H.-C.C., A.B.S.III, and M.P. contributed unique reagents; S.P.A. and A.F. wrote the paper. Every author has read, edited, and approved the published version of the manuscript.

Chapter V:

'Enhanced Ability of Plant-Derived PGT121 Glycovariants to Eliminate HIV-1-Infected Cells.'

Sai Priya Anand*, Shilei Ding*, William D. Tolbert, Jérémie Prévost, Jonathan Richard, Hwi Min Gil, Gabrielle Gendron-Lepage, Wing-Fai Cheung, Haifeng Wang, Rebecca Pastora, Hirak Saxena, Warren Wakarchuk, Halima Medjahed, Bruce D. Wines, P. Mark Hogarth, George M. Shaw, Malcom A. Martin, Dennis R. Burton, Lars Hangartner, David T. Evans, Marzena Pazgier, Doug Cossar, Michael D. McLean, and Andrés Finzi.

*S.P.A. and S.D. contributed equally, author order was determined alphabetically

Published in *Journal of Virology* (August 2021)

S.P.A., S.D., and A.F. conceived the study; S.P.A., S.D., M.P., D.C., M.D.M., and A.F. designed experimental approaches; S.P.A., S.D., J.P., J.R., H.M.G., and G.G-L. performed cellular experiments; S.P.A., S.D., J.P., D.T.E., and A.F. analyzed and interpreted the cellular experiments; W.D.T. and M.P. performed structural analyses; W.-F.C., H.S., and W.W. developed/performed glycosylation analyses; H.W., R.P., D.C., and M.D.M. performed and analyzed plant experiments; H.M., B.D.W., P.M.H., G.M.S., M.A.M., D.R.B., and L.H. contributed unique reagents; S.P.A. and A.F. wrote the paper. Every author has read, edited, and approved the published version of the manuscript.

TABLE OF CONTENTS

ABSTRACT ..... *iii*

RÉSUMÉ ..... *v*

ACKNOWLEDGMENTS ..... *vii*

PREFACE ..... *ix*

CONTRIBUTION OF AUTHORS ..... *xv*

LIST OF FIGURES ..... *xxiii*

LIST OF TABLES ..... *xxvi*

LIST OF ABBREVIATIONS ..... *xxvii*

CHAPTER I General Introduction *1*

1.1 HIV-1 and AIDS 2

1.1.1 Viral Origin and Classification 2

1.1.2 Viral Structure and Genome Organization 4

1.1.3 Replication cycle 6

1.1.3.1 Viral entry and early replication stages 7

1.1.3.2 Late replication stages 10

1.1.4 Accessory proteins 13

1.1.4.1 Nef 13

1.1.4.2 Vif 13

1.1.4.3 Vpr 14

1.1.4.4 Vpu 14

1.1.5 Envelope glycoproteins 15

1.1.5.1 gp120 18

1.1.5.2 gp41 18
1.1.5.3 Glycoprotein endocytosis 19
1.1.5.3.1 Modes of Endocytosis 20
1.1.5.4 Glycoprotein conformation 21
1.2 HIV-1 pathogenesis 23
1.2.1 Stages of infection 23
1.2.2 Antiretroviral therapies 25
1.2.3 HIV-1 vaccine strategies 26
1.2.4 HIV-1 cure strategies 27
1.3 Humoral immune responses against HIV-1 infection 29
1.3.1 IgG structure 29
1.3.2 Neutralizing response 30
1.3.3 Non-neutralizing response 32
1.3.4 Fc-mediated antibody functions and Fc receptors 34
1.3.4.1 Modulation of Fc-mediated antibody functions 38
1.3.5 IgG Fc glycosylation 39
1.3.5.1 IgG Fc glycosylation and Fc-mediated functionality 41
1.3.5.2 Modulation of IgG Fc glycosylation 42
1.3.6 Viral mechanisms to evade antibody recognition 43
1.4 Thesis Rationale and Objectives 45
CHAPTER II Two families of Env antibodies efficiently engage Fc-gamma receptors and eliminate HIV-1-infected cells 47
2.1 Preface to Chapter 2 47
2.2 Abstract 48

2.3 Introduction 48

2.4 Material and Methods 50

2.5 Results 55

Anti-CoRBS and anti-Cluster A Abs synergize to engage a soluble recombinant dimeric form of FcγRIIIa 55

Anti-CoRBS and anti-Cluster A Abs must recognize the same gp120 subunit in order to engage with dimeric FcγRIIIa 57

Anti-CoRBS and Anti-Cluster A Abs present in HIV-1+ sera are required for efficient engagement of FcγRIIIa 59

Anti-CoRBS and Anti-Cluster A Abs are required for efficient binding of FcγRIIIa to infected cells 61

Anti-CoRBS and Anti-Cluster A Abs are required for efficient ADCC-mediated killing of HIV-1 infected cells 64

Fc regions of anti-cluster A and anti-CoRBS Abs are required to engage FcγRIIIa and mediate ADCC 66

2.6 Discussion 71

2.7 References 76

CHAPTER III Antibody-induced internalization of HIV-1 Env proteins limits the surface expression of the closed conformation of Env 84

3.1 Preface to Chapter 3 84

3.2 Abstract 85

3.3 Introduction 86

3.4 Material and Methods 88

3.5 Results 93

bNAbs induce Env internalization from the cell surface 93

Antibody-induced internalization of cell surface-expressed HIV-1 Env 99

A dynamin inhibitor attenuates bNAb-induced Env internalization and increases the susceptibility of infected cells to ADCC *104*

3.6 Discussion 107

3.7 References 110

CHAPTER IV HIV-1 Envelope Glycoprotein Cell Surface Localization is Associated with Antibody-Induced Internalization ***117***

4.1 Preface to Chapter 4 117

4.2 Abstract 118

4.3 Introduction 119

4.4 Material and Methods 120

4.5 Results and Discussion 125

HIV-1 Env 'opening' accelerates its antibody-mediated internalization from the cell surface *125*

Visualizing nNAb mediated Env internalization from the cell surface *128*

Different membrane microdomains could determine antibody-mediated Env internalization *130*

4.6 References 134

CHAPTER V Enhanced ability of plant-derived PGT121 glycovariants to eliminate HIV-1-infected cells ***138***

5.1 Preface to Chapter 5 138

5.2 Abstract 139

5.3 Introduction 140

5.4 Material and Methods 142

5.5 Results 148

Generation of near-homogeneous plant-derived PGT121 glycovariants *148*

Fc glycosylation does not affect the ability of PGT121 to recognize infected cells nor its neutralization capacity *149*
The Fc glycosylation profile of PGT121 regulates its capacity to mediate ADCC *151*
The Fc glycosylation profile of PGT121 modulates FcγRIIIa interaction and ADCC against infected primary CD4+ T cells *153*
Susceptibility of ex-vivo-expanded primary CD4+ T cells from HIV-1-infected individuals to PGT121-mediated ADCC *157*
The Fc regions of N. benthamiana-derived and mammalian cell-derived PGT121 are structurally similar with differences in N297 sugar composition *159*
5.6 Discussion 165
5.7 References 168
CHAPTER VI General Discussion ***177***
6.1 Summary of main findings 178
6.1.1 Contribution to current knowledge 180
6.2 Outstanding questions and future work 183
6.3 Towards an HIV-1 Cure 189
6.4 Concluding remarks 191
REFERENCES ***192***
APPENDIX Permissions to use copyright material ***224***

LIST OF FIGURES

Figure Title	Page Number
Figure 1.1. Mature HIV-1 virion structure.	5
Figure 1.2. HIV-1 genomic organization.	5
Figure 1.3. HIV-1 Replication Cycle.	7
Figure 1.4. HIV Entry.	9
Figure 1.5. Envelope glycoprotein composition.	17
Figure 1.6. Stages of HIV-1 infection.	24
Figure 1.7. Structure of IgG.	30
Figure 1.8. Epitopes recognized by bNAbs.	31
Figure 1.9. Env conformations recognized by bNAbs and nNAbs.	34
Figure 1.10. Fc-mediated effector functions.	35
Figure 1.11. Human Fc gamma receptors (FcγRs) and their leukocyte expression patterns.	37
Figure 1.12. Structure of IgG and the IgG N-linked glycan.	40
Figure 1.13. Sequential Processing of the Antibody Glycan	41
Figure 2.1. Anti-CoRBS and Anti-Cluster A Abs synergize to engage dimeric FcγRIIIa.	56
Figure 2.2. Anti-CoRBS and anti-Cluster A Abs must engage with the same gp120 subunit in order to recruit dimeric FcγRIIIa.	58
Figure 2.3. Dimeric FcγRIIIa engagement by HIV+ sera is driven by anti-CoRBS and anti-cluster A Abs.	60
Figure 2.4. Anti-CoRBS and anti-Cluster A Abs are required for efficient engagement of FcγRIIIa to infected cells.	62
Figure 2.5. CD4mc in combination with Fab'2 but not Fab'1 fragments of anti-CoRBS Abs are sufficient to expose cluster A epitopes.	63

Figure 2.6. ADCC against HIV-1-infected cells expressing Env in its CD4-bound conformation is enhanced by the combination of anti-CoRBS and anti-cluster A Abs. 65
Figure 2.7. Introduction of LALA mutations in the Fc portion of both CoRBS and Anti-cluster A antibodies decreases engagement of dimeric FcγRIIIa and ADCC against HIV-1-infected cells 67
Figure 2.8. The Fc portion from both anti-CoRBS and anti-Cluster A Abs are required to engage dimeric FcγRIIIa. 69
Figure 2.9. The Fc from both anti-CoRBS and anti-cluster A Abs are required to mediate potent ADCC against HIV-1-infected cells. 70
Figure 2.10. Model of the dimeric rsFcγRIIIa engagement by anti-CoRBS and anti-cluster A Abs bound to their cognate epitopes within the same gp120 subunit. 74
Figure 3.1. Broadly neutralizing antibodies but not non-neutralizing antibodies induce Env internalization. 94
Figure 3.2. Binding of bNAbs but not nNAbs decreases Env expression from the surface of T/F virus-infected cells. 95
Figure 3.3. Nef and Vpu protect infected cells from recognition by CD4i antibodies. 97
Figure 3.4. Nef and Vpu are dispensable for bNAbs-mediated Env internalization. 98
Figure 3.5. Antibody-induced internalization of Env from the surface of transfected cells. 100
Figure 3.6. bNAb-triggered Env internalization is temperature-dependent manner. 101
Figure 3.7. Fab fragments fail to induce Env internalization. 103
Figure 3.8. bNAb-mediated Env internalization is Dynamin dependent. 105
Figure 3.9. A dynamin inhibitor enhances the ADCC activity of bNAbs. 106
Figure 3.10. bNAb-Env complexes accumulate in an early endosome compartment. 108
Figure 4.1. Antibody-internalization of HIV-1 Env from the cell-surface can be accelerated upon the selective opening of Env. 127

Figure 4.2. Antibody-induced internalization of Env from the surface of transfected cells 129
Figure 4.3. Differential localization of antibody-Env complexes visualized by lipid microdomain fractionation. 132
Figure 5.1. N-linked glycans of *N. benthamiana*-produced PGT121 glycovariants 149
Figure 5.2. Fc glycosylation does not affect the ability of PGT121 to recognize infected cells or its neutralization capacity 150
Figure 5.3. Fc glycosylation profile of PGT121 regulates its ADCC capacity against infected cells 152
Figure 5.4. Fc glycosylation profile of PGT121 modulates FcγRIIIa interaction and ADCC against infected primary CD4+ T cells 155
Figure 5.5. Susceptibility of *ex vivo*-expanded endogenously infected primary CD4+ T cells from HIV-1-infected individuals to PGT121-mediated ADCC 158
Figure 5.6. Structural characterization of the Fc regions of *N. benthamiana*-produced PGT121 161
Figure 5.7. Comparison of the overall structures of *N. benthamiana* expressed and mammalian expressed human Fc domains 164
Figure 6.1 Overview of three different mechanisms described in this thesis to harness Fc-mediated immune responses against HIV-1-infected cells 179
Figure 6.2 Introduction of LALA mutations in the Fc portion of both CoRBS and anti-cluster A antibodies decreases engagement of dimeric FcγRIIa. 186

LIST OF TABLES

Table Title	Page Number
Table 1.1 Characteristics of Abs used in this thesis	34
Table 5.1. Functionalities of PGT121 glycovariants targeting infected primary CD4+ T cells	156
Table 5.2. Data collection and refinement statistics for fucosylated and afucosylated human Fc from *N. benthamiana*	162

LIST OF ABBREVIATIONS

6HB: 6-Helix Bundle
Ab: Antibody
ADCC: Antibody-dependent cellular cytotoxicity
ADCML: Antibody-dependent complement-mediated lysis
ADCP: Antibody-dependent cellular phagocytosis
AIDS: Acquired immunodeficiency syndrome
AP-1: Adaptor Protein -1
AP-2: Adaptor Protein -2
APOBEC: Apolipoprotein B mRNA Editing Enzyme Catalytic Polypeptide
ART: Anti-Retroviral Therapy
AZT: Azidothymidine
BAR: Bin/Amphiphysin/Rvs
bNAb: Broadly Neutralizing Antibody
BST-2: Bone Marrow Stromal Antigen 2
CA: Capsid
CCR5: C-C Chemokine Receptor Type 5
CD: Cluster of Differentiation
CD4mc: CD4 mimetic compounds
CDK9: Cyclin-Dependant Protein Kinase-9
CDR: Complement Determining Regions
CoRBS: Co-Receptor Binding Site
COVID-19: Coronavirus Disease
CRF: Circulating Recombinant Forms
CT: Cytoplasmic Tail
CTL: Cytotoxic T Lymphocyte
CXCR4: C-X-C Chemokine Receptor 4
DC: Dendritic Cells
DNA: Deoxyribonucleic Acid
dNTP: Deoxyribonucleic Acid
DRM: Detergent-Resistant Membranes
dsDNA: Double stranded DNA
Env: Envelope glycoprotein
ER: Endoplasmic Reticulum
ERAD: ER-Associated Degradation
ESCRT: Endosomal Sorting Complex Required for Transport
Fab: Antigen Binding Fragment
Fc: Fragment Crystallizable Region

FcR: Fc Receptor
FcγR: Fc Gamma Receptors
FcRn: Neonatal Fc Receptor
Fuc: Fucose
Gag: Group-Specific Antigen
Gag-Pol: Gag-protease-reverse transcriptase-integrase polyprotein
Gal: Galactose
GALT: Gut Associated Lymphoid Tissue
GlcNAc: N-Acetylglucosamine
GM1: monosialotetrahexosylganglioside
Gp41: Glycoprotein 41 KDa
Gp120: Glycoprotein 120 KDa
Gp160: Glycoprotein 160 KDa
GPI: Glycosylphosphatidilinositol
HR1: Heptad Repeat 1
HR2: Heptad Repeat 2
HIV-1: Human Immunodeficiency Virus type 1
HIV-2: Human Immunodeficiency Virus type 2
HLA: Human Leukocyte Antigen
HTLV-III: Human T-lymphotropic virus III
HVTN: HIV Vaccine Trials Network
IC: Inhibitory Concentration
Ig: Immunoglobulin
IFN: Interferon
IL: Interleukin
IN: Integrase
INSTI: Integrase Strand Transfer Inhibitors
ITAM: Immunoreceptor Tyrosine-based Activation Motif
ITIM: Immunoreceptor Tyrosine-based Inhibitory Motif
LAV: Lymphadenopathy-Associated Virus
LEDGF: Lens-Epithelium-Derived Growth Factor
LLP: Lentiviral Lytic Peptide
LPA: Latency-Promoting Agents
LRA: Latency-Reversing Agents
LTNP: Long-Term Non-Progressor
LTR: Long Terminal Repeat
MA: Matrix
mAb: Monoclonal Antibody
Man: Mannose

MLV: Murine-Leukemia Virus
MHC: Major Histocompatibility Complex
MIC: MHC-I chain-related
MPER: Membrane Proximal External Region
mRNA: Messenger RNA
NC: Nucleocapsid
Nef: Negative Regulatory Factor
NES: Nuclear Export Signal
Neu5Ac: N-Acetylneuraminic Acid
NFAT: Nuclear Factor of Activated T cells
NHP: Non-Human Primates
NK: Natural Killer
NKG2D: Natural Killer Group 2D
NRTI: Nucleoside Reverse Transcriptase Inhibitor
NNRTI: Non-Nucleoside Reverse Transcriptase Inhibitor
NF-κB: Nuclear Factor-kappa B
NPC: Nuclear Pore Complex
NTB-A: NK-T-B antigen
ORF: Open Reading Frame
PBS: Primer Binding Site
PH: Pleckstrin Homology
PI: Protease Inhibitor
PKC: Protein Kinase C
PI3-k: Phosphatidylinositol-3-kinase
PIC: Pre-Integration Complex
Pol: Polymerase
PPT: Polypurine Tract
PR: Protease
PrEP: pre-exposure prophylaxis
PRD: Proline/Arginine-Rich Domain
PTCs: Post-Treatment Controllers
pTEF: Positive Transcription Elongation Factor
PVR: Polio Virus Receptor (CD155)
Rab11-FIPs: Rabl1 Family Interacting Proteins
REGN-COV2: Cocktail of casirivimab/imdevimab by Regeneron
RER: Rough Endoplasmic Reticulum
Rev: Regulator of Virion
RIDS: Residual Immune Dysregulation Syndrome
RNA: Ribonucleic Acid

RRE: Rev Responsive Element
RT: Reverse Transcriptase
SARS-CoV-2: Severe Acute Respiratory Syndrome Coronavirus 2
sCD4: Soluble CD4
SERINC: Serine Incorporator Protein
SIV: Simian Immunodeficiency Virus
SHIV: Simian-Human Immunodeficiency Virus
SHM: Somatic Hypermutation
smFRET: single molecule Förster Resonance Energy Transfer
SP1: Spacer Peptide 1
SP2: Spacer Peptide 2
ssDNA: Single-Stranded DNA
ssRNA: Single-Stranded RNA
T/F: Transmitted/Founder
TAR: Transactivation-response Region
Tat: Transcriptional Transactivator
TGN: Trans-Golgi Network
TMD: Transmembrane Domain
TNF: Tumor Necrosis Factor
ULBP: UL16 glycoprotein Binding Protein
UTR: Untranslated Region
Vif: Viral Infectivity Factor
Vpr: Viral protein R
Vpu: Viral protein U
vDNA: Viral DNA
VISCONTI: Viro-Immunologic Sustained Control after Treatment Interruption
vRNA: Viral RNA
VSV: Vesicular stomatitis virus

CHAPTER I

General Introduction

This chapter provides a literature review of the topics relevant to the research presented in this thesis. Section 1.1 reviews the origin of HIV and the viral replication cycle. In Section 1.2, the pathogenesis of infection, current HIV therapies, and vaccines strategies are discussed. An introduction to humoral immune responses against HIV will be described in Section 1.3. Parts of a published review article [Anand, S.P. and Finzi, A., **2019**. Understudied factors influencing Fc-mediated immune responses against viral infections. *Vaccines*, 7(3)] are used throughout this chapter to provide a succinct overview of the four published research articles presented in this thesis. Finally, the rationale and main objectives of the research presented in Chapters 2 to 5 are outlined in section 1.4.

1.1 HIV-1 and AIDS

According to the UNAIDS 2020 report, more than 37 million individuals are currently living with the human immunodeficiency virus (HIV) globally and acquired immunodeficiency syndrome (AIDS)-related deaths have claimed the lives of an estimated 36.3 million people since the beginning of the HIV pandemic (https://www.unaids.org/en). With the increased availability of combination antiretroviral therapies (ART), most individuals now living with HIV have a longer lifespan (1). Behavioural interventions as well as the availability of ART for pre-exposure prophylaxis (PrEP) has further reduced the risk of HIV transmissions (2, 3). However, only ~ 73% of people living with HIV worldwide are on ART, leaving an estimated 15 million people that still do not have access to ART. Thus, complete treatment access remains a hurdle to curb the spread of HIV and untreated individuals experience a progressive decrease in their CD4+ T lymphocyte count, ultimately leading to life-threatening AIDS.

As of 2021, curative treatments and an effective vaccine have still not been established. Although disease symptoms and viral loads can be suppressed with ART, the need for a cure remains as infected individuals harbour 'HIV Reservoirs'. With ART-induced suppression of HIV replication, circulating CD4+ T cell numbers typically increase back to normal levels. Despite this, many patients still experience residual immune dysregulation syndrome (RIDS), whichis characterized by increased inflammation and coagulopathy and is associated with increased morbidity and mortality (4). As will be discussed in section 1.1.3, reverse transcribed HIV proviral DNA integrates into the host genome, where it can be transcribed to produce new virions. However, a fraction of infected CD4+ T cells harbour integrated replication-competent HIV DNA that remain transcriptionally silent, and these populations are understood to be latently infected cells that survive for years and can be reactivated once treatment is withdrawn. Thus, lifelong ART is necessary to prevent viral rebound from reservoirs and to prevent harmful levels of plasma viral load.

1.1.1 Viral Origin and Classification

In 1981, emerging cases of a syndrome characterized by immune dysfunction, lymphadenopathy, and opportunistic infections (pneumonia, mucosal candidiasis, and others)

were reported in the USA (5, 6). In 1982, the American Center for Disease Control published a first case definition of this disease state – AIDS (7). In 1983, the group of Dr. Luc Montagnier in France (8), and soon after the group of Dr. Robert Gallo in USA (9, 10), discovered the causative agent for the AIDS disease and termed them: lymphadenopathy-associated virus (LAV) and human T-lymphotropic virus -III (HTLV-III), respectively. In 1986, the term HIV was officially designated (11, 12). Additionally, in 1986, another related but genetically distinct human retrovirus was identified in AIDS patients in West Africa, which is now termed HIV type 2 (HIV-2) (13).

HIV is an enveloped virus belonging to the family of *Retroviridae*, genus of zoonotic lentiviruses (8, 9) that seeded infection in humans from cross-species transfer of simian immunodeficiency virus (SIV) found in non-human primates (14). HIV is broadly classified into two types, HIV-1 and HIV-2, and while both HIV-1 and HIV-2 can cause AIDS, infection with HIV-2 results in a longer asymptomatic phase and has a lower transmission frequency because of lower plasma viral loads in infected individuals (15). The work presented in this thesis focuses on HIV-1, which is the most prevalent and widely distributed species.

A unique characteristic of retroviruses is the reverse transcription of their viral RNA into DNA, which is subsequently integrated into the host genome (16, 17). HIV-1 is highly genetically diverse due its error-prone reverse transcriptase, thus, leading to high recombination and mutation rates. It is phylogenetically characterized into the following groups: M (main), O (outlier), N (non-M/non-O/new) and P (pending classification) (18-21). Approximately 98% of global HIV-1 isolates belong to Group M (22) and these can be further subdivided into 9 subtypes/clades (A, B, C, D, F, G, H, J, and K) and at least 89 circulating recombinant forms (CRFs) (23, 24). CRFs are a result of co-infection with different subtypes that lead to recombination events (25). HIV-1 groups M and N are closely related to SIVs that infect chimpanzees (SIVcpz) (26) and groups P and O are closely related to SIVs that infect gorillas (SIVgor) (27). HIV-2 is related to SIVs that infect sooty mangabeys (SIVsmm) (28) and macaques (SIVmac) (29).

1.1.2 Viral Structure and Genome Organization

HIV-1 viral particles are spherical in shape with an average diameter ranging from 100 to 120 nm (30). Each virion is surrounded by a lipid bilayer that originates from the host cell and that carries approximately 8-10 envelope glycoprotein (Env) trimers (31), with each monomer composed of an external glycoprotein subunit (gp120) non-covalently linked to a transmembrane spanning subunit (gp41). The inner surface of the viral membrane is lined with the matrix protein (MA) that forms hexamers and remains attached to the Env glycoproteins and contributes to the spherical shell structure of the virion (32). Within the HIV-1 particle, a core composed of ~1,500 monomers of capsid protein (CA), 250 CA hexamers, and 12 CA pentamers encapsulate the dimeric single-stranded viral RNA (vRNA/ssRNA) genome (30, 33, 34). The nucleocapsid (NC) binds to the vRNA and helps its encapsulation during assembly. An infectious virus also contains the enzymes protease (PR), integrase (IN), and reverse transcriptase (RT) (**Figure 1.1**). Additional viral proteins present in virions include viral infectivity factor (Vif) (35), viral protein R (Vpr) (36), and negative factor (Nef) (37); while the biological properties of incorporated Nef and Vpr have been studied, the role of incorporated Vif remains to be determined (38).

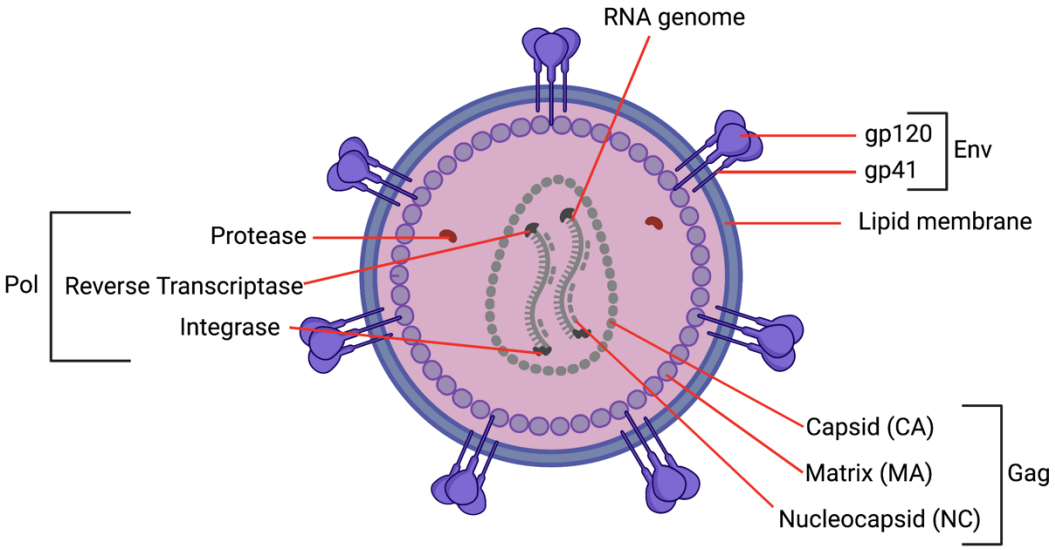

Figure 1.1 Mature HIV-1 virion structure. Schematic view of the mature HIV-1 particle detailing viral proteins and the virion structure. The HIV-1 Env composed of trimeric gp120–gp41 complexes are embedded in a lipid membrane. The cytoplasmic tail of gp41 interacts with the MA. The CA composes the conical core that contains two vRNAs surrounded by the NC protein. PR, RT, IN, Vpr, Vif, and Nef are also present in the virus. Diagram created with BioRender.com

The HIV-1 genome consists of two positive-sense single-strand RNA copies that are 9.2 kb each. The vRNA is capped at the 5’ end and polyadenylated at the 3’ end, like other eukaryotic mRNAs and both ends of the vRNA are flanked with non-coding repeat sequences called the 5’ and 3’ untranslated regions (UTRs). Each vRNA has nine overlapping open reading frames (ORFs) that code for fifteen viral proteins (**Figure 1.2**) (39).

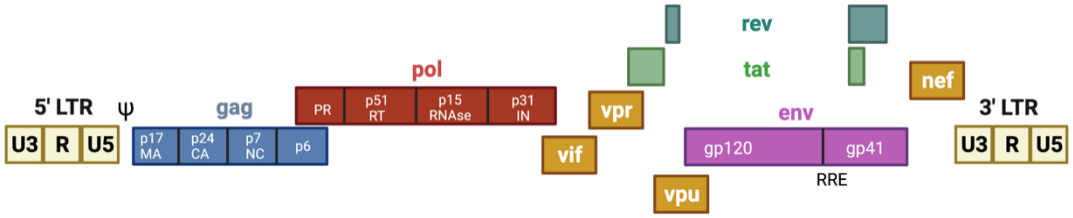

Figure 1.2 HIV-1 genomic organization. The HIV-1 genome organization with the 5' end and 3' end of the long terminal repeats (LTR) and the various open reading frames that code for the viral proteins and polyproteins are depicted in different colours. Diagram created with BioRender.com

After reverse transcription of the vRNA upon infection, the double-stranded DNA is integrated into the host cell genome in a mechanism coordinated by IN. The proviral DNA is flanked at both ends by long terminal repeat (LTR) sequences that are important for the integration (40). The three main enzymatic and structural products of the provirus are the structural group-specific antigen (Gag), envelope (Env), and polymerase (Pol), that are first transcribed into large polyprotein complexes and are later cleaved into different proteins (41). Following cleavage, the Gag precursor ($Pr55^{Gag}$) generates the MA (p17), CA (p24), nucleocapsid (NC; p7), and protein p6 (42). There also consist two spacer sequences, spacer peptide 1 (SP1) and spacer peptide 2 (SP2) that play important roles in regulating virion assembly and capsid maturation (43). The *env* gene encodes for the structural protein gp160, which is cleaved to form gp120 and gp41 subunits (44). Pol is cleaved into the viral enzymes protease (PR), reverse transcriptase (RT), and integrase (IN). The remainder of the viral proteins are regulatory and accessory proteins. The two regulatory proteins include the transcriptional transactivator (Tat) and regulator of virion (Rev). Whereas, the accessory proteins include viral protein U (Vpu), Vpr, Vif, and Nef.

1.1.3 Replication cycle

The replication cycle of HIV-1 can be divided into two distinct phases: the early and late stages. The early stage includes all the steps from viral entry to viral DNA integration. The late stage includes transcription of the HIV-1 DNA, translation of viral mRNA, virus assembly, and release of mature virions (**Figure 1.3**).

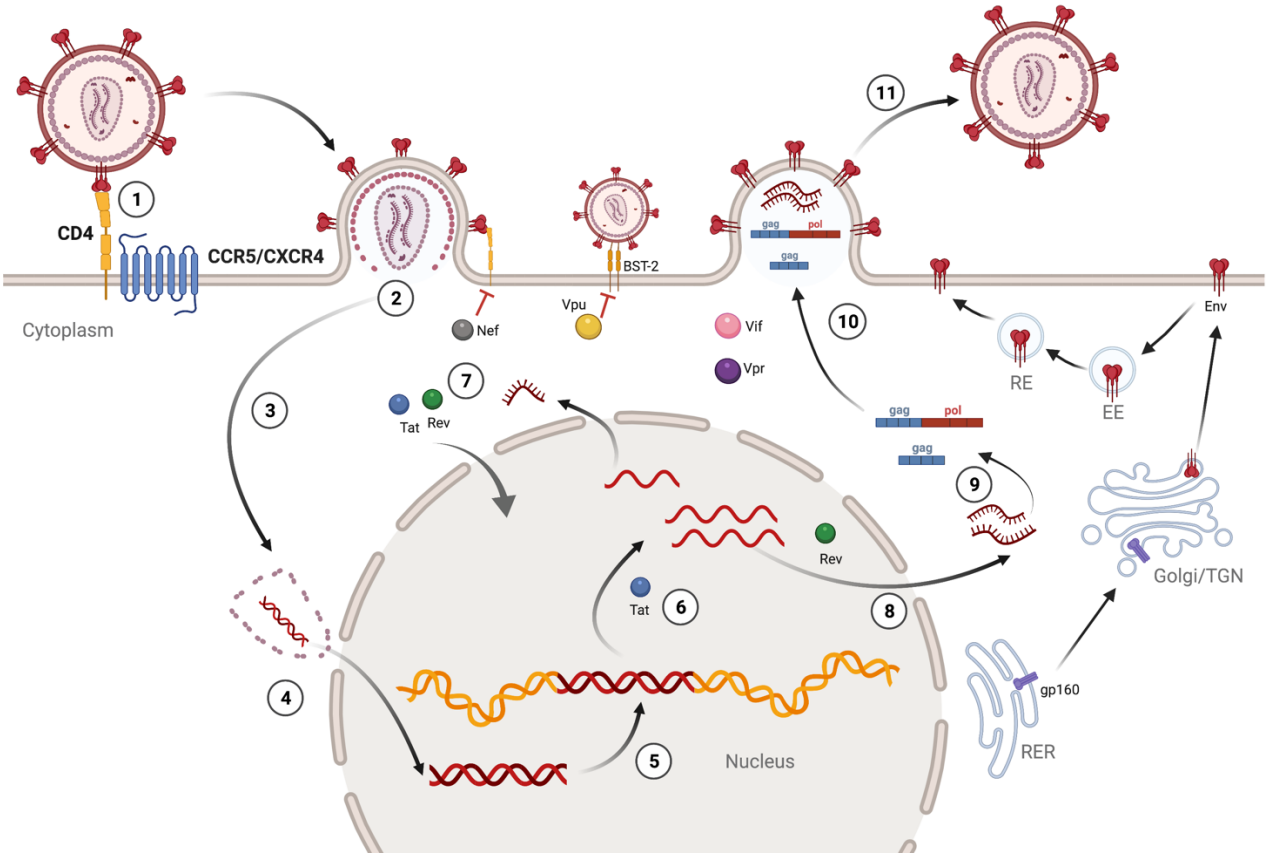

Figure 1.3 HIV-1 Replication Cycle. Schematic representation of the main stages of viral replication: (1) receptor interaction, (2) fusion and entry, (3) reverse transcription and translocation to the nucleus of the PIC (preintegration complex), (4) uncoating and nuclear import, (5) integration, (6) transcription, (7) nuclear export of multiply spliced and (8) unspliced or singly spliced transcripts, (9) translation of viral proteins, (10) viral assembly and budding, and (11) viral release and maturation. BST-2: bone marrow stromal cell 2; RER: rough endoplasmic reticulum, TGN: trans-golgi network; EE: early endosomes; RE: recycling endosomes. Diagram created with BioRender.com

1.1.3.1 Viral entry and early replication stages

HIV-1 infection begins with the entry of the virus into the host target cell. Initial studies showing striking depletion of CD4+ T cells in HIV-1-infected individuals suggested CD4 as the primary receptor required for viral entry (45). Thus, HIV-1 predominantly infects cells expressing the CD4 receptor, including CD4+ T lymphocytes, macrophages & dendritic cells. Entry can be summarized into three main phases: the interaction between Env and its receptor CD4 (46), the interaction between Env and its coreceptors: the C-X-C chemokine receptor type 4 (CXCR4) (47) or the C-C chemokine receptor type 5 (CCR5) (48-50), and the fusion of the

viral and cellular membranes. Viral particles that utilize the CCR5 receptor are denoted as R5 isolates and those utilizing the CXCR4 receptor are referred to as X4 isolates. A separate class of dual-tropic strains use both receptors and are referred to as R5X4 isolates (51). Some host proteins, such as lectins and proteoglycans, have been speculated to mediated non-specific attachment of the viral particle to the host cell,facilitating receptor binding and viral entry (52).

Protein-protein interactions between the gp120 subunit of the Env trimer and the CD4 receptor induce conformational changes within g120 to reposition and expose the otherwise buried variable loop 3 (V3) (53, 54). The V3 loop and bridging sheet aid the interaction of gp120 with the CXCR4 or CCR5 coreceptors, based on tropism (55). Upon coreceptor binding, a hydrophobic region called the fusion peptide is exposed from the N-terminus of the gp41 subunit and inserted into the target cell membrane (56, 57). A pre-hairpin intermediate is formed, and two heptad repeat regions (HR1 and HR2; also referred to as N-HR and C-HR) from each gp41 subunit come close together to form a 6-helix bundle (6HB). Thus, the 6HB is composed of a trimeric HR1 coiled-coil core surrounded by three HR2 helices that are packed in an antiparallel fashion (58-60) (**Figure 1.4**). This allows for the viral and target membrane to be brought into proximity a subsequently, the fusion pore formation leads to the delivery of the viral core into the target cell cytoplasm.

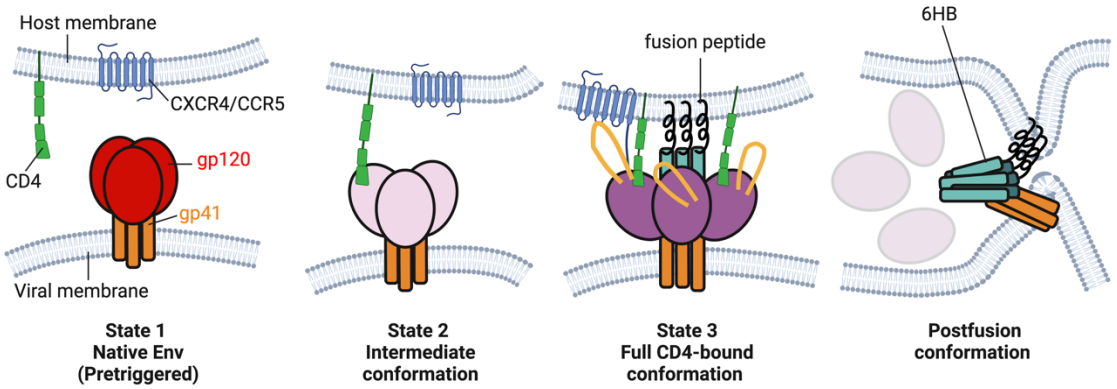

Figure 1.4 HIV Entry. Entry begins with binding of gp120 to its receptor CD4, which triggers a conformational change from 'closed' to partially 'open' (State 2) and further allows the binding of gp120 to its coreceptor (either CCR5 or CXCR4). Coreceptor binding results in triggering of the fusion machinery and formation of the six-helix bundle (6HB) required to drive fusion of the viral and host membranes. Diagram created with BioRender.com

After the entry process, the HIV vRNA is converted to DNA by RT, which possesses two enzymatic activities: (i) the DNA polymerase activity, which can either use RNA or DNA as a template, and (ii) the RNase H activity, which exclusively degrades RNA in the context of an RNA/DNA duplex (61). To begin this process, the $tRNA^{Lys3}$ is utilized as a primer to bind to the primer binding site (PBS) from the 5' end of HIV-1 RNA (62). As the RT catalyzes the synthesis of DNA, the RNase H activity of RT degrades the remaining 5' end of the template RNA on the RNA/DNA hybrid to free the antisense or (-) single-stranded DNA (ssDNA). The newly synthesized (-) ssDNA then hybridizes to the R regions present at the 3' end of the vRNA in a process called the first strand transfer (63). Since HIV carries two copies of genomic RNA, the first strand transfer can occur either in *cis* or *trans*, which accounts for high viral recombination (64). This transfer of DNA mediates the synthesis of the full-length (-) strand of the vDNA, while degrading the template RNA, except for the polypurine tract (PPT), which is resistant to RNase H activity and serves as the primer to produce the second sense or (+) DNA strand (65). HIV-1 has two PPTs located near the 3' end of the vRNA and another in the central region of the genome. Through a second strand transfer, DNA synthesized from the 3'-PPT is used as a primer for the synthesis of the 5' end of the (+) strand and elongation of this end proceeds through the central PPT, displacing the original strand and terminating at

~100 nucleotides from the cPPT (66). This process results in a linear double-stranded DNA product with a DNA flap in the (+) strand DNA, which plays a role in the nuclear localization of the pre-integration complex (PIC) (67). The PIC is composed of the newly synthesized proviral DNA and some viral proteins, such as IN, MA, RT, and Vpr (68-70).

Once inside the cell, the viral core undergoes progressive disassembly before integration. Within the HIV-1 field, the timing and location of CA disassembly or 'uncoating' is still under debate (71), with several studies explaining cytoplasmic uncoating (72), uncoating at the nuclear pore complex (NPC) (73), and nuclear uncoating (74, 75). In each model the reverse transcription of the vRNA into DNA is completed first (76). Over the past 2 years the field has seen compelling evidence using high-resolution microscopy favouring the completion of uncoating and reverse transcription in the nucleus to release the vDNA occurring close to the integration sites (75, 77).

The last step of the early stages of the HIV-1 life cycle is the integration of the viral DNA into the host cell genome (78). The viral enzyme IN plays a crucial role in this process along with the host protein lens epithelium-derived growth factor (LEDGF/p75) and other viral proteins (MA and Vpr) that aid in increasing integration efficiency (79). LEDGF prevents DNA circularization and the formation of 2-LTR circles since this form of the genome cannot be integrated (80). In the first step of integration (also called 3′ end processing), two nucleotides are removed from each 3′ end of the double-stranded DNA. In the second step (also called DNA-strand transfer), the 3′ ends of the DNA are covalently joined to the target DNA. Finally, the single-strand gaps (two-nucleotide overhangs) at the 5′ ends of the vDNA are repaired by cellular enzymes to complete integration (81).

1.1.3.2 Late replication stages

Following integration, the viral DNA is referred to as a 'provirus', and it serves as a template for the transcription of all the viral structural, regulatory, and accessory proteins. Initial viral transcription is mediated by the direct interaction between cellular transcription factors and cis-acting regulatory elements located in the LTR. These elements include a TATA box, three

tandem specificity protein-1 (SP1) binding sites, and two highly conserved nuclear factor kappa B (NF-κB) binding sites (83-85). Viral proteins Tat, Rev, and Nef are produced first from completely spliced transcripts (86, 87). The accumulation of Tat further stimulates transcription from the LTR, in a positive feedback manner. Tat shuttles back to the nucleus and binds to the positive transcription elongation factor, pTEFb, composed of cyclin T1 and the cyclin dependent kinase 9 (CDK9). This complex then binds the transactivation-response region (TAR), that is located downstream of the transcription initiation site and functions as an RNA regulatory signal (88), to enhance host RNA polymerase II processivity and promote efficient elongation of viral transcripts (89-91). The nuclear export of incompletely spliced transcripts coding for structural proteins and enzymes is prevented by cellular mechanisms and the primary role of Rev is to circumvent this system. Rev binds and multimerizes on the cis-acting RNA element called the Rev Responsive Element (RRE) present on both the singly spliced and unspliced transcripts (92, 93). Rev contains a nuclear export signal (NES) that allows its transport between the nucleus and cytoplasm (94).

HIV-1 has a compact genome with overlapping ORFs, and programmed frameshifting is utilized during translation (95). One example of this is the *gag-pol* transcript, which is subsequently translated into the Gag or Gag-Pol polyproteins at a 1:20 ratio. The 55 kilo Dalton (kDa) Gag protein (MA, CA, NC, and p6) is key for viral assembly. The production of Env on the rough endoplasmic reticulum (RER) is described in Section 1.1.5.

The N terminal of MA is myristoylated, thus, after synthesis, Gag associates to plasma membrane sites rich in the phosphoinositide phosphatidylinositol-4,5-bisphosphate (PI[4,5]P2) and cholesterol (96, 97). These regions are also known as lipid microdomains, where viral budding has been described to occur from. Microdomains are enriched with cholesterol, sphingolipids, and glycosylphosphatidylinositol (GPI)-anchored proteins, and the viral membrane contains higher levels of sphingolipids and cholesterol (98-100). Lipid microdomains are known to exist in the liquid-ordered (l_o) phase of plasma membranes that 'float' in the surrounding loosely packed liquid-disordered (l_d) phase (101). These floating microdomains have been termed 'lipid rafts' that can be biochemically isolated using sucrose

gradients as detergent-resistant membranes (DRM) at low temperatures due to their insolubility in nonionic detergents, like Triton X-100 (102). Studies have demonstrated colocalization of Gag with a microdomain associated ganglioside, monosialotetrahexosylganglioside (GM1) (103). Furthermore, evidence indicates Gag also restrictrs PI(4,5)P2 and cholesterol mobility in the plasma membrane to create a specific nanodomain platform for virus assembly (104).

The CA domain promotes the multimerization of Gag. The NC domain drives the packaging of the dimeric ssRNA, by interacting to the vRNA packaging signal sequence Psi (ψ) (105). There are a few mechanisms that have been proposed to explain how Env is incorporated into virions: (1) passive transport; (2) co-targeting of Gag and Env to microdomains; (3) direct interaction of MA domain of Gag with Env; (4) indirect interaction of Gag and Env with host cell proteins (106). Several studies support the third model of incorporation, wherein a direct interaction between the two proteins takes place at the assembly site (107-109). Furthermore, it has been suggested that the interaction of Gag with Env is required for the association of Env with lipid microdomains (110). However, some cytoplasmic tail truncated Env mutants can also be incorporated into virions (111), and thus, the dependence on Gag-Env interactions for Env incorporation remains to be clearly determined in the field.

The last stage of viral assembly process involves the budding and release of virions. The p6 domain at the C terminal of Gag serves as the docking site for the endosomal sorting complex required for transport (ESCRT), which is composed of cellular proteins that aid in membrane budding and scission processes (112). Released virions undergo a maturation process, and this is mediated by the PR domain that sequentially cleaves the Gag-Pol polyprotein to release PR, IN, RT enzymes (113). PR also cleaves Gag to release the MA, CA, and NC proteins. PR cleavage triggers morphological changes in the virion, resulting in mature infectious viral particles (Figure 1.1) (114).

1.1.4 Accessory proteins

1.1.4.1 Nef

Nef is a 27 – 35 kDa protein that is N-terminally myristoylated, which allows its association with the plasma membrane and incorporation into virions. Nef is very important for replication *in vivo* since patients infected with viruses lacking or harbouring a defective form of Nef demonstrate slower rates of disease progression (also known as long-term-non-progressors; LTNPs) (115). Additionally, in the absence of Nef, virions exhibit severe defects to enter the host cell (116).

Nef carries out a myriad of functions (117, 118), one of the major ones being the downregulation of the surface expressed of CD4 receptors during the early stages of infection (119). Nef interacts with the dileucine motif of the cytoplasmic tail of CD4 and bridges interaction with the adaptor protein complex 2 (AP-2) to enhance CD4 endocytosis through clathrin-coated pits, leading to its eventual lysosomal degradation through a phosphatidylinositol-3-kinase (PI3K) pathway (120, 121). Nef also down modulates other cellular proteins including the major histocompatibility complex class-I (MHC-I) molecules to protect infected cells from cytotoxic T lymphocyte recognition (122). Additionally, Nef down modulates expression of ligands of the activating natural killer group 2D receptor (NKG2D), including MHC-I chain-related A and B (MICA and MICB) and human cytomegalovirus UL16 glycoprotein binding protein (ULBP) 1-5 molecules (123, 124). NKG2D acts as a co-receptor for CD16a (Fc receptors will be further described in Section 1.3.4), and downregulation of its ligands interferes with overall Fc-mediated effector responses against HIV-1-infected cells (125). Recent findings have also revealed that Nef prevents the virion incorporation of cellular serine incorporator proteins 3 and 5 (SERINC3 and SERINC5), that otherwise block viral entry (126).

1.1.4.2 Vif

Vif is a 23 kDa cytoplasmic protein that is expressed late during the viral replication cycle. One of the main functions of Vif is to antagonize the host cellular restriction factor apolipoprotein B mRNA-editing enzyme, catalytic polypeptide like 3G (APOBEC3G) (127,

128). APOBEC3G is a member of the APOBEC family of editing enzymes that can mutate polynucleotides by deaminating cytidine (C) bases to uridine (U) in the viral DNA (129). Vif directly interacts with APOBEC3G and recruits a cullin5-based E3 ubiquitin ligase complex to polyubiquitinate APOBEC3G, leading to its proteasomal degradation (130, 131). Thus, Vif plays a critical role in the production of infectious virions. Other functions of Vif include inhibition of autophagy and inhibition of the interferon response (132, 133).

1.1.4.3 Vpr

Vpr is 15 kDa protein that is packaged into virions via a direct interaction with p6 domain of Gag and is important for the early stages of viral replication (134, 135), by aiding the nuclear import of the PIC (136). It can also later induce G_2 cell cycle arrest (137), modulate apoptosis (138, 139), aid with transactivation of the LTR (140), and regulate of NF-κB activity (141). By inducing infected cell cycle arrest in the G_2/M Phase, Vpr prevents infected cells from undergoing mitosis and inhibits cell proliferation, eventually leading to host cell apoptosis. However, Vpr also inhibits apoptosis by upregulating the bcl-2 oncogene and the anti-apoptotic effects of Vpr have been suggested to preserve a pool of infected cells that facilitate viral persistence and subsequent spread of HIV-1 (139). Additionally, Vpr can enhance the susceptibility of infected cells to NK-mediated killing by inducing cell surface expression of activating NKG2D ligands (142). Studies have suggested the importance of Vpr in overcoming restriction to viral replication in myeloid cells, such as macrophages and dendritic cells, since these are one of the first cell types to encounter HIV-1 in mucosal tissues (143, 144).

1.1.4.4 Vpu

Vpu is a 17 kDa transmembrane protein that contains a hydrophobic N-terminal membrane anchor and a hydrophilic C-terminus (145, 146). It is specific to HIV-1 and closely related SIVcpz and SIVgor (147). The phosphorylation of Vpu's cytoplasmic domain at Serine residues in position 52 and 56 by Casein kinase 2 is required for its activities in the replication cycle (148). These include degrading the CD4 receptor (149) as well as enhancing the release of virions by antagonizing the host protein bone marrow stromal cell 2 (BST-2): also known as CD317 or tetherin (150). The interaction of Vpu and CD4 also prevents the formation of

Env-CD4 complexes to subsequently enhance Env trafficking and incorporation. By interacting with the $SCF^{\beta\text{-}TrCP}$ E3 ubiquitin ligase complex, Vpu mediates the polyubiquitination of CD4 and its degradation via the ubiquitin-proteasome pathway; thus targeting CD4 degradation by an endoplasmic reticulum associated degradation (ERAD) pathway(151).

In the absence of Vpu, the restriction factor BST-2/ tetherin prevents virion release and promotes the accumulation of viral particles at the surface of infected cell. BST-2 is an interferon-induced dimeric protein that consists of an N-terminal cytoplasmic tail, a transmembrane domain (TMD), and a C-terminal glycophosphatidylinsitol (GPI) anchor, allowing it to interact with both the viral and cell membrane to cross-link budding virions. Vpu counteracts BST-2 via an interaction of the TMDs of both proteins (152). Vpu has been shown to block the trafficking of newly synthesized BST-2 but also downregulate BST-2 from the plasma membrane (153-155). BST-2 can be expressed in two distinct long and short isoforms, and Vpu preferentially targets the long form of the protein (156). Additionally, antagonism of BST-2 by Vpu also prevents the induction of the NF-κB pathway and thus, limits the activation of the innate immune response (157).

Vpu also interferes with the early innate immune responses by downmodulating several cellular proteins, including the NK cell ligands NK-T-B antigen (NTB-A) and polio virus receptor (PVR/CD155) from the infected cell surface; thus, affecting the recognition and elimination of infected cells by NK and cytotoxic T cells (158, 159).

1.1.5 Envelope glycoproteins

The mature Env trimeric protein of HIV-1 is the only viral protein exposed on the surface of viral particles and infected cells (160) and as mentioned in Section 1.1.3.1, it is essential for viral entry. The unprocessed 160 kDa Env glycoprotein precursor (gp160) is synthesized from a singly spliced, bicistronic *vpu/env* mRNA on the RER. The *env* gene encodes a signal peptide sequence at its N-terminus which targets it to the ER membrane, and this peptide is removed by cellular signal peptidases during translation (161). After production, within the ER, gp160

is glycosylated with *N*-linked and *O*-linked oligosaccharide side chains and it oligomerizes into trimers. More specifically, *N*-linked glycosylation occurs at Asparagine (Asn) residues (consensus sequence: NXT/S, where X represents any amino acid except proline). It follows an ordered assembly that begins in the ER with the attachment of a preassembled oligosaccharide and is followed by the enzymatic removal of sugar residues ('trimming') in the cis Golgi and addition of complex-type glycans ('processing') in the medial and late Golgi apparatus (further discussed in section 1.3.5). Additionally, during its trafficking through the trans-Golgi network (TGN), gp160 is proteolytically cleaved by cellular furin and furin-like proteases to produce gp120 and gp41 subunits of the trimeric functional Env (44, 162) (Figure 1.5). Trafficking through the Golgi has been demonstrated to be important for the appropriate addition of complex glycans; since Env trimers that bypass Golgi trafficking lack complex glycans, are uncleaved, and do not sample the native 'closed' conformation (163). Upon furin proteolytic cleavage, gp120 and gp41 subunits remain associated via non-covalent bonds (164, 165). Highly conserved Cys residues within the gp120 and g41 subunits also form intramolecular disulfide bonds to maintain the tertiary structure of Env. The highly conserved determinants of the functional Env protein are shielded by N-linked glycans or by structural constraints that have evolved because of immune pressure (166-168).

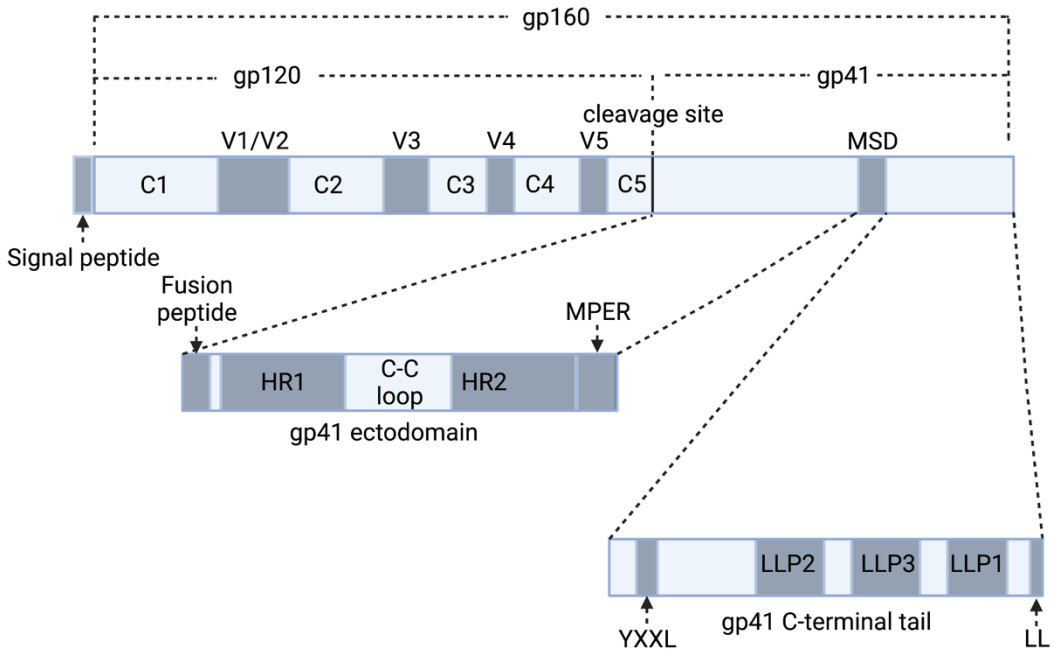

Figure 1.5 Envelope glycoprotein composition. Schematic representation of the HIV-1 Env, with the immature polyprotein labelled gp160 and the mature, cleaved protein labelled gp120 and gp41. The gp120 subunit is composed of five constant regions (C1–C5) and five variable domains (V1–V5). The gp41 subunit is composed of an ectodomain, membrane spanning domain (MSD) or transmembrane domain, and the C-terminal tail. Within the ectodomain are the heptad repeat regions (HR1 and HR2), and the membrane proximal external region (MPER). Within the C-terminal tail are the lentivirus lytic peptide sequences (LLP1, LLP2 and LLP3), and functional endocytic motifs YXXL (near the N terminus) and LL (dileucine; at the C terminus). Figure adapted from (169) with permission from Microbiology Society; diagram created with BioRender.com

In the field, researchers have faced several challenges to characterize the structural arrangement of the native Env trimer, due to its metastable conformation, insolubility of the membrane-bound proteins, and extensive glycosylation. Since 2013, a soluble gp140 form (known as SOSIP.664) derived from the sequence of a clade A HIV-1 isolate BG505 and stabilized by the introduction of artificial disulfide crosslinks between the gp120 and gp41 subunits (SOS) in combination with the I559P (IP) mutation, is being used for structural studies (170, 171). However, the introduction of SOSIP mutations have been shown to result in abnormal Env conformation transitions, and thus, this construct samples a different conformation compared to the native Env (172-174). Attempts to test SOSIP trimers as vaccine

immunogens in animal models has induced neutralizing antibodies against autologous viruses only, but not against a broad spectrum of circulating strains (175). Further work is required to acquire structural information about the unliganded native Env conformation since this represents the main antigenic target of antibodies.

Since there are non-covalent interactions between the gp120 and gp41 subunits, this can result in the spontaneous dissociation of gp120 from gp41, known as gp120 shedding, from the surface of productively infected cells (164, 165, 176). Consequently, significant levels of soluble gp120 can be found circulating in the blood and tissues of HIV-infected individuals (177-179). Shed gp120 can interact with CD4 receptors on the surface of uninfected bystander cells sensitizing them to antibody-dependent cellular cytotoxicity (ADCC) (180).

1.1.5.1 gp120

The gp120 subunit of Env consists of five constant domains (C1 to C5) and five variable domains (V1 to V5) (181). The constant domains form the core of the Env trimer, while the variable domains form the exterior of the gp120 subunit. Gp120 is highly glycosylated with N-linked and some O-linked glycans that shield the Env against immune recognition (182, 183). Thus, the overall structure of gp120 can be broken down into a gp41-interactive inner domain (conserved) and a glycosylated outer domain (variable). In its CD4-bound state, a four-stranded bridging sheet connects the inner and outer domains (184). Residues from the C1, C3 and C4 regions interact with the CD4 receptor (also known as CD4 binding site [CD4bs]) while residues from the V3 loop tip and the bridging sheet are important for co-receptor interaction (164, 176, 184-187). Non-neutralizing antibodies (further discussed in section 1.3.3) targeting the gp120 inner domain are known as anti-cluster A antibodies and belong to the larger family of CD4-induced (CD4i) antibodies.

1.1.5.2 gp41

The gp41 subunit is composed of an extracellular domain, a transmembrane domain, and a long C-terminal cytoplasmic tail (CT). The gp41 extracellular domain contains regions important for viral entry, including the fusion peptide (188), the HR1/HR2 domains (60), and

the membrane-proximal external region (MPER) (189). The MPER region is the main gp41 domain targeted by neutralizing antibodies (190). The transmembrane domain is composed of conserved residues that aid in Env anchoring to the plasma membrane (191). The CT is approximately 150 to 200 amino acids long and has been shown to be functionally important for viral replication, the incorporation of Env in virions, and cell surface expression of Env (192, 193). Within the CT, there are also other three segments known as the lentiviral lytic peptides (LLPs) (194) that have been implicated in many functions, including Env stability (195) and cell surface expression (196). Furthermore, a highly conserved motif (consensus sequence LWYIK) located near the N-terminus of the transmembrane domain regulates interaction of Env with cholesterol in the plasma membrane and mutations in this domain decrease HIV-1 infectivity (197).

1.1.5.3 Glycoprotein endocytosis

After Env is synthesized and the mature cleaved trimer reaches the cell surface, it is either incorporated onto budding virions or rapidly internalized (198, 199). This phenomenon was first demonstrated in the HIV field to be a mechanism in place to allow for antigen processing and presentation by MHC-II molecules (198). The CT interacts with components of the endosomal recycling compartments and endosomal recycling has been suggested to facilitate Env trafficking to the site of virion assembly and thus, its incorporation of Env into budding virions. More specifically, recycling of Env through endocytic recycling pathways is dependent upon Rab11a Family Interacting Proteins (FIPs), which are effector molecules that mediate sorting of cargo from the endosomal recycling compartment to the plasma membrane (200). Additionally, the retromer complex, which is involved in retrograde endosome-to-Golgi transport, also has a role in Env incorporation (201).

The CT of the gp41 subunit contains endocytic signals that contribute to constitutive endocytosis of endogenously synthesized Env upon its arrival to the plasma membrane. Two functional endocytic signals were discovered in the CT: a membrane proximal tyrosine-based sorting motif (consensus sequence: YXXΦ; where X represents any amino acid and Φ a hydrophobic amino acid) near the N terminus and a dileucine-based motif at the C terminus

that interact with clathrin adaptor proteins (AP-1 and AP-2), which concentrate proteins within clathrin-coated vesicles for endocytosis (202-206). Additional conserved tyrosine-based motifs are present within the CT and have variable effects on Env expression and incorporation in virions (205). Some immunological implications include evasion from antibody recognition, whereby mutations of these conserved endocytosis motifs in the cytoplasmic tail of Env have been shown to result in increased cell-surface expression of Env, which correlate with increased antibody binding and increased Fc-mediated effector responses (207).

1.1.5.3.1 Modes of Endocytosis

There is a high diversity of internalization routes in mammalian cells that can be dynamin-dependent and -independent. Dynamin is a large GTPase and upon GTP hydrolysis, mediates the fission of vesicles from the plasma membrane (208); the isoform dynamin-2 is ubiquitously expressed in all cell types. Dynamin proteins contain a pleckstrin homology (PH) domain, a GTPase effector domain (GED), and a C-terminal proline/arginine-rich domain (PRD). The PRD of dynamin interacts with a variety of proteins that contain SH3 domains (209). Thus, dynamin can interact directly with Bin/Amphiphysin/Rvs (BAR) adapter proteins that aid in membrane shaping, curvature, and scission (210). For the research presented in this thesis, experiments focused broadly on determining whether the mode of antibody-mediated Env endocytosis was dynamin-dependent or -independent (discussed in Chapter 3).

Dynamin-dependent mechanisms can be further categorized into clathrin-mediated and caveolar endocytosis. Clathrin-mediated endocytosis is the most widely studied pathway, where clathrin is recruited from the cytosol to form clathrin-coated pits with the aid of adaptor proteins and at least 40 different protein components (211). Caveolar budding occurs by the assembly of caveolins, integral membrane proteins that bind directly to membrane cholesterol, and aid in membrane curvature. Furthermore, lipids play an important role in endocytic mechanisms; with the depletion of cholesterol impacting formation of both clathrin-coated vesicles and flattening caveolae (212, 213).

1.1.5.4 Glycoprotein conformation

The conformational flexibility of the Env trimer can be broadly categorized into three different states through which it transitions upon CD4 interaction: State 1 (pre-triggered or 'closed'), State 2 (asymmetric intermediate), and State 3 (CD4-bound or 'open') (as illustrated in Figure 1.4) (214, 215). In its native and unliganded form, the trimer adopts its high-energy metastable 'closed' conformation, in which the variable loops protect the highly conserved inner regions from the immune system (216). Env trimers from primary HIV-1 isolates typically exist in State 1 (217). The interaction of CD4 with Env 'Phe 43 cavity', a hydrophobic pocket that allows for the insertion of the residue phenylalanine 43 of CD4, lowers the activation barrier between State 1 and downstream conformations (State 2, followed by State 3) (218). Following CD4 interaction, the V1 and V2 regions rearrange to expose the V3 loop that interacts with the coreceptor (215). Furthermore, three topological layers located in the inner domain of gp120 also affect the interaction of Env trimers with CD4 and control the transition between its unliganded and CD4-bound conformations (176).

Certain residues within the Phe43 cavity, particularly the amino acid at position 375, can influence the overall conformation of Env. Env trimers from group M strains usually have a serine at position 375, which allows Env to sample its 'closed' conformation. Whereas the substitution of serine with bulky residues, such as histidine or tryptophan, leads to Env trimers spontaneously sampling a more 'open' conformation, and thus, are better recognized by CD4i antibodies (219). This type of polymorphism has been observed in Env trimers from CRF01_AE strains, the major circulating strain in Southeast Asia (220, 221).

The CT of the gp41 subunit also influences the overall Env conformation, whereby substitutions or deletion of this domain increases exposure of epitopes that are normally hidden in the 'closed' conformation (222, 223). Some studies have described the effect of cholesterol, that is highly concentrated in lipid microdomains, on the conformation of Env trimers (224). By depleting cholesterol using either beta-cyclodextrins or mutating the LWYIK motif, a decrease in the conformational stability of Env is observed (225). In addition to cholesterol,

the removal of sphingolipids also significantly reduces viral production and infectivity (226, 227).

CD4 mimetic compounds (CD4mc) are small molecules that can bind within the Phe43 cavity of the gp120 subunit and have multifunctional properties, including neutralizing virions and can also enhance the neutralizing activity of otherwise non-neutralizing antibodies (nNAbs) (228-231). They can strongly induce conformational changes within the Env trimer to expose otherwise hidden highly conserved epitopes and promote elimination of infected cells by Fc-mediated effector functions (232). Additionally, these compounds also bind shed gp120 and thus, prevent the killing of HIV-1 uninfected bystander CD4+ T cells (180). Recent single molecule Förster resonance energy transfer (smFRET) microscopy studies have demonstrated an asymmetrical Env conformational State, State 2A, that can be induced with a combination of CD4mc, anti-cluster A antibodies, and anti-coreceptor binding site (CoRBS) antibodies (233).

1.2 HIV-1 pathogenesis

The transmission of HIV-1 results from direct contact with an infected individual's bodily fluids, including blood, vaginal fluids, pre-seminal fluids, semen, rectal fluids, and breast milk. The primary sources of transmission globally include unprotected sexual intercourse and the virus is transmitted through the genital tract or the rectal mucosa. Other forms of transmission include mother-to-child transmission during pregnancy and breastfeeding, blood transfusions, and the sharing of needles/syringes (234). Although the inoculum during transmission by any of these forms contains a mixture of genetically diverse HIV quasispecies, the initiation of infection usually begins from a single virus called the transmitted founder virus (T/F) (235, 236). These viruses have generally found to exhibit CCR5 tropism, have increased infectivity and replication capacities, harbour higher Env content, infect primarly CD4+ T cells, and are resistant to type I Interferons (IFN) (237, 238). Once infection is established, the clinical course of HIV infection can be described in three main stages: acute/early phase, chronic phase, and progression to AIDS (Figure 1.6).

1.2.1 Stages of infection

The acute/early phase (also known as primary infection) lasts a few weeks following exposure to the virus. The virus begins actively multiplying and plasma RNA levels reach a peak of several million copies per ml and in conjunction, there is a loss of CD4+ T cells in the blood and lymphoid tissues due to viral induced cell death (239, 240). More specifically, there is a significant depletion in peripheral and gut-associated lymphoid tissue (GALT) CD4+ T cells(241). Primary infection triggers the release of pro-inflammatory cytokines and during this phase, the latent reservoir is also established (242). The reservoir is maintained within memory CD4+ T cells, and are not considered to be productively infected; thus, are not targeted by ART (243).

This is followed by an asymptomatic chronic phase (also known as latency) in infected individuals. Without any treatment, this stage of disease progression could be short (3-5 years) or long (10-20 years) since this phase is characterized by relatively stable plasma viremia.

Meanwhile, there is also a continuous and gradual depletion of both infected and uninfected CD4+ T cells (244, 245).

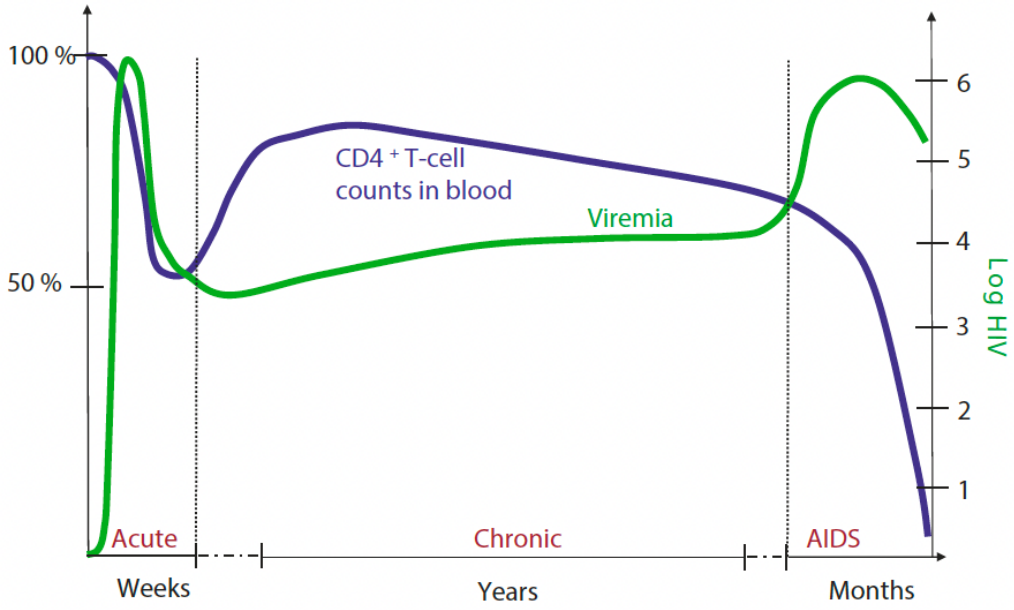

Figure 1.6 Stages of HIV-1 infection. Overall infection can be clinically described as acute, chronic, and AIDS. Changes in CD4 + T cell numbers and in viremia level over the course of infection are shown schematically. During the acute phase, viremia peaks and CD4 + cell counts decline. Infected individuals without ART progress to AIDS, with an accelerated CD4+ T cell loss and increase in viremia. Figure adapted from (246) with authorization by the Nature Publishing Group.

Although selective CD4+ T cell depletion is a hallmark of HIV infection and progression to AIDS, several infected cells with integrated proviral DNA survive. Different mechanisms can contribute to the depletion of CD4+ T cells, including direct cytopathic effects of the virus via syncytia formation, cell-cell fusion, and single cell swelling. Productively infected cells can undergo apoptosis via activation of caspase-3 or be killed by NK cells and HIV-specific CD8+ T cells (247-249). However, CD4+ T cell depletion is not only limited to infected cells. Viral proteins Tat, Vpr, Vpu, Nef, and soluble gp120 are released into circulation and can induce apoptosis in uninfected cells through surface-receptor binding (soluble gp120) or via cellular uptake (250, 251). Moreover, uninfected bystander CD4+ cells that have shed soluble gp120 bound to CD4 could potentially be destroyed by CD4i antibodies that can bind and mediate effector functions (180).

The development of opportunistic infections because of an immune system breakdown (*i.e.,* T cell depletion) eventually leads to the death of infected individuals. Thus, clinically, an HIV-infected individual can be defined as having AIDS when the CD4+ T cell count is lower than 200 cells/μl or if AIDS-defining conditions occur (252). Some of these conditions include candidiasis, Kaposi's sarcoma, cytomegalovirus retinitis, pneumonia, among others.

A subset of HIV-infected individuals called long-term non-progresses (LTNPs) maintain stable CD4+ T-cells and low plasma viremia without ART. There are also a minority of infected individuals, called viremic/elite controllers, that suppress viremia to undetectable levels, preserve their CD4+ T cell counts, and can go decades without ART and without progressing to AIDS (253). One of the major contributors to differences in disease progression are HIV-specific CD8+ T cell responses, where certain HLA haplotypes are associated with better viral control (254).

1.2.2 Antiretroviral therapies

In 1987, the first antiretroviral drug, zidovudine (azidothymidine or AZT), a nucleoside reverse transcriptase inhibitor (NRTI), that correlated with decreased mortality and frequency of opportunistic infections, was approved for treatment (255). However, using one drug alone could not be maintained due to the development of resistant strains (256). A better understanding of HIV biology aided the discovery of at least 28 other antiretroviral drugs belonging to different classes that target various stages of the replication cycle, including CCR5 inhibitors, fusion inhibitors, non-nucleoside reverse transcriptase inhibitors (NNRTIs), integrase strand transfer inhibitors (INSTIs), and protease inhibitors (257). Dual, and then later, triple, drug combination therapies from at least two different drug classes were established and this is now the approved standard care for HIV infection. Despite the tremendous success of ART, HIV persists in latently infected CD4+ T cells in infected individuals and lifelong therapy is required to avoid viral rebound (258, 259). However, lifelong therapy necessitates strict drug adherence and patients can endure undesired drug side effects.

1.2.3 HIV-1 vaccine strategies

A successful preventative vaccine remains elusive and to date, six vaccine candidates have completed efficacy trials; out of which only the RV144 trial demonstrated a modest efficacy of 31.2% in a three-year follow-up (260). The first two trials (VAX003 and VAX004), aimed to induce antibodies against a monomeric gp120 antigen. However, they failed to induce antibodies capable of neutralizing a wide range of HIV-1 variants (*i.e.,* broadly neutralizing antibodies [bNAbs]) and protect against HIV-1 acquisition (261). Subsequently, the STEP and Phambili trials tested recombinant adenovirus vectors (rAd5) encoding viral Gag, Pol, and Nef proteins to assess whether protection could be achieved by inducing cellular immunity. These trials demonstrated no overall protection and vaccinees in the STEP trial with pre-existing immunity to Ad5 had increased rates of HIV-1 infection (262, 263).

In 2009, the RV144 'Thai trail' of a prime with a recombinant canarypox vector (ALVAC vCP205) expressing *env*, *gag,* and *pol* genes and boost with recombinant gp120 provided the first clinical evidence of efficacy for any HIV-1 vaccine. This trial demonstrated 60.5% efficacy in the first year that waned to 31.2% three years postvaccination. The immune correlates of protection analyzed were mainly V1/V2-specific immunoglobulin (Ig)G responses, non-neutralizing IgG antibodies that mediated increased ADCC activity in the participants with decreased IgA responses, and stimulation of CD8+ T cells (260, 264).

More recently, the HIV Vaccine Trials Network 505 (HVTN 505) trial aimed to elicit both humoral and cellular responses by priming with DNA plasmids encoding for Gag, Pol, Nef, and Env proteins, followed by a boost with rAd5 encoding a Gag-Pol fusion and Env protein; however, this trial demonstrated no efficacy (265). The HVTN 702 'Uhambo trial', based on the RV144 trial with ALVAC expressing a subtype C Env and followed by a boost with subtype C gp120, was recently stopped in 2020 after an interim analysis found no prevention of infection (266). Another similar clinical trial, the HVTN 705 'Imbokodo trial', also reported no significant reduction in acquisition risk in August 2021. Currently, there are two ongoing HIV vaccine efficacy trials, Mosaico and PrEPVacc, that are evaluating the induction of Abs

and cellular responses, along with combining PreP in the latter strategy. Additionally, novel 'germline targeting' approaches aim to directly stimulate naïve B cells that encode for precursors to certain bNAbs (IAVI G001 and G002).

The challenges in developing a successful vaccine are mainly due to the variability of the virus, particularly Env, as well as in conclusively identifying the immune correlates of protection. If a vaccine can stimulate the production of cross-reactive bNAbs that can neutralize diverse strains of HIV-1 from multiple subtypes, it could likely confer protection against infection.

1.2.4 HIV-1 cure strategies

In broad terms, either a complete eradication of the latent reservoir (sterilizing cure) or a long-term control of viral replication in the absence of ART (functional cure) are required to achieve an HIV cure (267). As of 2021, only two individuals have been cured from HIV-1: the 'Berlin patient' and the 'London patient' (268, 269). They both developed acute myeloid leukaemia and were treated with allogeneic haematopoietic stem-cell transplantation using donors with a homozygous CCR5 (CCR5Δ32/Δ32) mutation whichresults in CD4+ T cellresistance to infection by R-tropic strains. ART was interrupted months after the transplantation and both individuals were in remission with undetectable plasma viral load. However, this treatment is not a viable option for all infected individuals without leukemia, given the high-risk complications during stem-cell transplantation. Moreover, some transplant patients suffer an eventual viral rebound with minority X-tropic strains (270).

Recent alternate cure strategies are trying to harness two different ideologies: the 'shock/kick and kill' and 'block and lock' strategies. The 'shock and kill' strategy aims to reactivate the provirus from its latent state using latency-reversing agents (LRAs), while ART prevents further rounds of replication. Examples of LRAs include histone deacetylase inhibitors and protein kinase C agonists (271, 272). The cellular reservoir is then cleared by immune system. The 'block and lock' strategy aims to transcriptionally silence HIV-1 by locking the promoter in deep latency using latency-promoting agents (LPAs). Examples of LPAs include Tat inhibitors and kinase inhibitors (273, 274). By boosting viral latency and making it irreversible, it could be possible to stop ART without viral rebound and establish a prolonged drug-free

remission. The early initiation of ART has also been linked to the reduced size of the viral reservoir and longer durations of undectable viral loads upon ART interruption (also known as post-treatment controllers [PTCs]). This was observed with patients of the Viro-Immunologic Sustained Control after Treatment Interruption (VISCONTI) cohort (275) and the 'Mississippi baby'; however, viral rebound still eventually reoccurred in the latter (276).

As will be further discussed in Section 1.3.2, the passive administration of neutralizing antibodies is also being tested in both animal studies and human clinical trials. Recent studies have demonstrated the potential of CD4mc in both therapeutic contexts and protection from transmission. Using macaques immunized with recombinant gp120, CD4mc was protective from multiple challenges with a heterologous simian-human immunodeficiency virus (SHIV) (277). SHIVs are chimeric viruses using SIV as a backbone and introducing Env from a particular HIV isolate, thus, are representative of a more relevant virus to use for non-human primates (NHP) studies (278). Additionally, using a humanized mice model, treatment with CD4mc in combination with CD4i-Abs significantly decreased HIV-1 replication, the viral reservoir, and viral rebound after ART interruption (279).

1.3 Humoral immune responses against HIV-1 infection

As mentioned earlier, the unliganded native Env represents the main antigenic target of neutralizing antibodies. Following infection, Env-specific antibodies are detectable during the acute phase, *i.e.*, during the first two to three weeks post infection. This initial antibody response is IgM antibodies directed against gp41 of the T/F strain (280). In the following weeks, class-switched IgA and IgG responses can be detected, which are also directed against viral proteins Gag or the V3 of gp120. However, these antibodies do not harbour potent neutralization capacities and do not impact the plasma viral load or exert much selective immune pressure on the Env. Neutralizing antibodies only against autologous viral strains are detectable two to three months post-infection, which mainly target the variable regions (V1V2 and the V3 loop) of Env (281), and these lead to the selection of escape mutants (282). In a subset of chronically infected individuals, cross-reactive neutralizing antibodies that target epitopes conserved across multiple strains can be produced upon persistent viral stimulation, and these are known as bNAbs (283).

1.3.1 IgG structure

Ig antibodies carry out a multitude of preventative and therapeutic antiviral activities and are symmetrically composed of two light (κ, λ) and heavy chains (μ, α, γ, δ, ε) that determines the overall class of the antibody. . The heavy and light chains of IgG are linked together via disulfide bonds and can be divided into two main functional units: antigen binding fragment (Fab) and crystallizable fragment (Fc) (Figure 1.7). The Fab fragment consists of the highly variable, genetically mutated regions of the heavy and light chains; each of the variable domains is composed of complementarity-determining regions (CDRs), which interact with an antigen and define the epitope specificity of the antibody. The Fc fragment, consists of half of the heavy chain and is composed of a set sequence and structure determining the isotype and effector functionality of the antibody, and in the case of IgG molecules: the subclass (IgG1, IgG2, IgG3, or IgG4). Thus, the functions of IgG can be classified into Fab- and Fc-mediated, wherein they can either neutralize viral particles via their Fab domains and interact with innate immune receptors, such as crystallizable fragment-gamma receptors (FcγRs), via their Fc domains (284).

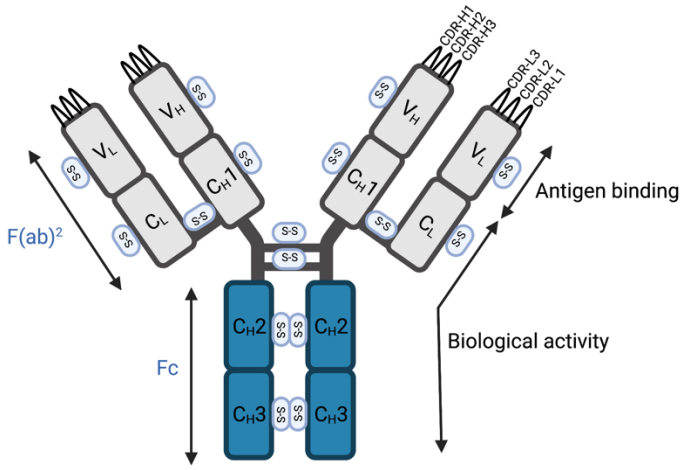

Figure 1.7 Structure of IgG. 150 kDa IgG molecule composed of two identical 50 kDa heavy (H) chains, and two identical 25 kDa light (L) chains, which are linked by disulfide bridges. CDR: complementarity-determining regions. Diagram created with BioRender.com.

1.3.2 Neutralizing response

NAbs against HIV target relatively conserved epitopes on the glycosylated Env trimer and harbour neutralization capacities against heterologous viral strains and therefore, can block viral entry by either preventing receptor/coreceptor binding or by preventing Env conformational changes (285, 286). BNAbs can neutralize majority of strains from diverse clades representing global circulating HIV-1. Notably, bNAbs can broadly be classified based on six distinct epitopes they target on the Env trimer: CD4bs, V2 apex, V3 glycan region, silent face, MPER, and the interface between gp120 and gp41(Figure 1.8) (287). As Env is heavily glycosylated, bNAbs target primarily glycan-dependent epitopes (288). Measurements of bNAb potency and breadth are traditionally determined *in vitro* by the concentration of antibody that inhibits either 50% (IC_{50}) or 80% (IC_{80}) of a fixed virus inoculum in a dose-response single-cycle infection assay.

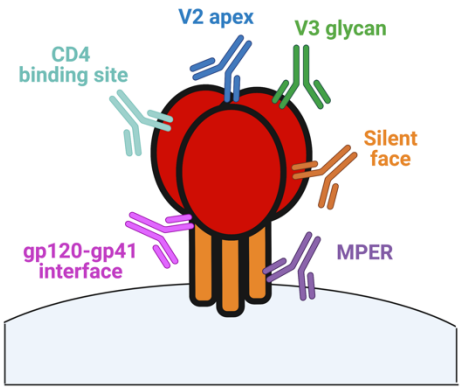

Figure 1.8 Epitopes recognized by bNAbs. Cartoon representation of the 'closed' Env trimer composed of three gp120 (red) and three gp41 subunits (orange). Antibodies targeting six distinct epitope regions on the trimer are presented. Diagram created with BioRender.com.

The production of bNAbs with very high breadth and potency can be found in less than 10% of infected individuals with persistent infection (289). Initially, naïve B cells recognize epitopes on the T/F or early autologous viral strains for the induction of the initial antibody response. Upon the selection of antibody-escape mutations, the humoral response adapts to the emergent diverse strains. A repeated evolution and co-evolution process between the viral strains and B cell specificities aids in the development of increased breadth of antibodies. With a high level of antigen exposure during persistent infection, bNAb lineages with unusually high levels of somatic hypermutation (SHM) including insertions, deletions, and long heavy chain CDRs, due to multiple rounds of affinity maturation, are formed (290).

When produced as monoclonals, the passive administration of bNAbs can protect against infection, as seen in animal model studieswith NHPs and humanized mice, as well as when used in a therapeutic context (291-294). Antibodies against the CD4bs, such as VRC01, 3BNC117, and VRC07, as well as antibodies targeting the V3 glycan region, such as 10-1074 and PGT121, have been tested in humans (295-299). Studies infusing bNAbs to infected participants showed rapid decreases in the plasma viral loads (296, 297). However, full viral suppression was only observed in a minority of study participants infected with bNAb-sensitive viruses, and the plasma viral load rebounded after a few weeks due to the

development of escape mutations. Conseqeuently, administration of a single bNAb only allows for a transient reduction of the plasma viral load before viral escape and increased viremia. As the understanding that viral escape can be avoided by combining multiple ART regimens targeting different steps of the viral replication cycle, a combination of multiple bNAbs targeting nonoverlapping epitopes on the Env trimer has also been utilized to prolong viral suppression (300). Thus, to overcome the generation of escape mutants, administering a combination of two bNAbs (3BNC117 and 10-1074) to viremic individuals infected with viruses sensitive to both bNAbs was attempted; this study demonstrated a reduction of viral load that was longer when compared to single bNAb-treatment (301).

Of note, two recent Antibody Mediated Prevention trials (HVTN704/HVTN085 and HVTN703/HPTN081), were conducted to determine whether VRC01 can prevent HIV-1 acquisition (302). Despite their lack of efficacy, analysis showed that protective capacity of passive immunization was limited only against highly sensitive viruses as well as serum neutralization titers. Currently ongoing clinical trials are evaluating combinatory bNAb transfusions to protect from HIV acquisition in vulnerable populations and are also evaluating the antiviral functions of bNAbs in viremic individuals (ClinicalTrials.gov Identifier: NCT04340596, NCT04319367, NCT03721510, NCT04811040, NCT03837756, and NCT04357821 to name a few).

1.3.3 Non-neutralizing response

During natural infection, majority of the elicited antibodies target Env sampling its State 2/3 conformations, and therefore exhibit little or no neutralizing activity against primary strains of HIV-1 harbouring ‘closed’ Env trimers(303, 304). Thus, these nNAbs are elicited upon the exposure of immunodominant epitopes via multiple mechanisms, including improper Env processing and shed soluble gp120.

As discussed, the antibody’s Fab domain is a major determinant of its neutralizing capacity, whereas the Fc domain of the antibody directly modulates Fc-mediated effector functions, including ADCC. These have been shown to be key for potent neutralizing antibodies targeting

the Env trimer, as well as functional nNAbs (305, 306). The importance of the Fc-mediated effector functions *in vivo* was first shown by Hessell *et al.*, where the passive administration of the antibody b12 (targeting the CD4bs) protected macaques against SHIV challenges, when compared with Fc-compromised b12 LALA (L234A/L235A) that resulted in a partial loss of protection (307). Many studies in the field have associated ADCC with the prevention of HIV acquisition and slow disease progression in human studies as well as with NHP and humanized mice (307-309). The levels of passively acquired ADCC-inducing antibodies have been associated with decreased acquisition and mortality in infected infants born from HIV-positive mothers, thus supporting the importance of ADCC-mediating antibodies in controlling HIV infection (310, 311). Furthermore, studies highlighting a role of ADCC-competent Abs in protection from HIV in vaccination (260), passive transfer (307), and natural viral control (312), support the development of a two-pronged vaccinal approach to induce Abs harbouring neutralization as well as strong effector functionalities.

As mentioned, the epitopes of most nNAbs are usually hidden in the 'closed' trimeric Env. Thus , the interaction of Env with CD4 exposes these CD4i epitopes (Figure 1.9) and some readily elicited antibodies recognize the CoRBS, V3 loop, or the gp41 subunit. More specifically, one family named the anti-cluster A antibodies, have been described to be potent ADCC mediators against HIV-1-infected cells when Env samples its CD4i conformation (313). Anti-cluster A Abs target the interface of layer 1 and 2 located the gp120 inner domain (composed of seven-stranded β-sandwich, layers 1 and 2, and N and C termini) (176, 314). CD4i epitopes can be exposed on the surface of cells infected with viruses defective for Nef and Vpu proteins and upon the binding of shed gp120 to CD4 on uninfected cells (306, 315). Furthermore, CD4mc which bind within the Phe-43 cavity of Env, leads to thermodynamic changes within the trimer similar, but not identical, to those induced by CD4 (233). Table 1.1 lists all the anti-Env antibodies used in this thesis along with their Env conformational preference.

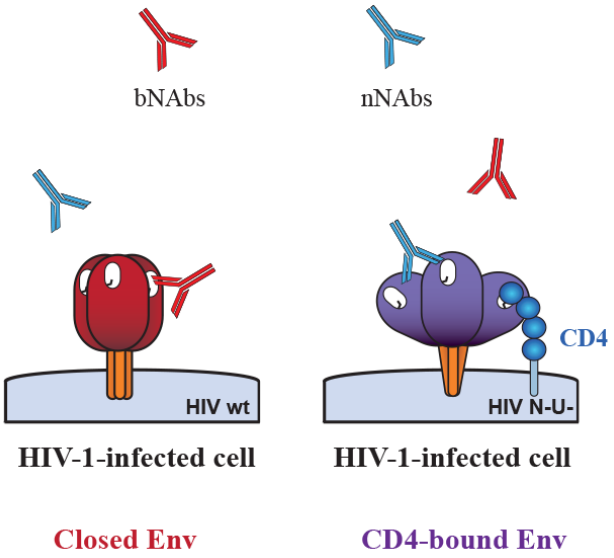

Figure 1.9 Env conformations recognized by bNAbs and nNAbs. The 'closed' State 1 trimer is preferentially bound by bNAbs and Env sampling the 'open' CD4-bound conformation is preferentially bound by nNAbs. N-U-: Nef and Vpu defective virus. Figure adapted from (306) with authorization from Elsevier.

Table 1.1 Characteristics of Abs used in this thesis

Epitope	Antibody	Conformation preference
V2 apex	PG9	Closed
V3-glycan	2G12	Independent
	PGT121	Closed
	PGT126	Closed
gp120-gp41 interface	PGT151	Intermediate
Cluster A	A32	CD4-bound/Open
	N5i5	CD4-bound/Open
CoRBS	17b	CD4-bound/Open
	N12i2	CD4-bound/Open
V3 loop	19b	CD4-bound/Open

1.3.4 Fc-mediated antibody functions and Fc receptors

The diverse Fc-mediated mechanisms to eliminate targets exposing vulnerable antigens include antibody-dependent cellular cytotoxicity (ADCC), antibody-dependent complement-mediated lysis (ADCML), and antibody-dependent cellular phagocytosis (ADCP) (Figure 1.10).

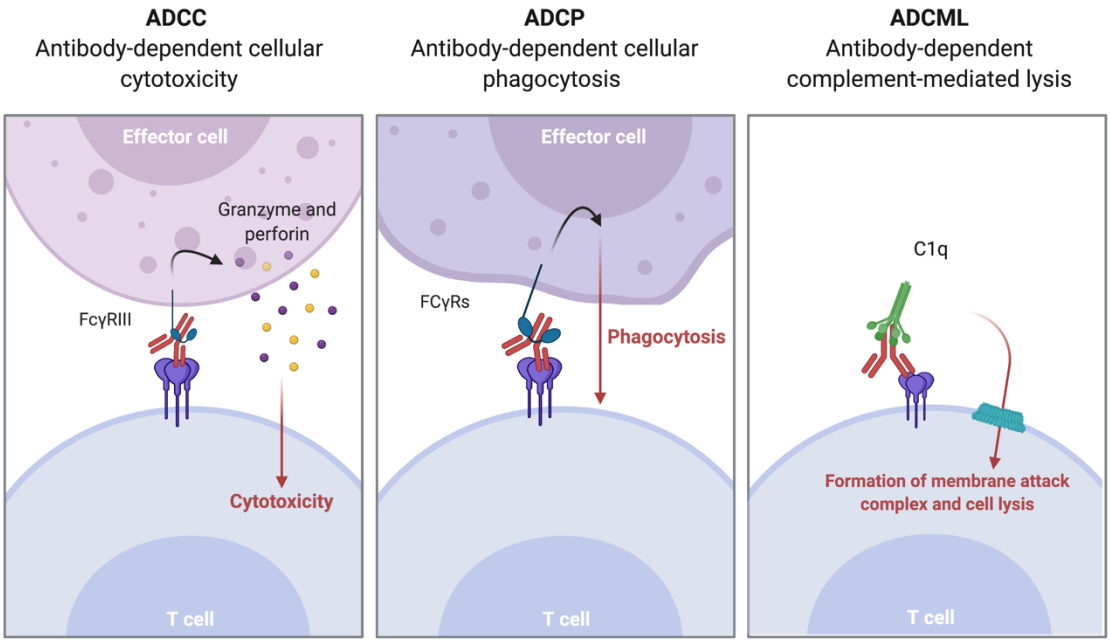

Figure 1.10 Fc-mediated effector functions. Schematic representation of processes antibody-dependent complement-mediated lysis (ADCML), antibody-dependent cellular cytotoxicity (ADCC), and antibody-dependent cellular phagocytosis (ADCP) mediated by Fc domain of IgG. Diagram created with BioRender.com.

These mechanisms are mediated via the Fc receptors (FcRs), which are a family of cell surface receptors that also specifically bind to the Fc portion of antibodies. There are two classes of FcRs that are functionally diverse: the activation and the inhibitory receptors, which transmit their signals via immunoreceptor tyrosine-based activation (ITAM) or inhibitory (ITIM) motifs, respectively. Human leukocytes express three main types of FcRs: FcγR (binds to IgG), FcεR (binds to IgE) and FcαR (binds to IgA). There are five IgG Fc receptors, which are the activatory FcγRI (CD64), FcγRIIa (CD32a), FcγRIIc (CD32c), FcγRIIIa (CD16a), FcγRIIIb (CD16b), and the inhibitory FcγRIIb (CD32b) (Figure 1.11); each of which have different cellular expression patterns and functions in the immune response (316, 317). Except for FcγRI, FcγRs are of low affinity for IgG and do not engage monomeric IgG at physiological conditions. These receptors require multimeric immune complexes for engagement and to trigger receptor cross-linking and subsequent cellular responses (318). The functional assays used in this thesis focus on effector cell activation via FcγRIIIa (CD16a), with it being expressed on NK cells, monocytes, and macrophages. Furthermore, FcγRIIIa binds IgG subclasses relatively differently, with higher affinities for IgG3 and IgG1 than IgG2 or IgG4

(319). The neonatal Fc receptor (FcRn), expressed on endothelial cells and circulating monocytes, is involved in IgG transport and recycling and prevents the intracellular degradation of antibodies (320).

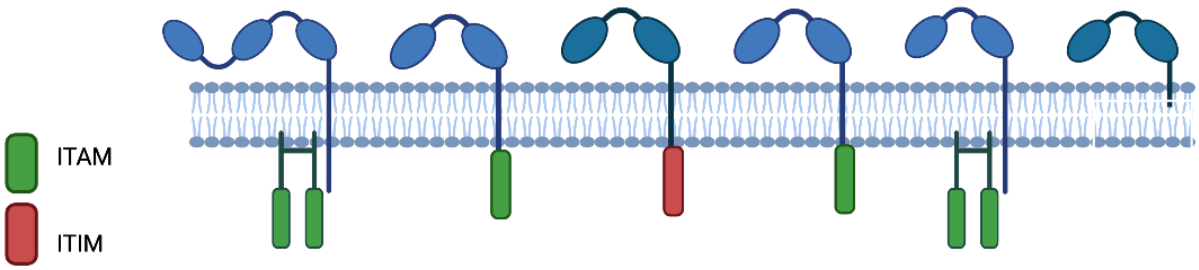

	FcγRI (CD64)	FcγRIIa (CD32a)	FcγRIIb (CD32b)	FcγRIIc (CD32c)	FcγRIIIa (CD16a)	FcγRIIIb (CD16b)
B cell	-	-	+	-	-	-
T cell	-	-	-	-	-	-
NK cell	-	-	-	(+)*	+	-
Monocyte	+	+	+	(+)*	+/-	-
Macrophage	+/-	+	+	-	+/-	-
Neutrophil	(+)	+	+	(+)*	-	+

Figure 1.11 Human Fc gamma receptors (FcγRs) and their leukocyte expression patterns. Schematic representation of activatory FcγRI (CD64), FcγRIIa (CD32a), FcγRIIc (CD32c), FcγRIIIa (CD16a), FcγRIIIb (CD16b), and inhibitory FcγRIIb (CD32b). +, constitutive expression; –, no expression; (+) inducible expression, (+) *, expression depends on *FCGR2C* allelic status. Diagram created with BioRender.com.

ADCC is mediated by effector cells, such as natural killer (NK) cells, neutrophils, macrophages, andmonocytes to eliminate virally infected cells (317). In humans, this response is initiated by the Fc regions of IgG1 or IgG3 subtypes that bind the activating FcγRIIIa (CD16a) receptor on effector cells (321). In addition to recognition via stress markers that are expressed on the surface on infected cells, NK cells can be activated via the Fc region of IgG that interacts with the FcγRIIIa. This is followed by clustering and cross-linking of FcγRs by immune complexes and intracellular signalling pathways are initiated via tyrosine phosphorylation of ITAM motifs. This in turn leads to the activation of kinases of the SYK and SRC family, as well as activation of the protein kinase C (PKC) pathway, resulting in a rapid increase in intracellular Ca^{2+} levels. Effector cellular activation is associated with activation of specific transcription factors that drive the expression and release of pro-inflammatory cytokines and chemokines, including interferon gamma (IFN-γ), tumor necrosis

factor (TNF), and β-chemokines that inhibit viral spread (322-324). Activation is also associated with the release of cytotoxic secretory granules (CD107a+) that traffic to the immunological synapse. More specifically, NK cells release perforin and granzyme proteins into the synaptic cleft (325, 326). Perforin is a pore-forming protein and granzyme B causes DNA fragmentation and apoptosis of the target cell (327).

ADCP is carried out by monocytes, macrophages, neutrophils, eosinophils and dendritic cells. These phagocytes can be engaged by either complement receptors or FcγRs, including FcγRIIa (CD32a) and FcγRI (CD64) (328, 329). In addition to clearing antibody-opsonized targets, phagocytosis and signalling via FcγRs also lead to the secretion of antiviral cytokines (330). ADCML is mediated by a multivalent interaction of the IgG Fc with the complement protein C1q to drive direct cytotoxicity, as well as other immunoregulatory functions involving enhancement of phagocytosis and stimulation of antigen-presenting cells (331, 332).

1.3.4.1 Modulation of Fc-mediated antibody functions

Numerous factors govern the magnitude of antibody-mediated effector functions against infected cells, which depend on the ability of immune complex formation and the efficiency with which effector cells are activated. The degree of antibody binding to antigens correlates with ADCC susceptibility, with lack of or excess binding disrupting effector functions (333, 334). Furthermore, antigen binding per se does not always trigger ADCC responses (335, 336), because a threshold of sufficienct FcγR interactions needs to be met (*i.e.* clustering of FcγRs) to activate effector cells (337). Since the affinity of antibodies for the majority of FcγRs, including FcγRIIa and FcγRIIIa, is low and in the micromolar range, only multivalent antibody-antigen immune complexes can exert enough avidity to cluster them (317, 321, 328, 338). Similarly, the stoichiometry and the orientation of the antibodies bound to the antigen, which dictate the accessibility of Fc domains to FcγRs, appear to play an important role (339, 340).

Amino acid mutations within the Fc portion of Abs can impact their ability to engage with FcγRs. Some of these modifications include the LALA (L234A/L235A) and GRLR

(G236R/L328R) mutations to decrease FcγR binding or the GASDALIE (G236A/S239D/A330L/I332E) and AAA (S298A/E333A/K334A) mutations to increase FcγR binding (341-343). Other mutations in the Fc domain include the YTE (M252Y/S254T/T256E) and LS (M428L/N434S) substitutions to enhance interactions with FcRn and consequently, increase the serum half-life of antibodies and extend their therapeutic effect (344, 345);. In the context of passive transfer, these modifications could limit the number of administrations. Moreover, FcγRs are polymorphic, where certain alleles exhibit higher affinity for Fc than others. Single-nucleotide polymorphisms (SNPs) have been described to occur in FcγRIIIa at protein position 158 (change from valine to phenylalanine). Since these SNPs affect FcR expression and IgG binding, and thus, affect the overall functionality of effector cells, they influence the humoral response against HIV-1 (346, 347). Overall, the level, specificity, isotype, and subclass of antibodies are characteristics that dictate the balance between Fc-mediated protection and disease progression.

1.3.5 IgG Fc glycosylation

Besides amino acid substitutions, the Fc glycosylation profile of IgG proteins can also be modified to enhance or reduce functionality. Glycosylation is an enzymatic co- and post-translational modification that adds sugar molecules onto proteins needed for their folding, stability, and functionality. More specifically, N-linked glycosylation involves the attachment of a carbohydrate molecule to the amide nitrogen of asparagine (N) (348). Every IgG Fc is glycosylated with an *N*-linked glycan at a single point in each heavy chain at asparagine 297 in the C_H2 domain that is essential for its thermodynamic stability and regulates the efficiency of Fc-FcγR interactions (Figure 1.12) (349). The lack of an *N*-linked glycan at Asn297 results in a lack of Fc-effector function. During recombinant IgG production, the glycan composition can be altered by knocking in/out glycosidases in the medium of production (for example, plant cells), or via *in vitro* enzymatic digestions (350).

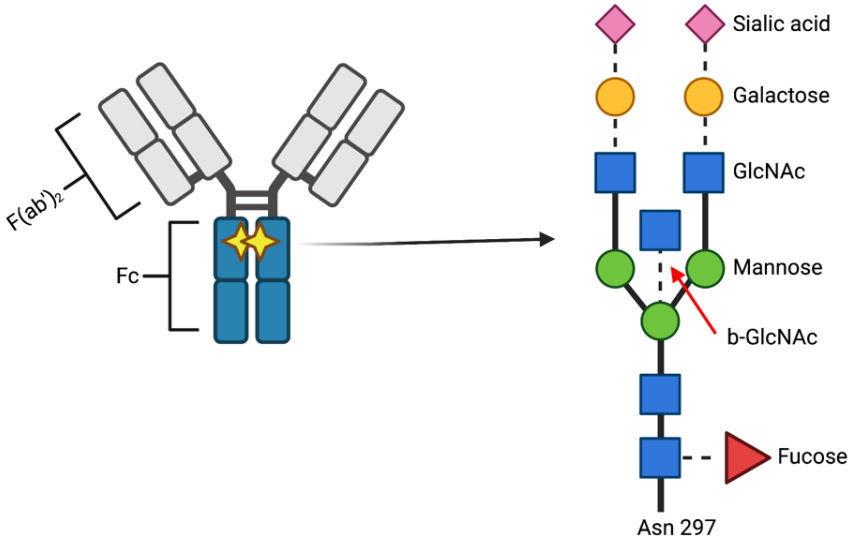

Figure 1.12 Structure of IgG and the IgG N-linked glycan. IgG proteins have a single N-linked glycosylation site at Asn297 of each heavy chain. The base glycan structure is pictured, with each of the four variably added glycan moieties presented with dotted lines. The largest possible IgG Fc N-linked glycan structure includes the fucose, bisecting GlcNAc (b-GlcNAc), galactose, and sialic acid moieties. Diagram created with BioRender.com.

Antibody *N*-linked glycans are sugar subunits including N-Acetylglucosamine (GlcNAc), mannose (Man), galactose (Gal), N-Acetylneuraminic acid (Neu5Ac), and fucose (Fuc). The process of *N*-glycosylation in eukaryotes takes place in the secretory pathway in the ER and is modified in the Golgi apparatus as enzymes called glycosyltransferases catalyze the addition and modification of these sugar subunits. The linkages between the sugars can occur in two major types, α and β, depending on stereochemistry. The glycan precursors are initially synthesized and linked to a dolichol molecule. As the antibody is synthesized in the ER, the glycan precursor, $Glc_3Man_9GlcNAc_2$, is attached to Asn297 by oligosaccharyltransferases. As the antibody traffics through the Golgi, the glycan is trimmed by glycosidases to have a core glycan composed of two GlcNAc molecules, and two additional Man antennae, each with a single GlcNAc attached (351, 352). This core glycan can be sequentially modified by the family of four glycosyltransferases: the fucosyltransferase enzymes that facilitate the addition of a core Fuc subunit (fucosylation), the galactosyltransferase enzymes that add one or two Gal molecules (galactosylation), the N-acetylglucosaminyltransferase enzymes that add a bisecting GlcNAc (b-GlcNAc; bisection), and the sialyltransferases enzymes that add one

sialic acid to each galactose subunit present (sialylation). Each glycan may or may not be modified by any of these specific glycosyltransferases, and thus, the presence or absence of these sugar subunits allows for the generation of 36 possible types of glycoforms. In humans, there exist up to 144 possible IgG glycan and subtype combinations, due to the presence of a terminal galactose, fucose, GlcNAc, or sialic acid. These glycans have been shown to influence the binding to FcγRs on effector cells and, consequently, alter antibody functionality (353).

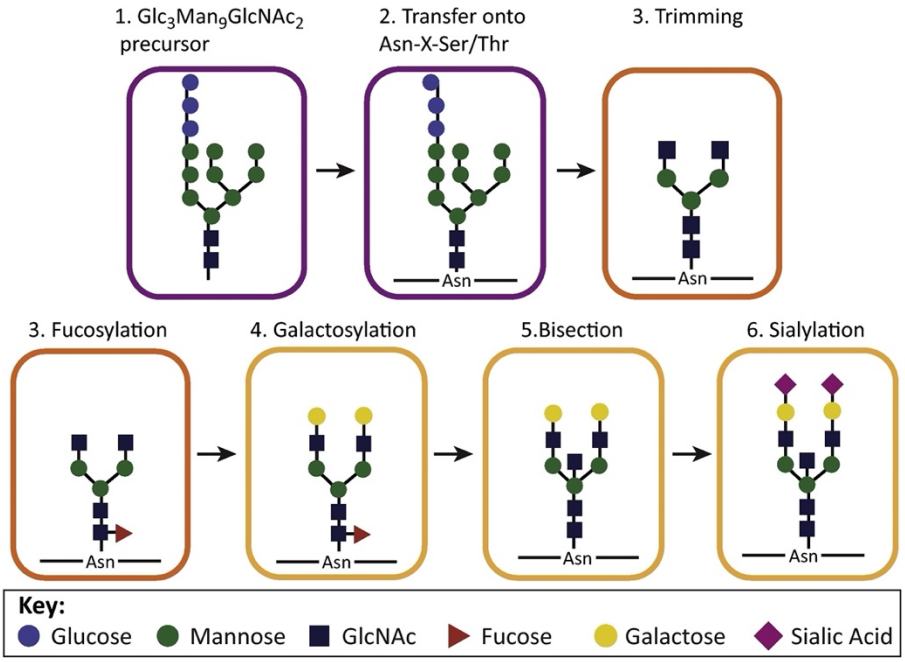

Figure 1.13 Sequential Processing of the Fc Glycan. The glycan precursor, $Glc_3Man_9GlcNAc_2$, is transferred onto the antibody in the ER (purple box). Upon entry into the Golgi, glycosidases and glycosyltransferases trim and extend the glycan into a classical antibody biantennary structure. The glycan is first trimmed into the Glc_4Man_3 precursor within the *cis* and medial Golgi (orange box). Then it is sequentially extended by four glycosyltransferases: (i) fucosyltransferases adds a fucose within the medial Golgi, and inside the *trans* Golgi (yellow box) (ii) galactosyltransferases adds one or two galactose molecules, (iii) N-acetylglucosaminyltransferases adds the b-GlcNAc, and (iv) sialyltransferases adds one or two sialic acids. Figure adapted from (353) with authorization from Elsevier.

1.3.5.1 IgG Fc glycosylation and Fc-mediated functionality

The Fc glycan structures affects binding to FcγRIIIa and FcγRIIIb through a glycan-glycan interaction, due to a unique glycan found in these human FcRs at position 162 that interacts

directly with the Fc-glycan within the IgG-Fc cavity (354). One of the most studied IgG glycan modification is that of the core Fuc. The absence of the core Fuc increases the affinity of FcγRIIIa more than 50-fold (355) and thus, the ADCC activity that can be modulated significantly (356). The presence of Fuc interferes with the glycan-glycan interaction between FcγRIIIa and the Fc region and thus, causes a steric hindrance and significantly reduces ADCC (357, 358). Thus, fucosyltransferase knockout cell lines are used to produce therapeutic monoclonal antibodies with optimized ADCC activity (359). Moreover, the process of bisection can also sterically hinder the addition of a Fuc moiety and thus, enhance ADCC activities (357, 360). Galactosylation has also been shown to enhance FcγRIIIa binding and modestly enhance ADCC *in vitro* (361-363). Lastly, preliminary evidence points towards sialylated IgGs having reduced binding to FcγRIIIa and enhanced anti-inflammatory activity (364-366).

In the context of HIV-1, studies have reported significant differences in the IgG glycosylation profiles depending on the disease status of HIV-1-infected individuals. Generally, infected individuals have more afucosylated, agalactosylated, and asialylated antibodies (367, 368). With respect to disease status, studies show that elite controllers harbour more afucosylated and fewer sialylated glycoforms compared to progressors (369). Additionally, afucosylated and galactosylated antibodies were shown to negatively correlate with levels of cell-associated HIV DNA and RNA in ART treated individuals (368).

1.3.5.2 Modulation of IgG Fc glycosylation

The production of monoclonal antibodies using plant-based systems is a promising recombinant protein production platform due to their low upstream production costs, high-yield, speed, and safety (370). Plant species utilized for protein production include the tobacco plant *Nicotiana benthamiana*. Current research to enhance the therapeutic activity of IgG and antibody-mediated effector functions against viral infections is focused on engineering the Fc-glycosylation status. Thus, using *N. benthamiana* to customize the *N*-glycans of IgG proteins harbours many advantageous traits, including its fast growth rate and its ability to express heterologous gene sequences (371).

Over the years, many parameters have been optimized to improve the efficiency with which *N. benthamiana* can transiently express recombinant proteins, involving a vacuum infiltration of its tissue with agrobacteria that harbour a DNA transgene for the protein of interest. Typical plant N-glycans consist of xylose and core fucose residues that are added by xylosyltransferases and fucosyltransferases, respectively. These plant-specific sugar residues have been reported to cause allergic responses in human (372). Consequently, current plant-based production systems have been optimized to bypass the addition of these undesired glycans by utilizing *N. benthamiana* plants that are knock out for xylosyltransferases and fucosyltransferases (373). Furthermore, mammalian glycoenzymes can be glycoengineered into *N. benthamiana* plant lines to produce proteins harbouring the appropriate *N*-glycosylation profile. This includes a transient expression of the mammalian fucosyltransferases, glactosyltransferases, and *N*-acetylglucosaminyltransferases (374). More importantly, *N. benthamiana* can generate proteins with homogenous *N*-glycosylation, promoting a profile consistency of IgG production.

Antibody glycoengineering has been exploited to improve the efficacy of bNAb-FcγR interactions against HIV-1-infected cells. This was accomplished using a 2G12 glycoform lacking the core fucose and plant-specific xylose to enhance antibody-dependent cell-mediated virus inhibition against HIV-1, along with significantly enhanced FcγRIIIa binding (375). Similar modifications were carried out for the bNAbs VRC01 and PG9, where the fucose- and xylose-free glycoforms had significantly higher affinities to form stable complexes with FcγRs and induce significantly higher ADCC against infected cells, respectively (376, 377).

1.3.6 Viral mechanisms to evade antibody recognition

As explained, since the HIV-1 Env trimer is the only viral antigen exposed on the surface of viral particles and infected cells, it represents the sole target of humoral immune responses and facilitates the generation of neutralizing and non-neutralizing antibodies. This imposes selective pressure on the HIV-1 Env, leading to the evolution of several features that diminish recognition by antibodies and elimination of infected cells. These include Env trimers

harbouring a high degree of glycosylation with *N*-linked carbohydrates and its constitutive internalization.

In the context of infection, the importance of Fc-mediated effector responses, particularly ADCC, has been extensively characterized in recent years (305). Nonetheless, HIV-1 has also evolved several mechanisms of immune evasion, and specifically the functional activities of certain accessory proteins and the structural features of Env that have been shown to reduce the susceptibility of infected cells to ADCC. As briefly mentioned, Vpu down modulates the restriction factor BST-2 that otherwise inhibits virion release at the surface of infected cells. Thus, abrogating the interaction of Vpu with BST-2 and when using viruses defective for Vpu, there is an increased accumulation of virions on the infected cell surface, increased sensitivity to opsonization, and elimination by Fc-mediated effector mechanisms (315, 378, 379). Moreover, downmodulating the CD4 receptor by Nef and Vpu also protects infected cells by preventing the interaction of Env and CD4, and consequently, preventing the exposure of CD4i epitopes that are normally hidden in the 'closed' Env trimer (315). Furthermore, Nef also downregulates the expression of NKG2D ligands, interfering with NK cell activation (124, 380).

It is now well established that the interaction of gp120 with CD4 is critical for the exposure of highly conserved epitopes (315, 378). Importantly, CD4i ADCC-mediating antibodies are naturally present in the sera of HIV-infected individuals, and HIV-1 has evolved to protect infected cells from antibody binding (306, 381). Thus, binding of shed gp120 to CD4 receptors on uninfected CD4+ T cells redirects ADCC responses away from the productively infected cells to bystander cells. This phenomenon results in the elimination of uninfected bystander cells. The *in vivo* effects of shed gp120 binding to the surface of bystander lymphocytes have been suggested to serve as effective targets that contribute to decreased CD4+ T cell counts in HIV-1-infected individuals (180, 382). This mechanism could also be in place to redirect effector cell responses away from productively infected cells, perhaps to promote viral replication, and could be another immune evasion strategy.

1.4 Thesis Rationale and Objectives

Several different cellular and viral factors contribute to the efficacy of Fc-mediated effector responses against HIV-1-infected cells. The shedding of gp120 can redirect humoral immune responses from infected to uninfected cells, the conformation of Env modulates antibody binding, antibody-binding stochiometry, the affinity of antibodies for FcγRs, FcR polymorphisms, and the modulation of stress ligands by accessory proteins are just a few examples of an expanding number of parameters governing Fc-effector functions. With the available knowledge in the field of the classes of bNAbs and nNAbs and their varying specificities, the question of how their activities could be harnessed to efficiently eliminate infected cells remains to be fully answered. Firstly, a comprehensive understanding of underlying factors that modulate the Fc-effector functionalities of Env-specific Abs is required to improve their use as immunotherapeutic agents for HIV cure approaches. Thus, the overarching aim of the research presented in this thesis was to investigate three mechanisms by which ADCC responses to clear HIV-1-infected cells are altered. With a focus towards boosting the Fc-effector functionality of IgG, my research had three broad objectives:

1. *To determine the synergistic abilities of two families of antibodies targeting distinct epitopes on the Env trimer to kill infected cells by ADCC.*

CD4i antibodies, and more specifically, anti-cluster A antibodies target an epitope commonly detected by antibodies present in sera from HIV-1-infected individuals (378). Previous work from our group has shown that CD4-mimetics and the bivalent interaction of another class of CD4i antibodies, CoRBS Abs, are required to sensitize HIV-1-infected cells to ADCC-mediated by anti-cluster A antibodies (180). However, detailed knowledge about the requirement of both these CD4i antibodies to activate effector cells was unclear. In Chapter 2, we study the engagement of CD16a by these two CD4i antibodies targeting nonoverlapping epitopes via recombinant dimeric FcγRIIIa proteins and a functional *in vitro* ADCC assay.

2. *To understand the impact of Env internalization from the surface of infected cells on antibody-Env immune complex recognition by effector cells.*

Since HIV-1 Env undergoes constitutive endocytosis, this phenotype has been correlated with decreased Fc-effector responses against infected cells. However, Env endocytosis mediated by antibodies, as seen with other viruses, including the respiratory syncytial virus (RSV) (383), was not fully studied in the context of HIV-1. Thus, we evaluate the stability of certain Env-antibody immune complexes on the surface of infected cells, the fate of endocytosed complexes, and the effect on ADCC *in vitro* in Chapter 3. These observations are then expanded in Chapter 4 to understand the underlying mechanisms that are associated with antibody-mediated Env internalization.

3. *To improve ADCC against infected cells by modulating the glycosylation profile of bNAbs.*

Finally, in Chapter 5, we exploit the transient formation of immune complexes on the infected cell surface, by enhancing the capacity of the Fc domain of a bNAb to engage with FcγRIIIa. The role of IgG N-glycosylation in mediating effective functional responses is clear, so understanding the effects of modulating Fc glycosylation to clinically relevant antibodies, such as PGT121 (299), is a crucial step toward harnessing this system to control disease progression.

The results generated from these four studies could be applied towards improving antibody functionality against HIV-1-infected cells and eventually, the potential development of a functional HIV-1 cure as discussed in Chapter 6.

CHAPTER II

Two families of Env antibodies efficiently engage Fc-gamma receptors and eliminate HIV-1-infected cells

Sai Priya Anand, Jérémie Prévost, Sophie Baril, Jonathan Richard, Halima Medjahed, Jean-Philippe Chapleau, William D. Tolbert, Sharon Kirk, Amos B. Smith III, Bruce D. Wines, Stephen J. Kent, P. Mark Hogarth, Matthew S. Parsons, Marzena Pazgier, and Andrés Finzi

2.1 Preface to Chapter 2

As discussed in Chapter 1, the 'open' CD4-bound Env conformation is recognized by commonly elicited non-neutralizing and ADCC-mediating antibodies present in the sera from HIV-1-infected individuals (232, 378). These nNAbs commonly target the highly conserved Cluster A epitope within the gp120 subunit (313, 335, 384). Furthermore, Richard *et al.* demonstrated that another class of anti-CoRBS Abs within HIV+ sera aid in anti-cluster A Ab binding to enhance the overall ADCC activities in the presence of CD4mc (336). With this information, whether the Fc-effector activities of Abs present in HIV+ sera was dependent only on anti-cluster A Abs or on both classes of Abs, was unclear. Thus, in this chapter we determine the requirement of both classes of antibodies to engage with FcγRIIIa and mediate ADCC. This information is crucial to determine which class of Ab would be necessary to efficiently activate effector cells for potential immunization strategies.

2.2 Abstract

HIV-1 conceals epitopes of its envelope glycoproteins (Env) recognized by antibody (Ab)-dependent cellular cytotoxicity (ADCC)-mediating antibodies. These Abs, including anti-coreceptor binding site (CoRBS) and anti-cluster A antibodies, preferentially recognize Env in its 'open' conformation. The binding of anti-CoRBS Abs has been shown to induce conformational changes that further open Env, allowing interaction of anti-cluster A antibodies. We explored the possibility that CoRBS Abs synergize with anti-cluster A Abs to engage Fc-gamma receptors to mediate ADCC. We found that binding of anti-CoRBS and anti-cluster A Abs to the same gp120 is required for interaction with soluble dimeric FcγRIIIa in enzyme-linked immunosorbent assays (ELISAs). We also found that Fc regions of both Abs are required to optimally engage FcγRIIIa and mediate robust ADCC. Taken together, our results indicate that these two families of Abs act together in a sequential and synergistic fashion to promote FcγRIIIa engagement and ADCC.

2.3 Introduction

Increasing evidence suggests that antibody (Ab)-dependent cellular cytotoxicity (ADCC) is an important host response that decreases human immunodeficiency virus type 1 (HIV-1) infection and replication (1-7). Analysis of the RV144 vaccine trial data suggested that increased ADCC activity was associated with decreased HIV-1 acquisition (8), and antibodies (Abs) with potent ADCC activity were isolated from RV144 vaccinees (9). The Fc portions of IgGs on opsonized targets trigger effector responses, including ADCC, by the ligation and cross-linking of specific Fc-gamma receptors (FcγR) expressed on effector cells (10). FcγRIIIa (CD16a) is the principal activating Fc receptor on natural killer (NK) cells, which are major mediators of ADCC.

There are many factors that can contribute to the ability of Abs to engage effector cells to clear infected cells, such as (i) the strength of IgG interactions with FcγRs; (ii) the density of IgG opsonization; and (iii) the orientation of the Fc portion (11, 12). Additionally, the interaction of FcγRs with Abs bound to distinct epitopes may have additive or synergistic effects on host immune responses. Previous reports have shown improved neutralization efficacy with two or

more monoclonal Abs (mAbs) targeting the Ebola virus (13), Hepatitis C virus (14) and HIV-1 (15). Using influenza A virus as a model, it has been shown that the combination of MAbs targeting different epitopes enhanced the induction of ADCC in an additive manner (16). These findings exemplify the complex interactions present in a polyclonal Ab response *in vivo*.

In the context of HIV-1, it has been shown that antibodies targeting the CD4-bound conformation of viral envelope glycoproteins (Env) mediate strong ADCC activity (17,–20). It should be noted that these Abs require infected cells to present Env in an 'open' conformation for ADCC to be achievable (18, 19, 21, 22). Several families of Abs can bind epitopes exposed in this conformation of Env, including anti-cluster A, anti-coreceptor binding site (anti-CoRBS), anti-V3, and anti-gp41 Abs (17). To avoid exposure of these CD4-induced epitopes, however, HIV-1 efficiently internalizes Env and prevents the accumulation of the CD4 receptor on the surface of infected cells through Nef and Vpu accessory proteins (20). Moreover, Vpu decreases Env levels at the cell surface by antagonizing the BST-2 host restriction factor which otherwise tethers budding viral particles (23, 24) (the impact of these accessory proteins on ADCC responses was recently reviewed in references 25-27).

In agreement with the susceptibility of the CD4-bound conformation of Env to ADCC, it has been shown that small-molecule CD4-mimetics (CD4mc) 'force' Env to adopt a similar conformation that enhances susceptibility of infected cells to ADCC triggered by antibodies within sera, breast milk, and cervicovaginal fluids from HIV-1-infected subjects (21, 28-30). The mechanism via which CD4mc facilitate anti-HIV-1 ADCC includes a synergistic interaction of Env with both CD4mc and anti-CoRBS Abs present in HIV-1-positive (HIV-1+) sera. The sequential binding of CD4mc and anti-CoRBS Abs opens the Env trimer and facilitates recognition by the anti-cluster A family of Abs. The members of the latter family of Abs recognize epitopes located in the gp120 inner domain which are occluded in the 'closed' native trimer (12, 20, 31-34) and are known to be responsible for the majority of the ADCC activity present in HIV-1+ sera (17, 19, 20, 31, 35). Accordingly, the addition of anti-cluster A Fab fragments has been shown to block most ADCC activity present in HIV-1+ sera (35). Interestingly, addition of Fab fragments from the 17b antibody, which belongs to the anti-

CoRBS family of anti-Env antibodies (36), also significantly blocked ADCC activity of HIV-1+ sera and in some cases to the same extent as anti-cluster A Fab fragments (35). Taken together, these studies suggested that there is a high degree of cooperation between anti-cluster A and anti-CoRBS Abs in the induction of effector functions. To mediate ADCC, Abs must bridge their Fab-bound cognate antigen with effector cells capable of recognizing Ab Fc via FcγR. While it was demonstrated that anti-CoRBS Abs facilitate the binding of anti-cluster A Abs to Env (29), it is still not known whether these two families of Abs also coordinate for FcγR engagement. Here we took advantage of the availability of a recently characterized dimeric recombinant soluble FcγRIIIa protein (11, 37-40) to evaluate whether these two families of anti-Env Abs coordinate for FcγR engagement and ADCC responses.

2.4 Material and Methods

Ethics Statement.

Written informed consent was obtained from all study participants [the Montreal Primary HIV Infection Cohort (71, 72) and the Canadian Cohort of HIV Infected Slow Progressors (73) (74)], and research adhered to the ethical guidelines of CRCHUM and was reviewed and approved by the CRCHUM institutional review board (ethics committee, approval number CE16.164-CA). Research adhered to the standards indicated by the Declaration of Helsinki. All participants were adult and provided informed written consent prior to enrolment in accordance with Institutional Review Board approval. All sera were heat-inactivated for 30min at 56°C and stored at 4°C until ready to use in subsequent experiments.

Isolation of Primary cells

CD4 T lymphocytes were purified from resting PBMCs by negative selection and activated as previously described (20, 21). Briefly, PBMC were obtained by leukapheresis. CD4+ T lymphocytes were purified using immunomagnetic beads as per the manufacturer's instructions (StemCell Technologies). CD4+ T lymphocytes were activated with phytohemagglutinin-L (10 µg/ mL) for 48 hours and then maintained in RPMI 1640 complete medium supplemented with rIL-2 (100 U/mL).

Viral production and Infections

Vesicular stomatitis viruses G (VSVG)-pseudotyped viruses were produced and titrated as described (19). Viruses were used to infect activated primary CD4 T cells from healthy HIV-1 negative donors by spin infection at 800 x g for 1 hour in 96-well plates at 25°C.

CD4-mimetics

The small CD4-mimetic compound BNM-III-170 was synthesized as described (42). The compounds were dissolved in dimethyl sulfoxide (DMSO) at a stock concentration of 10mM and diluted to 25µM in blocking buffer for the indirect ELISA assays and 50µM in PBS for cell-surface staining or in RPMI-1640 complete medium for ADCC assays.

Antibodies and Sera

The anti-cluster A mAbs A32 and N5i5 were conjugated with Alexa-Fluor 647 probe (Thermo Fisher Scientific) as per the manufacturer's protocol and used for cell-surface staining of HIV-1-infected primary CD4+ T cells. Additionally, the following anti-Env mAbs were also used for cell-surface staining: N12i2 LALA, N5i5 LALA, the Fab fragments, Fab′2 fragments or full CoRBS mAbs 17b and N12-i2. Goat anti-human Alexa Fluor-647 secondary Ab (Thermo Fisher Scientific) was used to determine overall antibody and sera binding and AquaVivid (Thermo Fisher Scientific) as a viability dye. AlexaFluor 647-conjugated Streptavidin was used to determine biotin-tagged dimeric recombinant soluble FcγRIIIa (V158) binding. Sera from HIV-infected and healthy donors were collected, heat-inactivated and conserved as previously described (19).

Protein production of recombinant proteins

FreeStyle 293F cells (Invitrogen) were grown in FreeStyle 293F medium (Invitrogen) to a density of 1 x 10^6 cells/ml at 37°C with 8% CO_2 with regular agitation (150 rpm). Cells were transfected with a codon-optimized plasmid expressing His6-tagged wild-type or mutant HIV-1 YU2 gp120 using the ExpiFectamine 293 transfection reagent, as directed by the manufacturer (Invitrogen). One week later, the cells were pelleted and discarded. The supernatants were filtered (0.22µm filter) (Thermo Fisher Scientific) and the gp120

glycoproteins were purified by nickel affinity columns, as directed by the manufacturer (Invitrogen). Monomeric gp120 was subsequently purified by fast protein liquid chromatography (FPLC), as reported previously (44). The gp120 preparations were dialyzed against phosphate-buffered saline (PBS) and stored in aliquots at -80°C. To assess purity, recombinant proteins were loaded on SDS-PAGE polyacrylamide gels in the absence of beta-mercaptoethanol and stained with Coomassie blue.

The biotin-tagged dimeric recombinant soluble FcγRIIIa (V158) protein was produced and characterized as described (38) with additional purification using a Superdex 200 10/300 GL column (GE Life Sciences).

ELISA-based rsFcγRIIIa dimer-binding assay

Non-saturating concentrations of recombinant gp120 glycoproteins in its full-length form (0.4μg/ml) or lacking its V1, V2, V3 and V5 variable regions (0.25μg/ml) were prepared in PBS as well as bovine serum albumin (BSA) (2μg/ml) as negative control were adsorbed to plates (MaxiSorp; Nunc) overnight at 4°C. Coated wells were subsequently blocked with blocking buffer (tris-buffered saline (TBS) containing 0.1% Tween-20 and 1% (w/v) BSA for 1 hour at room temperature. Anti-HIV-1 Env monoclonal antibodies (1μg/ml) or HIV+ sera (1:1000 dilution) were diluted in blocking buffer and incubated with the gp120-coated wells for 1 hour at room temperature. When indicated, 25μM of BNM-III-170, or equivalent amounts of DMSO, was diluted with the antibodies. Plates were washed four times with washing buffer (TBS containing 0.1% Tween-20). This was followed by an incubation with 0.1μg/ml purified dimeric rsFcγRIIIa-biotin in blocking buffer for 1 hour at room temperature. Horseradish peroxidase-conjugated (HRP) antibody specific for the Fc region of human IgG (Pierce) or High Sensitivity Streptavidin-HRP (Thermo Fisher) (1/1000 in blocking buffer) was added for 1 hour at room temperature, followed by four washes. HRP enzyme activity was determined after the addition of a 1:1 mix of Western Lightning oxidizing and luminol reagents (Perkin Elmer Life Sciences). Light emission was measured with the LB 941 TriStar luminometer (Berthold Technologies).

Flow Cytometry Analysis

Cell-surface staining was performed as previously described (19, 21, 46). Cells infected with HIV-1 primary isolates were identified by intracellular staining of HIV-1 p24 using the Cytofix/Cytoperm Fixation/Permeabilization Kit (BD Biosciences) and the PE-conjugated anti-p24 mAb, clone KC57 (Beckman Coulter). The percentage of infected cells (p24+ cells) was determined by gating the living cell population based on viability dye staining with AquaVivid (Thermo Fisher Scientific). Samples were analyzed on an LSRII cytometer (BD Biosciences), and data analysis was performed using FlowJo vX.0.7 (Tree Star).

FACS-based ADCC assay

Measurement of ADCC using the FACS-based assay was performed at 48h post-infection as previously described (20, 46, 69, 75). Briefly, infected primary CD4+ T cells were stained with AquaVivid viability dye and cell proliferation dye (eFluor670; eBioscience) and used as target cells. Autologous PBMC effectors cells, stained with another cellular marker (cell proliferation dye eFluor450; eBioscience), were added at an effector: target ratio of 10:1 in 96-well V-bottom plates (Corning). Indicated concentrations of ADCC-mediating mAbs (0.3125, 0.625, 1.25, 2.5 or 5µg/ml) with 50µM of BNM-III-170, or equivalent amounts of DMSO, when specified were added to appropriate wells and cells were incubated for 15 min at room temperature. The plates were subsequently centrifuged for 1 min at 300 x g, and incubated at 37°C, 5% CO_2 for 5 hours before being fixed in a 2% PBS-formaldehyde solution. Samples were acquired on an LSRII cytometer (BD Biosciences) and data analysis was performed using FlowJo vX.0.7 (Tree Star). The percentage of ADCC was calculated with the following formula: (% of p24+ cells in Targets plus Effectors) − (% of p24+ cells in Targets plus Effectors plus Abs) / (% of p24+ cells in Targets) by gating on infected live target cells.

In silico modelling

Models of the engagement of dimeric rsFcγRIIIa receptor by anti-CoRBS and anti-cluster A Abs IgGs bound to the target monomeric gp120 immobilized on a plate surface were built based on available crystal structures. First the crystal structures of complexes of N5-i5 Fab-$gp120_{93TH057}$ coree-d1d2CD4 (PDB code 4H8W, (12)) and 17b Fab-$gp120_{HXBC2}$ core-d1d2CD4

(PDB code 1RZJ, (65)) were superimposed based on gp120 with the IgG for each antibody built by overlaying the murine antibody subclass IgG1 (PDB code 1IGY (76)) onto Fabs from the two complexes. The model was assembled assuming monovalent binding of IgG1, and the dimeric rsFcγRIIIa receptor was built using the crystallographic dimer of FcγRIIa-HR (PDB code: 3RY5, high-responder polymorphism FcγRIIa (68)) as a template. The interaction between N5-i5 and 17b Fcs and dimeric rsFcγRIIIa was modeled based on the complex of FcγRIIIa bound to the Fc of IgG1 (PDB code 1E4K (77)).

Statistical Analyses

Statistics were analyzed using GraphPad Prism version 6.01 (GraphPad, San Diego, CA, USA). Every data set was tested for statistical normality, and this information was used to apply the appropriate (parametric or nonparametric) statistical test. P values of <0.05 were considered significant; significance values are indicated as * $p<0.05$, ** $p<0.01$, *** $p<0.001$, **** $p < 0.0001$.

2.5 Results

Anti-CoRBS and anti-Cluster A Abs synergize to engage a soluble recombinant dimeric form of FcγRIIIa

We recently developed an ELISA to model the cross-linking of FcγRs by Abs, a process essential to initiate ADCC responses. Using this assay, we showed that recombinant FcγR dimer engagement of Abs induced by the RV144 vaccine regimen correlated with a functional measure of ADCC (41). As such, we implemented this ELISA to assess anti-cluster A and anti-CoRBS Ab engagement with recombinant soluble dimeric FcγRIIIa (rsFcγRIIIa). Initially, ELISA plates were coated with recombinant gp120 and the ability of gp120-bound anti-cluster A (A32) and/or anti-CoRBS (17b) Abs to engage soluble rsFcγRIIIa was determined. Despite detectable binding of both A32 and 17b to the gp120-coated plates (**Figure 2.1C**), we noted poor binding of rsFcγRIIIa to either Ab alone or both Abs in combination (**Figure 2.1A**). Since we recently reported that anti-CoRBS Abs facilitate anti-cluster A Ab binding upon addition of CD4mc BNM-III-170 (29), we evaluated if this small molecule CD4mc could facilitate rsFcγRIIIa engagement. Plates were coated with recombinant gp120 and then antibody and rsFcγRIIIa binding was measured by ELISA in the presence of BNM-III-170. Consistent with the CD4-induced (CD4i) nature of anti-cluster A and anti-CoRBS Abs and capacity of BNM-III-170 to stabilize gp120 in a CD4-bound conformation (42), both Abs bound gp120 slightly better in the presence of BNM-III-170 (**Figure 2.1C**). Interestingly, only the combination of A32 and 17b resulted in efficient engagement between Abs and rsFcγRIIIa (**Figure 2.1A**). To confirm that the CD4-bound conformation of gp120 facilitates rsFcγRIIIa engagement by anti-cluster A and anti-CoRBS Abs, this Env conformation was stabilized by deleting the V1, V2, V3 and V5 variable regions (ΔV1V2V3V5) (43, 44). Using this stabilized recombinant gp120, we observed that neither anti-cluster A (A32, N5-i5) nor anti-CoRBS (17b, N12-i2) Abs could independently engage the rsFcγRIIIa. We noted, however, that utilizing any combination of Abs exhibiting these two specificities resulted in a dramatic increase in rsFcγRIIIa engagement (**Figure 2.1B**) - despite similar overall binding of the Abs to the CD4-bound-stabilized gp120 (**Figure 2.1D**).

Cumulatively, these data indicate that anti-cluster A and anti-CoRBS Abs synergize to engage with FcγRIIIa.

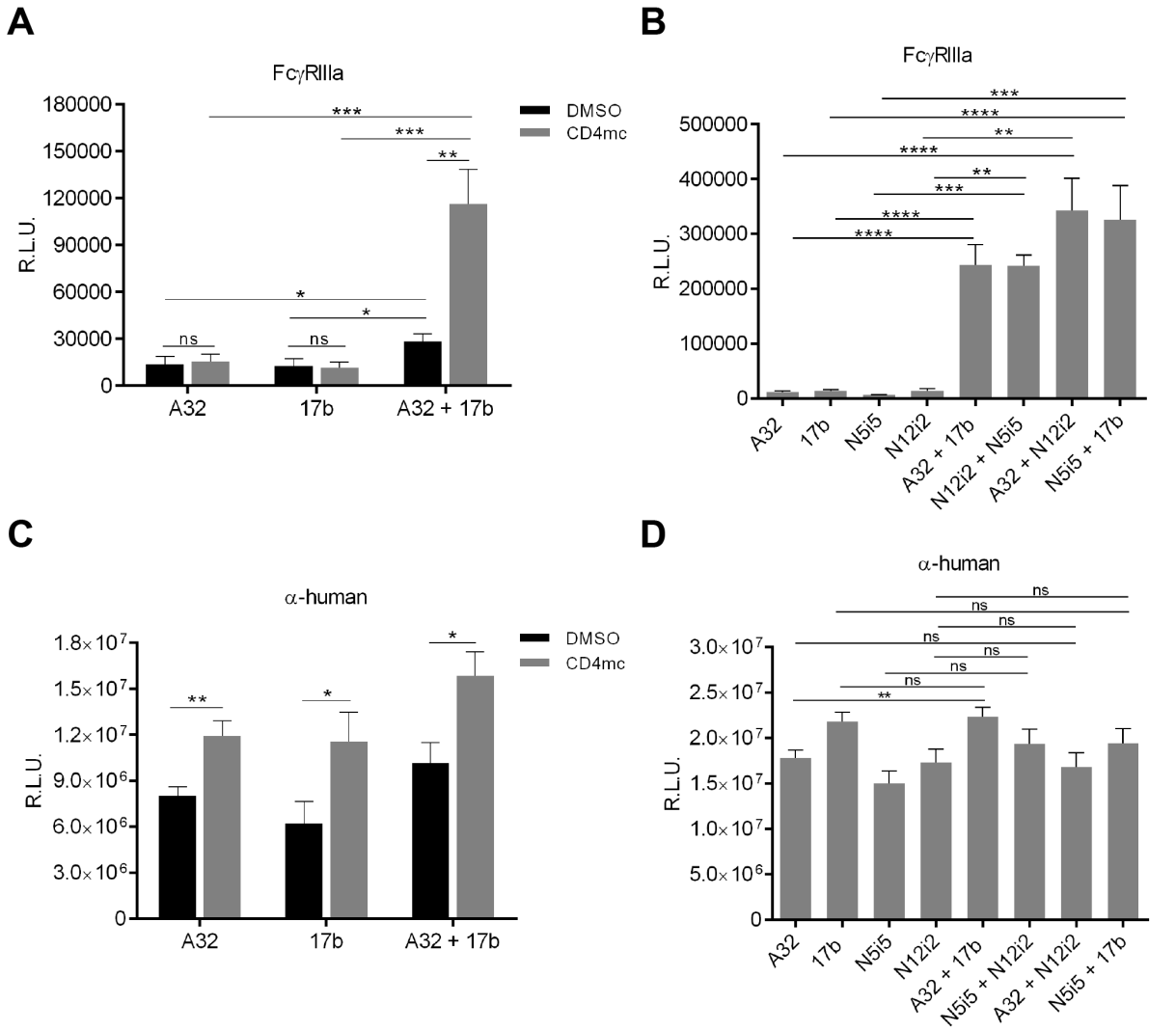

Figure 2.1. Anti-CoRBS and Anti-Cluster A Abs synergize to engage dimeric FcγRIIIa. (**A**,**C**) Indirect ELISA using recombinant full length YU2 gp120 protein (0.4µg/mL) or using (**B,D**) recombinant YU2 ΔV1V2V3V5 gp120 protein (0.25µg/mL). (**A-D**) gp120-coated wells were incubated with a total concentration of 1µg/mL of primary antibodies (**A,C**) +/- BNM-III-170 (25 µM). Antibody binding to gp120 was detected using (**A-B**) a biotin-tagged dimeric rsFcγRIIIa (0.1µg/mL) followed by the addition of HRP-conjugated Streptavidin or using (**C-D**) HRP-conjugated anti-human secondary antibody. Graphs represent Relative Light Units (R.L.U.) obtained from at least 5 independent experiments done in quadruplicate with the error bars indicating Mean +/- SEM. Statistical significance was tested using an unpaired t-test or a Mann-Whitney U test based on statistical normality (* $p<0.05$, ** $p<0.01$, *** $p<0.001$, **** $p<0.0001$; ns, non significant).

Anti-CoRBS and anti-Cluster A Abs must recognize the same gp120 subunit in order to engage with dimeric FcγRIIIa

In theory, due to their non-overlapping epitopes, anti-cluster A and anti-CoRBS Abs could bind the same gp120-coated monomer or two different adjacent gp120-coated monomers to facilitate rsFcγRIIIa engagement. To distinguish between these two possibilities, we coated equivalent amounts of CD4-bound stabilized (ΔV1V2V3V5) gp120 mutants that were competent to engage with anti-cluster A but presented decreased binding to anti-CoRBS (R419D) Abs or that were competent to bind anti-CoRBS but had decreased binding to anti-cluster A (W69A) Abs (**Figure 2.2B**). Strikingly, A32 and 17b were only able to engage rsFcγRIIIa when bound to the CD4-bound stabilized gp120 wt (having intact epitopes for anti-cluster and CoRBS Abs) (**Figure 2.2A**). Indeed, despite similar overall binding of A32 and 17b to wells coated with an equimolar ratio of R419D and W69A CD4-bound stabilized recombinant gp120s, poor rsFcγRIIIa engagement was observed. These data suggest that both A32 and 17b must bind the same gp120 to efficiently engage with FcγRIIIa.

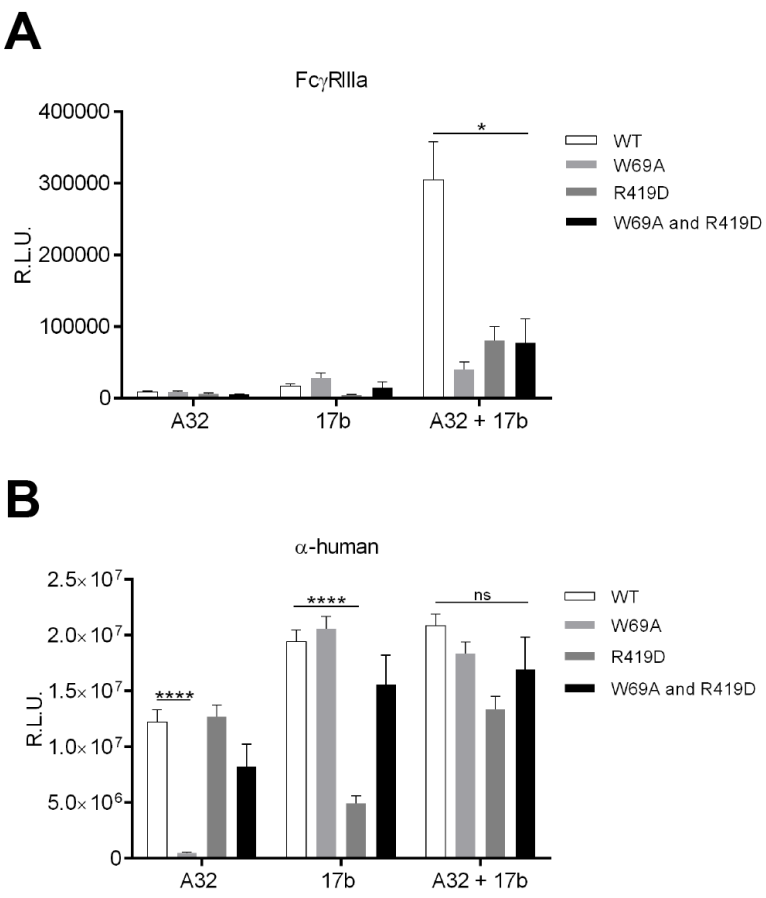

Figure 2.2. Anti-CoRBS and anti-Cluster A Abs must engage with the same gp120 subunit in order to recruit dimeric FcγRIIIa.
Indirect ELISA using recombinant YU2 ΔV1V2V3V5 gp120 protein (WT), its mutated counterpart (W69A or R419D) or an equimolar mixture of both mutated gp120 (W69A and R419D). gp120-coated wells were incubated with a total concentration of 1µg/mL of primary antibodies. Antibody binding to gp120 was detected using (**A**) a biotin-tagged dimeric rsFcγRIIIa (0.1µg/mL) followed by the addition of HRP-conjugated Streptavidin or using (**B**) HRP-conjugated anti-human secondary antibody. Graphs represent Relative Light Units (R.L.U.) obtained from 5 independent experiments done in quadruplicate with the error bars indicating mean +/- SEM. Statistical significance was tested using an unpaired t-test or a Mann-Whitney U test based on statistical normality (* $p<0.05$, **** $p<0.0001$; ns, non significant).

Anti-CoRBS and Anti-Cluster A Abs present in HIV-1+ sera are required for efficient engagement of FcγRIIIa

Since the two families of Abs tested in this study are easily elicited following HIV-1 infection (19, 29, 31, 45), we evaluated their contribution to the capacity of sera from 15 chronically HIV-1-infected individuals to bind to the rsFcγRIIIa by ELISA using the gp120 stabilized in the CD4-bound conformation (ΔV1V2V3V5). Compared to sera from 5 healthy HIV-1-uninfected donors, rsFcγRIIIa was efficiently engaged by Abs present in most HIV-1+ sera tested (**Figure 2.3A**). Interestingly, the addition of A32 or 17b Fab fragments to the HIV-1+ sera significantly blocked the binding of rsFcγRIIIa (**Figure 2.3A**). Addition of A32 and 17b fragments in combination significantly diminished rsFcγRIIIa engagement, to the level of sera from healthy uninfected (HIV-) individuals (**Figure 2.3A**). Similarly, gp120 mutants with impaired ability to engage anti-cluster A (W69A) and/or anti-CoRBS (R419D) Abs failed to facilitate rsFcγRIIIa engagement with bound Abs (**Figure 2.3B**). As such, suggesting that anti-cluster A and anti-CoRBS Abs represent the majority of Abs able to recruit FcγRIIIa in HIV-1+ sera towards Env in the CD4-bound conformation.

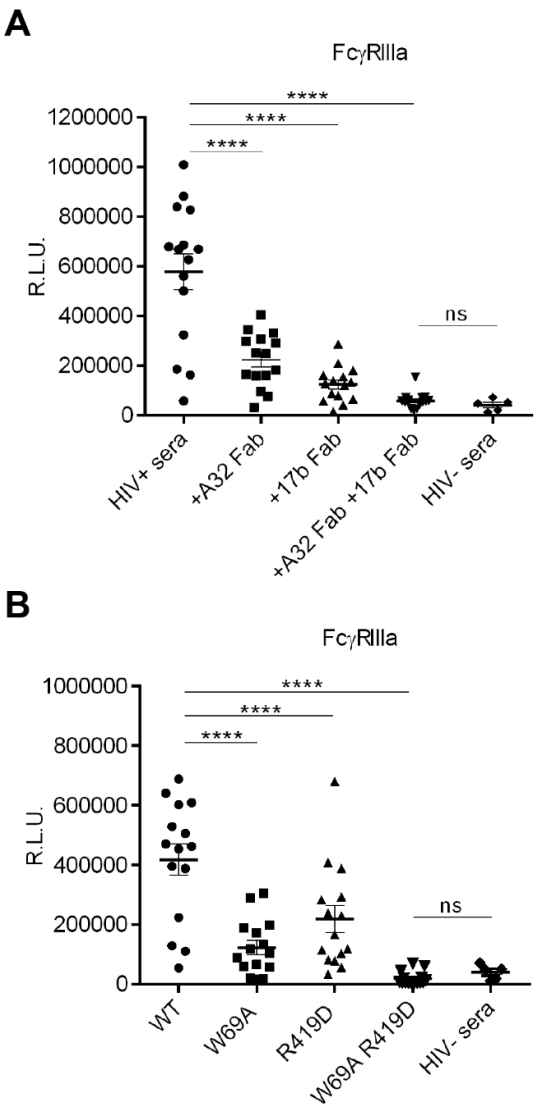

Figure 2.3. Dimeric FcγRIIIa engagement by HIV+ sera is driven by anti-CoRBS and anti-cluster A Abs.

(**A**) Indirect ELISA using recombinant YU2 ΔV1V2V3V5 gp120 protein (0.25µg/mL). gp120-coated wells were incubated with sera from 15 chronically HIV-1-infected individuals +/- A32 Fab and/or 17b Fab fragments (1µg/mL). (**B**) Indirect ELISA using recombinant YU2 ΔV1V2V3V5 gp120 protein (WT) or its mutated counterparts (W69A, R419D or the double mutant W69A/R419D). Sera binding to gp120 was detected using biotin-tagged dimeric rsFcγRIIIa (0.1 µg/mL) followed by the addition of HRP-conjugated Streptavidin. Sera from 5 healthy individuals were used as a negative control. Graphs represent Relative Light Units (R.L.U.) obtained from 3 independent experiments done in quadruplicate with the error bars indicating mean +/- SEM. Statistical significance was tested using a paired t-test or a Wilcoxon matched-pair signed-rank test (based on statistical normality) to compare HIV+ sera datasets together and a Mann-Whitney U test to compare HIV+ sera with HIV- sera (**** $p<0.0001$; ns, non significant).

Anti-CoRBS and Anti-Cluster A Abs are required for efficient binding of FcγRIIIa to infected cells

The above work and prior studies used plate bound Env proteins to measure engagement of FcγRIIIa. We therefore developed a more physiological system to measure this interaction, using HIV-1-infected cells. Primary CD4+ T cells were infected with a primary transmitted/founder (T/F) virus CH58 (CH58 T/F) either wild-type (WT) or defective for Nef and Vpu expression (N-U-). The N-U- virus was used to present Env in the CD4-bound conformation at the surface of infected cells (19, 20). Infected cells were identified by intracellular p24 staining. As previously shown (29), cells infected with the wild-type virus and therefore exposing Env in its untriggered 'closed' conformation were poorly recognized by A32 or 17b in the absence of the CD4mc BNM-III-170. BNM-III-170 enhanced recognition of the infected cells by 17b but not A32 (**Figure 2.4C**). In agreement with the ability of 17b to facilitate A32 binding to Env in the presence of CD4mc (29) (**Figure 2.5**), recognition of infected cells in the presence of BNM-III-170 was significantly higher for the combination of 17b and A32 than for 17b alone. Cobinding of 17b and A32 to CD4mc-bound Env translated into an efficient and significant engagement of rsFcγRIIIa (**Figure 2.4A, B**). As expected, cells infected with the N-U- virus presented Env in its CD4-bound conformation. As such, N-U- virus-infected cells were efficiently recognized by 17b, A32 and the combination of both Abs (**Figure 2.4G, H**). Interestingly, however, only the combination of A32 and 17b was able to engage dimeric rsFcγRIIIa (**Figure 2.4E, F**). Thus anti-cluster A and anti-CoRBS Abs are required to efficiently bind rsFcγRIIIa to infected cells.

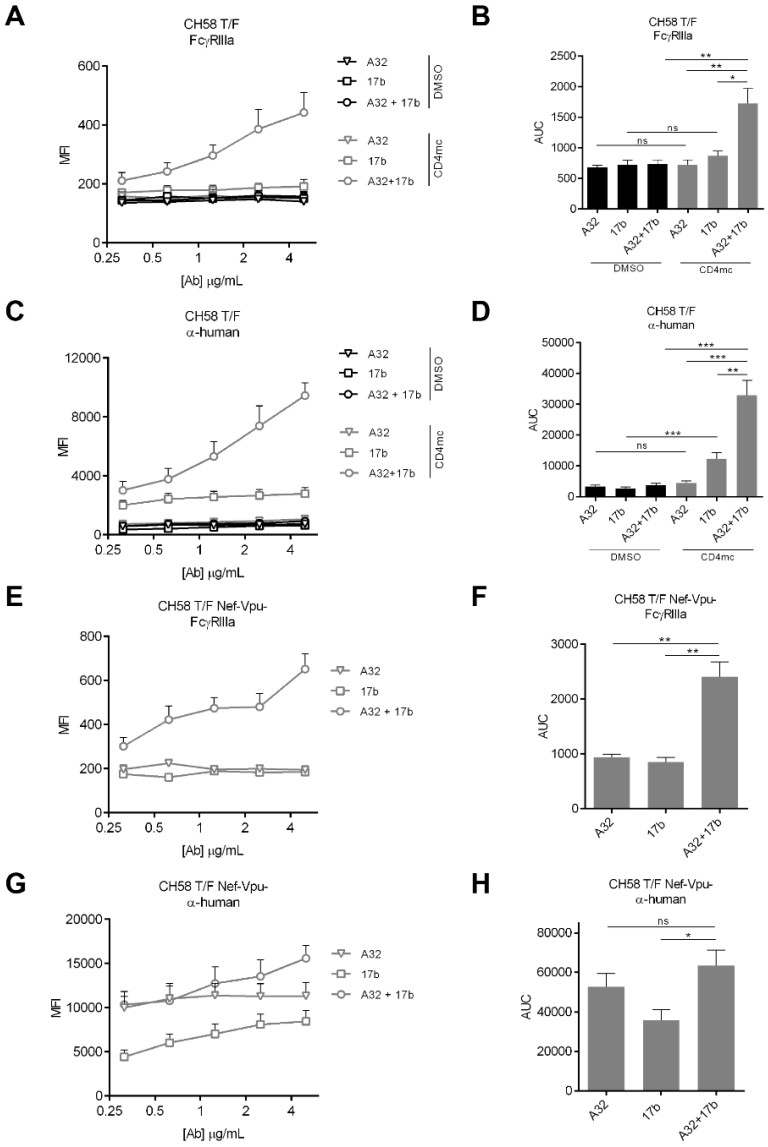

Figure 2.4. Anti-CoRBS and anti-Cluster A Abs are required for efficient engagement of FcγRIIIa to infected cells.

Cell-surface staining of primary CD4+ T cells infected with CH58 T/F virus either (**A**-**D**) WT or (**E-H**) defective for Nef and Vpu expression (N-U-) with various concentrations of A32 and 17b alone or in combination (1:1 ratio). (**A-D**) Staining with CH58 T/F WT virus was done +/- BNM-III-170 (50µM). Antibody binding was detected using (**A-B, E-F**) a biotin-tagged dimeric rsFcγRIIIa (0.2µg/mL) followed by the addition of AlexaFluor 647-conjugated streptavidin or using (**C-D, G-H**) AlexaFluor 647-conjugated anti-human secondary antibody. (**A,C,E,G**) Graphs represent mean fluorescence intensities (MFI) in the infected (p24+) population obtained from 5 independent experiments with the error bars indicating mean +/- SEM. (**B,D,F,H**) Areas under the curve (AUC) were calculated based on MFI datasets using GraphPad Prism software. Statistical significance was tested using an unpaired t-test or a Mann-Whitney U test based on statistical normality (* $p<0.05$, ** $p<0.01$, *** $p<0.001$; ns, non significant).

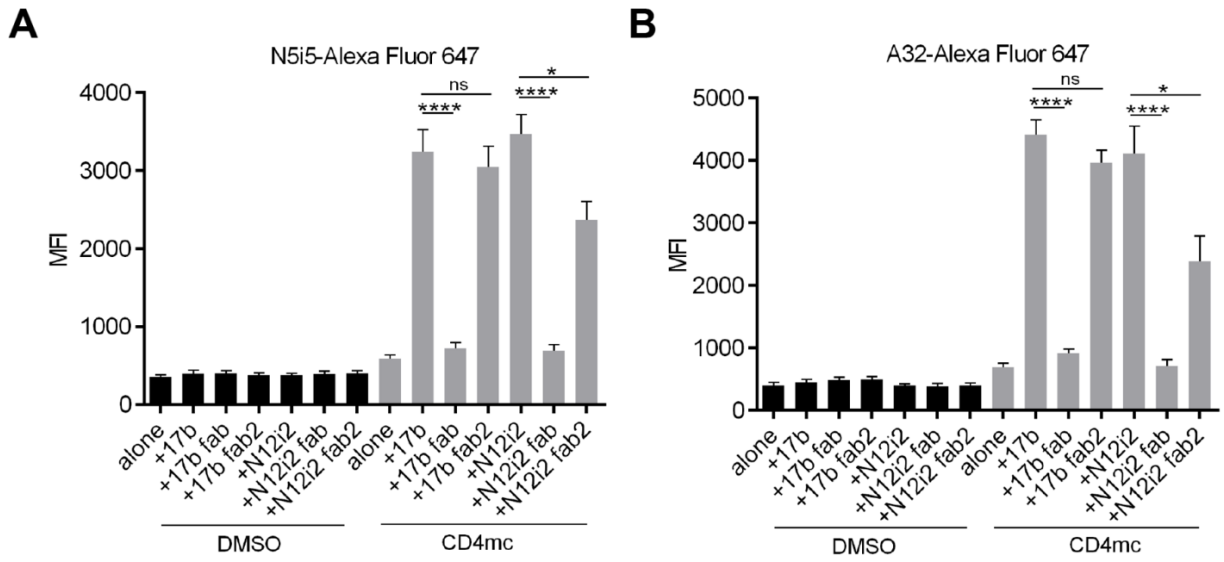

Figure 2.5. CD4mc in combination with Fab'2 but not Fab'1 fragments of anti-CoRBS Abs are sufficient to expose cluster A epitopes.

Cell-surface staining of primary CD4+ T cells infected with CH58 T/F WT virus with (**A**) AlexaFluor 647-conjugated N5i5 or (**B**) AlexaFluor 647-conjugated A32 with 1.25 µg/mL of CoRBS antibodies +/- BNM-III-170 (50µM). Graphs represent the mean fluorescence intensities (MFI) in the infected (p24+) population obtained from 5 independent experiments with the error bars indicating mean +/- SEM. Statistical significance was tested using an unpaired t-test (* $p<0.05$, **** $p<0.0001$; ns, non significant).

Anti-CoRBS and Anti-Cluster A Abs are required for efficient ADCC-mediated killing of HIV-1 infected cells

To evaluate whether engagement of rsFcγRIIIa translates into ADCC, primary CD4+ T cells from at least five healthy uninfected (HIV-) donors were infected with CH58 T/F WT and N-U- viruses and evaluated for their susceptibility to ADCC mediated by effector cells present in autologous PBMCs. ADCC was assessed using an assay measuring the elimination of infected (p24+ cells) (19-21, 30, 46). In agreement with the lack of rsFcγRIIIa binding to wild-type infected cells treated with A32, 17b or A32/17b in the absence of the BNM-III-170 CD4mc (**Figure 2.4A**), only low ADCC activity was observed for A32, 17b or A32/17b in the absence of BNM-III-170 (**Figure 2.6A, B**). Significant ADCC activity was only observed upon addition of the small molecule CD4mc BNM-III-170 with the combination of A32 and 17b Abs as predicted by rsFcγRIIIa binding. As previously reported, cells exposing Env in its CD4-bound conformation due to Nef and Vpu deletions were susceptible to ADCC mediated by A32 (19, 20) but not 17b (17). However, the combination of A32 and 17b further enhanced ADCC (**Figure 2.6C, D**). Altogether this data suggest that anti-cluster A and anti-CoRBS Abs cooperate for ADCC activity against infected cells by better engaging FcγRIIIa.

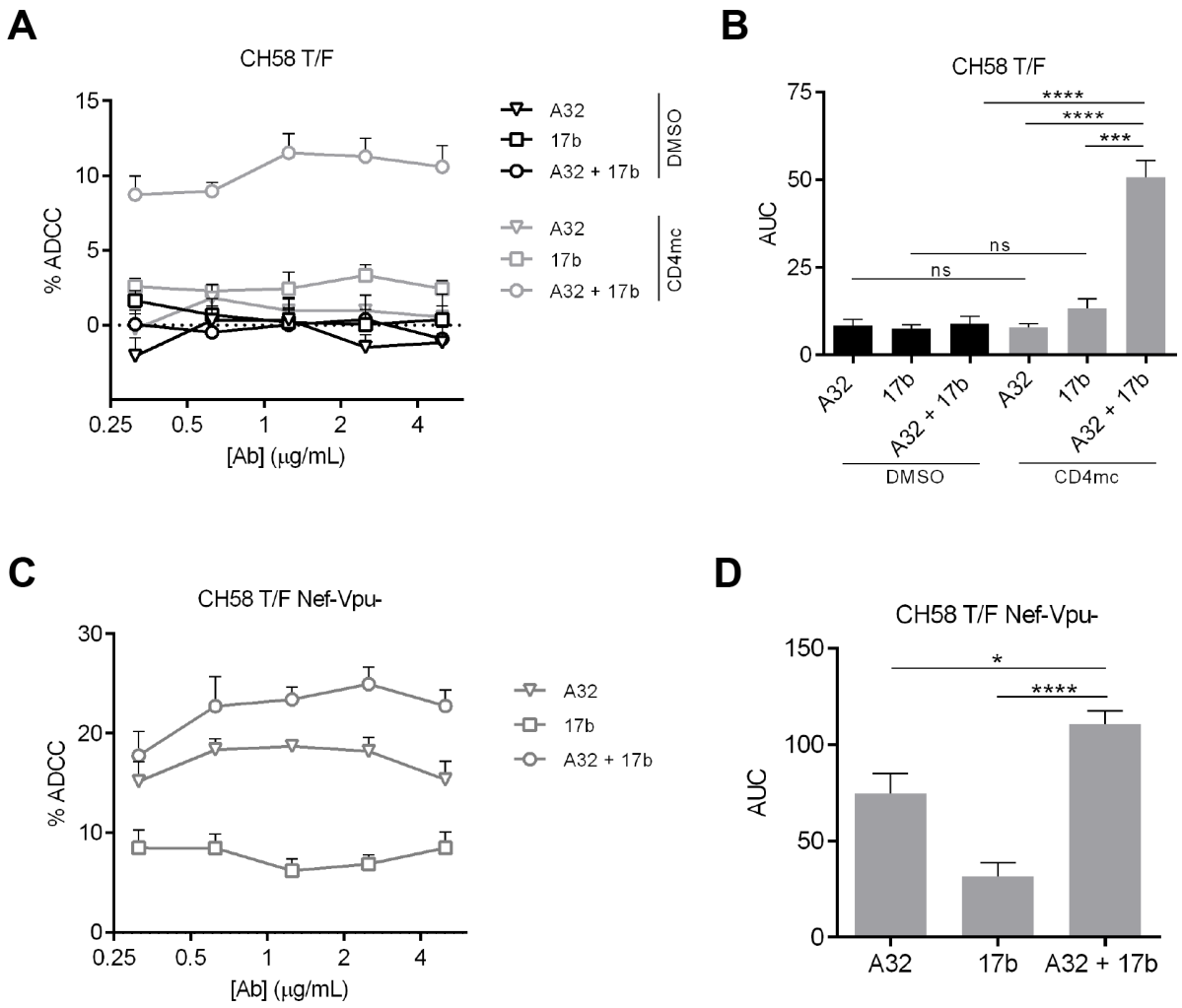

Figure 2.6. ADCC against HIV-1-infected cells expressing Env in its CD4-bound conformation is enhanced by the combination of anti-CoRBS and anti-cluster A Abs. Primary CD4+ T cells from at least 5 different healthy donors were infected with CH58 T/F virus either (**A-B**) WT or (**C-D**) defective for Nef and Vpu expression (N-U-) and used as target cells and autologous PBMC as effector cells in a FACS-based ADCC assay (29). (**A-B**) ADCC with CH58 T/F WT was done +/- BNM-III-170 (50µM). Shown in (**A,C**) are the percentages of ADCC-mediated killing obtained with various concentrations of A32 and 17b alone or in combination (1:1 ratio). (**B,D**) Areas under the curve (AUC) were calculated based on ADCC datasets using GraphPad Prism software. Data is representative of 5 independent experiments with the error bars indicating mean +/- SEM. Statistical significance was tested using an unpaired t-test or a Mann-Whitney U test based on statistical normality (* $p<0.05$, *** $p<0.001$, **** $p<0.0001$; ns, non significant).

Fc regions of anti-cluster A and anti-CoRBS Abs are required to engage FcγRIIIa and mediate ADCC

To evaluate how the combination of anti-cluster A and anti-CoRBS Abs facilitate engagement of rsFcγRIIIa, we introduced double leucine to alanine substitutions at positions 234 and 235 (LALA) of the Fc region of anti-CoRBS (N12i2) and anti-cluster A (N5i5) Abs. The LALA mutation significantly decreases Ab engagement with FcγRIIIa (47-49). First, we evaluated the ability of the unmutated Abs and their LALA counterparts to engage rsFcγRIIIa by ELISA. As shown in **Figure 2.7A**, only the combination of Fc-competent anti-cluster A and anti-CoRBS Abs engaged rsFcγRIIIa, despite similar levels of Ab binding to coated gp120 in conditions containing single Abs or combinations of LALA mutant Abs (**Figure 2.7B**). These results were corroborated by experiments assessing rsFcγRIIIa engagement with Abs bound to cells infected with wild-type and N-U- viruses. In cells infected with the wild-type virus, anti-cluster A and anti-CoRBS Abs were able to efficiently engage the rsFcγRIIIa upon small molecule CD4mc BNM-III-170 addition, but only if Fc-competent Abs were used (**Figure 2.7C**). Similarly, only combinations of Fc-competent anti-cluster A and anti-CoRBS Abs were able to engage rsFcγRIIIa to Nef-Vpu- infected cells (**Figure 2.7D**). Importantly, rsFcγRIIIa engagement translated into ADCC activity (**Figure 2.7E, F**). Likewise, even though Fab'2 fragments of anti-CoRBS Abs sufficiently expose anti-cluster A epitopes in the presence of CD4mc (29) (**Figure 2.5**), only the combination of anti-cluster A Abs with full IgG anti-CoRBS Abs, not Fab2 fragments, optimally recruited rsFcγRIIIa and mediated potent ADCC in the presence of CD4mc (**Figures 2.8** and **2.9**). Thus, the data suggest that a threshold of FcγRIIIa engagement is required to mediate ADCC. Moreover, our results indicate that both Fc regions of these two families of Abs are required to engage FcγRIIIa to mediate ADCC.

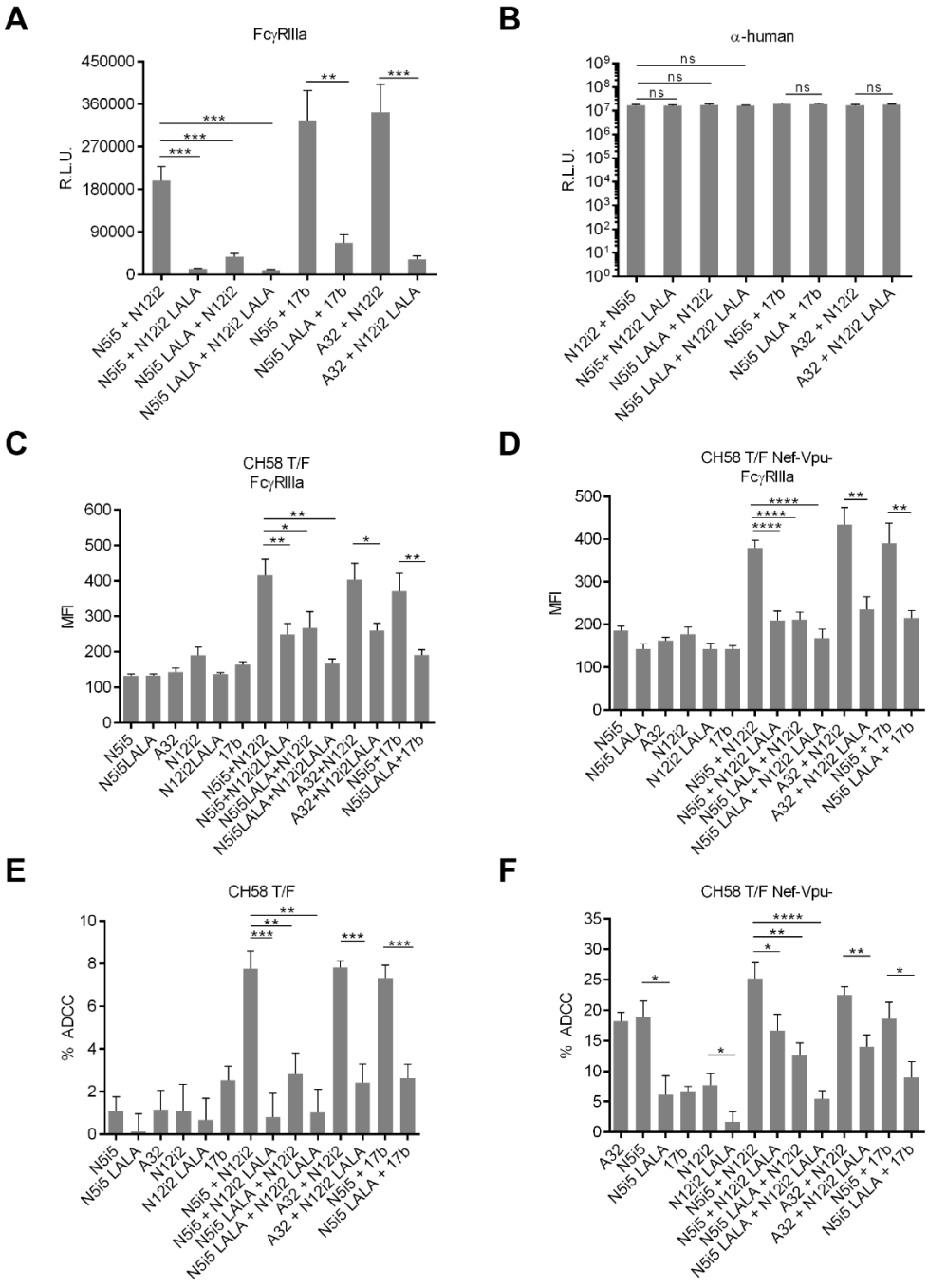

Figure 2.7. Introduction of LALA mutations in the Fc portion of both CoRBS and Anti-cluster A antibodies decreases engagement of dimeric FcγRIIIa and ADCC against HIV-1-infected cells

(**A, B**) Indirect ELISA using recombinant YU2 ΔV1V2V3V5 gp120 protein (0.25µg/mL) with a total concentration of 1µg/mL of primary antibodies. Antibody binding to gp120 was detected using (**A**) a biotin-tagged dimeric rsFcγRIIIa (0.1µg/mL) followed by the addition of HRP-conjugated Streptavidin or using (**B**) HRP-conjugated anti-human secondary antibody. (**A-B**) Graphs represent Relative Light Units (R.L.U.) obtained from at least 5 independent

Figure 2.7. Introduction of LALA mutations in the Fc portion of both CoRBS and Anti-cluster A antibodies decreases engagement of dimeric FcγRIIIa and ADCC against HIV-1-infected cells (continued):

experiments done in quadruplicate with the error bars indicating Mean +/- SEM. (**C, D**) Cell-surface staining of primary CD4+ T cells infected with CH58 T/F virus either (**C**) WT or (**D**) defective for Nef and Vpu expression (N-U-) with a total concentration of 2.5 μg/mL of primary antibodies. (**C**) Staining with CH58 T/F WT virus was done in the presence of BNM-III-170 (50μM). (**C-D**) Antibody binding was detected using a biotin-tagged dimeric rsFcγRIIIa (0.2μg/mL) followed by the addition of AlexaFluor 647-conjugated streptavidin. Graphs represent mean fluorescence intensities (MFI) in the infected (p24+) population obtained from 5 independent experiments with the error bars indicating Mean +/- SEM. (**E-F**) Primary CD4+ T cells from at least 5 different healthy donors infected with CH58 T/F virus either (**E**) WT or (F) defective for Nef and Vpu expression (N-U-) were used as target cells and autologous PBMC as effector cells in a FACS-based ADCC assay (29). (**E**) ADCC with CH58 T/F WT was done in the presence of BNM-III-170 (50μM). Shown in (**E-F**) are the percentages of ADCC-mediated killing obtained with a total concentration of 2.5μg/mL of antibodies. Data is representative of 5 independent experiments with the error bars indicating mean +/- SEM. Statistical significance was tested using an unpaired t-test or a Mann-Whitney U test based on statistical normality (* $p<0.05$, ** $p<0.01$, *** $p<0.001$, **** $p<0.0001$; ns, non significant).

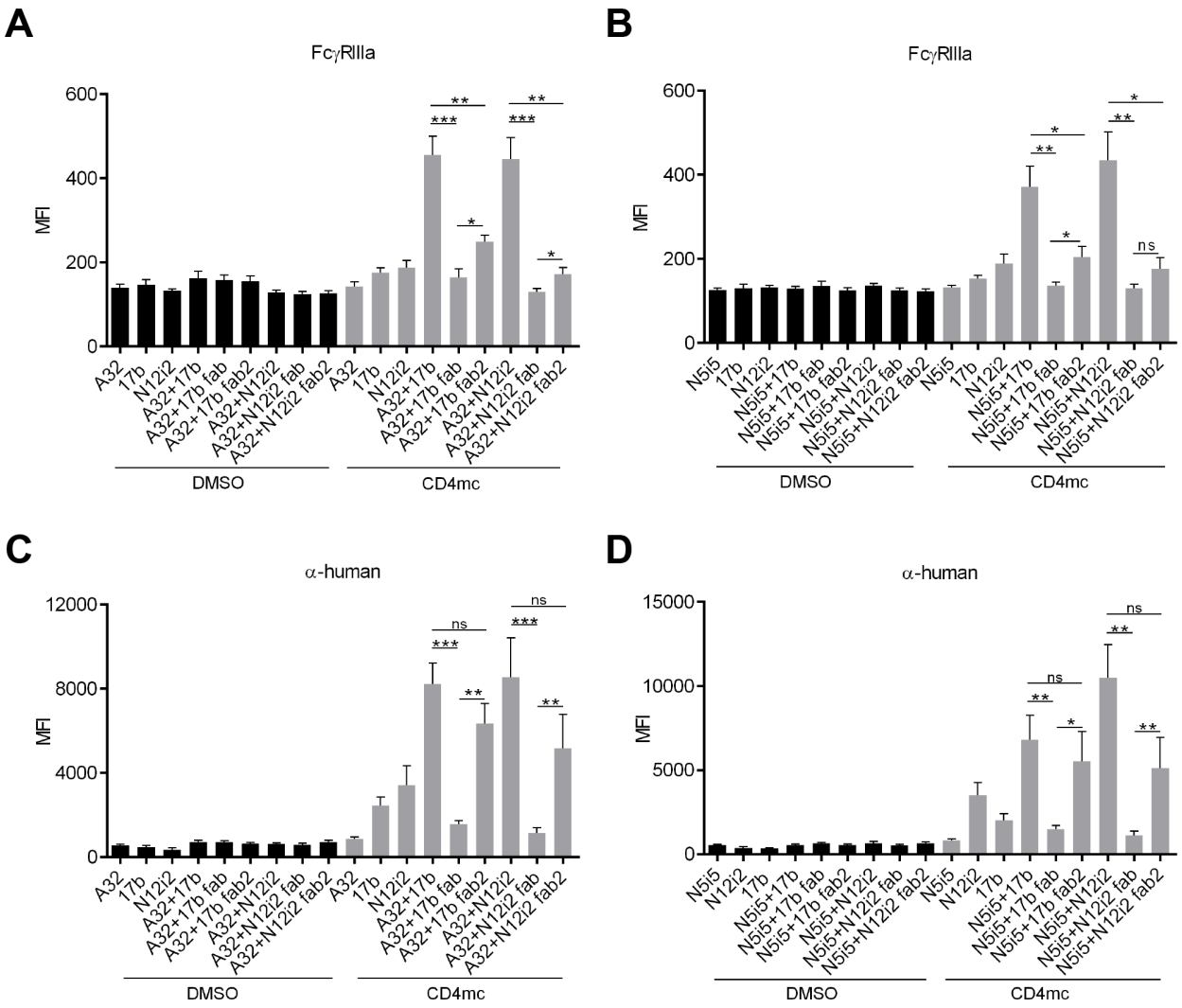

Figure 2.8. The Fc portion from both anti-CoRBS and anti-Cluster A Abs are required to engage dimeric FcγRIIIa.

Cell-surface staining of primary CD4+ T cells infected with CH58 T/F WT virus with a total concentration of 2.5µg/mL of primary antibodies +/- BNM-III-170 (50µM). Antibody binding was detected either by (**A**, **B**) biotin-tagged dimeric rsFcγRIIIa (0.2 µg/mL) followed by the addition of Alexa Fluor 647-conjugated streptavidin or by (**C**, **D**) Alexa Fluor 647-conjugated anti-human secondary antibody. Graphs represent the mean fluorescence intensities (MFI) in the infected (p24+) population obtained from 5 independent experiments with the error bars indicating mean +/- SEM. Statistical significance was tested using an unpaired t-test or a Mann-Whitney U test based on statistical normality (* $p<0.05$, ** $p<0.01$, *** $p<0.001$; ns, non significant).

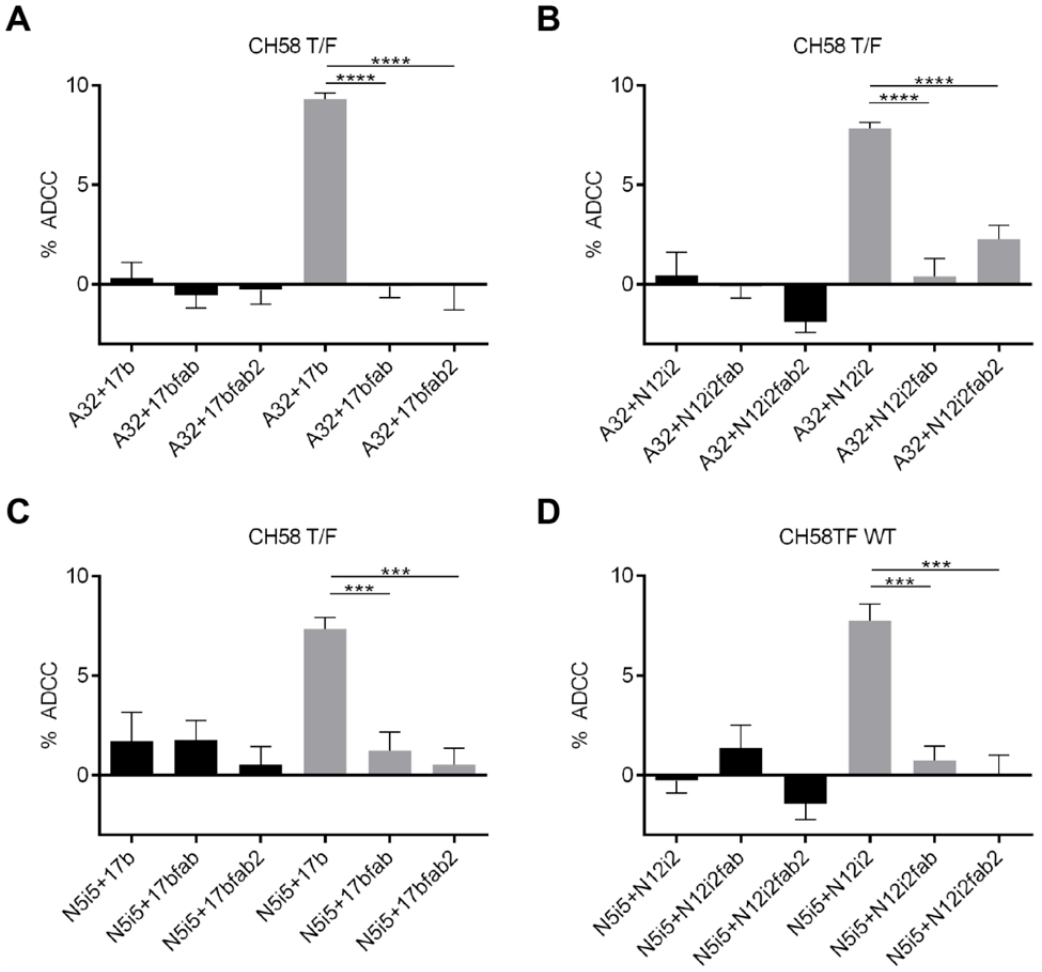

Figure 2.9. The Fc from both anti-CoRBS and anti-cluster A Abs are required to mediate potent ADCC against HIV-1-infected cells.

Primary CD4+ T cells from at least five different healthy donors were infected with CH58 T/F WT virus and used as target cells. Autologous PBMC were used as effector cells in a FACS-based ADCC assay. Shown in **(A-D)** are the percentages of ADCC-mediated killing obtained with a total concentration of 2.5 μg/mL of antibodies in the absence (black bars) or presence (grey bars) of BNM-III-170 (50μM). Data is representative of 5 independent experiments with the error bars indicating mean +/- SEM. Statistical significance was tested using an unpaired t-test (*** $p<0.001$, **** $p < 0.0001$).

2.6 Discussion

HIV-1 has evolved several evasion mechanisms to evade the humoral response elicited against its envelope glycoproteins, including conformational masking of vulnerable epitopes, high sequence variability in the variable loops and extensive glycosylation (50-52). The conformational dynamics of Env also constitute a major barrier for Env inactivation by Abs. The functional Env trimer mainly exists in an untriggered 'closed' conformation (State 1) that cannot be seen by non-neutralizing Abs (nnAbs). However, Env has intrinsic access to the 'open' CD4-bound conformation (State 3) through one necessary conformational intermediate (State 2) in which only one protomer is competent for CD4 binding (53, 54). Primary Tier 2 viruses are more 'closed', with elevated State 1 occupancy, explaining why they are resistant to binding and neutralization by nnAbs (54). CD4 and CD4mc interaction modifies the conformational landscape towards State 3 by lowering the energy barrier to 'open' states 2/3, rendering Env vulnerable to nnAb attack (18, 54-56). The majority of the antibodies elicited during natural infection are strain-specific neutralizing or nnAbs (57) and thought to play a minimal role in controlling viral replication. Recent studies, however, showed that these antibodies can exert a constant selection pressure and alter the course of HIV-1-infection *in vivo* (58, 59). Non-neutralizing Abs with Fc-effector function are present in HIV-1+ sera and have been shown to mediate potent ADCC activity against cells presenting Env in its 'open' CD4-bound conformation (17-21, 26, 30, 60-62). Among the different nnAbs tested for their ADCC activity, the anti-cluster A family of Abs were identified as being the most potent against target cells expressing Env in this 'open' conformation (17, 31, 33, 35). Of note, these Abs can be readily elicited in non-human primates with monomeric gp120 immunogens (22). Additional nnAbs such as anti-CoRBS Abs, which are unable to mediate potent ADCC activity on their own (17), were shown to facilitate engagement of anti-cluster A Abs and potentiate their ADCC activity (29). Here we provide evidence that anti-cluster A and anti-CoRBS Abs collaborate in engaging the dimeric form of the FcγRIIIa receptor when bound to the cognate epitopes within the same monomeric gp120. We utilized a novel probe, a covalent FcγRIIIa dimer as a surrogate of FcγRIIIa present on effector cells (11, 38, 40, 41, 63) and showed that sequential binding of antibodies specific for these two CD4i epitope targets is required for effective receptor engagement and potent ADCC. Recent structural studies defined the Env

epitopes recognized by anti-cluster A and anti-CoRBS Abs at the atomic level and mapped the cluster A epitope region to the C1-C2 regions of the gp120 inner domain in its CD4-bound conformation (12, 32, 33, 64) and CoRBS to the bridging sheet and the base of the V3 loop of the CD4-triggered gp120 (65-67). These two epitopes are not overlapping. In order to validate our findings of collaboration in effective engagement of the dimeric Fc-gamma receptor by antibodies specific for these two epitopes targets we prepared a model of the putative immune-complex that needs to be formed on the gp120 antigen in order to engage a covalent FcγRIIIa dimer (**Figure 2.10**). We used the crystallographic dimer of FcγRIIa-HR (PDB code: 3RY5), a high-responder polymorphism FcγRIIa (68) as a template to generate the putative FcγRIIIa dimer. As predicted, the anti-cluster A N5-i5 and anti-CoRBS 17b antibodies bind to non-overlapping sites on the same gp120 protomer such that their Fc domains are brought in close proximity (**Figure 2.10**). Simple adjustment of Fc positions, which could be mediated by the IgG1 hinge region, orients the Fcs to permit interactions with the FcγRIIIa dimer (**Figure 2.10**). Taken together the in silico modelling clearly confirms the possibility of complex formation in which the anti-cluster A and anti-CoRBS Abs are bound to the same gp120 antigen and their Fc domains engaged in an interaction with the dimeric Fc gamma receptor. However, whether the same configuration is maintained on trimeric Env remains to be shown.

Although our results reveal that anti-cluster A and anti-CoRBS Abs collaborate to trigger anti-HIV-1 ADCC, it is important to note that a collaboration between these Abs is only required for ADCC in the context of CD4mc. Indeed, target cells infected with N-U- viruses bind A32 and are susceptible to ADCC through A32 alone. Similarly, gp120-coated CD4+ T cells are susceptible to ADCC triggered by A32 alone (46, 69). The exact mechanisms behind the differential requirement for anti-CoRBS Abs for ADCC against target cells infected with wild type virus in the presence of CD4mc and target cells coated with gp120 or infected with N-U-viruses remain undetermined. One possible contributor to this phenomenon is the sparse density and/or proximity of Env on cells infected with wild type virus, increasing the need for multiple Abs per Env spike (70). Another possible contributor is that the conformational changes in Env induced by cell surface CD4 (present on target cells coated with gp120 or infected with N-U- viruses) is sufficient to allow binding to cell surface co-receptors and

negate the need for anti-CoRBS Abs to reveal the A32 epitope (12, 20). The conformational changes in Env induced by CD4mc, however, are not sufficient to allow co-receptor binding to Env, thus necessitating anti-CoRBS Ab binding to reveal the A32 epitope (29).

Taken together, our data identifies a complex interplay between two families of easy-to-elicit antibodies, present in most HIV-1-infected individuals, with good potential to eliminate HIV-1-infected cells, provided that the Env in the target cell is in a more open conformation. Interestingly, small molecule CD4-mimetics have been shown to 'open up' the Env trimer (21, 22, 30), therefore, this data suggests that strategies aimed at stabilizing 'open' Env conformations with CD4mc might expedite the design of new strategies aimed at fighting HIV-1 infection.

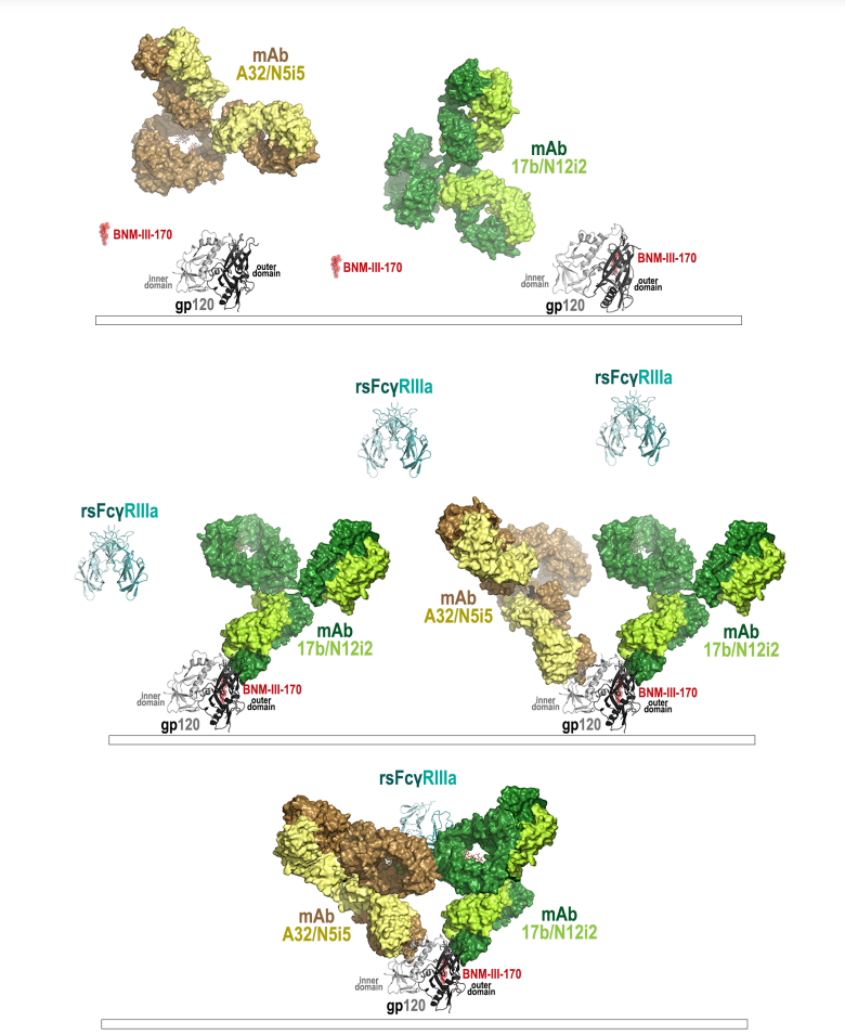

Figure 2.10. Model of the dimeric rsFcγRIIIa engagement by anti-CoRBS and anti-cluster A Abs bound to their cognate epitopes within the same gp120 subunit.
The model was built using representative anti-CoRBS and anti-cluster A Abs for which crystal structures of Fab-antigen complexes are available and the dimeric rsFcγRIIIa receptor as described in the materials and methods section. Monomeric gp120 (shown in grey and black for inner and outer domain, respectively) immobilized on a plate surface is triggered by the small CD4 mimetic compound BNM-III-170 to expose the co-receptor binding site (top panel). gp120 in the BNM-III-170-bound conformation is recognized first by anti-CoRBS Ab (17b or N12i2) followed by anti-cluster A Ab (A32 or N5i5) binding (middle panel). The proximity of the CoRBS and cluster A regions within the gp120 antigen permits easy engagement of Ab Fc domains into the complex with the dimeric rsFcγRIIIa receptor (bottom panel). Only minimal adjustment of positions (possibly mediated by the IgG hinge region) of anti-CoRBS and anti-cluster A bound to the same gp120 molecule is required for engagement of the dimeric rsFcγRIIIa receptor. *In vivo*, an array of identical complexes that involve two Abs bound to the same gp120 antigen and the dimeric rsFcγRIIIa receptor is presumably required to effectively stimulate an effector cell.

Acknowledgments

We thank the CRCHUM Flow Cytometry and BSL-3 platforms for technical assistance and Mario Legault for cohort coordination and clinical samples.

This work was supported by CIHR foundation grant 352417 to A.F. Support for this work was also provided by NIH via NIH grants NIAID R01 to A.F. and M.P. (AI129769) and NIAID R01 to M.P. (AI116274). A.F. is the recipient of a Canada Research Chair on Retroviral Entry (no. RCHS0235). J.R. is the recipient of Mathilde Krim Fellowships in Basic Biomedical Research from amfAR. J.P. is the recipient of a CIHR PhD fellowship award. The funders had no role in study design, data collection and analysis, decision to publish, or preparation of the manuscript. We declare that we have no competing interests.

The views expressed in this presentation are those of the authors and do not reflect the official policy or position of the Uniformed Services University, U.S. Army, the Department of Defense, or the U.S. Government.

2.7 References

1. Alpert MD, Harvey JD, Lauer WA, Reeves RK, Piatak M, Jr., Carville A, Mansfield KG, Lifson JD, Li W, Desrosiers RC, Johnson RP, Evans DT. 2012. ADCC develops over time during persistent infection with live-attenuated SIV and is associated with complete protection against SIV(mac)251 challenge. PLoS Pathog 8:e1002890.
2. Banks ND, Kinsey N, Clements J, Hildreth JE. 2002. Sustained antibody-dependent cell-mediated cytotoxicity (ADCC) in SIV-infected macaques correlates with delayed progression to AIDS. AIDS Res Hum Retroviruses 18:1197-1205.
3. Baum LL, Cassutt KJ, Knigge K, Khattri R, Margolick J, Rinaldo C, Kleeberger CA, Nishanian P, Henrard DR, Phair J. 1996. HIV-1 gp120-specific antibody-dependent cell-mediated cytotoxicity correlates with rate of disease progression. J Immunol 157:2168-2173.
4. Chung AW, Isitman G, Navis M, Kramski M, Center RJ, Kent SJ, Stratov I. 2011. Immune escape from HIV-specific antibody-dependent cellular cytotoxicity (ADCC) pressure. Proc Natl Acad Sci U S A 108:7505-7510.
5. Forthal DN, Landucci G, Haubrich R, Keenan B, Kuppermann BD, Tilles JG, Kaplan J. 1999. Antibody-dependent cellular cytotoxicity independently predicts survival in severely immunocompromised human immunodeficiency virus-infected patients. J Infect Dis 180:1338-1341.
6. Mabuka J, Nduati R, Odem-Davis K, Peterson D, Overbaugh J. 2012. HIV-specific antibodies capable of ADCC are common in breastmilk and are associated with reduced risk of transmission in women with high viral loads. PLoS Pathog 8:e1002739.
7. Sun Y, Asmal M, Lane S, Permar SR, Schmidt SD, Mascola JR, Letvin NL. 2011. Antibody-dependent cell-mediated cytotoxicity in simian immunodeficiency virus-infected rhesus monkeys. J Virol 85:6906-6912.
8. Haynes BF, Gilbert PB, McElrath MJ, Zolla-Pazner S, Tomaras GD, Alam SM, Evans DT, Montefiori DC, Karnasuta C, Sutthent R, Liao HX, DeVico AL, Lewis GK, Williams C, Pinter A, Fong Y, Janes H, DeCamp A, Huang Y, Rao M, Billings E, Karasavvas N, Robb ML, Ngauy V, de Souza MS, Paris R, Ferrari G, Bailer RT, Soderberg KA, Andrews C, Berman PW, Frahm N, De Rosa SC, Alpert MD, Yates NL, Shen X, Koup RA, Pitisuttithum P, Kaewkungwal J, Nitayaphan S, Rerks-Ngarm S, Michael NL, Kim JH. 2012. Immune-correlates analysis of an HIV-1 vaccine efficacy trial. N Engl J Med 366:1275-1286.
9. Bonsignori M, Pollara J, Moody MA, Alpert MD, Chen X, Hwang KK, Gilbert PB, Huang Y, Gurley TC, Kozink DM, Marshall DJ, Whitesides JF, Tsao CY, Kaewkungwal J, Nitayaphan S, Pitisuttithum P, Rerks-Ngarm S, Kim JH, Michael NL, Tomaras GD, Montefiori DC, Lewis GK, Devico A, Evans DT, Ferrari G, Liao HX, Haynes BF. 2012. Antibody-Dependent Cellular Cytotoxicity-Mediating Antibodies from an HIV-1 Vaccine Efficacy Trial Target Multiple Epitopes and Preferentially Use the VH1 Gene Family. J Virol 86:11521-11532.

10. Hogarth PM, Pietersz GA. 2012. Fc receptor-targeted therapies for the treatment of inflammation, cancer and beyond. Nat Rev Drug Discov 11:311-331.
11. Wines BD, Billings H, McLean MR, Kent SJ, Hogarth PM. 2017. Antibody Functional Assays as Measures of Fc Receptor-Mediated Immunity to HIV - New Technologies and their Impact on the HIV Vaccine Field. Curr HIV Res 15:202-215.
12. Acharya P, Tolbert WD, Gohain N, Wu X, Yu L, Liu T, Huang W, Huang CC, Kwon YD, Louder RK, Luongo TS, McLellan JS, Pancera M, Yang Y, Zhang B, Flinko R, Foulke JS, Jr., Sajadi MM, Kamin-Lewis R, Robinson JE, Martin L, Kwong PD, Guan Y, DeVico AL, Lewis GK, Pazgier M. 2014. Structural Definition of an Antibody-Dependent Cellular Cytotoxicity Response Implicated in Reduced Risk for HIV-1 Infection. J Virol 88:12895-12906.
13. Howell KA, Brannan JM, Bryan C, McNeal A, Davidson E, Turner HL, Vu H, Shulenin S, He S, Kuehne A, Herbert AS, Qiu X, Doranz BJ, Holtsberg FW, Ward AB, Dye JM, Aman MJ. 2017. Cooperativity Enables Non-neutralizing Antibodies to Neutralize Ebolavirus. Cell Rep 19:413-424.
14. Carlsen TH, Pedersen J, Prentoe JC, Giang E, Keck ZY, Mikkelsen LS, Law M, Foung SK, Bukh J. 2014. Breadth of neutralization and synergy of clinically relevant human monoclonal antibodies against HCV genotypes 1a, 1b, 2a, 2b, 2c, and 3a. Hepatology 60:1551-1562.
15. Walker LM, Huber M, Doores KJ, Falkowska E, Pejchal R, Julien JP, Wang SK, Ramos A, Chan-Hui PY, Moyle M, Mitcham JL, Hammond PW, Olsen OA, Phung P, Fling S, Wong CH, Phogat S, Wrin T, Simek MD, Koff WC, Wilson IA, Burton DR, Poignard P. 2011. Broad neutralization coverage of HIV by multiple highly potent antibodies. Nature 477:466-470.
16. He W, Tan GS, Mullarkey CE, Lee AJ, Lam MM, Krammer F, Henry C, Wilson PC, Ashkar AA, Palese P, Miller MS. 2016. Epitope specificity plays a critical role in regulating antibody-dependent cell-mediated cytotoxicity against influenza A virus. Proc Natl Acad Sci U S A 113:11931-11936.
17. Ding S, Veillette M, Coutu M, Prevost J, Scharf L, Bjorkman PJ, Ferrari G, Robinson JE, Sturzel C, Hahn BH, Sauter D, Kirchhoff F, Lewis GK, Pazgier M, Finzi A. 2016. A Highly Conserved Residue of the HIV-1 gp120 Inner Domain Is Important for Antibody-Dependent Cellular Cytotoxicity Responses Mediated by Anti-cluster A Antibodies. J Virol 90:2127-2134.
18. Prevost J, Richard J, Ding S, Pacheco B, Charlebois R, Hahn BH, Kaufmann DE, Finzi A. 2018. Envelope glycoproteins sampling states 2/3 are susceptible to ADCC by sera from HIV-1-infected individuals. Virology 515:38-45.
19. Veillette M, Coutu M, Richard J, Batraville LA, Dagher O, Bernard N, Tremblay C, Kaufmann DE, Roger M, Finzi A. 2015. The HIV-1 gp120 CD4-Bound Conformation Is Preferentially Targeted by Antibody-Dependent Cellular Cytotoxicity-Mediating Antibodies in Sera from HIV-1-Infected Individuals. J Virol 89:545-551.

20. Veillette M, Desormeaux A, Medjahed H, Gharsallah NE, Coutu M, Baalwa J, Guan Y, Lewis G, Ferrari G, Hahn BH, Haynes BF, Robinson JE, Kaufmann DE, Bonsignori M, Sodroski J, Finzi A. 2014. Interaction with cellular CD4 exposes HIV-1 envelope epitopes targeted by antibody-dependent cell-mediated cytotoxicity. J Virol 88:2633-2644.
21. Richard J, Veillette M, Brassard N, Iyer SS, Roger M, Martin L, Pazgier M, Schon A, Freire E, Routy JP, Smith AB, 3rd, Park J, Jones DM, Courter JR, Melillo BN, Kaufmann DE, Hahn BH, Permar SR, Haynes BF, Madani N, Sodroski JG, Finzi A. 2015. CD4 mimetics sensitize HIV-1-infected cells to ADCC. Proc Natl Acad Sci U S A 112:E2687-2694.
22. Madani N, Princiotto AM, Mach L, Ding S, Prevost J, Richard J, Hora B, Sutherland L, Zhao CA, Conn BP, Bradley T, Moody MA, Melillo B, Finzi A, Haynes BF, Smith Iii AB, Santra S, Sodroski J. 2018. A CD4-mimetic compound enhances vaccine efficacy against stringent immunodeficiency virus challenge. Nat Commun 9:2363.
23. Neil SJ, Zang T, Bieniasz PD. 2008. Tetherin inhibits retrovirus release and is antagonized by HIV-1 Vpu. Nature 451:425-430.
24. Van Damme N, Goff D, Katsura C, Jorgenson RL, Mitchell R, Johnson MC, Stephens EB, Guatelli J. 2008. The interferon-induced protein BST-2 restricts HIV-1 release and is downregulated from the cell surface by the viral Vpu protein. Cell Host Microbe 3:245-252.
25. Veillette M, Richard J, Pazgier M, Lewis GK, Parsons MS, Finzi A. 2016. Role of HIV-1 Envelope Glycoproteins Conformation and Accessory Proteins on ADCC Responses. Curr HIV Res 14:9-23.
26. Richard J, Prevost J, Alsahafi N, Ding S, Finzi A. 2018. Impact of HIV-1 Envelope Conformation on ADCC Responses. Trends Microbiol 26:253-265.
27. Forthal DN, Finzi A. 2018. Antibody-Dependent Cellular Cytotoxicity (ADCC) in HIV Infection. AIDS doi:10.1097/QAD.0000000000002011.
28. Lee WS, Richard J, Lichtfuss M, Smith AB, 3rd, Park J, Courter JR, Melillo BN, Sodroski JG, Kaufmann DE, Finzi A, Parsons MS, Kent SJ. 2015. Antibody-Dependent Cellular Cytotoxicity against Reactivated HIV-1-Infected Cells. J Virol 90:2021-2030.
29. Richard J, Pacheco B, Gohain N, Veillette M, Ding S, Alsahafi N, Tolbert WD, Prevost J, Chapleau JP, Coutu M, Jia M, Brassard N, Park J, Courter JR, Melillo B, Martin L, Tremblay C, Hahn BH, Kaufmann DE, Wu X, Smith AB, 3rd, Sodroski J, Pazgier M, Finzi A. 2016. Co-receptor Binding Site Antibodies Enable CD4-Mimetics to Expose Conserved Anti-cluster A ADCC Epitopes on HIV-1 Envelope Glycoproteins. EBioMedicine doi:10.1016/j.ebiom.2016.09.004.
30. Richard J, Prevost J, von Bredow B, Ding S, Brassard N, Medjahed H, Coutu M, Melillo B, Bibollet-Ruche F, Hahn BH, Kaufmann DE, Smith AB, 3rd, Sodroski J, Sauter D, Kirchhoff F, Gee K, Neil SJ, Evans DT, Finzi A. 2017. BST-2 Expression Modulates Small CD4-Mimetic Sensitization of HIV-1-Infected Cells to Antibody-Dependent Cellular Cytotoxicity. J Virol 91.

31. Guan Y, Pazgier M, Sajadi MM, Kamin-Lewis R, Al-Darmarki S, Flinko R, Lovo E, Wu X, Robinson JE, Seaman MS, Fouts TR, Gallo RC, DeVico AL, Lewis GK. 2013. Diverse specificity and effector function among human antibodies to HIV-1 envelope glycoprotein epitopes exposed by CD4 binding. Proc Natl Acad Sci U S A 110:E69-78.
32. Tolbert WD, Gohain N, Veillette M, Chapleau JP, Orlandi C, Visciano ML, Ebadi M, DeVico AL, Fouts TR, Finzi A, Lewis GK, Pazgier M. 2016. Paring Down HIV Env: Design and Crystal Structure of a Stabilized Inner Domain of HIV-1 gp120 Displaying a Major ADCC Target of the A32 Region. Structure 24:697-709.
33. Tolbert WD, Gohain N, Alsahafi N, Van V, Orlandi C, Ding S, Martin L, Finzi A, Lewis GK, Ray K, Pazgier M. 2017. Targeting the Late Stage of HIV-1 Entry for Antibody-Dependent Cellular Cytotoxicity: Structural Basis for Env Epitopes in the C11 Region. Structure 25:1719-1731 e1714.
34. Finzi A, Xiang SH, Pacheco B, Wang L, Haight J, Kassa A, Danek B, Pancera M, Kwong PD, Sodroski J. 2010. Topological layers in the HIV-1 gp120 inner domain regulate gp41 interaction and CD4-triggered conformational transitions. Mol Cell 37:656-667.
35. Ferrari G, Pollara J, Kozink D, Harms T, Drinker M, Freel S, Moody MA, Alam SM, Tomaras GD, Ochsenbauer C, Kappes JC, Shaw GM, Hoxie JA, Robinson JE, Haynes BF. 2011. An HIV-1 gp120 envelope human monoclonal antibody that recognizes a C1 conformational epitope mediates potent antibody-dependent cellular cytotoxicity (ADCC) activity and defines a common ADCC epitope in human HIV-1 serum. J Virol 85:7029-7036.
36. Ding S, Veillette M, Coutu M, Prevost J, Scharf L, Bjorkman PJ, Ferrari G, Robinson JE, Sturzel C, Hahn BH, Sauter D, Kirchhoff F, Lewis GK, Pazgier M, Finzi A. 2015. A Highly Conserved Residue of the HIV-1 gp120 Inner Domain Is Important for Antibody-Dependent Cellular Cytotoxicity Responses Mediated by Anti-cluster A Antibodies. J Virol 90:2127-2134.
37. Wyatt R, Moore J, Accola M, Desjardin E, Robinson J, Sodroski J. 1995. Involvement of the V1/V2 variable loop structure in the exposure of human immunodeficiency virus type 1 gp120 epitopes induced by receptor binding. J Virol 69:5723-5733.
38. Wines BD, Vanderven HA, Esparon SE, Kristensen AB, Kent SJ, Hogarth PM. 2016. Dimeric FcgammaR Ectodomains as Probes of the Fc Receptor Function of Anti-Influenza Virus IgG. J Immunol 197:1507-1516.
39. Lee WS, Kristensen AB, Rasmussen TA, Tolstrup M, Ostergaard L, Sogaard OS, Wines BD, Hogarth PM, Reynaldi A, Davenport MP, Emery S, Amin J, Cooper DA, Kan VL, Fox J, Gruell H, Parsons MS, Kent SJ. 2017. Anti-HIV-1 ADCC Antibodies following Latency Reversal and Treatment Interruption. J Virol 91.
40. Vanderven HA, Wragg K, Ana-Sosa-Batiz F, Kristensen AB, Jegaskanda S, Wheatley AK, Wentworth D, Wines BD, Hogarth PM, Rockman S, Group IFPSW, Kent SJ. 2018.

Anti-influenza Hyperimmune Immunoglobulin Enhances Fc-functional Antibody Immunity during Human Influenza Infection. J Infect Dis doi:10.1093/infdis/jiy328.
41. McLean MR, Madhavi V, Wines BD, Hogarth PM, Chung AW, Kent SJ. 2017. Dimeric Fcgamma Receptor Enzyme-Linked Immunosorbent Assay To Study HIV-Specific Antibodies: A New Look into Breadth of Fcgamma Receptor Antibodies Induced by the RV144 Vaccine Trial. J Immunol 199:816-826.
42. Melillo B, Liang S, Park J, Schon A, Courter JR, LaLonde JM, Wendler DJ, Princiotto AM, Seaman MS, Freire E, Sodroski J, Madani N, Hendrickson WA, Smith AB, 3rd. 2016. Small-Molecule CD4-Mimics: Structure-Based Optimization of HIV-1 Entry Inhibition. ACS Med Chem Lett 7:330-334.
43. Kwon YD, Finzi A, Wu X, Dogo-Isonagie C, Lee LK, Moore LR, Schmidt SD, Stuckey J, Yang Y, Zhou T, Zhu J, Vicic DA, Debnath AK, Shapiro L, Bewley CA, Mascola JR, Sodroski JG, Kwong PD. 2012. Unliganded HIV-1 gp120 core structures assume the CD4-bound conformation with regulation by quaternary interactions and variable loops. Proc Natl Acad Sci U S A 109:5663-5668.
44. Coutu M, Finzi A. 2015. HIV-1 gp120 dimers decrease the overall affinity of gp120 preparations for CD4-induced ligands. J Virol Methods 215-216:37-44.
45. Decker JM, Bibollet-Ruche F, Wei X, Wang S, Levy DN, Wang W, Delaporte E, Peeters M, Derdeyn CA, Allen S, Hunter E, Saag MS, Hoxie JA, Hahn BH, Kwong PD, Robinson JE, Shaw GM. 2005. Antigenic conservation and immunogenicity of the HIV coreceptor binding site. J Exp Med 201:1407-1419.
46. Richard J, Prevost J, Baxter AE, von Bredow B, Ding S, Medjahed H, Delgado GG, Brassard N, Sturzel CM, Kirchhoff F, Hahn BH, Parsons MS, Kaufmann DE, Evans DT, Finzi A. 2018. Uninfected Bystander Cells Impact the Measurement of HIV-Specific Antibody-Dependent Cellular Cytotoxicity Responses. MBio 9.
47. Hezareh M, Hessell AJ, Jensen RC, van de Winkel JG, Parren PW. 2001. Effector function activities of a panel of mutants of a broadly neutralizing antibody against human immunodeficiency virus type 1. J Virol 75:12161-12168.
48. Arduin E, Arora S, Bamert PR, Kuiper T, Popp S, Geisse S, Grau R, Calzascia T, Zenke G, Kovarik J. 2015. Highly reduced binding to high and low affinity mouse Fc gamma receptors by L234A/L235A and N297A Fc mutations engineered into mouse IgG2a. Mol Immunol 63:456-463.
49. Hessell AJ, Hangartner L, Hunter M, Havenith CE, Beurskens FJ, Bakker JM, Lanigan CM, Landucci G, Forthal DN, Parren PW, Marx PA, Burton DR. 2007. Fc receptor but not complement binding is important in antibody protection against HIV. Nature 449:101-104.
50. Kwong PD, Doyle ML, Casper DJ, Cicala C, Leavitt SA, Majeed S, Steenbeke TD, Venturi M, Chaiken I, Fung M, Katinger H, Parren PW, Robinson J, Van Ryk D, Wang L, Burton DR, Freire E, Wyatt R, Sodroski J, Hendrickson WA, Arthos J. 2002. HIV-1 evades antibody-mediated neutralization through conformational masking of receptor-binding sites. Nature 420:678-682.

51. Wyatt R, Kwong PD, Desjardins E, Sweet RW, Robinson J, Hendrickson WA, Sodroski JG. 1998. The antigenic structure of the HIV gp120 envelope glycoprotein. Nature 393:705-711.
52. Wyatt R, Sodroski J. 1998. The HIV-1 envelope glycoproteins: fusogens, antigens, and immunogens. Science 280:1884-1888.
53. Ma X, Lu M, Gorman J, Terry DS, Hong X, Zhou Z, Zhao H, Altman RB, Arthos J, Blanchard SC, Kwong PD, Munro JB, Mothes W. 2018. HIV-1 Env trimer opens through an asymmetric intermediate in which individual protomers adopt distinct conformations. Elife 7.
54. Munro JB, Gorman J, Ma X, Zhou Z, Arthos J, Burton DR, Koff WC, Courter JR, Smith AB, 3rd, Kwong PD, Blanchard SC, Mothes W. 2014. Conformational dynamics of single HIV-1 envelope trimers on the surface of native virions. Science 346:759-763.
55. Herschhorn A, Ma X, Gu C, Ventura JD, Castillo-Menendez L, Melillo B, Terry DS, Smith AB, 3rd, Blanchard SC, Munro JB, Mothes W, Finzi A, Sodroski J. 2016. Release of gp120 Restraints Leads to an Entry-Competent Intermediate State of the HIV-1 Envelope Glycoproteins. MBio 7.
56. Ma X, Lu M, Acharya P, Gorman J, Druz A, Terry DS, Geng H, Dandey V, Zi Y, Baldwin P, Eng ET, Zhou Z, Zhao H, Altman RB, Arthos J, Potter CS, Carragher B, Blanchard SC, Kwong PD, Munro JB, Mothes W. 2017. Single-molecule imaging delineates asymmetric intermediates during the opening of the HIV-1 envelope trimer. In revision
57. Kwong PD, Mascola JR. 2012. Human antibodies that neutralize HIV-1: identification, structures, and B cell ontogenies. Immunity 37:412-425.
58. Moody MA, Gao F, Gurley TC, Amos JD, Kumar A, Hora B, Marshall DJ, Whitesides JF, Xia SM, Parks R, Lloyd KE, Hwang KK, Lu X, Bonsignori M, Finzi A, Vandergrift NA, Alam SM, Ferrari G, Shen X, Tomaras GD, Kamanga G, Cohen MS, Sam NE, Kapiga S, Gray ES, Tumba NL, Morris L, Zolla-Pazner S, Gorny MK, Mascola JR, Hahn BH, Shaw GM, Sodroski JG, Liao HX, Montefiori DC, Hraber PT, Korber BT, Haynes BF. 2015. Strain-Specific V3 and CD4 Binding Site Autologous HIV-1 Neutralizing Antibodies Select Neutralization-Resistant Viruses. Cell Host Microbe 18:354-362.
59. Horwitz JA, Bar-On Y, Lu CL, Fera D, Lockhart AAK, Lorenzi JCC, Nogueira L, Golijanin J, Scheid JF, Seaman MS, Gazumyan A, Zolla-Pazner S, Nussenzweig MC. 2017. Non-neutralizing Antibodies Alter the Course of HIV-1 Infection In Vivo. Cell 170:637-648 e610.
60. Alsahafi N, Ding S, Richard J, Markle T, Brassard N, Walker B, Lewis GK, Kaufmann DE, Brockman MA, Finzi A. 2016. Nef Proteins from HIV-1 Elite Controllers Are Inefficient at Preventing Antibody-Dependent Cellular Cytotoxicity. J Virol 90:2993-3002.

61. Prevost J, Zoubchenok D, Richard J, Veillette M, Pacheco B, Coutu M, Brassard N, Parsons MS, Ruxrungtham K, Bunupuradah T, Tovanabutra S, Hwang KK, Moody MA, Haynes BF, Bonsignori M, Sodroski J, Kaufmann DE, Shaw GM, Chenine AL, Finzi A. 2017. Influence of the Envelope gp120 Phe 43 Cavity on HIV-1 Sensitivity to Antibody-Dependent Cell-Mediated Cytotoxicity Responses. J Virol 91.
62. Prevost J, Richard J, Medjahed H, Alexander A, Jones J, Kappes JC, Ochsenbauer C, Finzi A. 2018. Incomplete Downregulation of CD4 Expression Affects HIV-1 Env Conformation and Antibody-Dependent Cellular Cytotoxicity Responses. J Virol 92.
63. Madhavi V, Kulkarni A, Shete A, Lee WS, McLean MR, Kristensen AB, Ghate M, Wines BD, Hogarth PM, Parsons MS, Kelleher A, Cooper DA, Amin J, Emery S, Thakar M, Kent SJ, Group ES. 2017. Effect of Combination Antiretroviral Therapy on HIV-1-specific Antibody-Dependent Cellular Cytotoxicity Responses in Subtype B- and Subtype C-Infected Cohorts. J Acquir Immune Defic Syndr 75:345-353.
64. Gohain N, Tolbert WD, Acharya P, Yu L, Liu T, Zhao P, Orlandi C, Visciano ML, Kamin-Lewis R, Sajadi MM, Martin L, Robinson JE, Kwong PD, DeVico AL, Ray K, Lewis GK, Pazgier M. 2015. Cocrystal Structures of Antibody N60-i3 and Antibody JR4 in Complex with gp120 Define More Cluster A Epitopes Involved in Effective Antibody-Dependent Effector Function against HIV-1. J Virol 89:8840-8854.
65. Huang CC, Venturi M, Majeed S, Moore MJ, Phogat S, Zhang MY, Dimitrov DS, Hendrickson WA, Robinson J, Sodroski J, Wyatt R, Choe H, Farzan M, Kwong PD. 2004. Structural basis of tyrosine sulfation and VH-gene usage in antibodies that recognize the HIV type 1 coreceptor-binding site on gp120. Proc Natl Acad Sci U S A 101:2706-2711.
66. Zhang Y, Guo J, Huang L, Tian J, Yao X, Liu H. 2018. The molecular mechanism of two coreceptor binding site antibodies X5 and 17b neutralizing HIV-1: Insights from molecular dynamics simulation. Chem Biol Drug Des 92:1357-1365.
67. Huang CC, Tang M, Zhang MY, Majeed S, Montabana E, Stanfield RL, Dimitrov DS, Korber B, Sodroski J, Wilson IA, Wyatt R, Kwong PD. 2005. Structure of a V3-containing HIV-1 gp120 core. Science 310:1025-1028.
68. Ramsland PA, Farrugia W, Bradford TM, Sardjono CT, Esparon S, Trist HM, Powell MS, Tan PS, Cendron AC, Wines BD, Scott AM, Hogarth PM. 2011. Structural basis for Fc gammaRIIa recognition of human IgG and formation of inflammatory signalling complexes. J Immunol 187:3208-3217.
69. Richard J, Veillette M, Batraville LA, Coutu M, Chapleau JP, Bonsignori M, Bernard N, Tremblay C, Roger M, Kaufmann DE, Finzi A. 2014. Flow cytometry-based assay to study HIV-1 gp120 specific antibody-dependent cellular cytotoxicity responses. J Virol Methods 208:107-114.
70. Klein JS, Bjorkman PJ. 2010. Few and far between: how HIV may be evading antibody avidity. PLoS Pathog 6:e1000908.

71. Fontaine J, Chagnon-Choquet J, Valcke HS, Poudrier J, Roger M. 2011. High expression levels of B lymphocyte stimulator (BLyS) by dendritic cells correlate with HIV-related B-cell disease progression in humans. Blood 117:145-155.
72. Fontaine J, Coutlee F, Tremblay C, Routy JP, Poudrier J, Roger M. 2009. HIV infection affects blood myeloid dendritic cells after successful therapy and despite nonprogressing clinical disease. J Infect Dis 199:1007-1018.
73. Peretz Y, Ndongala ML, Boulet S, Boulassel MR, Rouleau D, Cote P, Longpre D, Routy JP, Falutz J, Tremblay C, Tsoukas CM, Sekaly RP, Bernard NF. 2007. Functional T cell subsets contribute differentially to HIV peptide-specific responses within infected individuals: correlation of these functional T cell subsets with markers of disease progression. Clin Immunol 124:57-68.
74. Kamya P, Boulet S, Tsoukas CM, Routy JP, Thomas R, Cote P, Boulassel MR, Baril JG, Kovacs C, Migueles SA, Connors M, Suscovich TJ, Brander C, Tremblay CL, Bernard N. 2011. Receptor-ligand requirements for increased NK cell polyfunctional potential in slow progressors infected with HIV-1 coexpressing KIR3DL1*h/*y and HLA-B*57. J Virol 85:5949-5960.
75. Richard J, Veillette M, Ding S, Zoubchenok D, Alsahafi N, Coutu M, Brassard N, Park J, Courter JR, Melillo B, Smith AB, 3rd, Shaw GM, Hahn BH, Sodroski J, Kaufmann DE, Finzi A. 2016. Small CD4 Mimetics Prevent HIV-1 Uninfected Bystander CD4 + T Cell Killing Mediated by Antibody-dependent Cell-mediated Cytotoxicity. EBioMedicine 3:122-134.
76. Harris LJ, Skaletsky E, McPherson A. 1998. Crystallographic structure of an intact IgG1 monoclonal antibody. J Mol Biol 275:861-872.
77. Sondermann P, Huber R, Oosthuizen V, Jacob U. 2000. The 3.2-A crystal structure of the human IgG1 Fc fragment-Fc gammaRIII complex. Nature 406:267-273.

CHAPTER III

Antibody-induced internalization of HIV-1 Env proteins limits the surface expression of the closed conformation of Env

Sai Priya Anand, Jonathan Grover, William D. Tolbert, Jérémie Prévost, Jonathan Richard, Shilei Ding, Sophie Baril, Halima Medjahed, David T. Evans, Marzena Pazgier, Walther Mothes, and Andrés Finzi

3.1 Preface to Chapter 3

As described in Chapter 1, HIV-1 has evolved to acquire several strategies to limit the exposure of its Env on the surface of infected cells. Interestingly, it has been reported that the interaction of some antibodies with viral glycoproteins expressed on the surface of Respiratory Syncytial virus (RSV) (383) and Feline Coronavirus (385) infected cells accelerates glycoprotein internalization and decreases its exposure to the immune system. These studies suggested that the stability of antigen-antibody complexes on the surface of infected cells could contribute to modulating humoral responses against infected cells. The applicability of this phenotype in the context of HIV-1-infected cells was unclear in the field and in this chapter we attempt to uncover a phenotype of antibody-induced HIV-1 Env internalization. The results of this study have important implications in understanding underlying causes that could hinder ADCC responses to clear HIV-1-infected cells.

3.2 Abstract

To minimize immune responses against infected cells, HIV-1 limits the surface expression of its envelope glycoprotein (Env). Here we demonstrate that this mechanism is specific for the Env conformation and affects the efficiency of ADCC. Using flow cytometry and confocal microscopy we show that broadly neutralizing antibodies (bNAbs) targeting the 'closed' conformation of Env induce its internalization from the surface. In contrast, non-neutralizing antibodies (nNAbs) are displayed on the cell surface for prolonged period of times. The bNAb-induced Env internalization can be decreased by blocking dynamin function, which translates into higher susceptibility of infected cells to antibody-dependent cellular cytotoxicity (ADCC). Our results suggest that antibody-mediated Env internalization is a mechanism used by HIV-1 to evade immune responses against the 'closed' conformation of Env expressed on HIV-1-infected cells.

3.3 Introduction

Human immunodeficiency virus type 1 (HIV-1) envelope glycoproteins (Env) are exposed on the surface of viral particles and infected cells. Antibodies (Abs) targeting Env can therefore either neutralize viral particles, or mediate different immune responses including antibody-dependent cellular cytotoxicity (ADCC) against infected cells. ADCC has been associated with decreased HIV-1 transmission and disease progression (1-5). Antibodies with ADCC activity, in the presence of low plasma IgA Env-specific Abs, inversely correlated with HIV-1 acquisition in the partially successful Thai RV144 vaccine trial (6).

HIV-1 has evolved several mechanisms to avoid the elimination of infected cells via ADCC. Env in its 'open' CD4-bound conformation is particularly vulnerable to ADCC activity (7-9). HIV-1 keeps Env in its 'closed' (State 1) conformation on the surface of infected cells by preventing the accumulation of the CD4 receptor via Nef and Vpu-mediated downregulation (9-11). The virus also evades ADCC by antagonizing BST-2 (9, 12-14) through its Vpu accessory protein. In addition to these evasion mechanisms, the virus minimizes Env accumulation at the cell surface by internalizing Env (15). HIV-1 Env has a long C-terminal cytoplasmic domain, which is involved in the regulation of Env trafficking and contains several endocytic signals, including membrane-proximal tyrosine-based sorting motifs and dileucine motifs (16-18). Mutations of these motifs have been shown to result in increased cell-surface expression of Env, which correlates with increased ADCC responses (15, 19, 20). Internalizing envelope glycoproteins from the cell surface to avoid humoral immune responses does not appear to be restricted to HIV-1; Equine Herpesvirus-1 (21) and Pseudorabies virus (22) also downregulate their envelope glycoproteins to avoid antibody-dependent complement-mediated lysis. Thus, internalization of viral envelope glycoproteins from the surface of infected host cells appears to be a mechanism employed by many viruses to minimize recognition by the immune system (23-26).

The ability of antigen-Ab complexes to remain on the surface of infected cells might be another factor modulating humoral responses against different viruses. It has been reported previously that the interaction of some Abs with Env glycoproteins expressed on the surface of

Respiratory Syncytial virus (RSV) (27) and Feline Coronavirus (28) infected cells accelerates their internalization and decreases their exposure to the immune system. Here we evaluated the fate of HIV-1 Env expression at the surface of cells upon antibody binding and made the surprising observation that the binding of broadly neutralizing antibodies (bNAbs) but not non-neutralizing antibodies (nNAbs) induced Env-Ab complex internalization and reduced ADCC responses mediated by bNAbs. These data indicate that HIV-1 specifically evades immune responses against the closed conformation of Env.

3.4 Material and Methods

Plasmids and cell lines

293T human embryonic kidney cells (American Type Culture Collection) were maintained at 37°C under 5% CO_2 in Dulbecco's modified Eagle's medium (Invitrogen) containing 5% fetal bovine serum (Sigma) and 100µg/ml of penicillin-streptomycin (Mediatech). The E168K mutation was introduced into the previously described pcDNA3.1 expressing codon-optimized HIV-1 JRFL envelope glycoproteins (34) using the QuickChange II XL site-directed mutagenesis protocol (Stratagene). Other plasmids used to transfect 293T cells include pcDNA3.1 human CD4 expressor and pIRES-GFP vector (9, 43). The pCAGGS codon-optimized JR-FL gp160 plasmid was a kind gift from Joseph Sodroski (63). The pECFP Lamin B Receptor plasmid was a kind gift from Melissa Rolls and Tom Rapoport (64).

Isolation of Primary cells, Viral production, and Infections

CD4+ T lymphocytes were purified from resting PBMCs by negative selection and activated as previously described (8, 9). Briefly, PBMC were obtained by leukapheresis from at least five different healthy HIV-uninfected individuals. CD4+ T lymphocytes were purified by negative selection using immunomagnetic beads as per the manufacturer's instructions (StemCell Technologies). CD4+ T lymphocytes were activated with phytohemagglutinin-L (10 µg/ mL) for 48 hours and then maintained in RPMI 1640 complete medium supplemented with rIL-2 (100 U/mL).

To ensure similar levels of infection between viruses, vesicular stomatitis viruses G (VSVG)-pseudotyped viruses were produced and titrated as described (8). Viruses were used to infect activated primary CD4 T cells from healthy HIV-1 negative donors by spin infection at 800 x g for 1 hour in 96-well plates at 25°C.

Antibodies

Anti-HIV-1 gp120 mAbs recognizing CD4-induced epitopes (A32, 17b; obtained from NIH AIDS Reagent Program), the outer domain (2G12; obtained from NIH AIDS Reagent Program) and the gp120-gp41 interface (PGT151; obtained from International AIDS Vaccine Initiative [IAVI]) were conjugated with Alexa-Fluor 488 or 594 (Thermo Fisher Scientific) as

per the manufacturer's protocol and used for confocal microscopy analyses of cell-surface staining of 293T-transfected cells. Additionally, the following anti-Env mAbs were also used for cell-surface staining: PGT126 (IAVI), PG9 (Polymun), N5-i5, N12-i2. Fab fragments were generated by papain digest of the corresponding antibody. Briefly purified IgGs were incubated at 37°C overnight with immobilized papain (G Biosciences) and then filtered to remove the papain. Fabs were separated from undigested IgG and Fc by passage over a HiTrap protein A column (GE Healthcare) equilibrated with phosphate buffered saline (PBS) pH 7.2. Flow through fractions were concentrated and further purified by gel filtration chromatography on a Superdex 200 gel filtration column (GE Healthcare) equilibrated in 25 mM Tris-HCl pH 8.5 and 150 mM sodium chloride. Fab fractions with elution times roughly correlating to 50 kDa were combined and concentrated prior to use. Goat anti-human Alexa Fluor-647 secondary Ab (Thermo Fisher Scientific) was used to determine overall antibody binding and AquaVivid (Thermo Fisher Scientific) as a viability dye. Mouse monoclonal EEA1 (14/EEA1) and LAMP1 (H4A3) antibodies were obtained from BD Transduction Laboratories. Alexa-Fluor 568 goat anti-mouse was obtained from ThermoFisher Scientific.

Flow Cytometry Analysis of Cell Surface Staining

Cell-surface staining was performed as previously described (8, 9). Cells infected with HIV-1 primary isolates were identified by intracellular staining of HIV-1 Gag using the Cytofix/Cytoperm Fixation/Permeabilization Kit (BD Biosciences) and the PE-conjugated anti-Gag mAb, clone KC57 (Beckman Coulter). The percentage of infected cells (Gag+ or GFP+ cells) was determined by gating the living cell population based on viability dye staining with AquaVivid (Thermo Fisher Scientific). For the cell surface staining of transfected 293T cells, 3x105 293T cells were transfected by the calcium phosphate method with the Env-expressing plasmids along with a pIRES-GFP vector, at a ratio of 2 μg of pcDNA3.1 or JRFL Env to 0.5 μg of green fluorescence protein (GFP). Sixteen hours post-transfection, cells were washed with fresh medium and cell surface staining was carried out twenty-found hours later. Samples were analyzed on an LSRII cytometer (BD Biosciences), and data analysis was performed using FlowJo vX.0.7 (Tree Star).

Antibody-induced internalization assay

48 h post-infection or post-transfection, HIV-1-infected primary CD4+ T cells or Env-transfected 293T cells, respectively, were incubated with 5μg/mL anti-Env antibodies for 30 mins at 4°C. Excess antibodies were washed three times with cold serum-free media. This was followed by incubation at 37°C to start the internalization process. After different time points, cells were fixed with 2% paraformaldehyde. For flow cytometry analyses, to visualize remaining antigen-antibody complexes on the cell surface, cells were stained with a goat anti-human conjugated with Alexa Fluor-647 secondary Ab (Thermo Fisher Scientific). As a control, cells were fixed after 4°C incubation (Time point 0 min). Dead cells were excluded by staining the cells with live/dead fixable AquaVivid stain (Thermo Fisher Scientific). The reduction in surface expression for a given time point was normalized by calculating with the following equation: [(Mean Fluorescence Intensity at *X* min)/(Mean Fluorescence Intensity 0 min)]x100.

For confocal microscopy analyses, 293T cells were plated in 10mm MatTek dishes with #0 coverslip bottoms. 293T cells were transfected with 1μg pCAGGS JR-FL Env (codon-optimized) plasmid and 100ng Lamin B Receptor-CFP plasmid (to locate the nuclear envelope) with or without 1μg human CD4 plasmid using Fugene 6 reagent according to the manufacturer's instructions. At 48 hours post transfection, cells were incubated with prelabeled antibodies diluted 1:250 in fresh media for the indicated amount of time, washed once with PBS + 0.5% BSA, and fixed with PBS + 4% paraformaldehyde (PFA) for 10 minutes. Cells were then placed in PBS + 0.01% sodium azide prior to imaging. For the 0-minute control, cells were fixed prior to antibody staining for 1 hour in PBS + 0.5% BSA. For endosomal staining, cells were first incubated with prelabeled 2G12 antibody for 180 minutes, followed by fixation, permeabilization (5 minutes with 0.1% TritonX-100), and staining for endogenous EEA1 or LAMP1.

Internalization inhibition assay

To inhibit antibody-induced internalization, a dynamin inhibitor was used before and during the internalization assay. Myristoylated dynamin inhibitory peptide (DIP, Tocris Bioscience)

was diluted in water prior to dilution in serum-free cell culture medium. After 1 hour of pre-treatment of infected or transfected cells with 50μM and 40μM DIP, respectively, at 37°C, fresh inhibitor was added to the cells together with antibodies to allow for their attachment and then during incubations at 37°C to induce their internalization. As a control, 20μg/mL of biotinylated transferrin was used to confirm the effectiveness of DIP and this was visualized with streptavidin-AlexaFluor-647 (data not shown).

Antibody-dependent cellular cytotoxicity assay

Measurement of ADCC using the FACS-based assay was performed at 48h post-infection as previously described (9, 47). Briefly, infected primary CD4+ T cells were stained with AquaVivid viability dye and cell proliferation dye (eFluor670; eBioscience) and used as target cells. Next, the target cells were treated with and without 50μM of DIP for 1 hour at 37°C. Autologous PBMC effectors cells, stained with another cellular marker (cell proliferation dye eFluor450; eBioscience), were added at an effector: target ratio of 10:1 in 96-well V-bottom plates (Corning). DIP was washed out before incubating the infected cells with effector cells to guarantee that the drug affected only the target cells and not the effector cells. 5μg/ml of mAbs were added to appropriate wells and cells were incubated for 15 min at room temperature. Subsequently the plates were centrifuged for 1 min at 300 x g, and incubated at 37°C, 5% CO_2 for 5 hours before being fixed in a 2% PBS-formaldehyde solution. Samples were acquired on an LSRII cytometer (BD Biosciences) and data analysis was performed using FlowJo vX.0.7 (Tree Star). The percentage of cytotoxicity was calculated with the following formula: (% of GFP+ cells in Targets plus Effectors) − (% of GFP+ cells in Targets plus Effectors plus mAbs)/(% of GFP+ cells in Targets) by gating on infected live target cells.

Confocal microscopy

Confocal imaging was performed using a Nikon Eclipse TE2000-E microscope equipped with 444, 488, and 561nm lasers, a Yokogawa CSU 10 spinning disc confocal laser scanning unit, and an Andor Zyla sCMOS camera. Images were analyzed manually using ImageJ (65). Briefly, regions of interest were drawn around entire cells and cytoplasmic regions. Total fluorescence for regions of interest were calculated as area x (mean – minimum). Surface

fluorescence was calculated as total minus cytoplasmic. Values are represented as ratios of surface / total and cytoplasmic / total, normalized to the 0min time point. Average intensity and area were measured and used to calculate total fluorescence and cytoplasmic fluorescence. Minimum intensity was subtracted from mean intensity to correct for cytoplasmic background fluorescence. Colocalization between Env and endosomal markers was quantified with the Pearson Correlation function using the JACoP plugin (66) for ImageJ.

Statistical Analyses

Statistics were analyzed using GraphPad Prism version 6.01 (GraphPad, San Diego, CA, USA). Every data set was tested for statistical normality, and this information was used to apply the appropriate (parametric or nonparametric) statistical test. P values of <0.05 were considered significant; significance values are indicated as * $p<0.05$, ** $p<0.01$, *** $p<0.001$, **** $p < 0.0001$.

3.5 Results

bNAbs induce Env internalization from the cell surface

To determine if Env-Abs complexes can remain stable over time at the surface of infected cells, we selected nine anti-Env Abs that recognize different conformations and epitopes of Env. These Abs target different sites on Env, such as the gp120-gp41 interface (PGT151) (29), glycans on the gp120 outer domain (2G12) (30), the V1/V2 apex (PG9) (31) and V3 glycans (PGT121, PGT126) (32) as well as CD4-induced (CD4i) targeting epitopes, including the co-receptor binding site (CoRBS; 17b, N12-i2) and the cluster A region in the gp120 inner domain (A32, N5-i5) (33). This panel of antibodies was selected because it can distinguish 'closed' versus 'open' trimers. Indeed, PGT151, PG9, PGT121 and PGT126 preferentially recognize the 'closed' trimer (34-37) whereas CD4i Abs 17b, N12-i2, A32 and N5-i5 binds epitopes only exposed in the 'open' trimer. 2G12 is an antibody that can recognize both forms of trimers (9, 37) but has a preference for the 'closed' form (36).

Primary CD4+ T cells were infected with a previously reported wild-type (wt) HIV-1 NL4.3 strain encoding a *gfp* reporter gene and an R5-tropic (ADA) envelope (9). Infected cells were identified based on GFP expression (GFP+). Cells were first incubated with monoclonal Abs at 4°C for thirty minutes, washed to remove excess antibody, and then incubated at 37°C for internalization to occur. After incubation at 37°C for different time intervals, Env-Ab complexes remaining at the cell surface were visualized with a fluorescent secondary anti-human antibody by flow cytometry. Under these experimental settings we observed that the binding of bNAbs (PG126, PGT151, PG9 and 2G12) significantly declined over time indicating Env internalization (**Figure 3.1**). In contrast, binding of the nNAbs (17b, N12-i2, A32 and N5-i5) was fairly steady. The reduction of cell-surface levels of Env was ~60% after six hours of incubation with PGT126, PG9, PGT151 and 2G12 at 37°C. Conversely, binding to surface Env was only reduced by ~20% upon incubation for the same time period at 37°C with N12-i2, N5-i5, A32 and 17b (**Figure 3.1 B and C**).

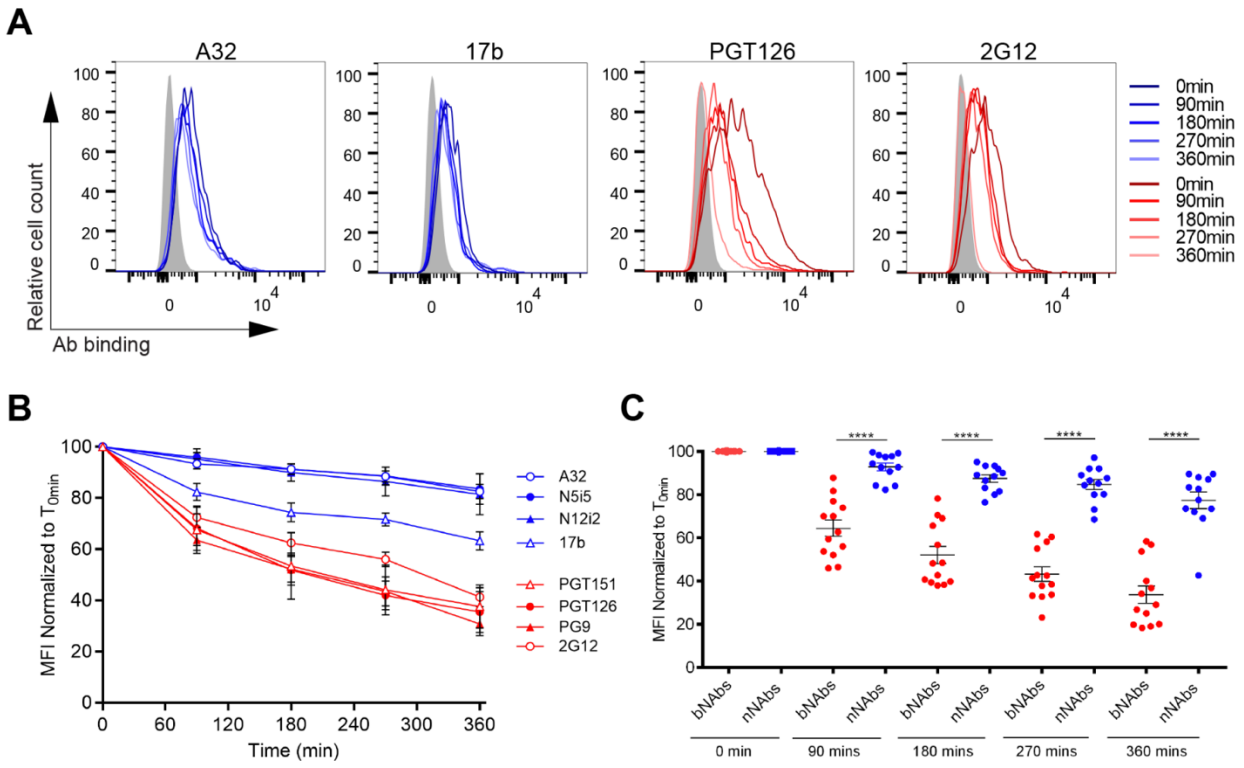

Figure 3.1. Broadly-neutralizing antibodies but not non-neutralizing antibodies induce Env internalization. A panel of bNAbs (PGT121, PGT126, PG9, 2G12) and nNAbs (A32, N5-i5, 17b, N12-i2) were used to stain the surface of primary CD4+ T cells infected with the NL4.3 GFP ADA- virus. (**A**) Histograms depicting representative staining of infected cells (GFP+) with A32, 17b, PGT126 and 2G12 mAbs over time or with mock infected cells (grey). (**B, C**) Quantification of remaining antibody-Env complexes on the cell-surface over different time points is expressed as percentage of MFI relative to the 0-minute time control. Error bars indicate mean +/- SEM. Statistical significance was tested using an unpaired t-test or a Mann-Whitney U test based on statistical normality (****p<0.0001).

To evaluate if this phenotype was restricted to the infectious molecular clone used, we infected primary CD4+ T cells with the transmitted/founder (T/F) virus CH58 (CH58 T/F) and performed the same experiments described above with the exception that infected cells were identified by intracellular Gag staining. Similar to what we obtained with NL4.3 ADA infected cells (**Figure 3.1**), bNAbs reduced by ~80% cell surface levels of CH58T/F Env after six hours of incubation at 37°C, whereas incubation with nNAbs only reduced Env by ~20% during the same time period (**Figure 3.2**).

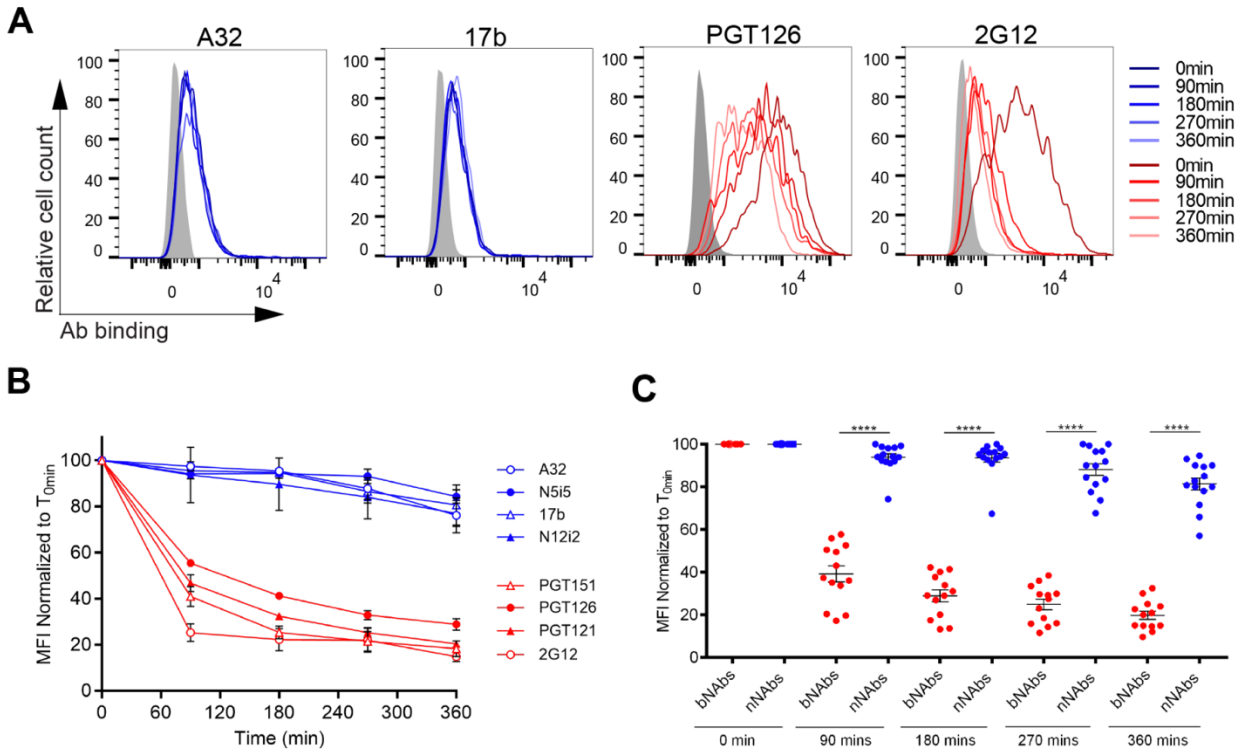

Figure 3.2. Binding of bNAbs but not nNAbs decreases Env expression from the surface of T/F virus-infected cells.
A panel of bNAbs (PGT121, PGT126, PG9, 2G12) and nNAbs (A32, N5-i5, 17b, N12-i2) were used to stain the surface of primary CD4+ T cells infected with CH58 T/F virus. (**A**) Histograms depicting representative staining of infected cells (Gag+) with A32, 17b, PGT126 and 2G12 mAbs over time or with mock infected cells. (**B, C**) Quantification of remaining antibody-Env complexes on the cell-surface over different time points is expressed as percentage of MFI relative to the 0-minute time control. Error bars indicate mean +/- SEM. Statistical significance was tested using an unpaired t-test or a Mann-Whitney U test based on statistical normality (****p<0.0001).

It is now well established that the conformation of Env at the cell surface influences antibody binding and ADCC responses (38-40). Non-neutralizing antibodies and bNAbs target different Env conformations, with most bNAbs preferentially recognizing Env in its 'closed' conformation (State 1) (36) whereas the nNAbs herein target epitopes that are only exposed upon Env interaction with CD4 (9, 37, 41, 42). To verify if the differences in cell-surface reduction of Env between bNAbs and nNAbs was due to their differential recognition of infected cells, we infected primary CD4+ T cells with NL4.3 ADA defective for Nef and Vpu accessory proteins (Nef-Vpu-) that fails to downregulate CD4. This virus was used to present Env in its CD4-bound 'open' conformation at the surface of infected cells and enhance recognition of infected cells by the nNAbs used in this study (8, 9) (**Figure 3.3**). As expected, deletion of Vpu enhances the overall levels of Env at the cell surface as measured by 2G12, known to bind to both 'open' and 'closed' conformations of Env (7, 9, 43) (**Figure 3.3A**). This phenomenon has been well established and is due to the accumulation of BST-2-trapped viral particles at the cell surface which results in Env accumulation (9, 12, 14). In agreement with their CD4-induced nature, the recognition of infected cells by the nNAbs tested (A32, 17b, N12-i2, N5-i5) was dramatically enhanced by deletion of Nef and Vpu. Deletion of these accessory genes impair the ability of HIV-1 to downregulate CD4 from the cell surface, thus resulting in increased Env-CD4 interactions and the subsequent exposure of CD4i epitopes (**Figure 3.3B**) (9). Despite their improved capacity to recognize Env at the surface of Nef-Vpu- infected cells, nNAbs only reduced Env from the cell surface by ~20% after six hours, while bNAbs reduced Env levels by ~60% within the same time period (**Figure 3.4**). Altogether these results indicate that the conformation specificity of antibody-mediated internalization of Env is not affected by changes in surface expression and that Nef and Vpu accessory proteins are not involved in the bNAb-mediated reduction of Env from the cell surface.

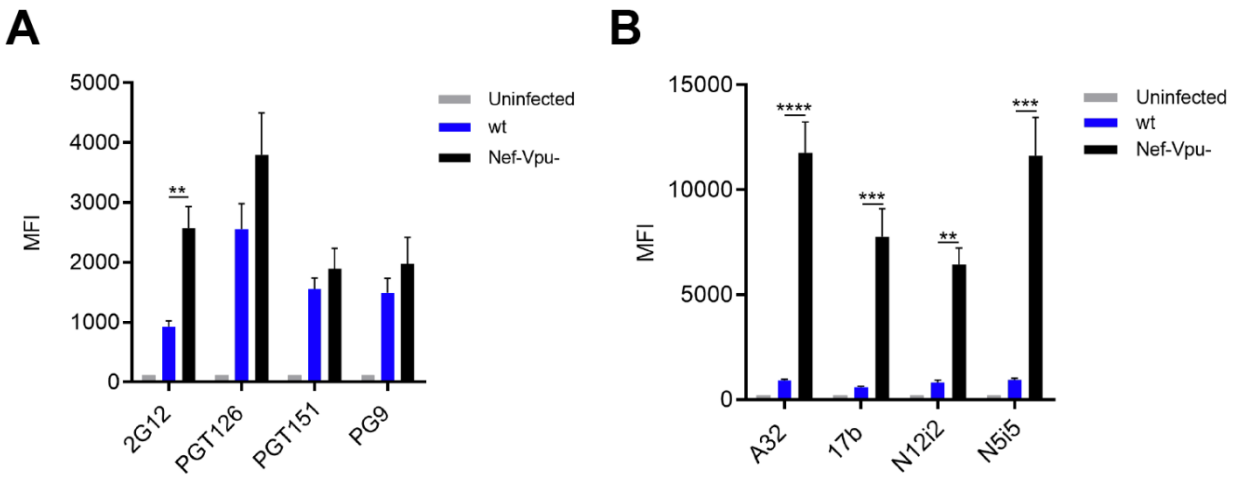

Figure 3.3. Nef and Vpu protect infected cells from recognition by CD4i antibodies. Primary CD4+ T cells infected with NL4.3 GFP ADA-based viruses either wt or defective for Nef and Vpu expression (Nef-Vpu-) were stained with (**A**) bNAbs (2G12, PGT126, PGT151, PG9) or (**B**) anti-cluster A (A32, N5-i5) and CoRBS (N12-i2, 17b) antibodies. Error bars indicate mean +/- SEM. Statistical significance was tested using an unpaired t-test or a Mann-Whitney U test based on statistical normality (**p<0.01, ***p<0.001, ****p<0.0001).

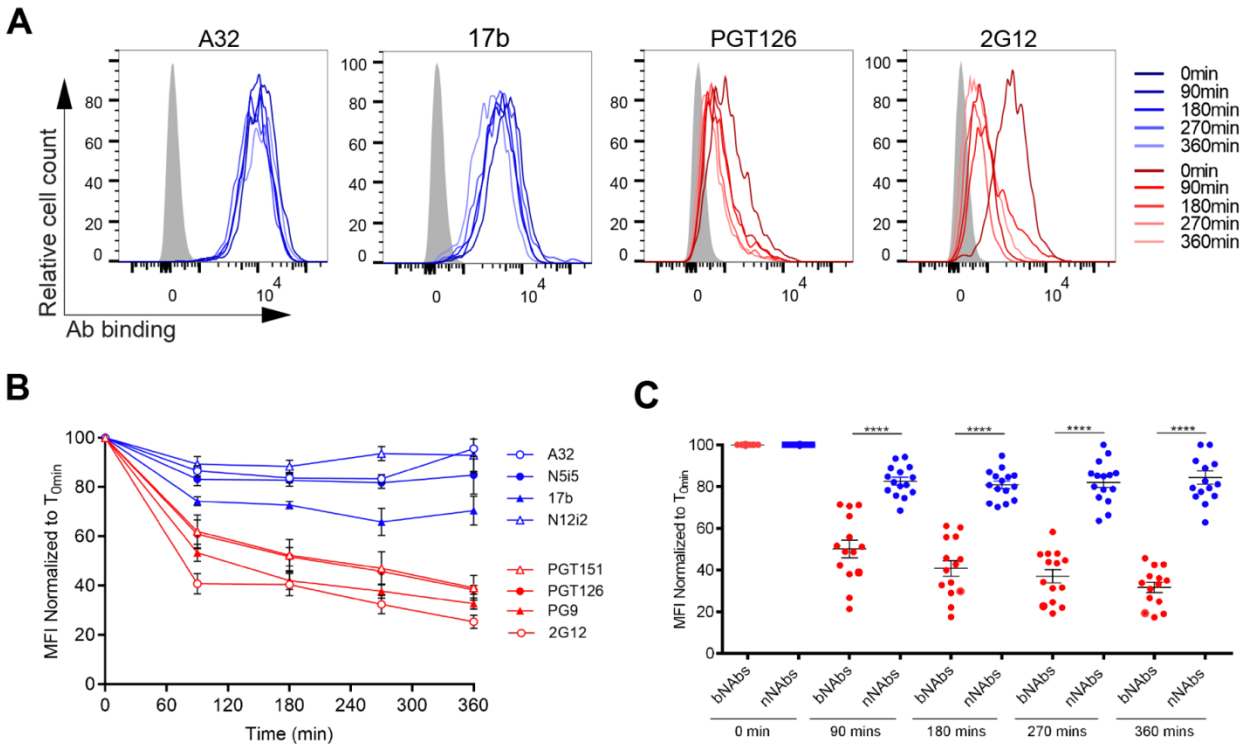

Figure 3.4. Nef and Vpu are dispensable for bNAbs-mediated Env internalization. Cell-surface staining of primary CD4+ T cells infected with NL4.3 GFP ADA-based virus defective for Nef and Vpu expression using a panel of bNAbs (PGT126, PGT151, PG9, 2G12) and nNAbs (A32, N5-i5, 17b, N12-i2). (**A**) Histograms depicting representative staining of infected cells (GFP+) with A32, 17b, PGT126 and 2G12 mAbs over time or with mock infected cells (grey). (**B, C**) Quantification of remaining antibody-Env complexes on the cell-surface over different time points is expressed as percentage of MFI relative to the 0-minute time control. Error bars indicate mean +/- SEM. Statistical significance was tested using an unpaired t-test or a Mann-Whitney U test based on statistical normality (****p<0.0001).

Antibody-induced internalization of cell surface-expressed HIV-1 Env

To confirm that Env-bNAb complexes were internalized upon incubation at 37°C, we performed confocal microscopy studies in parallel to flow cytometry. Since primary CD4+ T cells are small and poorly adherent, we used HEK 293T cells for these studies. 293T cells were transfected with a primary Tier 2 Env (JRFL) and incubated them forty-eight hours post transfection with Alexa-Fluor conjugated bNAbs (2G12, PG9 and PGT151) or nNAbs (17b, A32) for various time-points at 37°C before fixing, and analysis by flow cytometry and confocal imaging. Since A32 and 17b don't recognize the unliganded EnvJRFL, Env was co-transfected together with the CD4 receptor to trigger the exposure of the CD4i epitopes recognized by these nNAbs (9, 43). Flow cytometry confirmed that the bNAbs 2G12, PG9 and PGT151 were much faster internalized as compared to the nNAbs 17b and A32, thus pheno-copying the results from T cells (**Figure 3.5A**). Parallel confocal imaging demonstrated that, upon the addition of bNAbs PGT151 and 2G12, Env moved from the plasma membrane into intracellular compartments after sixty minutes of incubation at 37°C. In contrast, the binding of A32 and 17b didn't change the cell surface localization of Env (**Figure 3.5B-C**). These results were consistent with those obtained using infected primary CD4+ T cells (**Figures 3.1, 3.2 and 3.4**). Interestingly, the quantification of internalization measured by microscopy correlated well with the quantification of cell surface Env measured by flow cytometry (**Figure 3.5D**), suggesting that both assays measure Env internalization. Further supporting this possibility, we observed that bNAb-induced Env reduction from the cell surface was blocked if cells were incubated at 4°C for the entirety of the internalization assay, a temperature known to block molecular trafficking events (**Figure 3.6**).

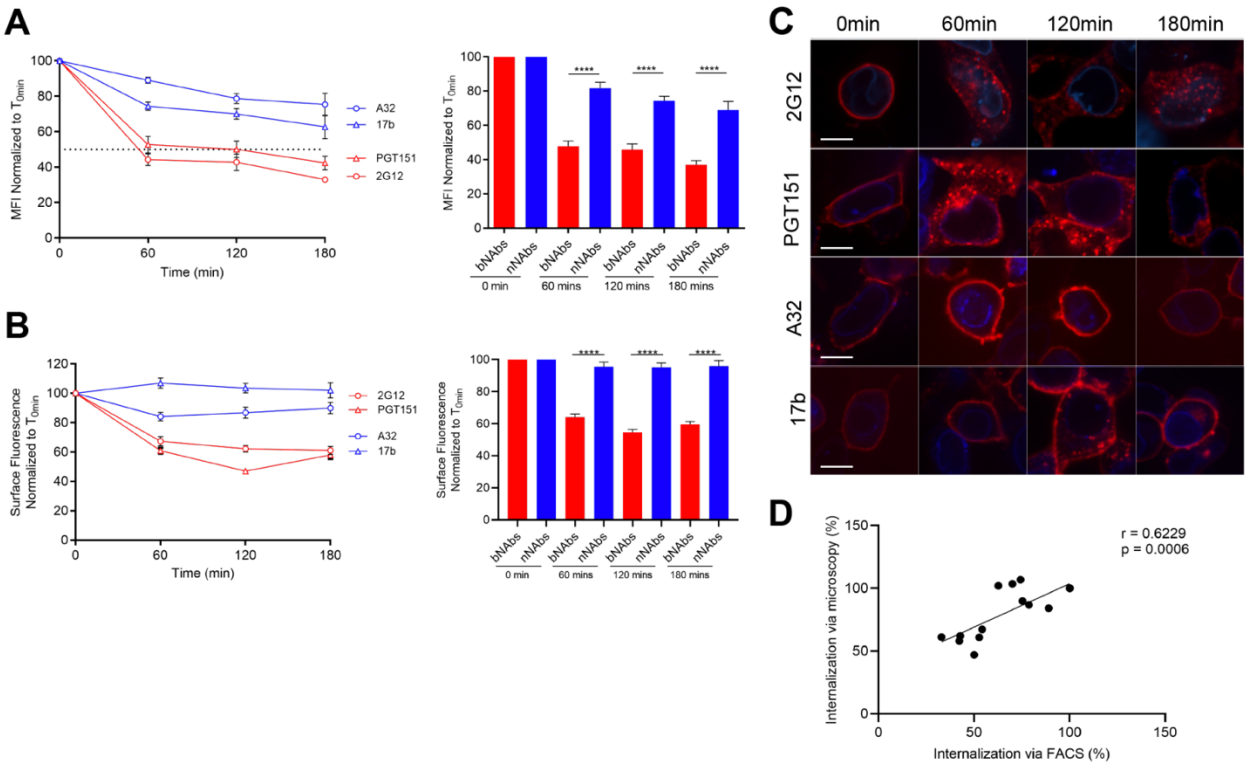

Figure 3.5. Antibody-induced internalization of Env from the surface of transfected cells. 293T cells were transfected with plasmids encoding HIV-1_{JRFL} Env alone or together with human CD4 receptor to expose CD4i epitopes. Env expressed in the absence of CD4 were visualized with 2G12 and PGT151. Env co-expressed with CD4 was visualized with 17b and A32. (**A**) Flow-cytometric analysis of Env internalization from the surface of 293T-transfected cells. The level of the remaining surface-expressed Env after internalization is expressed as percentage of MFI relative to the 0-minute time control. (**B**) Confocal microscopy analysis of antibody-induced internalization. Remaining antibody-Env complexes over different time points is expressed as percentage of surface fluorescence relative to the 0-minute control. (**C**) For confocal microscopy 293T cells were also transfected with the Lamin B Receptor-CFP plasmid (a nuclear envelope marker used to identify transfected cells). Images show the localization of antibody-Env complexes at different time points (0min, 60mins, 120mins and 180mins). Images represent a single confocal z-section through the middle of the cell; 20 cells were imaged per condition and representative images are shown, scale bar, 10μm. (**D**) Correlation of the quantification of Env internalization by confocal microscopy with internalization by flow cytometry using a Pearson correlation test. Error bars indicate mean +/- SEM. Statistical significance was tested using an unpaired t-test or a Mann-Whitney U test based on statistical normality (***p<0.001, ****p<0.0001).

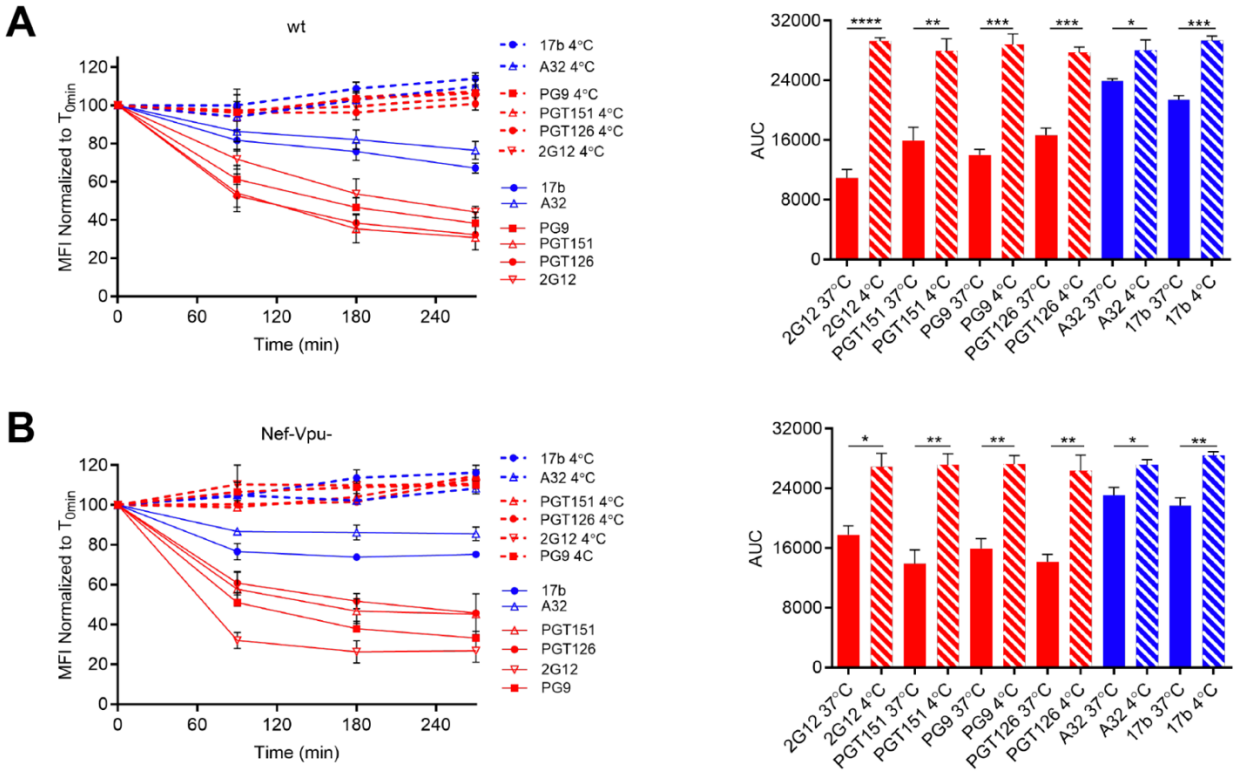

Figure 3.6. bNAb-triggered Env internalization is temperature-dependent manner. Cell-surface staining of primary CD4+ T cells infected with NL4.3 GFP ADA-based viruses either wt (**A**) or defective for Nef and Vpu (Nef-Vpu-) expression (**B**) with A32, 17b, PGT151, PG9 and 2G12 mAbs. (*Left)* Quantification of remaining antibody-Env complexes on the cell-surface over different time points (90mins, 180mins and 270 mins) at 4°C (dotted lines) or 37°C (solid lines) is expressed as percentage of MFI relative to the 0-minute time control. (*Right*) Areas under the curve (AUC) were calculated based on MFI data sets using GraphPad Prism software. Error bars indicate mean +/- SEM. Statistical significance was tested using an unpaired t-test or a Mann-Whitney U test based on statistical normality (*p<0.05, **p<0.01, ***p<0.001, ****p<0.0001).

It has been previously suggested that Ab-mediated crosslinking facilitates internalization of RSV fusion proteins. In this study, RSV Env endocytosis was significantly reduced when Fab fragments were used instead of their full mAbs counterpart (27). To verify whether this was the case for HIV-1 Env, we performed side-by-side comparisons on the ability of full-length Abs versus their Fab fragments to reduce Env levels at the cell surface upon incubation at 37°C, as measured by flow cytometry. A32 and 17b Fab fragments behaved similar to the full-length Abs. However, PG9, PGT151 and 2G12 Fab fragments were significantly less efficient than their IgG counterparts at inducing internalization of Env (**Figure 3.7**). These data suggest that the crosslinking of Env trimers at the cell surface stimulates bNAb-mediated internalization.

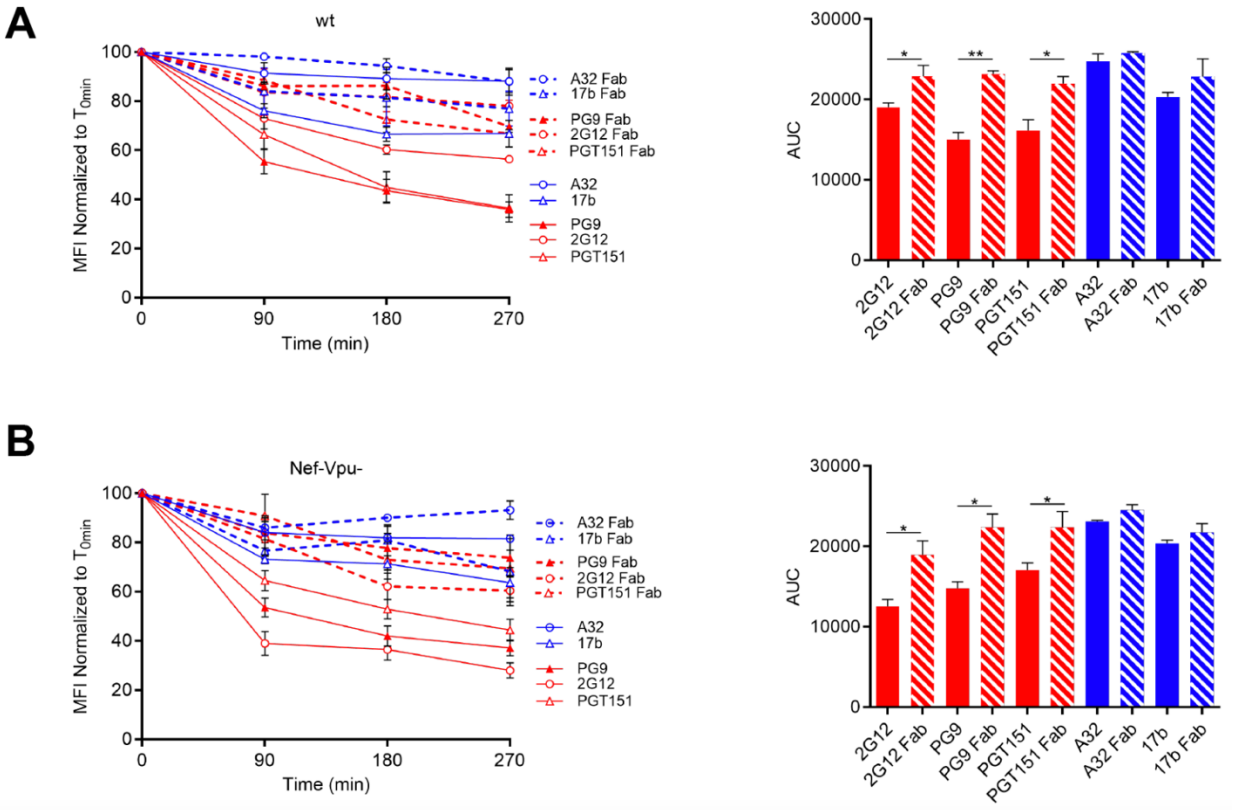

Figure 3.7. Fab fragments reduce the induction of Env internalization.
Cell-surface staining of primary CD4+ T cells infected with NL4.3 GFP ADA (**A**) or defective for Nef and Vpu (Nef-Vpu-) expression (**B**) was performed with A32, 17b, PGT151, PG9 and 2G12 mAbs (solid lines) or their Fab fragments (dotted lines). (*Left*) Quantification of remaining antibody-Env complexes on the cell-surface over different time points (90mins, 180mins and 270mins) is expressed as percentage of MFI relative to the 0-minute time control. (*Right*) Areas under the curve (AUC) were calculated based on MFI data sets using GraphPad Prism software. Error bars indicate mean +/- SEM. Statistical significance was tested using an unpaired t-test or a Mann-Whitney U test based on statistical normality (*p<0.05, **p<0.01).

A dynamin inhibitor attenuates bNAb-induced Env internalization and increases the susceptibility of infected cells to ADCC

To further confirm that internalization was involved in the observed bNAb-induced reduction of Env from the cell surface, we decided to block the function of dynamin, a GTPase implicated in endocytic membrane fission events (44). Primary CD4+ T cells were infected with NL4.3 ADA GFP or CH58 T/F and dynamin was inhibited with the dynamin inhibitory peptide (DIP). This peptide blocks the binding of dynamin to amphiphysin and has been shown to reduce endocytic events (27, 45, 46). Addition of DIP significantly reduced bNAb-induced Env internalization in infected cells as measured by flow cytometry (**Figure 3.8A and B**) and confocal microscopy using Env_{JRFL}-transfected 293T cells (**Figure 3.8C and D**). No statistical differences in the internalization rates of Env bound by nNAbs, with or without added DIP were observed. Thus, this reiterates the observation that the binding of these Abs does not promote Env internalization.

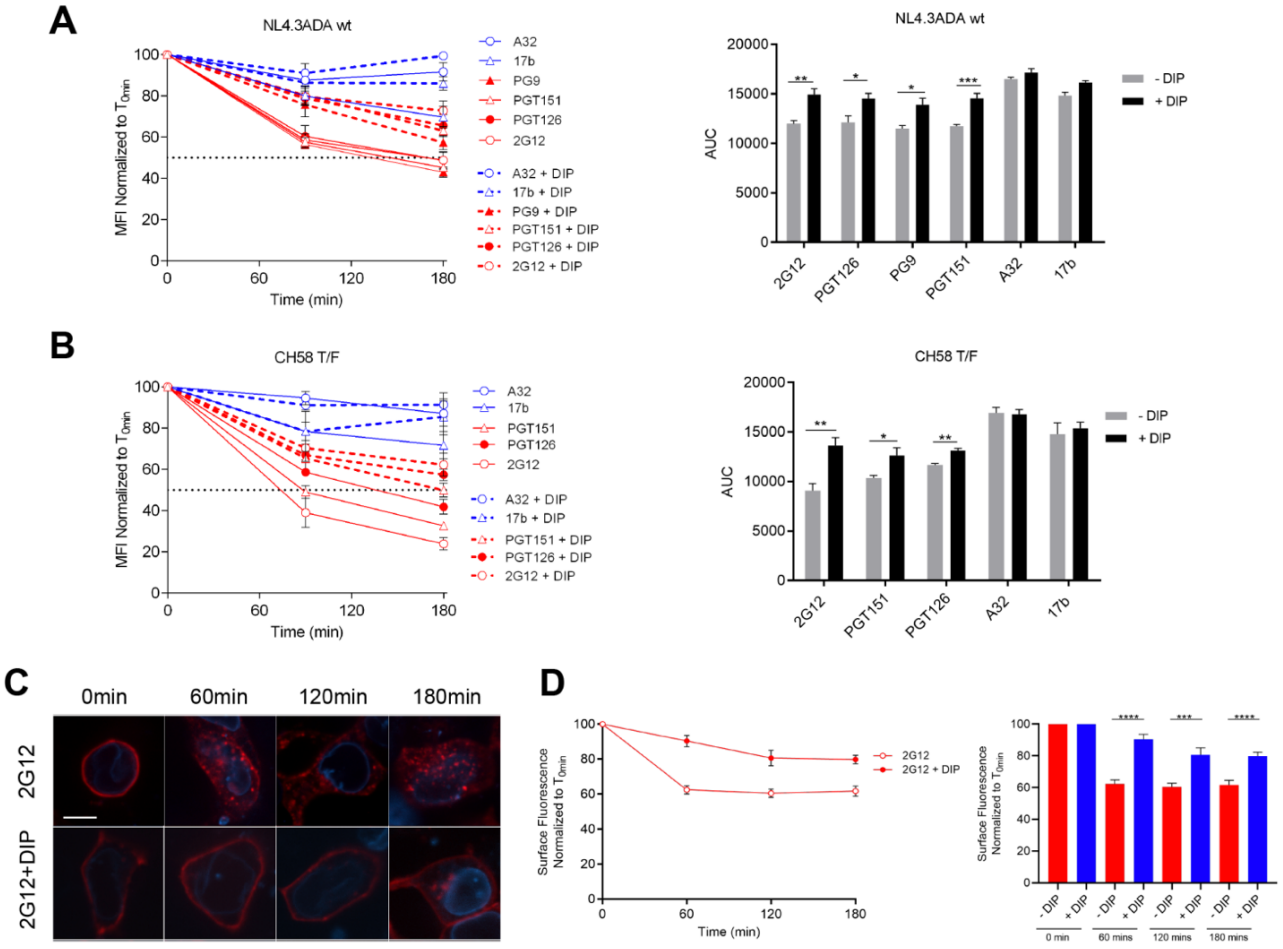

Figure 3.8. bNAb-mediated Env internalization is Dynamin dependent.
Cell-surface staining of primary CD4+ T cells infected with either NL4.3 GFP ADA-based virus (**A**) or CH58 T/F virus (**B**) with A32, 17b, PGT151, PGT126, PG9 and 2G12 mAbs in the presence or absence of 50μM of DIP. (*Left)* Quantification of remaining antibody-Env complexes on the cell-surface over different time points (90mins and 180mins) is expressed as percentage of MFI relative to the 0-minute time control. (*Right*) Areas under the curve (AUC) were calculated based on MFI data sets using GraphPad Prism software. Cell-surface staining of 293T cells transfected with HIV-1_{JRFL} Env along with the Lamin B Receptor-CFP plasmid to locate the nuclear envelope with Alexa-Fluor 594 conjugated 2G12 mAb in the presence or absence of 40μM DIP. (**C**) Images show the localization of antibody-Env complexes at different time points (0min, 60mins, 120mins and 180mins). Images represent a single confocal z-section through the middle of the cell; 20 cells were imaged per condition and representative images are shown, scale bar, 10μm. (**D**) Quantification of remaining antibody-Env complexes over different time points is expressed as percentage of surface fluorescence relative to the 0-minute control. Error bars indicate mean +/- SEM. Statistical significance was tested using an unpaired t-test or a Mann-Whitney U test based on statistical normality (*p<0.05, **p<0.01, ***p<0.001, ****p<0.0001).

Since DIP treatment resulted in an accumulation of bNAb/Env complexes at the surface of HIV-1-infected cells, we evaluated whether it had any impact on the ability of bNAbs to mediate ADCC. Primary CD4+ T cells were infected with the NL4.3 ADA GFP wt virus and their susceptibility to ADCC was measured using a previously described FACS-based assay (9, 47). Interestingly, we observed a significant increase in ADCC responses mediated by PGT126, PGT151, PG9 and 2G12 upon DIP treatment (**Figure 3.9**) but not of direct killing (*i.e.*, in the absence of Abs; not shown). Thus, this suggests that under normal conditions bNAb-mediated Env internalization reduces their capacity to trigger ADCC.

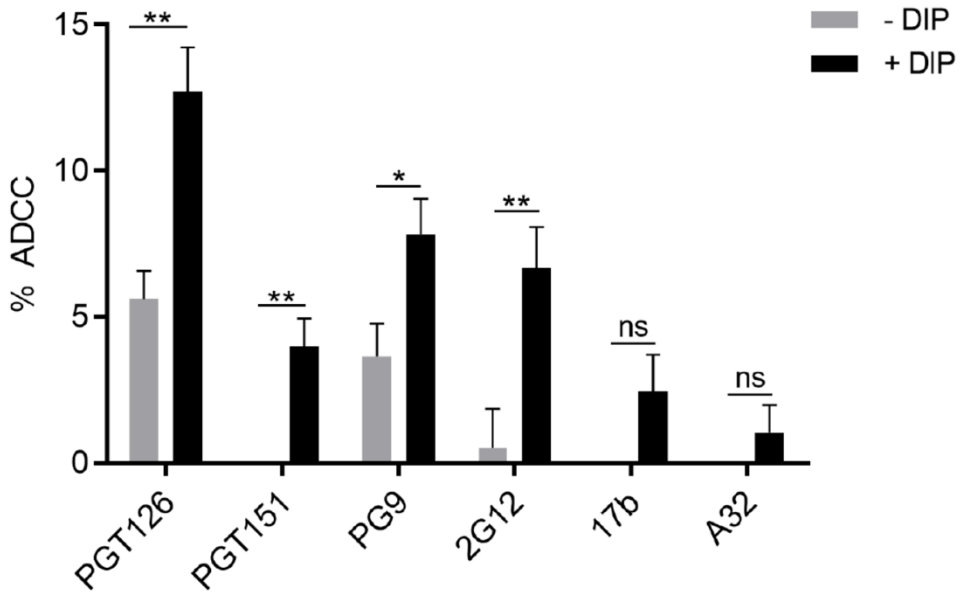

Figure 3.9. A dynamin inhibitor enhances the ADCC activity of bNAbs.
Primary CD4 T cells isolated from at least 3 different healthy donors were infected with NL4.3 GFP ADA virus and used as target cells. Autologous PBMC were used as effector cells in a FACS-based ADCC assay (9, 47). Shown are the percentages of ADCC-mediated killing obtained with A32, 17b, PGT126, PGT151, PG9 and 2G12 mAbs in the presence or absence of 50µM of DIP or the vehicle control. Error bars indicate mean +/- SEM. Statistical significance was tested using an unpaired t-test or a Mann-Whitney U test based on statistical normality (*$p<0.05$, **$p<0.01$).

3.6 Discussion

Here we report that antibody-bound Env proteins are internalized from the surface of HIV-1-infected cells in a conformation-specific manner. bNAbs that preferentially recognize 'closed' Env conformations trigger rapid Env internalization. When this process was decreased using a Dynamin inhibitor, the susceptibility of infected cells to ADCC mediated by bNAbs was enhanced. Thus, suggesting that bNAb-triggered Env internalization impairs their ability to mediate robust ADCC responses. In contrast, nNAb specific for 'open' Env conformation remain exposed on the surface of infected cells for prolonged periods of time. As such, differential internalization of Env-antibody complexes is likely an immune evasion mechanism that HIV-1 evolved to limit the surface exposure of Env in 'closed' conformations while distracting the immune system with the display of Env proteins in 'open' conformations that ultimately result in non-neutralizing immune responses.

Specifically, the native Env trimer mainly exists in an untriggered 'closed' conformation (State 1). The interaction with the CD4 receptor lowers the energy barrier to reach the 'open' states 2/3 (34, 36). Natural HIV-1 infection elicits mainly nNAbs, which poorly recognize the 'closed' Env and are only able to recognize highly conserved epitopes exposed upon the 'opening' of Env (8, 48). Despite poor neutralizing activity, these nNAbs have been shown to exert a constant selection pressure and alter the course of HIV-1-infection *in vivo* (49-51) and can mediate potent ADCC activity against cells presenting Env in its 'open' CD4-bound conformation (7, 9, 38, 52). It is interesting to note that the nNAbs used in this study can form a stable complex with Env on the cell-surface for a prolonged amount of time. Conversely, the bNAbs tested induced faster Env internalization rates. Since these bNAbs recognize the 'closed' conformation of Env, these results suggest that Env sampling its State 1 conformation might be located in discrete membrane micro-domains that could be prone to antibody-mediated internalization. Additional studies are required to explore this interesting possibility. Of note, bNAb-Env complexes don't appear to follow the degradative pathway since the intracellular compartments where they accumulate over time are negative for the lysosomal marker Lamp1 (**Figure 3.10**). Rather, Env accumulated in endosomes positive for early endosome marker EEA1 (**Figure 3.10**). It is intriguing to speculate that this endocytic pathway

could be related to the observed role for recycling endosomes in the incorporation of Env into budding virions (53-55).

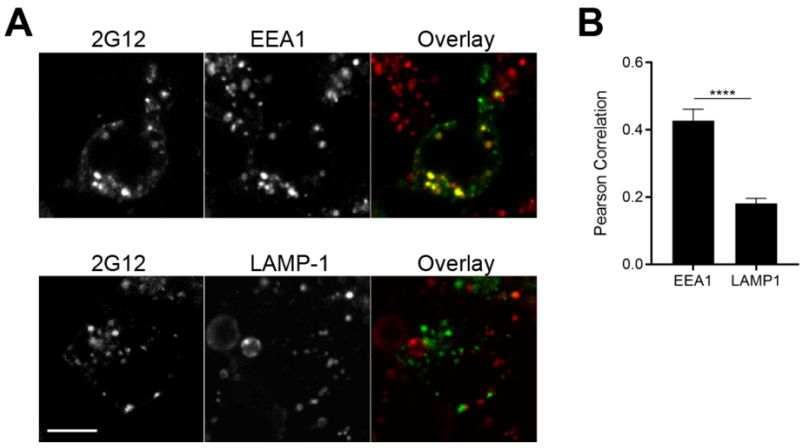

Figure 3.10. bNAb-Env complexes accumulate in an early endosome compartment. 293T cells were transfected with a codon-optimized JR-FL Env plasmid. 48 hours post-transfection, cells were incubated with AlexaFluor488-2G12 for 180 minutes. Cells were then fixed, permeabilized and stained for endogenous EEA1 or LAMP1 proteins, followed by Alexa568 secondary antibodies (**A**). Representative images are shown. Colocalization was quantified for 20 cells per condition using the Pearson Correlation (**B**). Values shown represent mean ± SEM. Scale bar = 10 μm. Statistical significance was tested using an unpaired t-test (****$p<0.001$)

Previous reports have shown that humoral immune responses, such as antibody-dependent complement-mediated lysis, are decreased by internalization of surface-expressed viral glycoproteins upon the binding of antibodies (22, 23). Here we show that this also applies to ADCC. The surprising differences observed between bNAbs and nNAbs studied here suggest that different Env populations sampling different conformations co-exist at the surface of infected cells. Envs sampling the 'closed' conformation could potentially facilitate the elicitation of bNAbs. Therefore, it is tempting to speculate that the virus minimizes the exposure of Env sampling the 'closed' conformation while tolerating the exposure of limited amounts of Env in the 'open' conformation. The 'open' Env could act as a decoy since it is well established that this conformation fails to elicit bNAbs. The nNAbs that are elicited

instead fail to neutralize viral particles or mediate ADCC against wild-type infected cells (9-11, 43, 56, 57).

It is becoming increasingly clear that several factors contribute to ADCC responses against HIV-1-infected cells: Env conformation (58), CD4 (8, 9, 11) and BST-2 downregulation (12-14), gp120 shedding (37, 59), the stability of Env-Ab complexes at the cell surface (60) which are driven by the affinity of Abs for Env (61), Env internalization (15), cell surface expression of stress ligands (56, 62) and now antibody-induced Env internalization. Additional work will be required to tease apart the differential contribution of each of these factors in ADCC. Further dissecting the mechanisms underlying antibody-induced Env internalization might help in the development of new generations of bNAbs that are able to efficiently eliminate HIV-1-infected cells.

Acknowledgments

This study was supported by a CIHR foundation grant 352417 to A.F., by NIH grant R01 AI129769 to M.P. and A.F., by NIH grants R01 GM116654 and P01-GM56550 to W.M., by NIH grant R01 AI116274 to M.P., and by NIH grant R01 AI121135 to D.T.E. A.F. is the recipient of a Canada Research Chair on Retroviral Entry. J.P. is the recipient of a CIHR doctoral fellowship. J.R. is the recipient of an amfAR Mathilde Krim Fellowship in Basic Biomedical Research, and S.D. is a recipient of an FRQS postdoctoral fellowship. The funders had no role in study design, data collection and analysis, decision to publish, or preparation of the manuscript. The authors have no conflicts of interest to report.

The views expressed in this presentation are those of the authors and do not reflect the official policy or position of the Uniformed Services University, U.S. Army, the Department of Defense, or the U.S. Government.

3.7 References

1. Baum LL, Cassutt KJ, Knigge K, Khattri R, Margolick J, Rinaldo C, Kleeberger CA, Nishanian P, Henrard DR, Phair J. 1996. HIV-1 gp120-specific antibody-dependent cell-mediated cytotoxicity correlates with rate of disease progression. J Immunol 157:2168-2173
2. Chung AW, Isitman G, Navis M, Kramski M, Center RJ, Kent SJ, Stratov I. 2011. Immune escape from HIV-specific antibody-dependent cellular cytotoxicity (ADCC) pressure. Proc Natl Acad Sci U S A 108:7505-7510.
3. Forthal DN, Landucci G, Haubrich R, Keenan B, Kuppermann BD, Tilles JG, Kaplan J. 1999. Antibody-dependent cellular cytotoxicity independently predicts survival in severely immunocompromised human immunodeficiency virus-infected patients. J Infect Dis 180:1338-1341.
4. Mabuka J, Nduati R, Odem-Davis K, Peterson D, Overbaugh J. 2012. HIV-specific antibodies capable of ADCC are common in breastmilk and are associated with reduced risk of transmission in women with high viral loads. PLoS Pathog 8:e1002739.
5. Sun Y, Asmal M, Lane S, Permar SR, Schmidt SD, Mascola JR, Letvin NL. 2011. Antibody-dependent cell-mediated cytotoxicity in simian immunodeficiency virus-infected rhesus monkeys. J Virol 85:6906-6912.
6. Haynes BF, Gilbert PB, McElrath MJ, Zolla-Pazner S, Tomaras GD, Alam SM, Evans DT, Montefiori DC, Karnasuta C, Sutthent R, Liao HX, DeVico AL, Lewis GK, Williams C, Pinter A, Fong Y, Janes H, DeCamp A, Huang Y, Rao M, Billings E, Karasavvas N, Robb ML, Ngauy V, de Souza MS, Paris R, Ferrari G, Bailer RT, Soderberg KA, Andrews C, Berman PW, Frahm N, De Rosa SC, Alpert MD, Yates NL, Shen X, Koup RA, Pitisuttithum P, Kaewkungwal J, Nitayaphan S, Rerks-Ngarm S, Michael NL, Kim JH. 2012. Immune-correlates analysis of an HIV-1 vaccine efficacy trial. N Engl J Med 366:1275-1286.
7. Prevost J, Richard J, Ding S, Pacheco B, Charlebois R, Hahn BH, Kaufmann DE, Finzi A. 2018. Envelope glycoproteins sampling states 2/3 are susceptible to ADCC by sera from HIV-1-infected individuals. Virology 515:38-45.
8. Veillette M, Coutu M, Richard J, Batraville LA, Dagher O, Bernard N, Tremblay C, Kaufmann DE, Roger M, Finzi A. 2015. The HIV-1 gp120 CD4-Bound Conformation Is Preferentially Targeted by Antibody-Dependent Cellular Cytotoxicity-Mediating Antibodies in Sera from HIV-1-Infected Individuals. J Virol 89:545-551.
9. Veillette M, Desormeaux A, Medjahed H, Gharsallah NE, Coutu M, Baalwa J, Guan Y, Lewis G, Ferrari G, Hahn BH, Haynes BF, Robinson JE, Kaufmann DE, Bonsignori M, Sodroski J, Finzi A. 2014. Interaction with cellular CD4 exposes HIV-1 envelope epitopes targeted by antibody-dependent cell-mediated cytotoxicity. J Virol 88:2633-2644.
10. Alsahafi N, Ding S, Richard J, Markle T, Brassard N, Walker B, Lewis GK, Kaufmann DE, Brockman MA, Finzi A. 2016. Nef Proteins from HIV-1 Elite Controllers Are

Inefficient at Preventing Antibody-Dependent Cellular Cytotoxicity. J Virol 90:2993-3002.
11. Prevost J, Richard J, Medjahed H, Alexander A, Jones J, Kappes JC, Ochsenbauer C, Finzi A. 2018. Incomplete Downregulation of CD4 Expression Affects HIV-1 Env Conformation and Antibody-Dependent Cellular Cytotoxicity Responses. J Virol 92.
12. Arias JF, Heyer LN, von Bredow B, Weisgrau KL, Moldt B, Burton DR, Rakasz EG, Evans DT. 2014. Tetherin antagonism by Vpu protects HIV-infected cells from antibody-dependent cell-mediated cytotoxicity. Proc Natl Acad Sci U S A 111:6425-6430.
13. Alvarez RA, Hamlin RE, Monroe A, Moldt B, Hotta MT, Rodriguez Caprio G, Fierer DS, Simon V, Chen BK. 2014. HIV-1 Vpu antagonism of tetherin inhibits antibody-dependent cellular cytotoxic responses by natural killer cells. J Virol 88:6031-6046.
14. Richard J, Prevost J, von Bredow B, Ding S, Brassard N, Medjahed H, Coutu M, Melillo B, Bibollet-Ruche F, Hahn BH, Kaufmann DE, Smith AB, 3rd, Sodroski J, Sauter D, Kirchhoff F, Gee K, Neil SJ, Evans DT, Finzi A. 2017. BST-2 Expression Modulates Small CD4-Mimetic Sensitization of HIV-1-Infected Cells to Antibody-Dependent Cellular Cytotoxicity. J Virol 91.
15. von Bredow B, Arias JF, Heyer LN, Gardner MR, Farzan M, Rakasz EG, Evans DT. 2015. Envelope Glycoprotein Internalization Protects Human and Simian Immunodeficiency Virus Infected Cells from Antibody-Dependent Cell-Mediated Cytotoxicity. J Virol doi:10.1128/JVI.01911-15.
16. Boge M, Wyss S, Bonifacino JS, Thali M. 1998. A membrane-proximal tyrosine-based signal mediates internalization of the HIV-1 envelope glycoprotein via interaction with the AP-2 clathrin adaptor. J Biol Chem 273:15773-15778.
17. Byland R, Vance PJ, Hoxie JA, Marsh M. 2007. A conserved dileucine motif mediates clathrin and AP-2-dependent endocytosis of the HIV-1 envelope protein. Mol Biol Cell 18:414-425.
18. Blot G, Janvier K, Le Panse S, Benarous R, Berlioz-Torrent C. 2003. Targeting of the human immunodeficiency virus type 1 envelope to the trans-Golgi network through binding to TIP47 is required for env incorporation into virions and infectivity. J Virol 77:6931-6945.
19. Bu Z, Ye L, Vzorov A, Taylor D, Compans RW, Yang C. 2004. Enhancement of immunogenicity of an HIV Env DNA vaccine by mutation of the Tyr-based endocytosis motif in the cytoplasmic domain. Virology 328:62-73.
20. Fultz PN, Vance PJ, Endres MJ, Tao B, Dvorin JD, Davis IC, Lifson JD, Montefiori DC, Marsh M, Malim MH, Hoxie JA. 2001. In vivo attenuation of simian immunodeficiency virus by disruption of a tyrosine-dependent sorting signal in the envelope glycoprotein cytoplasmic tail. J Virol 75:278-291.
21. van der Meulen KM, Nauwynck HJ, Pensaert MB. 2003. Absence of viral antigens on the surface of equine herpesvirus-1-infected peripheral blood mononuclear cells: a strategy to avoid complement-mediated lysis. J Gen Virol 84:93-97.

22. Van de Walle GR, Favoreel HW, Nauwynck HJ, Pensaert MB. 2003. Antibody-induced internalization of viral glycoproteins and gE-gI Fc receptor activity protect pseudorabies virus-infected monocytes from efficient complement-mediated lysis. J Gen Virol 84:939-948
23. Favoreel HW, Van Minnebruggen G, Van de Walle GR, Ficinska J, Nauwynck HJ. 2006. Herpesvirus interference with virus-specific antibodies: bridging antibodies, internalizing antibodies, and hiding from antibodies. Vet Microbiol 113:257-263.
24. Vogt C, Eickmann M, Diederich S, Moll M, Maisner A. 2005. Endocytosis of the Nipah virus glycoproteins. J Virol 79:3865-3872.
25. Popa A, Carter JR, Smith SE, Hellman L, Fried MG, Dutch RE. 2012. Residues in the hendra virus fusion protein transmembrane domain are critical for endocytic recycling. J Virol 86:3014-3026.
26. Moll M, Klenk HD, Herrler G, Maisner A. 2001. A single amino acid change in the cytoplasmic domains of measles virus glycoproteins H and F alters targeting, endocytosis, and cell fusion in polarized Madin-Darby canine kidney cells. J Biol Chem 276:17887-17894.
27. Leemans A, De Schryver M, Van der Gucht W, Heykers A, Pintelon I, Hotard AL, Moore ML, Melero JA, McLellan JS, Graham BS, Broadbent L, Power UF, Caljon G, Cos P, Maes L, Delputte P. 2017. Antibody-Induced Internalization of the Human Respiratory Syncytial Virus Fusion Protein. J Virol 91.
28. Dewerchin HL, Cornelissen E, Nauwynck HJ. 2006. Feline infectious peritonitis virus-infected monocytes internalize viral membrane-bound proteins upon antibody addition. J Gen Virol 87:1685-1690.
29. Falkowska E, Le KM, Ramos A, Doores KJ, Lee JH, Blattner C, Ramirez A, Derking R, van Gils MJ, Liang CH, McBride R, von Bredow B, Shivatare SS, Wu CY, Chan-Hui PY, Liu Y, Feizi T, Zwick MB, Koff WC, Seaman MS, Swiderek K, Moore JP, Evans D, Paulson JC, Wong CH, Ward AB, Wilson IA, Sanders RW, Poignard P, Burton DR. 2014. Broadly neutralizing HIV antibodies define a glycan-dependent epitope on the prefusion conformation of gp41 on cleaved envelope trimers. Immunity 40:657-668.
30. Calarese DA, Scanlan CN, Zwick MB, Deechongkit S, Mimura Y, Kunert R, Zhu P, Wormald MR, Stanfield RL, Roux KH, Kelly JW, Rudd PM, Dwek RA, Katinger H, Burton DR, Wilson IA. 2003. Antibody domain exchange is an immunological solution to carbohydrate cluster recognition. Science 300:2065-2071.
31. Julien JP, Lee JH, Cupo A, Murin CD, Derking R, Hoffenberg S, Caulfield MJ, King CR, Marozsan AJ, Klasse PJ, Sanders RW, Moore JP, Wilson IA, Ward AB. 2013. Asymmetric recognition of the HIV-1 trimer by broadly neutralizing antibody PG9. Proc Natl Acad Sci U S A 110:4351-4356.
32. Walker LM, Huber M, Doores KJ, Falkowska E, Pejchal R, Julien JP, Wang SK, Ramos A, Chan-Hui PY, Moyle M, Mitcham JL, Hammond PW, Olsen OA, Phung P, Fling S, Wong CH, Phogat S, Wrin T, Simek MD, Koff WC, Wilson IA, Burton DR, Poignard

P. 2011. Broad neutralization coverage of HIV by multiple highly potent antibodies. Nature 477:466-470.
33. Anand SP, Prevost J, Baril S, Richard J, Medjahed H, Chapleau JP, Tolbert WD, Kirk S, Smith AB, 3rd, Wines BD, Kent SJ, Hogarth PM, Parsons MS, Pazgier M, Finzi A. 2019. Two Families of Env Antibodies Efficiently Engage Fc-Gamma Receptors and Eliminate HIV-1-Infected Cells. J Virol 93.
34. Herschhorn A, Ma X, Gu C, Ventura JD, Castillo-Menendez L, Melillo B, Terry DS, Smith AB, 3rd, Blanchard SC, Munro JB, Mothes W, Finzi A, Sodroski J. 2016. Release of gp120 Restraints Leads to an Entry-Competent Intermediate State of the HIV-1 Envelope Glycoproteins. MBio 7.
35. Ma X, Lu M, Gorman J, Terry DS, Hong X, Zhou Z, Zhao H, Altman RB, Arthos J, Blanchard SC, Kwong PD, Munro JB, Mothes W. 2018. HIV-1 Env trimer opens through an asymmetric intermediate in which individual protomers adopt distinct conformations. Elife 7.
36. Munro JB, Gorman J, Ma X, Zhou Z, Arthos J, Burton DR, Koff WC, Courter JR, Smith AB, 3rd, Kwong PD, Blanchard SC, Mothes W. 2014. Conformational dynamics of single HIV-1 envelope trimers on the surface of native virions. Science 346:759-763.
37. Richard J, Prevost J, Baxter AE, von Bredow B, Ding S, Medjahed H, Delgado GG, Brassard N, Sturzel CM, Kirchhoff F, Hahn BH, Parsons MS, Kaufmann DE, Evans DT, Finzi A. 2018. Uninfected Bystander Cells Impact the Measurement of HIV-Specific Antibody-Dependent Cellular Cytotoxicity Responses. MBio 9.
38. Richard J, Prevost J, Alsahafi N, Ding S, Finzi A. 2017. Impact of HIV-1 Envelope Conformation on ADCC Responses. Trends Microbiol doi:10.1016/j.tim.2017.10.007.
39. Veillette M, Richard J, Pazgier M, Lewis GK, Parsons MS, Finzi A. 2016. Role of HIV-1 Envelope Glycoproteins Conformation and Accessory Proteins on ADCC Responses. Curr HIV Res 14:9-23.
40. Forthal DN, Finzi A. 2018. Antibody-Dependent Cellular Cytotoxicity (ADCC) in HIV Infection. AIDS doi:10.1097/QAD.0000000000002011.
41. Anand SP, Prévost J, Baril S, Richard J, Medjahed H, Chapleau J-P, Tolbert WD, Kirk S, Smith AB, Wines BD. 2018. Two families of Env antibodies efficiently engage Fc-gamma receptors and eliminate HIV-1-infected cells. Journal of Virology:JVI. 01823-01818.
42. Richard J, Pacheco B, Gohain N, Veillette M, Ding S, Alsahafi N, Tolbert WD, Prevost J, Chapleau JP, Coutu M, Jia M, Brassard N, Park J, Courter JR, Melillo B, Martin L, Tremblay C, Hahn BH, Kaufmann DE, Wu X, Smith AB, 3rd, Sodroski J, Pazgier M, Finzi A. 2016. Co-receptor Binding Site Antibodies Enable CD4-Mimetics to Expose Conserved Anti-cluster A ADCC Epitopes on HIV-1 Envelope Glycoproteins. EBioMedicine doi:10.1016/j.ebiom.2016.09.004.

43. Veillette M, Coutu M, Richard J, Batraville LA, Desormeaux A, Roger M, Finzi A. 2014. Conformational evaluation of HIV-1 trimeric envelope glycoproteins using a cell-based ELISA assay. J Vis Exp doi:10.3791/51995:51995.
44. Ferguson SM, De Camilli P. 2012. Dynamin, a membrane-remodelling GTPase. Nat Rev Mol Cell Biol 13:75-88.
45. Grabs D, Slepnev VI, Songyang Z, David C, Lynch M, Cantley LC, De Camilli P. 1997. The SH3 domain of amphiphysin binds the proline-rich domain of dynamin at a single site that defines a new SH3 binding consensus sequence. J Biol Chem 272:13419-13425.
46. Falgairolle M, O'Donovan MJ. 2015. Pharmacological Investigation of Fluoro-Gold Entry into Spinal Neurons. PLoS One 10:e0131430.
47. Richard J, Veillette M, Batraville LA, Coutu M, Chapleau JP, Bonsignori M, Bernard N, Tremblay C, Roger M, Kaufmann DE, Finzi A. 2014. Flow cytometry-based assay to study HIV-1 gp120 specific antibody-dependent cellular cytotoxicity responses. J Virol Methods 208:107-114.
48. Decker JM, Bibollet-Ruche F, Wei X, Wang S, Levy DN, Wang W, Delaporte E, Peeters M, Derdeyn CA, Allen S, Hunter E, Saag MS, Hoxie JA, Hahn BH, Kwong PD, Robinson JE, Shaw GM. 2005. Antigenic conservation and immunogenicity of the HIV coreceptor binding site. J Exp Med 201:1407-1419.
49. Kwong PD, Mascola JR. 2012. Human antibodies that neutralize HIV-1: identification, structures, and B cell ontogenies. Immunity 37:412-425.
50. Horwitz JA, Bar-On Y, Lu CL, Fera D, Lockhart AAK, Lorenzi JCC, Nogueira L, Golijanin J, Scheid JF, Seaman MS, Gazumyan A, Zolla-Pazner S, Nussenzweig MC. 2017. Non-neutralizing Antibodies Alter the Course of HIV-1 Infection In Vivo. Cell 170:637-648 e610.
51. Moody MA, Gao F, Gurley TC, Amos JD, Kumar A, Hora B, Marshall DJ, Whitesides JF, Xia SM, Parks R, Lloyd KE, Hwang KK, Lu X, Bonsignori M, Finzi A, Vandergrift NA, Alam SM, Ferrari G, Shen X, Tomaras GD, Kamanga G, Cohen MS, Sam NE, Kapiga S, Gray ES, Tumba NL, Morris L, Zolla-Pazner S, Gorny MK, Mascola JR, Hahn BH, Shaw GM, Sodroski JG, Liao HX, Montefiori DC, Hraber PT, Korber BT, Haynes BF. 2015. Strain-Specific V3 and CD4 Binding Site Autologous HIV-1 Neutralizing Antibodies Select Neutralization-Resistant Viruses. Cell Host Microbe 18:354-362.
52. Ding S, Tolbert WD, Prevost J, Pacheco B, Coutu M, Debbeche O, Xiang SH, Pazgier M, Finzi A. 2016. A Highly Conserved gp120 Inner Domain Residue Modulates Env Conformation and Trimer Stability. J Virol doi:10.1128/JVI.01068-16.
53. Kirschman J, Qi M, Ding L, Hammonds J, Dienger-Stambaugh K, Wang JJ, Lapierre LA, Goldenring JR, Spearman P. 2018. HIV-1 Envelope Glycoprotein Trafficking through the Endosomal Recycling Compartment Is Required for Particle Incorporation. J Virol 92.

54. Qi M, Chu H, Chen X, Choi J, Wen X, Hammonds J, Ding L, Hunter E, Spearman P. 2015. A tyrosine-based motif in the HIV-1 envelope glycoprotein tail mediates cell-type- and Rab11-FIP1C-dependent incorporation into virions. Proc Natl Acad Sci U S A 112:7575-7580.
55. Qi M, Williams JA, Chu H, Chen X, Wang JJ, Ding L, Akhirome E, Wen X, Lapierre LA, Goldenring JR, Spearman P. 2013. Rab11-FIP1C and Rab14 direct plasma membrane sorting and particle incorporation of the HIV-1 envelope glycoprotein complex. PLoS Pathog 9:e1003278.
56. Alsahafi N, Richard J, Prevost J, Coutu M, Brassard N, Parsons MS, Kaufmann DE, Brockman M, Finzi A. 2017. Impaired downregulation of NKG2D ligands by Nef protein from elite controllers sensitizes HIV-1-infected cells to ADCC. J Virol doi:10.1128/JVI.00109-17.
57. Ding S, Veillette M, Coutu M, Prevost J, Scharf L, Bjorkman PJ, Ferrari G, Robinson JE, Sturzel C, Hahn BH, Sauter D, Kirchhoff F, Lewis GK, Pazgier M, Finzi A. 2016. A Highly Conserved Residue of the HIV-1 gp120 Inner Domain Is Important for Antibody-Dependent Cellular Cytotoxicity Responses Mediated by Anti-cluster A Antibodies. J Virol 90:2127-2134.
58. Richard J, Prevost J, Alsahafi N, Ding S, Finzi A. 2018. Impact of HIV-1 Envelope Conformation on ADCC Responses. Trends Microbiol 26:253-265.
59. Richard J, Veillette M, Ding S, Zoubchenok D, Alsahafi N, Coutu M, Brassard N, Park J, Courter JR, Melillo B, Smith AB, 3rd, Shaw GM, Hahn BH, Sodroski J, Kaufmann DE, Finzi A. 2016. Small CD4 Mimetics Prevent HIV-1 Uninfected Bystander CD4 + T Cell Killing Mediated by Antibody-dependent Cell-mediated Cytotoxicity. EBioMedicine 3:122-134.
60. Bruel T, Guivel-Benhassine F, Amraoui S, Malbec M, Richard L, Bourdic K, Donahue DA, Lorin V, Casartelli N, Noel N, Lambotte O, Mouquet H, Schwartz O. 2016. Elimination of HIV-1-infected cells by broadly neutralizing antibodies. Nat Commun 7:10844.
61. Ivan B, Sun Z, Subbaraman H, Friedrich N, Trkola A. 2019. CD4 occupancy triggers sequential pre-fusion conformational states of the HIV-1 envelope trimer with relevance for broadly neutralizing antibody activity. PLoS Biol 17:e3000114.
62. Parsons MS, Richard J, Lee WS, Vanderven H, Grant MD, Finzi A, Kent SJ. 2016. NKG2D acts as a co-receptor for natural killer cell-mediated anti-HIV-1 antibody-dependent cellular cytotoxicity. AIDS Res Hum Retroviruses doi:10.1089/AID.2016.0099.
63. Mao Y, Wang L, Gu C, Herschhorn A, Desormeaux A, Finzi A, Xiang SH, Sodroski JG. 2013. Molecular architecture of the uncleaved HIV-1 envelope glycoprotein trimer. Proc Natl Acad Sci U S A doi:10.1073/pnas.1307382110.
64. Rolls MM, Stein PA, Taylor SS, Ha E, McKeon F, Rapoport TA. 1999. A visual screen of a GFP-fusion library identifies a new type of nuclear envelope membrane protein. J Cell Biol 146:29-44.

65. Schneider CA, Rasband WS, Eliceiri KW. 2012. NIH Image to ImageJ: 25 years of image analysis. Nat Methods 9:671-675.
66. Bolte S, Cordelieres FP. 2006. A guided tour into subcellular colocalization analysis in light microscopy. J Microsc 224:213-232.

CHAPTER IV

HIV-1 Envelope Glycoprotein Cell Surface Localization is Associated with Antibody-Induced Internalization

Sai Priya Anand, Jérémie Prévost, Jade Descôteaux-Dinelle, Jonathan Richard, Dung N. Nguyen, Halima Medjahed, Hung-Ching Chen, Amos B. Smith III, Marzena Pazgier, and Andrés Finzi

4.1 Preface to Chapter 4

The findings reported in Chapter 3 highlight that antibody-bound Env proteins are internalized from the surface of HIV-1-infected cells in a conformation-specific manner, with the binding of bNAbs that preferentially recognize the 'closed' Env triggering rapid Env internalization. This process could be circumvented using a dynamin inhibitor, suggesting that bNAb-triggered Env internalization impairs their ability to mediate ADCC. Thus, in this chapter we attempt to gain a better understanding of this mechanism by which bNAbs induce Env internalization and nNAb-bound Env persists on the cell surface for longer periods of time. The results of this study have important implications in understanding underlying causes that could hinder ADCC responses to clear HIV-1-infected cells. Consequently, a better understanding of Ab-induced Env internalization might help in the development of Abs with improved Fc-effector capacities.

4.2 Abstract

To minimize immune responses against infected cells, HIV-1 has evolved different mechanisms to limit the surface expression of its envelope glycoproteins (Env). Recent observations suggest that the binding of certain broadly neutralizing antibodies (bNAbs) targeting the 'closed' conformation of Env induces its internalization. On the other hand, non-neutralizing antibodies (nNAbs) that preferentially target Env in its 'open' conformation, remain bound to Env on the cell-surface for longer periods of time. In this study, we attempt to better understand the underlying mechanisms behind the differential rates of antibody-mediated Env internalization. We demonstrate that 'forcing' open Env using CD4 mimetics allows for nNAb binding and results in similar rates of Env internalization as those observed upon the bNAb binding. Moreover, we can identify distinct populations of Env that are differentially targeted by Abs that mediate faster rates of internalization, suggesting that the mechanism of antibody-induced Env internalization partially depends on the localization of Env on the cell surface.

4.3 Introduction

Envelope glycoproteins (Env) of the human immunodeficiency virus (HIV-1) have long C-terminal cytoplasmic tails containing specific trafficking signals (1, 2). These allow for the endocytosis of Env from the surface of infected cells, which has been suggested to be a mechanism in place to minimize recognition by the host immune system. Mutations of these motifs have been shown to result in increased cell surface expression of Env and to correlate with increased Fc-mediated effector responses, such as antibody-dependent cellular cytotoxicity (ADCC), against infected cells (3). Additionally, we have recently reported that the binding of broadly neutralizing antibodies (bNAbs) to Env accelerates its internalization from the surface of infected cells (4). On the contrary, the binding of non-neutralizing antibodies (nNAbs) induced Env internalization at a significantly slower rate, allowing Env to remain on the cell surface for a prolonged period (4). This phenomenon has also been observed with other retroviral glycoproteins, including the murine leukemia virus (MLV), where the binding of certain antibodies initiates signalling cascades within the cell, leading to cellular activation and enhancement of envelope glycoprotein internalization (5). Furthermore, we also observed that upon dynamin inhibition, antibody-mediated Env internalization is significantly reduced and the susceptibility of infected cells to ADCC responses mediated by bNAbs increased (4). Similarly, recent studies have also demonstrated enhancement of ADCC responses against human tumors upon temporary endocytosis inhibition (6). Thus, antibody-induced antigen internalization from the cell-surface decreases the overall recognition and elimination of target cells by immune cells.

In this study, we attempt to better understand the mechanisms by which bNAbs induce Env internalization and nNAb-bound Env persists on the cell surface for longer periods of time. Recent studies have highlighted the presence of different Env populations at the cell surface due to differential processing during its trafficking (7-9). To investigate whether the differences in antibody-mediated Env internalization is due to distinct populations of Env on the cell-surface being targeted, we utilize ligands such as small CD4-mimetics (CD4mc) and soluble CD4 (sCD4) to ‘force’ open the otherwise ‘closed’ Env populations and evaluate the rates of nNAbs internalization. Our observations indicate that in addition to the conformation

of Env and epitope availability, Env internalization also depends on its localization on the cell surface.

4.4 Material and Methods

Ethics Statement

Written informed consent was obtained from all study participants [the Montreal Primary HIV Infection Cohort] (10, 11). Research adhered to the ethical guidelines of CRCHUM and was reviewed and approved by the CRCHUM institutional review board (ethics committee, approval number CE16.164-CA). Research adhered to the standards indicated by the Declaration of Helsinki. All participants were adult and provided informed written consent prior to enrolment in accordance with Institutional Review Board approval.

Cell lines and primary cells

293T human embryonic kidney cells (obtained from ATCC) were cultured at 37°C under 5% CO_2 in Dulbecco's modified Eagle's medium (Wisent) containing 5% fetal bovine serum (VWR) and 100 µg/ml of penicillin-streptomycin (Wisent). Primary CD4+ T lymphocytes were purified from resting PBMCs by negative selection and activated as previously described (12, 13). Briefly, PBMC were obtained by leukapheresis. CD4+ T lymphocytes were purified using immunomagnetic beads as per the manufacturer's instructions (StemCell Technologies). CD4+ T lymphocytes were activated with phytohemagglutinin-L (PHA-L; 10 µg/ mL) for 48 hours and then maintained in RPMI 1640 (Gibco) complete medium supplemented with rIL-2 (100 U/mL).

Plasmids and proviral constructs

The vesicular stomatitis virus G (VSV-G)-encoding plasmid (pSVCMV-IN-VSV-G) was previously described (14) . The infectious molecular clone (IMC) of the transmitted/founder (T/F) virus CH58 was inferred and constructed as previously described (15, 16). The CH58 IMC with the L193A change in the Env glycoprotein (L193A) or defective for Nef and Vpu expression (Nef-Vpu-) were described elsewhere (17, 18). The JRFL IMC was also previously reported (19). Plasmids used to transfect 293T cells include the pcDNA3.1 vector expressing

the codon-optimized HIV-1 JRFL envelope glycoproteins and the pcDNA3.1 human CD4 expressor (20, 21).

Viral production, Infections, and ex vivo amplification

To ensure similar levels of infection between viruses, vesicular stomatitis viruses G (VSVG)-pseudotyped viruses were produced and titrated as described (13). Viruses were used to infect activated primary CD4 T cells from healthy HIV-1 negative donors by spin infection at 800 x g for 1 hour in 96-well plates at 25°C. To expand endogenously infected CD4+ T cells, primary CD4+ T cells obtained from six antiretroviral therapy (ART)-treated HIV-1-infected individuals were isolated from PBMCs by negative selection. Purified CD4+ T cells were activated with PHA-L at 10 μg /mL for 48 hours and then cultured for at least 6 days in RPMI-1640 complete medium supplemented with rIL-2 (100U/mL).

Antibodies and Reagents

Anti-HIV-1 gp120 mAbs recognizing CD4-induced epitopes (19b, 17b; obtained from NIH AIDS Reagent Program), the outer domain (2G12; obtained from NIH AIDS Reagent Program) and the gp120-gp41 interface (PGT151; obtained from IAVI) were used for cell-surface staining of infected cells. Additionally, the following constructs were also used for cell-surface staining: 17b-sCD4 and 19b-sCD4 constructs, which are hybrid proteins and consist of anti-gp120 Abs linked to the C-terminus of soluble CD4 (sCD4; D1D2 domains) via a flexible linker on each heavy chain (22). Goat anti-human IgG Alexa Fluor-647 secondary Ab (Thermo Fisher Scientific) was used to determine overall antibody binding and AquaVivid (Thermo Fisher Scientific) as a viability dye. The sCD4 protein was produced and purified as previously described (23). The small molecule CD4 mimetic compound (CD4mc) BNM-III-170 were synthesized as described previously (24, 25). The CD4mc was analyzed, dissolved in dimethyl sulfoxide (DMSO) at a stock concentration of 10 mM, aliquoted, and stored at −80 °C until further use. For western blot analyses, a mouse anti-CD71 monoclonal antibody (clone OKT-9; Thermo Fisher Scientific) was used as a control for detergent soluble membranes (DSM) and was followed by incubation with a horseradish peroxidase (HRP)-conjugated antibody specific for the Fc region of mouse IgG (Thermo Fisher Scientific). An HRP-

conjugated cholera toxin subunit B (CTx-B) (Invitrogen) was used to detect ganglioside GM1 as a control for detergent-resistant membranes (DRM), and HRP-conjugated streptavidin (Thermo Fisher Scientific) was used to detect cell-surface biotinylated Env. For confocal microscopy analyses, DAPI (Sigma) was used for nucleic acid staining. 19b and 17b were conjugated with Alexa-Fluor 647 and 594 probes (Thermo Fisher Scientific), respectively, as per the manufacturer's protocol and used for confocal microscopy analyses. Alternatively, staining with 17b-sCD4 was performed in combination with the goat anti-human IgG Alexa Fluor 594 secondary Ab (Thermo Fisher Scientific).

Antibody-induced internalization assay by flow cytometry

48 hours post-infection, HIV-1-infected primary CD4+ T cells were incubated with 5μg/mL of anti-Env antibodies or 10 μg/mL of 19b-sCD4 or 17b-sCD4 chimeric protein for 30 mins at room temperature to allow for antibody attachment. To allow nnAbs binding, either sCD4 (10 μg/mL) or the CD4-mimetic compound BNM-III-170 (5 μM) were also added to the cells. To remove unbound antibodies, cells were washed three times with cold phosphate-buffered saline (PBS). This was followed by incubation at 37°C to start the internalization process. After different time points, cells were fixed with 2% paraformaldehyde (PFA) in PBS. To visualize remaining antigen-antibody complexes on the cell surface, cells were stained with a goat anti-human conjugated with Alexa Fluor-647 secondary Ab (Thermo Fisher Scientific). Some cells were fixed after the primary incubation with the anti-Env antibodies as a control (Time point 0 min). Dead cells were excluded using the live/dead fixable AquaVivid stain (Thermo Fisher Scientific). The reduction in surface expression for a given time point was normalized by using the following equation: [(Mean Fluorescence Intensity at *X* min) / (Mean Fluorescence Intensity at 0 min)] x 100.

HIV-1-infected cells were identified by intracellular staining of HIV-1 p24 using the Cytofix/Cytoperm Fixation/Permeabilization Kit (BD Biosciences) and the PE-conjugated anti-p24 mAb (clone KC57; Beckman Coulter). The percentage of infected cells (p24+) was determined by gating the living cell population based on viability dye staining with AquaVivid

(Thermo Fisher Scientific). Samples were analyzed on an LSRII cytometer (BD Biosciences), and data analysis was performed using FlowJo v10.7.2 (Tree Star).

Antibody-induced internalization assay by confocal microscopy

For confocal microscopy analyses, 293T cells were plated in poly-D-lysine coated 14mm MatTek dishes with #0 coverslip bottoms. 293T cells were transfected with 1µg JRFL Env (codon-optimized) plasmid with or without 1µg human CD4 plasmid. At 48 hours post transfection, cells were incubated with prelabeled anti-gp120 antibodies (5 µg/mL) (+/- 5 µM of BNM-III-170) or a mix of 17b-sCD4 (10 µg/mL) and pre-coupled anti-human IgG (1:1000 dilution) in fresh media for 20 minutes, washed twice with PBS + 0.5% BSA, and incubated for the indicated amount of time at 37°C to start the internalization process. After different time points, cells were fixed with PBS + 4% PFA for 30 minutes and then placed in PBS prior to imaging. All high-resolution images were obtained using a Zeiss AxioObserver Z1 Yokogawa CSU-X1 Spinning disk confocal microscope equipped with Piezo objectives, an Evolve EMCCD (512x512, 16bit) monochrome camera (Photometrics), and 405-, 488-, and 561-nm lasers. Images were analyzed manually using ImageJ (26). Briefly, regions of interest were drawn around entire cells and cytoplasmic regions. Total fluorescence for regions of interest were calculated as the area × (mean – minimum). Surface fluorescence was calculated as the total fluorescence minus the cytoplasmic fluorescence. Values are represented as surface/total ratios, normalized to the 0-min time point. The average intensity and area were measured and used to calculate the total fluorescence and the cytoplasmic fluorescence. The minimum intensity was subtracted from the mean intensity to correct for cytoplasmic background fluorescence.

Biochemical isolation of lipid microdomains and Western Blot analysis

48 hours post-transfection, Env-expressing 293T cells (2 x 10^7 to 4 x 10^7) were washed twice with ice-cold PBS and cell-surface proteins were biotinylated using EZ-Link™ Sulfo-NHS-LC-Biotin (Thermo Fisher Scientific) as per the manufacturer's protocol for 30 minutes at 4°C. Cells were incubated with 10µg/mL of respective anti-Env antibodies for cell-surface staining for 30 minutes at room temperature. Cells were then lysed on ice for 30 min in 1 ml of 1%

Triton X-100 TNE lysis buffer (25 mM Tris [pH 7.5], 150 mM NaCl, 5 mM EDTA) supplemented with protease inhibitor cocktail (Thermo Fisher Scientific). The cell lysates were homogenized with a tissue grinder (Fisher) and centrifuged for 5 min at 720 × g at 4°C in a microcentrifuge. The supernatant was mixed with 1 mL of 80% sucrose in TNE lysis buffer, placed at the bottoms of ultracentrifuge tubes, and overlaid with 6 mL of 30% and 3 mL of 5% sucrose in TNE lysis buffer. The lysates were ultracentrifuged at 4°C in a TH641 rotor (Thermo Fisher Scientific) for 16 hours at 38,000 rpm. After centrifugation, the Triton X-100-insoluble, low-density material was visible as a band migrating on the boundary between 5 and 30% sucrose. One 4mL and two 3mL fractions were collected from the top; 100µl of each fraction was analyzed immediately by Western blotting and the rest was used for immunoprecipitation. Precipitation antibody-bound biotinylated cell-surface JRFL envelope glycoproteins from cell lysates were performed for 1 hour at 4°C in the presence of 50 µL of 10% protein A-Sepharose (Cytiva). Aliquots of sucrose gradient fractions were analyzed by sodium dodecyl sulfate-polyacrylamide gel electrophoresis (SDS-PAGE) on 10% polyacrylamide gels. The proteins were transferred to supported nitrocellulose membranes and probed with either HRP-conjugated streptavidin (1:2500), anti-CD71 (1:1000) followed by HRP-conjugated anti-mouse IgG (1:10,000) or HRP-conjugated CTx-B (200ng/mL). HRP enzyme activity was determined after the addition of a 1:1 mix of Western Lightning oxidizing and luminol reagents (PerkinElmer Life Sciences).

Statistical Analyses

Statistics were analyzed using GraphPad Prism version 9.1.1 (GraphPad). Every data set was tested for statistical normality, and this information was used to apply the appropriate (parametric or nonparametric) statistical test. P values of <0.05 were considered significant; significance values are indicated as * $p<0.05$, ** $p<0.01$, *** $p<0.001$, **** $p < 0.0001$.

4.5 Results and Discussion

HIV-1 Env 'opening' accelerates its antibody-mediated internalization from the cell surface

We first determined the rate of cell-surface Env internalization upon the addition of certain nNAbs, the coreceptor binding site antibody 17b and the V3 crown antibody 19b, from the surface of primary CD4+ T cells infected with the transmitted/founder (T/F) virus CH58. As our previous observations (4), the binding of nNAbs to surface Env remained steady over the course of 3 hours at 37°C and antibody bound Env levels only reduced by ~20% (**Figure 4.1A**). Upon the addition of a CD4mc, BNM-III-170, Env adopts its downstream CD4-bound conformation (27). This allows for enhanced nNAb binding that preferentially recognize epitopes normally hidden in the 'closed' Env, including enhanced 17b and 19b binding (12, 28, 29). In the presence of BNM-III-170, surface levels of 17b and 19b-bound Env significantly declined by ~80% after 3 hours, at a similar rate as the bNAb PGT151, indicating Env internalization (**Figure 4.1A**).

We confirmed these observations with soluble CD4 (sCD4), a version of the CD4 receptor lacking its transmembrane region. In this condition, sCD4 interacts with Env in *trans* and we observed faster rates of nNAb-induced Env internalization (**Figure 4.1B**). Furthermore, we also used Ab-sCD4 hybrid proteins which are designed to harbour two sCD4 molecules linked to a single antibody of interest (22). Using 17b-sCD4 and 19b-sCD4 hybrids, surface levels of Env significantly declined by ~60% from the surface of primary CD4+ T cells infected with the JRFL virus (**Figure 4.1B**). Using other methods to selectively 'open up' the Env independently of CD4, we introduced the L193A substitution in Env, a mutation known to stabilize Env downstream conformations (18, 30). In a similar fashion as with the addition of BNM-III-170, surface levels of 17b- and 19b-bound Env declined by ~80% over 3 hours at 37°C using cells infected with the CH58 L193A virus (**Figure 4.1C**).

Interestingly, the deletion of Nef and Vpu, which impairs the capacity of the virus to downregulate CD4 resulting in Env sampling its 'open' conformation, (13) significantly slowed down the rate of 17b and 19b-mediated Env internalization (**Figure 4.1D**) (4) when

compared to the accelerated rates seen in the presence of BNM-III-170 in **Figure 4.1A**. Thus, these results suggest that 'opening' the Env is not sufficient to induce its internalization since soluble CD4, but not membrane-anchored CD4 (mCD4) are able to mediate nNAb-induced internalization. Whether this phenotype is related to the mode of interaction being in *trans* for sCD4 versus in *cis* for mCD4 (13), remains to be determined. Hypothetically, endogenous CD4 expression might result in Env-CD4 complex co-trafficking and the redirection of Env to different microdomains at the cell surface that are refractory to antibody-induced internalization.

We further confirmed our observations of antibody-mediated internalization upon the selective opening of Env with *ex vivo*-expanded endogenously infected CD4+ T cells. Primary CD4+ T cells were isolated from antiretroviral therapy (ART)-treated HIV-1-infected individuals and activated with PHA-L/IL-2, where viral replication was followed by intracellular p24 staining. In agreement with the results obtained with CH58 T/F and JRFL-infected primary CD4+ T cells, the binding of 19b and 17b induces Env internalization from the surface of endogenously infected primary CD4+ T cells in the presence of BNM-III-170 (**Figure 4.1E**), sCD4 or when using Ab-sCD4 hybrid protein (**Figure 4.1F**). Altogether, the results from our flow cytometry experiments are suggestive of coexisting Env populations at the cell surface that can undergo faster or slower internalization.

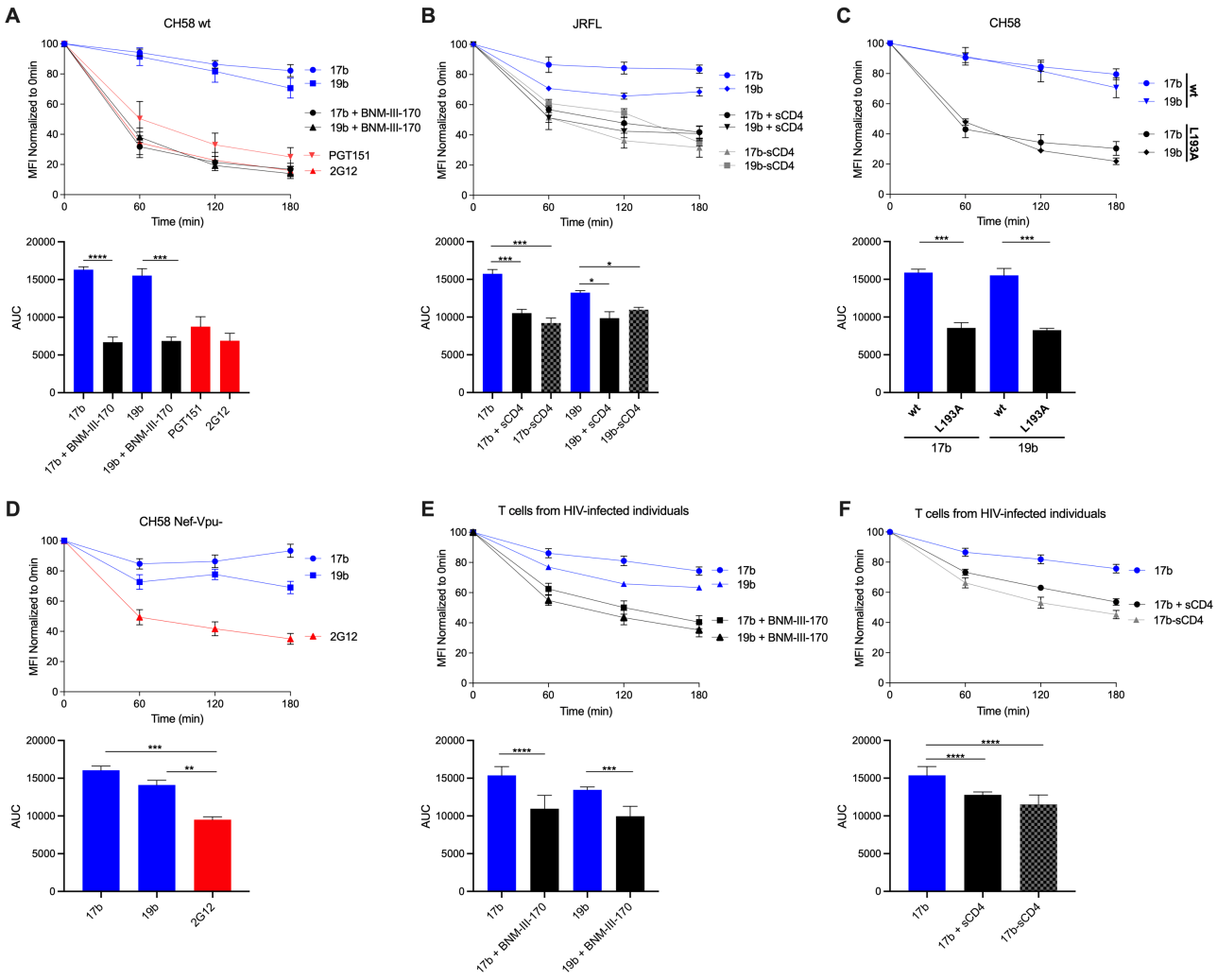

Figure 4.1. Antibody-induced internalization of HIV-1 Env from the cell-surface can be accelerated upon the selective opening of Env.
(**A-D**) Cell surface staining of primary CD4+ T cells infected *in vitro* with (**A**) CH58 T/F virus, (**B**) JRFL wt virus, (**C**) CH58 T/F wt or L193A virus, and (**D**) CH58 T/F virus defective for Nef and Vpu expression was performed 48h post-infection. (**E-F**) Primary CD4+ T cells from at least three different HIV-1-infected individuals were isolated and reactivated with PHA-L for 48 h, followed by incubation with IL-2 to expand the endogenous virus. Cell surface staining of endogenously infected primary CD4+ T cells was performed upon reactivation. (**A-F**) Antibody binding was detected using Alexa Fluor 647-conjugated anti-human secondary Abs. (Top) Quantification of remaining antibody-Env complexes on the cell surface over different timepoints is expressed as percentage of the MFI relative to the 0 min timepoint control. (Bottom) Areas under the curve (AUC) were calculated based on MFI data sets using GraphPad Prism software. Error bars indicate means ± the SEM. Statistical significance was tested using an unpaired t test or a Mann-Whitney U test based on statistical normality (*, $P<0.05$; **, $P<0.01$; ***, $P < 0.001$; ****, $P < 0.0001$).

Visualizing nNAb mediated Env internalization from the cell surface

We confirmed our observations obtained with infected primary CD4+ T cells (**Figure 4.1**) using 293T cells transfected with plasmids encoding the tier 2 JRFL Env alone or together with a human CD4 receptor. Using flow cytometry, we observe an increase in 17b- and 19b-binding to the Env in the presence of CD4mc. Once again, in these conditions, the overall levels of 17b- and 19b-bound Env significantly decreases within 3 hours (**Figure 4.2A**). However, upon CD4 co-transfection, which allows for greater overall nNAb binding, we observe decreased rates of Env internalization (**Figure 4.2A**). To visualize the phenotype of nNAb-induced internalization, we performed confocal microscopy experiments with transfected 293T cells. Cells were incubated 48 hours post-transfection with Alexa Fluor-conjugated nNAbs for up to 2 hours at 37°C before fixing and analysis by imaging. In the presence of BNM-III-170, we can visualize a rapid internalization of 19b and 17b-bound Env from the cell surface compared to the antibody alone (**Figure 4.2B, C**). A similar phenotype was observed with Env bound by the 17b-sCD4 chimeric protein (**Figure 4.2C**). Similar to the results obtained with the Nef and Vpu deleted virus (**Figure 4.1D**), CD4 co-expression did not results in Env internalization, and rather the remaining surface fluorescence was significantly higher (**Figure 4.2B, C**). Overall, indicating that, interaction with CD4 in cis allows for antibody-Env complexes to remain on the surface for a longer period. These observations confirm previous observations (4), wherein the rates of nNAb-mediated Env internalization were significantly slower upon the co-transfection of the CD4 receptor. Thus, CD4mc or sCD4 speed up Env internalization but membrane-anchored CD4 allows the Env-antibody complexes to remain on the cell surface for a longer period.

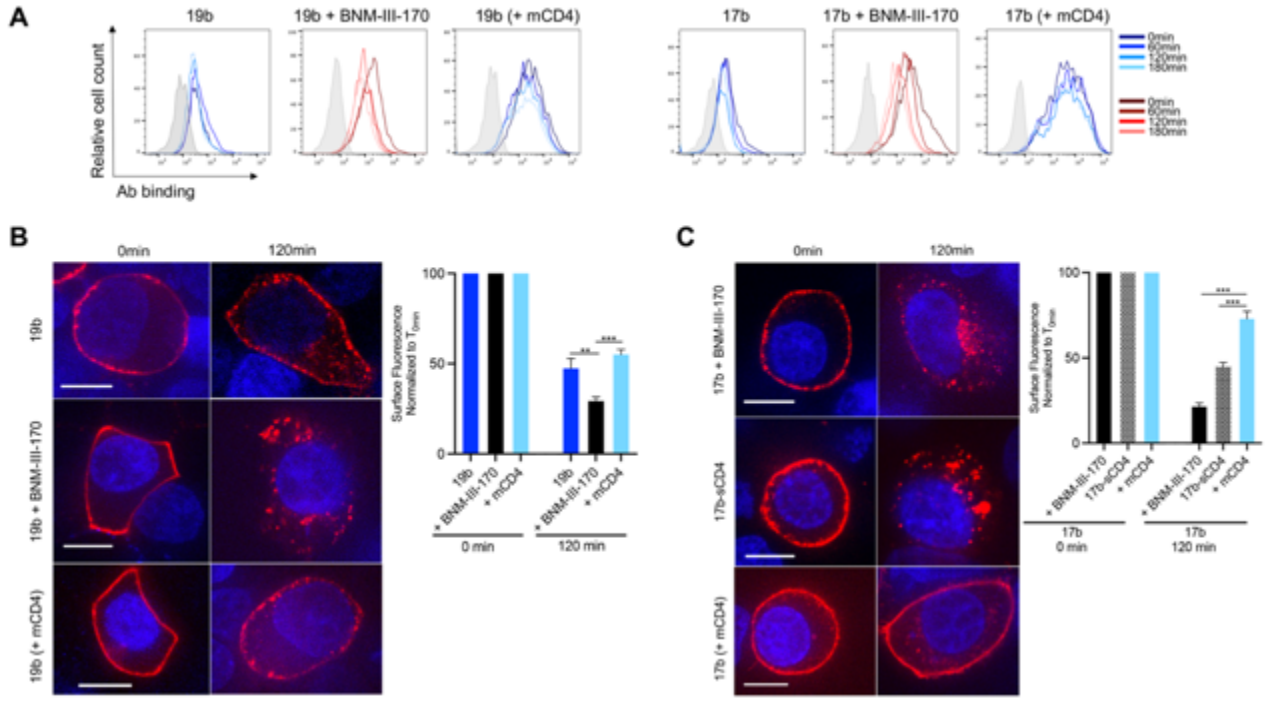

Figure 4.2. Antibody-induced internalization of Env from the surface of transfected cells. (**A**) Cell surface staining of 293T cells transfected with plasmid encoding JRFL Env alone or together with an expressor of the human CD4 receptor was performed 48h post-transfection. Ab binding was quantified at 0-, 60-, 120- and 180-minutes using flow cytometry. Histograms depict representative staining of transfected cells and untransfected (gray) with 17b or 19b Abs. (**B, C**) 293T cells were transfected with a plasmid encoding JRFL Env alone or together with an expressor of the human CD4 receptor and were stained with (**B**) 19b conjugated with Alexa Fluor 647 or (**C**) 17b conjugated with Alexa Fluor 594 for confocal microscopy analyses to visualize internalization. Alternatively, staining with 17b-sCD4 was done in combination with the goat anti-human IgG Alexa Fluor 594 secondary Ab. (**B-C**, Left panels) Images show the localization of antibody-Env complexes at different time points (0 and 120 min). Images represent a single confocal z-section through the middle of the cell; at least 25 cells were imaged per condition, and representative images are shown. Scale bar, 10 μm. (**B-C**, Right panels) The remaining cell-surface antibody-Env complexes over different time points are expressed as percentages of the surface fluorescence relative to the 0 min timepoint control. Error bars indicate means ± the SEM. Statistical significance was tested using an unpaired t test or a Mann-Whitney U test based on statistical normality (**, $P<0.01$; ***, $P < 0.001$). mCD4; membrane-anchored CD4.

Different membrane microdomains could determine antibody-mediated Env internalization

Since we observed striking differences in nNAb-induced internalization rates depending on the presence of membrane-anchored CD4, we sought to determine if this could be due a difference in the localization of antibody-Env complexes at the plasma membrane. First, we biotinylated Env trimers expressed on the surface of 293T cells, allowed 19b binding, pulled out Env-19b complexes using immunoprecipitation, and resolved surface Env using streptavidin via western blot. We observe that with cells expressing only the JRFL Env, 19b precipitates out mainly the uncleaved Env (gp160). Whereas, with cells expressing both the JRFL Env and human CD4, 19b precipitates out both the uncleaved (gp160) and cleaved Env (gp120) (**Figure 4.3A**). This is likely due to the conformational flexibility of the uncleaved Env that facilitates its recognition by nNAbs. Env epitopes recognized by these nNAbs are occluded in the cleaved Env (31-33), therefore requiring the 'opening' of Env by CD4 for their interaction to occur. Of note, and in agreement with previous publications, we observe two bands of distinct molecular weight for the uncleaved gp160 that were previously associated to their glycosylation content (**Figure 4.3A**) (7, 34).

The Env trimer has been described to be contained in lipid microdomains (commonly known as 'lipid rafts') on the infected cell surface from where budding occurs (35-38). These specialized membrane microdomains are enriched with cholesterol and sphingolipids and are reported to play an important role in endocytic processes (39). To assess the association of rapidly internalized antibody-Env complexes with microdomains, we biochemically isolated lipid microdomains by membrane fractionation using a sucrose gradient (40). We identified the detergent-resistant membranes (DRMs or 'lipid rafts') using the ganglioside GM1 and the transferrin receptor (CD71) was used to identify the detergent soluble membranes (DSMs) (**Figure 4.3B**). Cell-surface biotinylated Env trimers complexed with antibodies undergoing fractionation using sucrose gradients were resolved via immunoprecipitation, followed by western blotting. Using this technique, we observed an enrichment of bNAb-bound (PGT151) cleaved Env (gp120) in the DRM (top) fractions (**Figure 4.3C**). Since bNAb-bound Env internalizes rapidly, this initial observation indicates that the Env-antibody complexes that are present in the DRM (top) fractions, and thus, associated with lipid microdomains, undergo

rapid internalization. On the other hand, when we used 19b we preferentially detected uncleaved Env (gp160) which was located in both the DSM (bottom) and DRM (top) fractions (**Figure 4.3D**). Interestingly, we observed that the slower migrating gp160 band, which was reported to have complex glycans, is enriched in the DRM (top) fractions, while the gp160 band with the lower molecular weight, reported to be composed primarily of oligomannose glycans, appeared in the DSM (bottom) fractions (7, 34). Upon addition of BNM-III-170, the cleaved Env (gp120) appears in the DRM (top) fractions (**Figure 4.3E**). The presence of cleaved Env in the fractions that are associated with lipid microdomains upon the addition of BNM-III-170, could explain the rapid Env internalization in the conditions that CD4mc are present. Consistent with our observations that co-expression of CD4 slows down nNAb-internalization, we observe an accumulation of the cleaved Env (gp120) localization to the DSM (bottom) fractions (**Figure 4.3F**). An enrichment of Ab-Env complexes away from lipid microdomains in the presence of membrane-anchored CD4 could explain the slower antibody-mediated Env internalization seen in these conditions. Thus, cleaved or uncleaved Env-antibody complexes that are present in DSM (bottom) fractions, and do not associate with lipid microdomains, remain on the cell surface for a prolonged period. Our observations suggest that the association of antibody-bound functionally cleaved Env (gp120) with lipid microdomains could influence its accelerated internalization. Future studies need to confirm these observations in a more physiological system with primary CD4+ T cells.

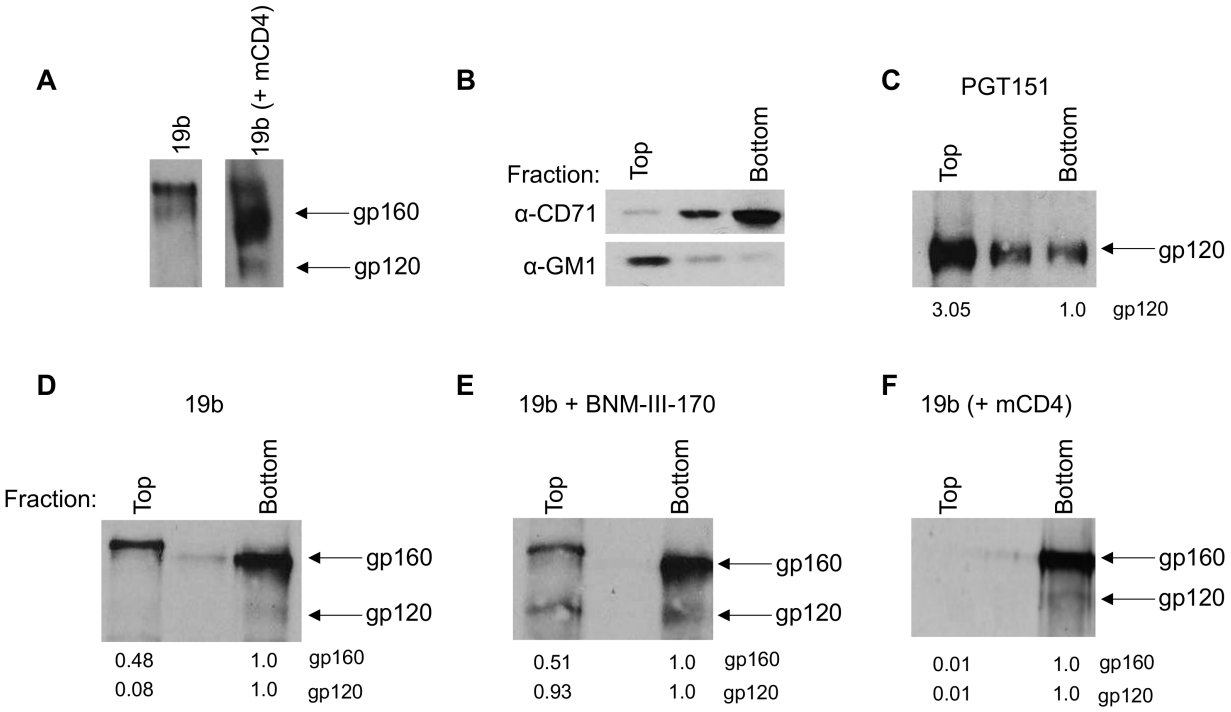

Figure 4.3. Differential localization of antibody-Env complexes visualized by lipid microdomain fractionation.

293T cells were transfected with a plasmid encoding JRFL Env alone or together with an expressor of the human CD4 receptor and 48 hours post-transfection all cell-surface proteins were biotinylated. (**A**) Immunoprecipitation of cell-surface biotinylated Env from cells transfected to express the (left) JRFL Env alone or (right) with the human CD4 receptor after incubation with 19b. Further, cell lysates were fractionated on a sucrose density gradient as described in Materials and Methods. (**B**) Equal volumes of individual fractions were resolved by SDS-PAGE, transferred to a nitrocellulose membrane, and probed with HRP-conjugated CTx-B to detect DRM marker ganglioside GM1 or with OKT-9 antibody to detect DSM marker CD71. (**C-F**) Immunoprecipitation of cell-surface biotinylated Env from individual sucrose gradient fractions using (**C**) PGT151, (**D**) 19b, (**E**) 19b with 5μM BNM-III-170 from cells expressing the JRFL Env only and (**F**) 19b from cells expressing both the JRFL Env and human CD4 receptor. Values represent densities of respective band intensities quantified using ImageJ normalized to the bottom fractions. (**B-F**) Representative blots from at least three independent experiments are shown. mCD4; membrane-anchored CD4

Collectively, our results suggest that in addition to the different populations and conformations of Env that co-exist on the cell surface, antibody-mediated Env internalization could also be attributed to the localization of Env in discrete microdomains. Further studies to confirm the differential localization of antibody-Env complexes using high-resolution microscopic studies are warranted (41). Our results could steer the selection of antibody therapeutics against HIV-1 that allow for the Env to remain stable on the surface of infected cells and thus, enhance its recognition by the immune system.

Acknowledgments

The authors thank the CRCHUM Cellular Imaging, Flow Cytometry, and Biosafety Level 3 Laboratory Platforms as well as Mario Legault for cohort coordination and clinical samples. The authors thank Dennis Burton for the JRFL IMC, Beatrice H. Hahn for the CH58 wt IMC, Frank Kirchhoff for the CH58 Nef-Vpu- IMC, and Joseph Sodroski for helpful discussions regarding the project. This work was supported by a CIHR foundation grant #352417 to A.F. Support for this work was also provided by NIH R01 to A.F. and M.P. (AI129769) and to A.F. (AI148379 and AI150322) and P01 AI120756 to Georgia Tomaras and M.P. This study was also supported by grant P01-GM56550/AI150471 to A.B.S. and A.F. A.F. is the recipient of a Canada Research Chair on Retroviral Entry #RCHS0235 950-232424. S.P.A. and J.P. are recipients of CIHR doctoral fellowships. The funders had no role in study design, data collection and analysis, decision to publish, or preparation of the manuscript.

4.6 References

1. Boge M, Wyss S, Bonifacino JS, Thali M. 1998. A membrane-proximal tyrosine-based signal mediates internalization of the HIV-1 envelope glycoprotein via interaction with the AP-2 clathrin adaptor. J Biol Chem 273:15773-8.
2. Byland R, Vance PJ, Hoxie JA, Marsh M. 2007. A conserved dileucine motif mediates clathrin and AP-2-dependent endocytosis of the HIV-1 envelope protein. Mol Biol Cell 18:414-25.
3. von Bredow B, Arias JF, Heyer LN, Gardner MR, Farzan M, Rakasz EG, Evans DT. 2015. Envelope Glycoprotein Internalization Protects Human and Simian Immunodeficiency Virus-Infected Cells from Antibody-Dependent Cell-Mediated Cytotoxicity. J Virol 89:10648-55.
4. Anand SP, Grover JR, Tolbert WD, Prévost J, Richard J, Ding S, Baril S, Medjahed H, Evans DT, Pazgier M. 2019. Antibody-induced internalization of HIV-1 Env proteins limits the surface expression of the closed conformation of Env. Journal of virology:JVI. 00293-19.
5. Panova V, Attig J, Young GR, Stoye JP, Kassiotis G. 2020. Antibody-induced internalisation of retroviral envelope glycoproteins is a signal initiation event. PLoS Pathog 16:e1008605.
6. Chew HY, De Lima PO, Gonzalez Cruz JL, Banushi B, Echejoh G, Hu L, Joseph SR, Lum B, Rae J, O'Donnell JS, Merida de Long L, Okano S, King B, Barry R, Moi D, Mazzieri R, Thomas R, Souza-Fonseca-Guimaraes F, Foote M, McCluskey A, Robinson PJ, Frazer IH, Saunders NA, Parton RG, Dolcetti R, Cuff K, Martin JH, Panizza B, Walpole E, Wells JW, Simpson F. 2020. Endocytosis Inhibition in Humans to Improve Responses to ADCC-Mediating Antibodies. Cell 180:895-914 e27.
7. Zhang S, Nguyen HT, Ding H, Wang J, Zou S, Liu L, Guha D, Gabuzda D, Ho DD, Kappes JC, Sodroski J. 2021. Dual Pathways of Human Immunodeficiency Virus Type 1 Envelope Glycoprotein Trafficking Modulate the Selective Exclusion of Uncleaved Oligomers from Virions. J Virol 95.
8. Zou S, Zhang S, Gaffney A, Ding H, Lu M, Grover JR, Farrell M, Nguyen HT, Zhao C, Anang S, Zhao M, Mohammadi M, Blanchard SC, Abrams C, Madani N, Mothes W, Kappes JC, Smith AB, 3rd, Sodroski J. 2020. Long-Acting BMS-378806 Analogues Stabilize the State-1 Conformation of the Human Immunodeficiency Virus (HIV-1) Envelope Glycoproteins. J Virol doi:10.1128/JVI.00148-20.
9. Salimi H, Johnson J, Flores MG, Zhang MS, O'Malley Y, Houtman JC, Schlievert PM, Haim H. 2020. The lipid membrane of HIV-1 stabilizes the viral envelope glycoproteins and modulates their sensitivity to antibody neutralization. J Biol Chem 295:348-362.
10. Fontaine J, Chagnon-Choquet J, Valcke HS, Poudrier J, Roger M. 2011. High expression levels of B lymphocyte stimulator (BLyS) by dendritic cells correlate with HIV-related B-cell disease progression in humans. Blood 117:145-55.
11. Fontaine J, Coutlee F, Tremblay C, Routy JP, Poudrier J, Roger M. 2009. HIV infection affects blood myeloid dendritic cells after successful therapy and despite nonprogressing clinical disease. J Infect Dis 199:1007-18.

12. Richard J, Veillette M, Brassard N, Iyer SS, Roger M, Martin L, Pazgier M, Schon A, Freire E, Routy JP, Smith AB, 3rd, Park J, Jones DM, Courter JR, Melillo BN, Kaufmann DE, Hahn BH, Permar SR, Haynes BF, Madani N, Sodroski JG, Finzi A. 2015. CD4 mimetics sensitize HIV-1-infected cells to ADCC. Proc Natl Acad Sci U S A 112:E2687-94.
13. Veillette M, Desormeaux A, Medjahed H, Gharsallah NE, Coutu M, Baalwa J, Guan Y, Lewis G, Ferrari G, Hahn BH, Haynes BF, Robinson JE, Kaufmann DE, Bonsignori M, Sodroski J, Finzi A. 2014. Interaction with cellular CD4 exposes HIV-1 envelope epitopes targeted by antibody-dependent cell-mediated cytotoxicity. J Virol 88:2633-44.
14. Lodge R, Lalonde JP, Lemay G, Cohen EA. 1997. The membrane-proximal intracytoplasmic tyrosine residue of HIV-1 envelope glycoprotein is critical for basolateral targeting of viral budding in MDCK cells. EMBO J 16:695-705.
15. Salazar-Gonzalez JF, Salazar MG, Keele BF, Learn GH, Giorgi EE, Li H, Decker JM, Wang S, Baalwa J, Kraus MH, Parrish NF, Shaw KS, Guffey MB, Bar KJ, Davis KL, Ochsenbauer-Jambor C, Kappes JC, Saag MS, Cohen MS, Mulenga J, Derdeyn CA, Allen S, Hunter E, Markowitz M, Hraber P, Perelson AS, Bhattacharya T, Haynes BF, Korber BT, Hahn BH, Shaw GM. 2009. Genetic identity, biological phenotype, and evolutionary pathways of transmitted/founder viruses in acute and early HIV-1 infection. J Exp Med 206:1273-89.
16. Ochsenbauer C, Edmonds TG, Ding H, Keele BF, Decker J, Salazar MG, Salazar-Gonzalez JF, Shattock R, Haynes BF, Shaw GM, Hahn BH, Kappes JC. 2012. Generation of Transmitted/Founder HIV-1 Infectious Molecular Clones and Characterization of Their Replication Capacity in CD4 T Lymphocytes and Monocyte-Derived Macrophages. J Virol 86:2715-28.
17. Heigele A, Kmiec D, Regensburger K, Langer S, Peiffer L, Sturzel CM, Sauter D, Peeters M, Pizzato M, Learn GH, Hahn BH, Kirchhoff F. 2016. The Potency of Nef-Mediated SERINC5 Antagonism Correlates with the Prevalence of Primate Lentiviruses in the Wild. Cell Host Microbe 20:381-91.
18. Prevost J, Richard J, Ding S, Pacheco B, Charlebois R, Hahn BH, Kaufmann DE, Finzi A. 2018. Envelope glycoproteins sampling states 2/3 are susceptible to ADCC by sera from HIV-1-infected individuals. Virology 515:38-45.
19. O'Brien WA, Koyanagi Y, Namazie A, Zhao JQ, Diagne A, Idler K, Zack JA, Chen IS. 1990. HIV-1 tropism for mononuclear phagocytes can be determined by regions of gp120 outside the CD4-binding domain. Nature 348:69-73.
20. Mao Y, Wang L, Gu C, Herschhorn A, Xiang SH, Haim H, Yang X, Sodroski J. 2012. Subunit organization of the membrane-bound HIV-1 envelope glycoprotein trimer. Nat Struct Mol Biol 19:893-9.
21. Bour S, Schubert U, Strebel K. 1995. The human immunodeficiency virus type 1 Vpu protein specifically binds to the cytoplasmic domain of CD4: implications for the mechanism of degradation. J Virol 69:1510-20.
22. Richard J, Nguyen D, Tolbert WD, Gasser R, ding s, Vezina D, Yu Gong S, Prevost J, Gendron-Lepage G, Medjahed H, Gottumukkala S, Finzi A, Pazgier M. 2021. Across functional boundaries: making non-neutralizing antibodies to neutralize HIV-1 and

mediate Fc-mediated effector killing of infected cells. bioRxiv doi:10.1101/2021.08.13.456231:2021.08.13.456231.
23. Finzi A, Xiang SH, Pacheco B, Wang L, Haight J, Kassa A, Danek B, Pancera M, Kwong PD, Sodroski J. 2010. Topological layers in the HIV-1 gp120 inner domain regulate gp41 interaction and CD4-triggered conformational transitions. Mol Cell 37:656-67.
24. Melillo B, Liang S, Park J, Schon A, Courter JR, LaLonde JM, Wendler DJ, Princiotto AM, Seaman MS, Freire E, Sodroski J, Madani N, Hendrickson WA, Smith AB, 3rd. 2016. Small-Molecule CD4-Mimics: Structure-Based Optimization of HIV-1 Entry Inhibition. ACS Med Chem Lett 7:330-4.
25. Chen J, Park J, Kirk SM, Chen HC, Li X, Lippincott DJ, Melillo B, Smith AB, 3rd. 2019. Development of an Effective Scalable Enantioselective Synthesis of the HIV-1 Entry Inhibitor BNM-III-170 as the Bis-Trifluoroacetate Salt. Org Process Res Dev 23:2464-2469.
26. Schneider CA, Rasband WS, Eliceiri KW. 2012. NIH Image to ImageJ: 25 years of image analysis. Nat Methods 9:671-5.
27. Laumaea A, Smith AB, 3rd, Sodroski J, Finzi A. 2020. Opening the HIV envelope: potential of CD4 mimics as multifunctional HIV entry inhibitors. Curr Opin HIV AIDS 15:300-308.
28. Richard J, Veillette M, Ding S, Zoubchenok D, Alsahafi N, Coutu M, Brassard N, Park J, Courter JR, Melillo B, Smith AB, 3rd, Shaw GM, Hahn BH, Sodroski J, Kaufmann DE, Finzi A. 2016. Small CD4 Mimetics Prevent HIV-1 Uninfected Bystander CD4 + T Cell Killing Mediated by Antibody-dependent Cell-mediated Cytotoxicity. EBioMedicine 3:122-34.
29. Anand SP, Prévost J, Baril S, Richard J, Medjahed H, Chapleau J-P, Tolbert WD, Kirk S, Smith AB, Wines BD. 2018. Two families of Env antibodies efficiently engage Fc-gamma receptors and eliminate HIV-1-infected cells. Journal of Virology:JVI. 01823-18.
30. Herschhorn A, Ma X, Gu C, Ventura JD, Castillo-Menendez L, Melillo B, Terry DS, Smith AB, 3rd, Blanchard SC, Munro JB, Mothes W, Finzi A, Sodroski J. 2016. Release of gp120 Restraints Leads to an Entry-Competent Intermediate State of the HIV-1 Envelope Glycoproteins. MBio 7:doi:10.1128/mBio.01598-16.
31. Haim H, Salas I, Sodroski J. 2013. Proteolytic processing of the human immunodeficiency virus envelope glycoprotein precursor decreases conformational flexibility. J Virol 87:1884-9.
32. Alsahafi N, Bakouche N, Kazemi M, Richard J, Ding S, Bhattacharyya S, Das D, Anand SP, Prévost J, Tolbert WD, Lu H, Medjahed H, Gendron-Lepage G, Ortega Delgado GG, Kirk S, Melillo B, Mothes W, Sodroski J, Smith AB, 3rd, Kaufmann DE, Wu X, Pazgier M, Rouiller I, Finzi A, Munro JB. 2019. An Asymmetric Opening of HIV-1 Envelope Mediates Antibody-Dependent Cellular Cytotoxicity. Cell Host Microbe 25:578-587.e5.
33. Castillo-Menendez LR, Witt K, Espy N, Princiotto A, Madani N, Pacheco B, Finzi A, Sodroski J. 2018. Comparison of Uncleaved and Mature Human Immunodeficiency Virus Membrane Envelope Glycoprotein Trimers. J Virol 92.

34. Stieh DJ, King DF, Klein K, Aldon Y, McKay PF, Shattock RJ. 2015. Discrete partitioning of HIV-1 Env forms revealed by viral capture. Retrovirology 12:81.
35. Campbell SM, Crowe SM, Mak J. 2001. Lipid rafts and HIV-1: from viral entry to assembly of progeny virions. J Clin Virol 22:217-27.
36. Nguyen DH, Hildreth JE. 2000. Evidence for budding of human immunodeficiency virus type 1 selectively from glycolipid-enriched membrane lipid rafts. J Virol 74:3264-72.
37. Tedbury PR, Freed EO. 2014. The role of matrix in HIV-1 envelope glycoprotein incorporation. Trends Microbiol 22:372-8.
38. Waheed AA, Freed EO. 2010. The Role of Lipids in Retrovirus Replication. Viruses 2:1146-1180.
39. Laude AJ, Prior IA. 2004. Plasma membrane microdomains: organization, function and trafficking. Mol Membr Biol 21:193-205.
40. Popik W, Alce TM, Au WC. 2002. Human immunodeficiency virus type 1 uses lipid raft-colocalized CD4 and chemokine receptors for productive entry into CD4(+) T cells. J Virol 76:4709-22.
41. Chojnacki J, Eggeling C. 2018. Super-resolution fluorescence microscopy studies of human immunodeficiency virus. Retrovirology 15:41.

CHAPTER V

Enhanced Ability of Plant-Derived PGT121 Glycovariants to Eliminate HIV-1-Infected Cells

Sai Priya Anand*, Shilei Ding*, William D. Tolbert, Jérémie Prévost, Jonathan Richard, Hwi Min Gil, Gabrielle Gendron-Lepage, Wing-Fai Cheung, Haifeng Wang, Rebecca Pastora, Hirak Saxena, Warren Wakarchuk, Halima Medjahed, Bruce D. Wines, P. Mark Hogarth, George M. Shaw, Malcom A. Martin, Dennis R. Burton, Lars Hangartner, David T. Evans, Marzena Pazgier, Doug Cossar, Michael D. McLean and Andrés Finzi

5.1 Preface to Chapter 5

As described in Chapter 1, the antiviral activities of the highly potent bNAb, PGT121, are currently being evaluated in clinical trials for HIV-1 prevention and therapy. Two recent studies showed that the neutralization capacity of PGT121 is sufficient to protect infection since the Fc-impaired versions of PGT121 provided similar levels of protection as their wild-type counterparts (386, 387). However, these studies were performed with primarily fucosylated PGT121 and did not comprehensively explore the capacity of PGT121 to clear the cellular reservoir. Thus, in this chapter, we attempt to better understand the importance of the Fc-effector functions of PGT121 in clearing HIV-1-infected cells by modulating its glycosylation profile using a plant-based system. These results are important in informing the design of numerous ongoing and future human clinical trials utilizing bNAbs for HIV-1 remission.

5.2 Abstract

The activity of broadly neutralizing antibodies (bNAbs) targeting HIV-1 depends on pleiotropic functions including viral neutralization and the elimination of HIV-1-infected cells. Several *in vivo* studies have suggested that passive administration of bNAbs represents a valuable strategy for the prevention or treatment of HIV-1. Additionally, different strategies are currently being tested to scale-up the production of bNAbs to obtain the large quantities of antibodies required for clinical trials. Production of antibodies in plants permits low-cost and large-scale production of valuable therapeutics; furthermore, pertinent to this work, it also includes an advanced glycoengineering platform. In this study, we used *Nicotiana benthamiana* to produce different Fc-glycovariants of a potent bNAb, PGT121, with near-homogeneous profiles and evaluated their antiviral activities. Structural analyses identified a close similarity in overall structure and glycosylation patterns of Fc regions for these plant-derived Abs and mammalian cell-derived Abs. When tested for Fc-effector activities, afucosylated PGT121 showed significantly enhanced FcγRIIIa interaction and antibody dependent cellular cytotoxicity (ADCC) against primary HIV-1-infected cells, both *in vitro* and *ex vivo*. However, the overall galactosylation profiles of plant PGT121 did not affect ADCC activities against infected primary CD4+ T cells. Our results suggest that the abrogation of the Fc N-linked glycan fucosylation of PGT121 is a worthwhile strategy to boost its Fc-effector functionality.

5.3 Introduction

Human immunodeficiency virus type 1 (HIV-1) envelope glycoproteins (Env) represent the main virus-specific antigen exposed at the surface of viral particles and infected cells. As such, Env represents a unique target for neutralization and Fc-effector functions, such as antibody-dependent cellular cytotoxicity (ADCC). Several *in vivo* studies in humanized mice and non-human primate (NHP) models of HIV-1 infection (1-7), as well as in HIV-1-infected humans, have shown that passive administration of broadly neutralizing antibodies (bNAbs) can confer both effective pre-exposure prophylaxis and therapeutic control of viremia (8-12). The progress made over the last few years further spurred the interest to use bNAbs for protection and control of HIV-1 infection in ongoing clinical trials (NCT03707977, NCT04319367, and NCT03837756). With the expansion in the use of bNAbs, the large amounts of antibodies required to perform these studies, and the cost that is associated to produce them in mammalian cells is a significant barrier (13, 14). Alternate cost-effective platforms to express and purify these bNAbs are being explored. Strategies that are currently being tested to increase the production of monoclonal antibody therapeutics include bacteria such as *Escherichia coli* (15) and yeast such as *Pichia pastoris* (16).

Another platform gaining significant interest in the recent decade is the production of monoclonal antibodies (mAbs) and other biologic drugs in plant-based systems using *Nicotiana benthamiana* (17, 18). This allows the unlimited potential for large-scale, cost-effective production of valuable therapeutic proteins (19, 20). Additionally, production cost is not the only advantage of this technology. This method offers rapid development timelines since plant expression systems apply transient expression technology using Agrobacterium to introduce DNA expression vectors encoding mAbs of interest into the plant by horizontal gene transfer. This system allows mAb production of upwards of 10% total soluble protein biomass that usually peaks within one week, after which the plants can be harvested for product purification (21, 22).

Furthermore, plant expression systems now also harbour the advantage of an advanced glycoengineering platform (23). Since post-translational modifications are critical for the

functional activities of antibodies, glycoengineering is a valuable tool to improve their Fc-effector functions. Glycoengineered mAbs have already demonstrated their potential for other viral infections, including Zika (24), Dengue (25), Rabies (26) and West Nile virus (27). The glycosylation status of mAbs modulates Fc gamma receptors (FcγR) binding to improve or decrease Ab-mediated effector functions, such as ADCC. This is dictated by glycan moieties that can be added or removed from asparagine-297 (N297), the single N-linked glycosylation site of IgG Fc fragment. Mutations of N297 residue have been shown to diminish FcγR binding and specific Fc-glycan modifications have been shown to modulate Ab functionality (28-31). Concurrent with the research being done to glycoengineer Env-specific bNAbs against HIV-1 (32-35), we have utilized a *N. benthamiana*-based glycoengineering platform in this study that is valuable in the currently expanding field of HIV-1 bNAbs therapy.

Here we generated different glycoforms of the highly potent PGT121 bNAb, which recognizes the N332 supersite at the base of Env V3 loop (36-40). PGT121 has been shown to provide prolonged viral suppression in chronically infected rhesus macaques (1) and to mediate effective protection against cell-free viral mucosal (41, 42) and cell-associated intravenous (43) SHIV challenges. While bNAbs antiviral effects can be largely attributed to the ability of antibodies to neutralize viral particles (44), Fc-mediated functions have also been associated with optimal bNAb activity *in vivo* (1, 2, 45-48) but remains somewhat controversial in the context of protection against infection (49). We evaluated the abilities of these PGT121 glycovariants to interact with FcγRIIIa and mediate efficient ADCC against HIV-1 and SHIV-infected cells *in vitro* and *ex vivo*.

5.4 Material and Methods

Ethics Statement

Written informed consent was obtained from all study participants [the Montreal Primary HIV Infection Cohort (77, 78)] and research adhered to the ethical guidelines of CRCHUM and was reviewed and approved by the CRCHUM institutional review board (ethics committee, approval number CE16.164-CA). Research adhered to the standards indicated by the Declaration of Helsinki. All participants were adult and provided informed written consent prior to enrolment in accordance with Institutional Review Board approval.

Cell lines and Isolation of Primary CD4+ T cells

293T human embryonic kidney cells (obtained from ATCC) were maintained at 37°C under 5% CO_2 in Dulbecco's modified Eagle's medium (DMEM) (Wisent) containing 5% fetal bovine serum (VWR) and 100 µg/ml penicillin-streptomycin (Wisent). CEM.NKR-CCR5-sLTR-Luc cells and the CD16+ KHYG-1 effector cells were maintained at 37°C under 5% CO_2 in RPMI 1640 complete medium (Gibco) containing 10% fetal bovine serum (VWR) and 100 µg/ml penicillin-streptomycin (Wisent). Primary CD4+ T lymphocytes were purified from resting PBMCs by negative selection and activated as previously described (56, 73). Briefly, PBMCs were obtained by leukapheresis from 5 HIV-uninfected healthy adults. CD4+ T lymphocytes were purified using immunomagnetic beads as per the manufacturer's instructions (StemCell Technologies). CD4+ T lymphocytes were activated with phytohemagglutinin-L (PHA-L; 10 µg/mL) for 48 hours and then maintained in RPMI 1640 complete medium (Gibco) supplemented with rIL-2 (100 U/mL).

Plant derived protein production and purification

Methods for production of antibodies in plants have been published (18, 21, 79, 80). Expression vectors for plant-produced trastuzumab and PGT121 were assembled in a common plasmid backbone and included a double-enhancer version of the Cauliflower Mosaic Virus (CaMV) 35S promoter (EE35S) (81) driving expression of each of the respective heavy chain (HC) and light chain (LC) genes plus the same promoter driving expression of Tomato Bushy Stunt Virus P19 protein (22). A P19-only expression vector, assembled in similar fashion, was

also used in some plant treatments. Post-translational modification vectors were also assembled similarly: oligosaccharidyltransferase STT3D (82), driven by the *Arabidopsis* Act2 promoter (83); alpha-mannosidase GMII from *N. benthamiana* (Niben101Scf06280g02001.1; solgenomics.net), driven by the EE35S or Act2 promoters; N-acetylglucosaminyltransferase GnTII from *N. benthamiana* (Niben101Scf16329g00007.1; solgenomics.net), driven by the EE35S or Act2 promoters; human beta-1,4-galactosyltransferase (GalT; (84)), driven by the basal 35S promoter; human alpha-1,6-fucosyltransferase (FucT, NCBI Reference Sequence: NP_835368.1), driven by the Act2 promoter. All plant-produced antibody and glycomodification enzyme coding sequences were designed to incorporate preferred *N. benthamiana* codons according to published methods (85, 86). Antibodies were purified using Protein A (HiTrap MabSelect) and polished with Capto Q (HiTrap Capto Q) columns according to manufacturer protocols (Cytiva Life Sceinces, Chicago, IL). Purified antibodies were dialyzed against PBS. To assess purity, SDS-PAGE and immunoblotting was performed according to published methods (80). Galactosylated and fucosylated antibodies were confirmed via immunoblotting with biotinylated Ricinus communis Agglutinin I for galactose or biotinylated Aleuria aurantia Lectin for fucose (both lectins were from Vector Labs), followed by horseradish peroxidase conjugated streptavidin (HRP; BioLegend) and chemiluminescent signal development with SuperSignal West Pico Chemiluminescent Substrate (ThermoFisher) (data not shown). Glycan analyses were as described (21). Briefly, glycans were prepared using the GlykoPrep® Rapid N-Glycan Preparation kit (PROzyme, Hawyard, CA) and separated by hydrophilic-interaction liquid chromatography (HILIC) using a TSKgel Amide-80 column (Tosoh Bioscience, Grove City, OH), then identified by relative retention time and quantified using auto-integration of glycan peaks. Crystallizable fragments (Fcs) of N. *benthamiana* expressed afucosylated and fucosylated PGT121 IgG were generated by papain digest. Digested Fab and Fc were separated by protein A affinity purification on a HiTrap protein A affinity column (GE Healthcare, Piscataway, NJ) equilibrated in phosphate buffered saline (PBS). Fc fragment was eluted with 0.1 M glycine pH 3.0 and the pH of the eluted fractions raised by addition of 1 M Tris-HCl pH 8.5. Fc was separated from undigested IgG by gel filtration chromatography on a Superdex 200 16/60 column (GE Healthcare, Piscataway, NJ) equilibrated in 10 mM Tris-HCl pH 7.2 and 0.1 M ammonium acetate. Elution

fractions corresponding to the predicted Fc molecular weight were combined and concentrated to approximately 10 mg/ml for crystallization experiments.

Mammalian cell derived protein production and purification

PGT121 and PGT121 LALA antibodies produced in 293F cells were acquired from Scripps Research Institute Antibody Core Facility (La Jolla, CA). FreeStyle 293F cells (Thermo Fisher Scientific) were grown in FreeStyle 293F medium (Thermo Fisher Scientific) to a density of 1×10^6 cells/mL at 37°C with 8 % CO_2 with regular agitation (150 rpm). Cells were transfected with a plasmid expressing the dimeric recombinant soluble FcγRIIIa V^{158} (rsFcγRIIIa) (61) using ExpiFectamine 293 transfection reagent, as directed by the manufacturer (Thermo Fisher Scientific). One week later, cells were pelleted, and supernatants were filtered using a 0.22-μm-pore-size filter (Thermo Fisher Scientific). The rsFcγRIIIa proteins were purified by nickel affinity columns, as directed by the manufacturer (Thermo Fisher Scientific). Furthermore, the purified rsFcγRIIIa proteins were biotinylated using the EZ-Link™ Sulfo-NHS-LC-Biotinylation Kit as per manufacturer's instructions (Themo Fisher Scientific).

X-ray crystallography, structure solution, and refinement

Crystals of both Fc isoforms were grown by the hanging drop vapor diffusion method from 15% PEG 4000 and 0.1 M HEPES pH 7.0. Data were collected on crystals that had been flash frozen in liquid nitrogen. To prevent ice formation upon freezing, crystals were briefly soaked in crystallization buffer with 20% MPD added as a cryoprotectant. Data were collected on the National Synchrotron Light Source II (NSLS II) Highly Automated Macromolecular Crystallography (AMX) beam line (17-ID-1). Data were integrated and scaled with mosflm and scala from the CCP4 suite of programs. Structures were solved by molecular replacement with Phaser from the CCP4 suite based on the coordinates of 3AVE (a human fucosylated Fc). Refinement was carried out with Refmac and/or Phenix and model building was done with COOT. Data collection and refinement statistics are shown in **Table 5.2**. Ramachandran statistics were calculated with Molprobity and illustrations were prepared with Pymol Molecular graphics (http://pymol.org). Fucosylated and afucosylated Fc structures were deposited in the Protein Data Bank with PDB IDs 6VSL and 6VSZ respectively. The b-factor,

also called a temperature factor or atomic displacement parameter, indicates the precision of the atom positions in the crystallographic structures on macromolecules. A higher b-factor corresponds to the increased movement (disorder) of the given atom. Atom positions can be uncertain because of disorder in the crystal from which the structure was determined.

Viral production, infections, and ex vivo amplification

For *in vitro* infection, vesicular stomatitis virus G (VSV-G)-pseudotyped HIV-1_{JRCSF} (NIH AIDS Reagent Program), $SHIV_{AD8\text{-}EO}$ (kindly provided by Malcom Martin) and $SHIV_{BG505}$ infectious molecular clones (IMC) were produced in 293T cells and titrated as previously described (56). The $SHIV_{BG505}$ IMC harbours the T332N and S375Y mutations in its Env (87). Viruses were then used to infect CEM.NKr CCR5+ cells or primary CD4 T cells from healthy donors by spin infection at 800 x g for 1 h in 96-well plates at 25°C. To expand endogenously infected CD4+ T cells, primary CD4+ T cells obtained from four antiretroviral therapy (ART)-treated HIV-1-infected individuals were isolated from PBMCs by negative selection. Purified CD4+ T cells were activated with PHA-L at 10 µg /ml for 48 hours and then cultured for at least 6 days in RPMI-1640 complete medium supplemented with rIL-2 (100U/ml) to reach above 10% infection for ADCC assay. ADCC susceptibility was not assessed for one of the donors since it only reached 4% infection.

Flow Cytometry Analysis of Cell Surface Staining

Cell-surface staining of infected cells was performed as previously described (55, 63, 88). Binding to cell surface HIV-1 Env by anti-Env mAbs (5 µg/ml) was performed at 48 h post-infection. Goat anti-human Alexa-Fluor 647 secondary Abs (Thermo Fisher Scientific) was used to determine overall antibody binding and AquaVivid (Thermo Fisher Scientific) as a viability dye. Alexa-Fluor 647-conjugated streptavidin (Thermo Fisher Scientific) was used to determine biotin-tagged dimeric recombinant soluble FcγRIIIa (V158) binding. Cells were then permeabilized using the Cytofix/Cytoperm Fixation/Permeabilization Kit (BD Biosciences). HIV-1-infected cells were identified by intracellular staining of p24 using PE-conjugated anti-p24 mAb (clone KC57; Beckman Coulter) and SHIV-infected cells were identified by intracellular staining using Alexa Fluor 488-conjugated anti-p27 Abs (clone

2F12). The percentage of infected cells (p24+ or p27+ cells) was determined by gating the living cell population based on viability dye staining with AquaVivid (Thermo Fisher Scientific). Samples were analyzed on a Fortessa cytometer (BD Biosciences), and data analysis was performed using FlowJo v10.7.1 (Tree Star).

FACS-based ADCC assay

Measurement of ADCC using the FACS-based assay was performed at 48h post-infection as previously described (55, 63, 89) or after reaching 10% of p24+ cells during *ex vivo* expansion. Briefly, infected cells were stained with AquaVivid viability dye and cell proliferation dye (eFluor670; eBioscience) and used as target cells. Autologous PBMCs were used as effectors cells and were stained with another cellular dye (cell proliferation dye eFluor450; eBioscience). Effector and target cells were mixed at a ratio of 10:1 in 96-well V-bottom plates (Corning) and 5µg/ml of mAbs were added to appropriate wells. The plates were subsequently centrifuged for 1 min at 300 x g, and incubated at 37°C, 5% CO_2 for 5 hours before being fixed in a 2% PBS-formaldehyde solution. Samples were acquired on a Fortessa cytometer (BD Biosciences) and data analysis was performed using FlowJo v10.7.1 (Tree Star). The percentage of ADCC was calculated with the following formula: (% of p24+ or p27+ cells in Targets plus Effectors) − (% of p24+ or p27+ cells in Targets plus Effectors plus Abs) / (% of p24+ or p27+ cells in Targets) by gating on live target cells.

Luciferase-based ADCC assay

Measurement of ADCC responses using the luciferase reporter assay was performed as previously described with a NK cell line stably expressing human CD16a serving as effector cells (44, 57-59). The lymphocytic cell line CEM.NKR-CCR5-sLTR-Luc, which expresses the firefly luciferase (Luc) under the control of a Tat-inducible promoter, was infected with VSV G-pseudotyped $SHIV_{AD8\text{-}EO}$ and used as target cells. To avoid VSV G-pseudotyping replication-competent virus, a 2-bp deletion was introduced into the *vif* gene of $SHIV_{AD8\text{-}EO}$, resulting in a premature stop codon followed by a frameshift. At 2 days post-infection, effector cells were incubated with target cells for 8h, in triplicate, at a ratio of 10:1 in the presence of different concentrations of Abs ranging from 100µg/mL to 0.006 µg/mL using a 4-fold dilution

factor. The dose-dependent loss of Luc activity was measured as an indication of Ab-mediated killing of productively infected cells. Infected target cells incubated with effector cells in the absence of Ab were used to measure maximal Luc activity, and uninfected target cells cultured with effector cells were used to determine background Luc activity. ADCC activity as a percentage of relative light units (RLU) was calculated as follows: (mean RLU at a given antibody concentration − mean background RLU) / (mean maximal RLU − mean background RLU) × 100. Area under the curve (AUC) values for ADCC were calculated from percent relative light units (RLU), as previously described (44, 57-59).

Virus neutralization

Lentiviral particles were produced in HEK 293T using the standard calcium phosphate transfection technique. Two days post-transfection, cell supernatants were harvested. TZM-bl target cells were seeded at a density of 1 x 104 cells/well in 96-well luminometer-compatible tissue culture plates (Perkin Elmer) 24 hours before infection. Viral preparations were incubated for 1 hour at 37°C with serial dilutions of anti-Env antibodies in a final volume of 200 µL before being added to the target cells. After a 48-hour incubation at 37°C, the medium was removed from each well, and cells were lysed by the addition of 30 µL of passive lysis buffer (Promega) followed by one freeze-thaw cycle. An LB941 TriStar luminometer (Berthold Technologies) was used to measure the luciferase activity of each well after the addition of 100 µL of luciferin buffer (15mM $MgSO_4$, 15mM KPO_4 [pH 7.8], 1mM ATP, and 1mM dithiothreitol) and 50 µL of 1mM d-luciferin potassium salt (Prolume)

Statistical Analyses

Statistics were analyzed using GraphPad Prism version 9.0.0 (GraphPad, San Diego, CA, USA). Every data set was tested for statistical normality using the Shapiro-Wilk test, and this information was used to apply the appropriate (parametric or nonparametric) statistical test. P values of <0.05 were considered significant; significance values are indicated as * $p<0.05$, ** $p<0.01$, *** $p<0.001$, **** $p < 0.0001$.

5.5 Results

Generation of near-homogeneous plant-derived PGT121 glycovariants

Most therapeutic protein drugs, such as mAbs, exist as mixtures of glycoproteins that are identical in amino acid sequence composition yet variable in glycosylation profile due to a series of post-translational modifications. In this study, a versatile platform was used to produce Env-specific bNAb PGT121 with controlled post-translational glycomodification. This platform involved transient expression of antibody genes in a proprietary *Nicotiana benthamiana* plant line engineered for knock down of plant-specific α1,3-fucosylation and β1,2-xylosylation (KDFX) (18) thus producing mAbs with predominantly biantennary N-acetylglucosamine (GnGn) glycans (G0 glycoform). When mAbs were transiently co-expressed with human α-1,6 fucosyltransferase in KDFX plants, glycans bearing core fucose resulted; with human α-1,4 galactosyltransferase, glycans with galactose linkages being either mono- or di-antennary resulted (50, 51). In this study, we produced diverse PGT121 glycovariants that were purified from different plant treatments, resulting in mainly G0 (agalactosylated and afucosylated), G0F (agalactosylated and fucosylated), G2 (two galactose residues and afucosylated) or G2F (two galactose residues and fucosylated) glycans (**Figure 5.1**), respectively, with minor amounts of branched oligomannose residues. All plant treatments produced antibodies with highly homogeneous glycosylation profiles characterized by a single dominant glycan. MAb PGT121 produced in mammalian 293F cells was also used in this study; its glycosylation status has been previously reported as G0F (agalactosylated and fucosylated) with minor amounts of other N-linked glycans (42).

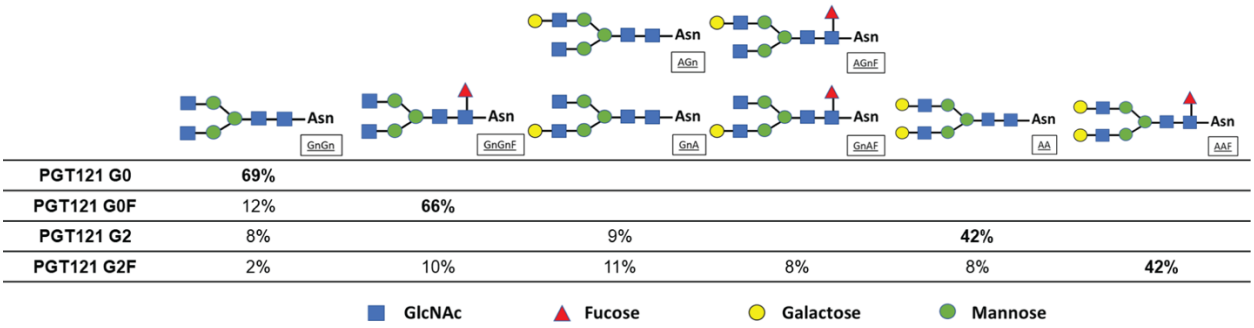

PGT121 G0	**69%**					
PGT121 G0F	12%	**66%**				
PGT121 G2	8%		9%		**42%**	
PGT121 G2F	2%	10%	11%	8%	8%	**42%**

Figure 5.1. N-linked glycans of *N. benthamiana*-produced PGT121 glycovariants
Percentage of predominant N-glycosylations on PGT121 G0, PGT121 G0F, PGT121 G2, and PGT121 G2F are presented in the table. Schematic diagrams are across the top, where Asn is asparagine 297; GnGn is diantennary N-Acetylglucosamine; F is fucose; A is galactose. Glycan species abundances are given as percentages and minor glycoforms are not indicated. Glycan nomenclature is further described by ProGlycAn (http://www.proglycan.com/protein-glycosylation-analysis/nomenclature).

Fc glycosylation does not affect the ability of PGT121 to recognize infected cells nor its neutralization capacity

Taking our panel of glycoengineered PGT121 mAbs, we first evaluated their overall binding capacity to Env on the surface of infected cells when compared to the 293F-produced PGT121. First, we used a lymphocytic cell line (CEM.NKr) infected with three different infectious molecular clones (IMC) expressing Env in its 'closed' conformation (HIV-1_{JRCSF} (52), $SHIV_{AD8\text{-}EO}$ (53) and $SHIV_{BG505}$ N332 S375Y (44)). As controls, we included a version of 293F-produced PGT121 with Fc mutations known to decrease FcγRIIIa interactions (L234A/L235A [LALA]) as well as a non-specific mAb, Trastuzumab, a HER2-specific mAb used in specific cancer immunotherapies (54) in our panel. Two days post-infection, cells were stained with the respective mAbs and all plant-produced PGT121 glycovariants recognized cells infected with the three IMCs to the same extent as 293F-produced PGT121 (**Figure 5.2A-C**). Furthermore, in agreement with an equivalent Env recognition by all PGT121 glycovariants, no significant differences in their ability to neutralize HIV-1_{JRCSF}, $SHIV_{AD8\text{-}EO}$ and $SHIV_{BG505}$ lentiviral particles were observed (**Figure 5.2D-F**). These results confirm that

modifying the Fc domain does not affect the antigen-recognition and neutralization capabilities of PGT121.

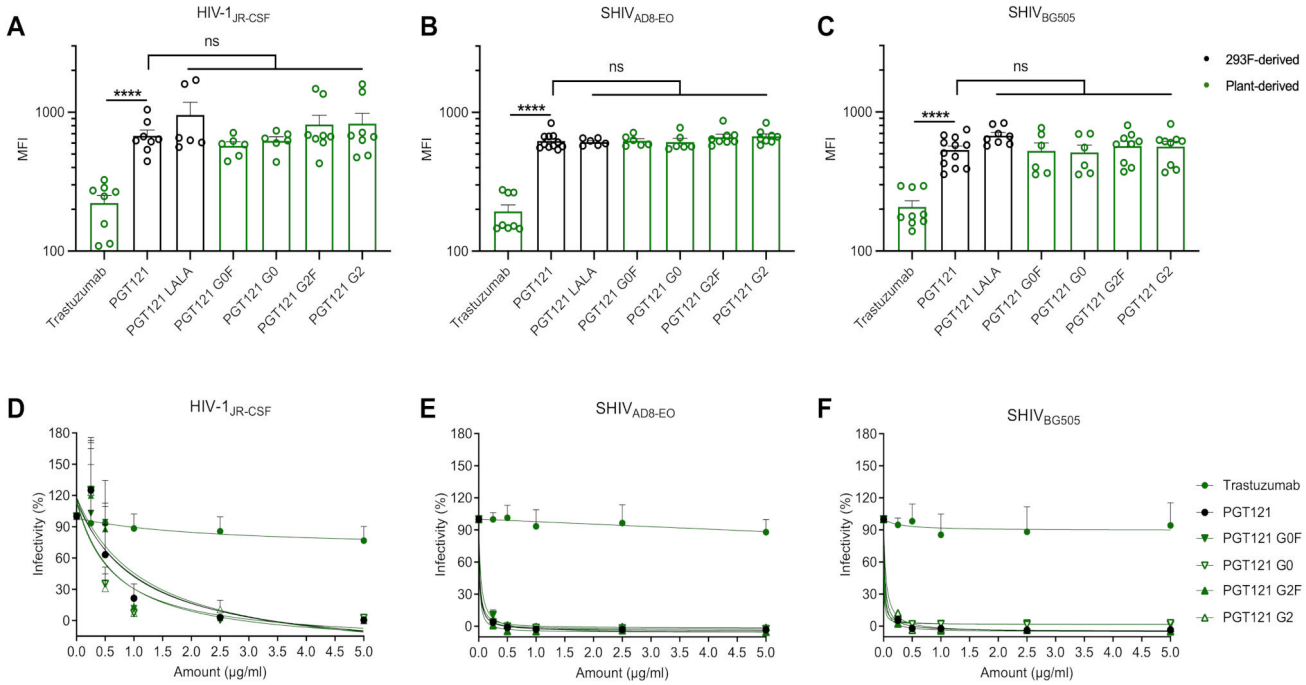

Figure 5.2. Fc glycosylation does not affect the ability of PGT121 to recognize infected cells or its neutralization capacity

Cell surface staining of CEM.NKr CCR5+ cells infected with (**A**) HIV-1_{JRCSF}, (**B**) $SHIV_{AD8-EO}$, and (**C**) $SHIV_{BG505}$ was performed 48h post-infection. Antibody binding was detected using Alexa Fluor 647-conjugated anti-human secondary Abs. (**A-C**) Graphs represent the median fluorescence intensities (MFI) in the infected (p24+ or p27+) population determined from at least 5 independent experiments, with the error bars indicating means ± SEM. Statistical significance was tested using an unpaired t test or a Mann-Whitney U test based on statistical normality (**** $P < 0.0001$; ns, nonsignificant). (**D-F**) Lentiviral particles produced from (**D**) HIV-1_{JRCSF}, (**E**) $SHIV_{AD8-EO}$, and (**F**) $SHIV_{BG505}$ IMCs. Viruses were incubated with serial dilutions of trastuzumab and PGT121 mAbs at 37°C for 1 h prior to infection of TZM-bl target cells. Infectivity at each Ab concentration tested is shown as the percentage of infection without Ab for each virus. Quadruplicate samples were analyzed in each experiment. (**D-F**) Data shown are the means of results obtained in at least 3 independent experiments. Error bars indicate means ± SEM. Black histogram/curves represent 293F cell-derived mAbs and green histogram/curves represent plant-derived mAbs.

The Fc glycosylation profile of PGT121 regulates its capacity to mediate ADCC

Next, we evaluated the efficacy of our panel of glycoengineered mAbs to eliminate infected cells. The susceptibility of CEM.NKR cells (infected HIV-1_{JRCSF}, $SHIV_{AD8\text{-}EO}$ and $SHIV_{BG505}$) to ADCC was measured with a previously described FACS-based ADCC assay that measures the elimination of productively infected cells by measuring the presence of intracellular HIV-1 or SHIV capsid antigens (p24+ and p27+, respectively) (44, 55, 56) (**Figure 5.3A-C**). As expected, no ADCC activity was observed with the negative control, trastuzumab. Furthermore, the capacity of PGT121 to mediate ADCC was significantly impaired by the introduction of the LALA mutations in its Fc domains. Despite equivalent recognition of Env (**Figure 5.2**), we observed significant differences in the abilities of the different PGT121 glycovariants to mediate ADCC. As expected, the plant-produced agalactosylated and fucosylated PGT121 (PGT121 G0F), gave similar results as that of the 293F-produced PGT121, where the N-linked glycans are also predominantly G0F. Although significant increases in ADCC activities were observed with the two afucosylated PGT121 mAbs (G0 and G2) compared to their fucosylated counterparts (G0F and G2F), the galactosylated mAb (PGT121 G2) harboured the most potent activity against CEM.NKR cells infected with HIV-1_{JRCSF} (**Figure 5.3A**). In contrast, no effect of galactosylation was seen against both SHIV-infected cells.

We confirmed the enhanced ADCC activity of galactosylated PGT121 using a different luciferase based ADCC assay that also relies on the specific elimination of infected cells (57). In this assay, infected CEM.NKR-CCR5-sLTR-Luc cells expressing a Tat-driven luciferase reporter gene serve as target cells, while a CD16+ NK cell line is used as effector cells (57-59). As luciferase is only expressed upon productive infection, elimination of infected cells can be calculated by the loss of luciferase activity. As expected, similar results were obtained with this assay, where the afucosylated mAb (PGT121 G2) had enhanced ADCC activity when compared to the fucosylated mAb (PGT121 G2F) (**Figure 5.3D, E**).

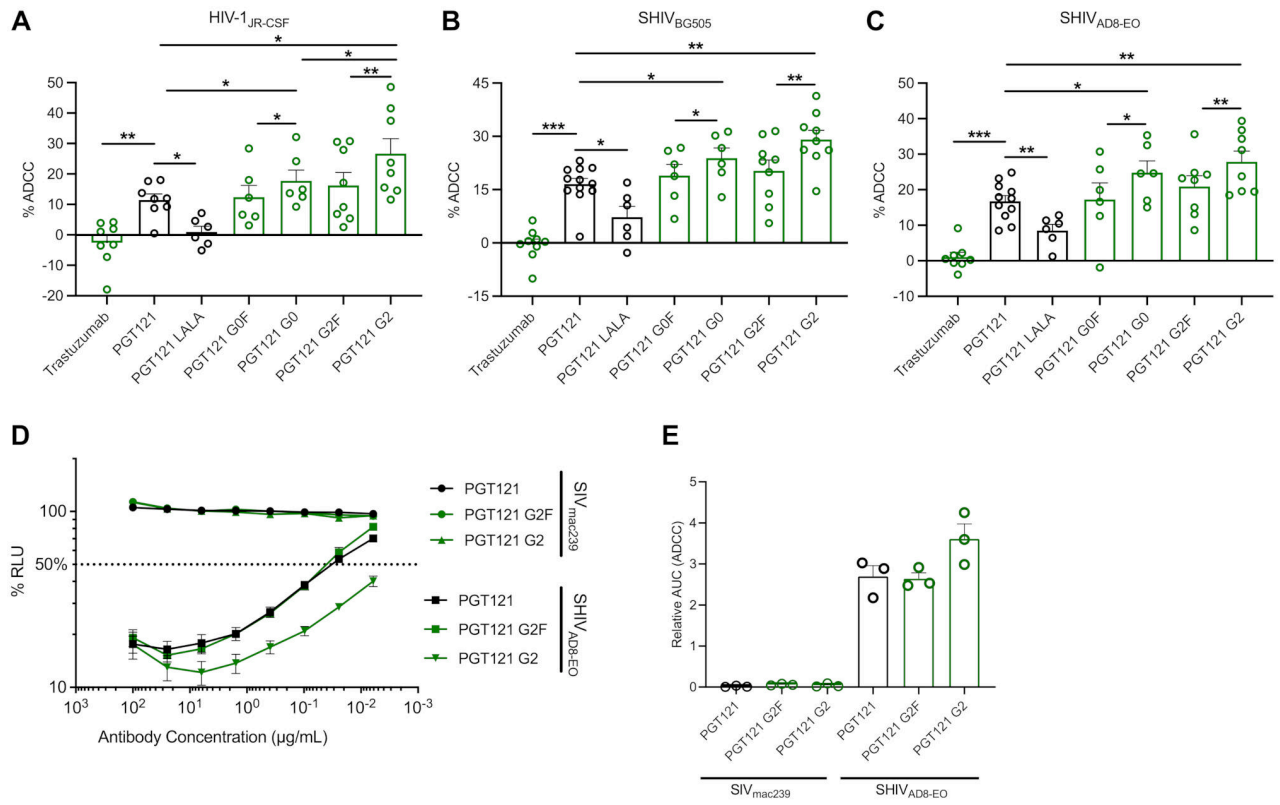

Figure 5.3. Fc glycosylation profile of PGT121 regulates its ADCC capacity against infected cells

CEM.NKR-CCR5-sLTR-Luc cells infected with (**A**) HIV-1_{JRCSF}, (**B**) $SHIV_{BG505}$, and (**C**) $SHIV_{AD8\text{-}EO}$ were used as target cells. PBMCs from uninfected donors were used as effector cells in a FACS-based ADCC assay. (**A-C**) The graphs shown represent the percentages of ADCC obtained in the presence of the respective antibodies. (**D-E**) For the luciferase assay, CEM.NKr-CCR5-sLTR-Luc cells infected with $SHIV_{AD8\text{-}EO}$, or SIV_{mac239} as a negative control. ADCC responses were measured as the dose-dependent loss of luciferase activity in relative light units (RLU) after incubation of infected CEM.NKR-CCR5-sLTR-Luc cells with CD16+ KHYG-1 effector cells in presence of antibody. Values are the means ± standard deviations (error bars) for triplicate wells, and the dotted line indicates half-maximal lysis of infected cells. (**E**) Area under the curve (AUC) values were calculated using from curves of increasing mAb concentrations shown in (**D**). Error bars indicate means ± SEM. Statistical significance was tested using a paired t test or Wilcoxon matched pairs signed rank test based on statistical normality (* $P < 0.05$; ** $P < 0.01$; *** $P < 0.001$). Black histogram bars represent 293F cell-derived mAbs and green histogram bars represent plant-derived mAbs.

The Fc glycosylation profile of PGT121 modulates FcγRIIIa interaction and ADCC against infected primary CD4+ T cells

To assess the activities of *N. benthamiana*-derived PGT121 mAbs in a more physiological setting, we aimed to validate our results obtained using infected CEM.NKr cell line with infected primary CD4+ T cells (**Figure 5.4**). We purified primary CD4+ T lymphocytes from resting PBMCs by negative selection and activated them with PHA-L/IL-2, followed by infection with HIV-1_{JRCSF}, $SHIV_{AD8\text{-}EO}$ or $SHIV_{BG505}$. Once again, all our plant-produced PGT121 glycovariants recognized cells infected with the three viruses to the same extent as the 293F-produced PGT121 (**Figure 5.4A-C**).

The N-linked glycosylation profile of IgG Fc portion has been described to strongly dictate their ability to interact with FcγRs (28, 60). To further evaluate the impact of PGT121 glycoforms on its interaction with FcγRIIIa, we incubated antibody-opsonized infected primary CD4+ T cells with a soluble recombinant dimeric FcγRIIIa protein that models the cross-linking of FcγRs by Abs, a process essential to activate effector cells (61-63). Despite equivalent recognition of Env, the fucosylated PGT121 mAbs had decreased dimeric FcγRIIIa engagement when compared to the afucosylated glycoforms (**Table 5.1 and Figure 5.4D-F**). Moreover, both the agalactosylated and galactosylated mAbs (PGT121 G0 and G2, respectively) had equivalent binding of FcγRIIIa in cells infected with all three viruses tested (**Figure 5.4D-F**).

To evaluate whether the engagement of FcγRIIIa translates to ADCC, primary CD4+ T cells from different healthy uninfected donors were infected with HIV-1_{JRCSF} and investigated for their ADCC susceptibility in presence of autologous effector cells. Similar ADCC responses were observed with significant enhancements in presence of the two afucosylated mAbs (PGT121 G0 and G2) (**Table 5.1 and Figure 5.4G**). Akin to the engagement of FcγRIIIa, the presence or absence of galactose did not impact ADCC responses. Moreover, the overall capacity of our panel of PGT121 glycoforms to recognize Env did not correlate with the differences in ADCC responses observed ($r = 0.6676$, $p = 0.1474$) (**Figure 5.4H**), while their ability to interact with the dimeric FcγRIIIa correlated significantly with ADCC activity

exhibited against HIV-1_{JRCSF} infected primary CD4+ T cells ($r = 0.9615$, $p = 0.0022$) (**Figure 5.4I**). Thus, the enhanced ADCC functionality observed with the afucosylated PGT121 mAbs appears to depend on their improved capacity to interact with FcγRIIIa.

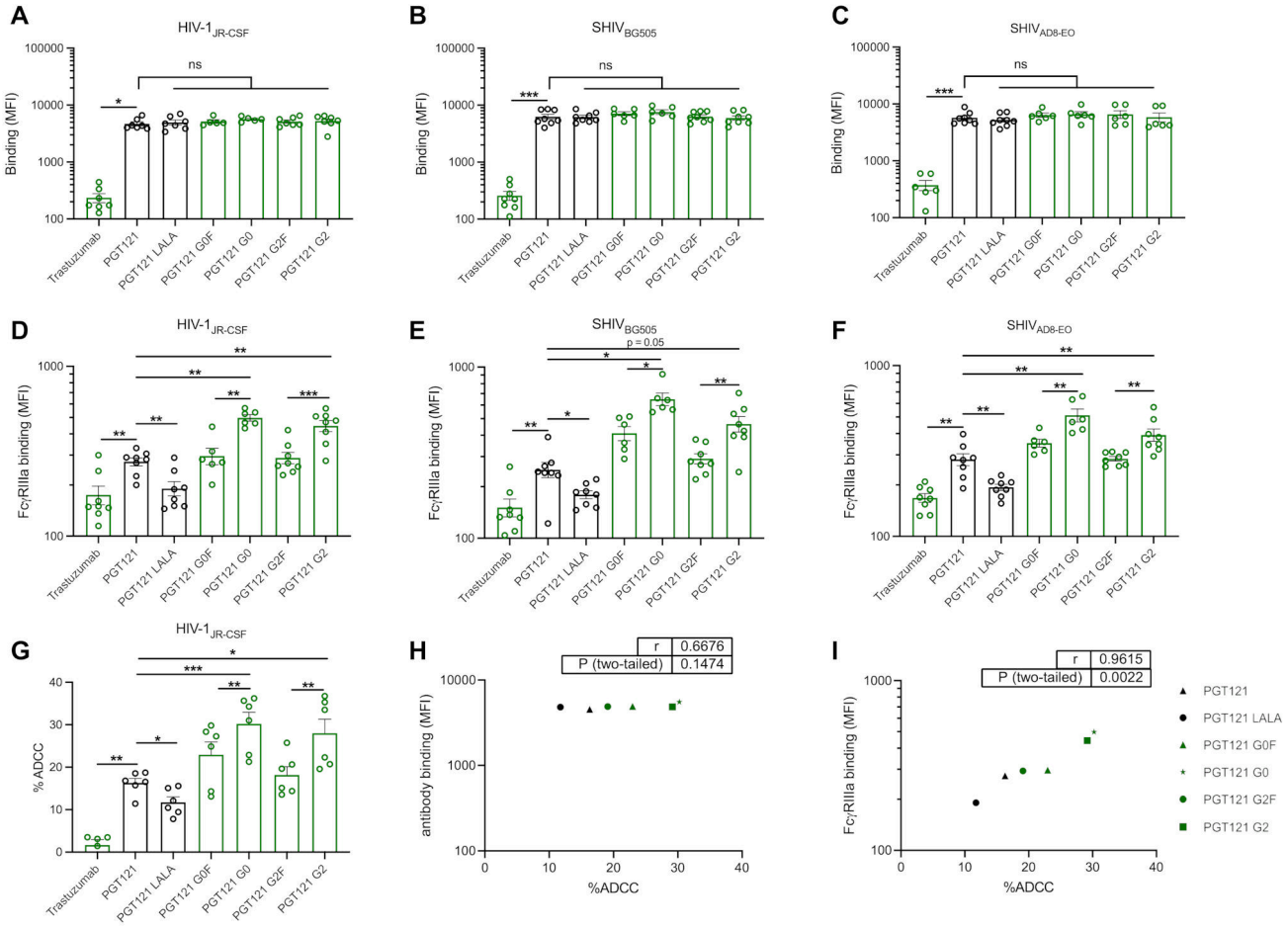

Figure 5.4. Fc glycosylation profile of PGT121 modulates FcγRIIIa interaction and ADCC against infected primary CD4+ T cells

Cell surface staining of primary CD4+ T cells infected with (**A, D**) HIV-1_{JRCSF}, (**B, E**) $SHIV_{AD8\text{-}EO}$, and (**C, F**) $SHIV_{BG505}$ was performed 48h post-infection. Antibody binding was detected either by (**A-C**) using Alexa Fluor 647-conjugated anti-human secondary Abs or by (**D-F**) using biotin-tagged dimeric rsFcγRIIIa (0.2 µg/ml) followed by the addition of Alexa Fluor 647-conjugated streptavidin. (**A-F**) Graphs represent the mean fluorescence intensities (MFI) in the infected (p24+ or p27+) population determined from at least 5 independent experiments, with the error bars indicating means ± SEM. (**G**) Primary CD4+ T cells infected with HIV-1_{JRCSF} were used as target cells. Autologous PBMCs were used as effector cells in a FACS-based ADCC assay. The graph shown represent the percentages of ADCC obtained in the presence of the respective antibodies. Statistical significance was tested using a paired t test or Wilcoxon matched pairs signed rank test based on statistical normality (*, $P < 0.05$; **, $P < 0.01$; ***, $P < 0.001$; ns, nonsignificant). Black histogram bars represent 293F cell-derived mAbs and green histogram bars represent plant-derived mAbs. (**H, I**) Correlations between the levels of ADCC and levels of (**H**) antibody binding or (**I**) FcγRIIIa binding as measured on primary CD4+ T cells infected with HIV-1_{JRCSF}. Statistical significance was tested using a Pearson correlation test. Black points represent 293F cell-derived mAbs and green points represent plant-derived mAbs.

Table 5.1. Functionalities of PGT121 glycovariants targeting infected primary CD4+ T cells [a, b]

HIV-1_{JRCSF}	Trastuzumab†	PGT121*	PGT121 LALA*	PGT121 G0F†	PGT121 G0†	PGT121 G2F†	PGT121 G2†
Antibody binding	**0.05**	**1.00**	**1.06**	**1.10**	**1.20**	**1.10**	**1.12**
FcγRIIIa binding	**0.64**	**1.00**	**0.70**	**1.18**	**1.82**	**1.05**	**1.63**
%ADCC	**0.10**	**1.00**	**0.72**	**1.39**	**1.85**	**1.12**	**1.72**

[a] Ab binding, FcγRIIIa binding and ADCC were measured as described in the Materials and Methods. Respective values obtained for each assay are normalized to the value obtained by PGT121

*, 293F-derived MAbs; †, plant-derived MAbs.

Susceptibility of ex-vivo-expanded primary CD4+ T cells from HIV-1-infected individuals to PGT121-mediated ADCC

Since our results indicate that Fc fucosylation of PGT121 plays an important role in modulating FcγRIIIa interaction and ADCC response efficacy, we further evaluated whether our panel of plant-derived PGT121 glycovariants were able to eliminate *ex vivo*-expanded endogenously infected CD4+ T cells. We isolated primary CD4+ T cells from four antiretroviral therapy (ART)-treated HIV-1-infected individuals and activated them with PHA-L/IL-2, where viral replication was followed by intracellular p24 staining. In agreement with the results obtained with HIV-1_{JRCSF} infected primary CD4+ T cells, endogenously infected primary CD4+ T cells were also more susceptible to ADCC mediated by afucosylated PGT121 mAbs. Similarly, these mAbs were also able to engage with the dimeric FcγRIIIa more efficiently than the fucosylated PGT121, despite their comparable binding to Env present on the surface of infected cells (**Figure 5.5A-C**).

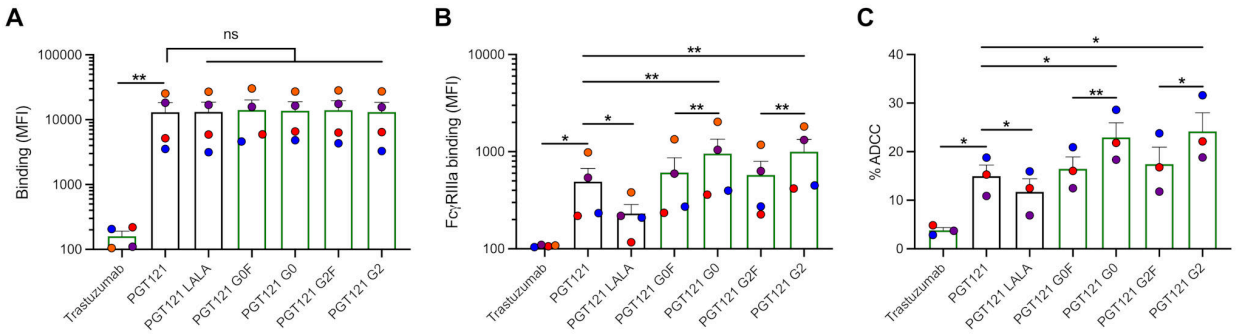

Figure 5.5. Susceptibility of *ex vivo*-expanded endogenously infected primary CD4+ T cells from HIV-1-infected individuals to PGT121-mediated ADCC

Primary CD4+ T cells from four different HIV-1-infected individuals were isolated and reactivated with PHA-L for 48 h, followed by incubation with IL-2 to expand the endogenous virus. Cell surface staining of infected primary CD4+ T cells was performed upon reactivation. Antibody binding was detected either by using (**A**) Alexa Fluor 647-conjugated anti-human secondary Abs or (**B**) biotin-tagged dimeric rsFcγRIIIa (0.2 µg/ml) followed by the addition of Alexa Fluor 647-conjugated streptavidin. (**A-B**) Graphs represent the mean fluorescence intensities (MFI) in the infected (p24+ or p27+) population determined from at four different donors, with the error bars indicating means ± SEM. (**C**) *Ex vivo*-expanded infected primary CD4+ T cells from three HIV-1-infected individuals were used as target cells. Autologous PBMCs were used as effector cells in a FACS-based ADCC assay. The graphs shown represent the percentages of ADCC obtained in the presence of the respective antibodies. ADCC susceptibility was only measured when the percentage of infection (p24+ cells) was higher than 10%. Statistical significance was tested using a paired t test or Wilcoxon matched pairs signed rank test based on statistical normality (*, $P < 0.05$; **, $P < 0.01$; ***, $P < 0.001$; ns, nonsignificant). Black histogram bars represent 293F cell-derived mAbs and green histogram bars represent plant-derived mAbs.

The Fc regions of N. benthamiana-derived and mammalian cell-derived PGT121 are structurally similar with differences in N297 sugar composition

Functional characterizations of our panel of glycoengineered PGT121 mAbs demonstrated significant differences in Fc-mediated effector activities when compared to mammalian cell derived PGT121. To understand if there are any differences in the overall structure and glycosylation pattern within the Fc region of our engineered mAbs we determined the 2.6 Å and 2.1 Å crystal structures of *N. benthamiana*-expressed galactosylated afucosylated (G2) and fucosylated (G2F) PGT121 Fcs, respectively (**Table 5.2 and Figure 5.6**). Both Fcs crystallized in the same P212121 space group with similar dimensions (**Table 5.2**) indicative of their close structural similarity. Indeed, a structural alignment confirms that the G2 and G2F Fcs are almost identical with a main chain atom root square deviation (RMSD) of 0.59 Å for the monomers A and B that assemble to form the Fc dimer (**Figure 5.6A and B**). In both structures, glycosyl groups attached to N297 were clearly visible permitting identification of the differences in sugar composition. As shown in **Figure 5.6C**, the N297 sugar of both variants consists of a core formed by two N-acetyl-D-glucosamines (with the first attached directly to N297) and one β-D-mannose with two branching arms, an α(1-3) arm [α3 arm] linked to the O3 of the mannose and an α(1-6) arm [α6 arm] linked to the O6. Both arms consist of an α-D-mannose followed by a N-acetyl-D-glucosamine. In addition, a terminal β-D-galactose is visible on the α6 arm (**Figure 5.6C**, colored in cyan); a corresponding terminal galactose on the α3 arm, if present, is not visible due to disorder. The only major difference between the G2 and G2F forms is the lack of fucosyl group in afucosylated G2. The fucosyl group branches directly off the first N-acetyl-D-glucosamine in the core attached to N297 in the G2F variant (**Figure 5.6C**, colored in green). Of note, although the density for the Fc glycan attached to monomers A and B is visible in both the G2 and G2F structures, in both cases better quality density is observed for chain A. Chain B makes fewer crystal contacts resulting in more movement and higher b-factors for the chain B CH2 domain and its attached glycan.

The CH2-CH3 homodimer is stabilized by interactions between the two CH3 domains in the dimer, which are largely identical in both Fc variants (**Figure 5.6A and B**). The glycans of opposing CH2 domains are in proximity but make no defined contacts to one another. The core

β-D-mannose and the α6 arm of the glycan are stabilized by phenylalanines 241 and 243 of the CH2 domain while the α3 arm is only stabilized by the opposing glycan in the dimer (**Figure 5.6D**). The α6 arm is also stabilized by a hydrogen bond to lysine 246. This added stability facilitates the resolution of a terminal β-D-galactose which is in turn stabilized by hydrogen bonds to the carbonyl oxygen of glutamate 258 and the side chain of threonine 260. Details of the α3 arm past the N-acetyl-D-glucosamine are not seen due to movement in the crystal.

The structures presented in **Figure 5.6** allowed us to compare our plant-derived G2 and G2F PGT121 Fc structures with previously published structures of mammalian cell-expressed Fc domains: a fucosylated Fc lacking the terminal galactose (G0F) (PDB ID: 3AVE), an afucosylated Fc (G0) (PDB ID: 2DTS), and a fucosylated Fc containing a terminal galactose (G2F) (PDB ID: 5VGP). As shown in **Figure 5.7A**, where the structures of the Fc dimer, the CH2-CH3 monomer and the individual CH2 and CH3 domains are overlaid, there is very close similarity between equivalent fucosylated and afucosylated variants of plant and mammalian derived Fcs. **Figure 5.7B** summarizes the RMSD values for all comparisons which show that the CH3 domain is the most structurally similar among the comparisons with RMSDs less than 1 Å. Bigger differences are seen for the both the plant and mammalian expressed afucosylated structures. The same holds true for the comparison of the CH_2 domains but the magnitude of the RMSD is higher, 1.1 to 1.5 Å, reflecting the influence of the glycan bound to N297. Looking at the Fc as a whole, a similar pattern emerges with a greater range of RMSD variation for the afucosylated as compared to the fucosylated Fc. This greater variability is more apparent in the dimer than the monomer, supporting the interpretation that these differences are a consequence of glycan composition. However, given these differences, both plant and mammalian expressed Fc domains are largely identical with respect to expression origin.

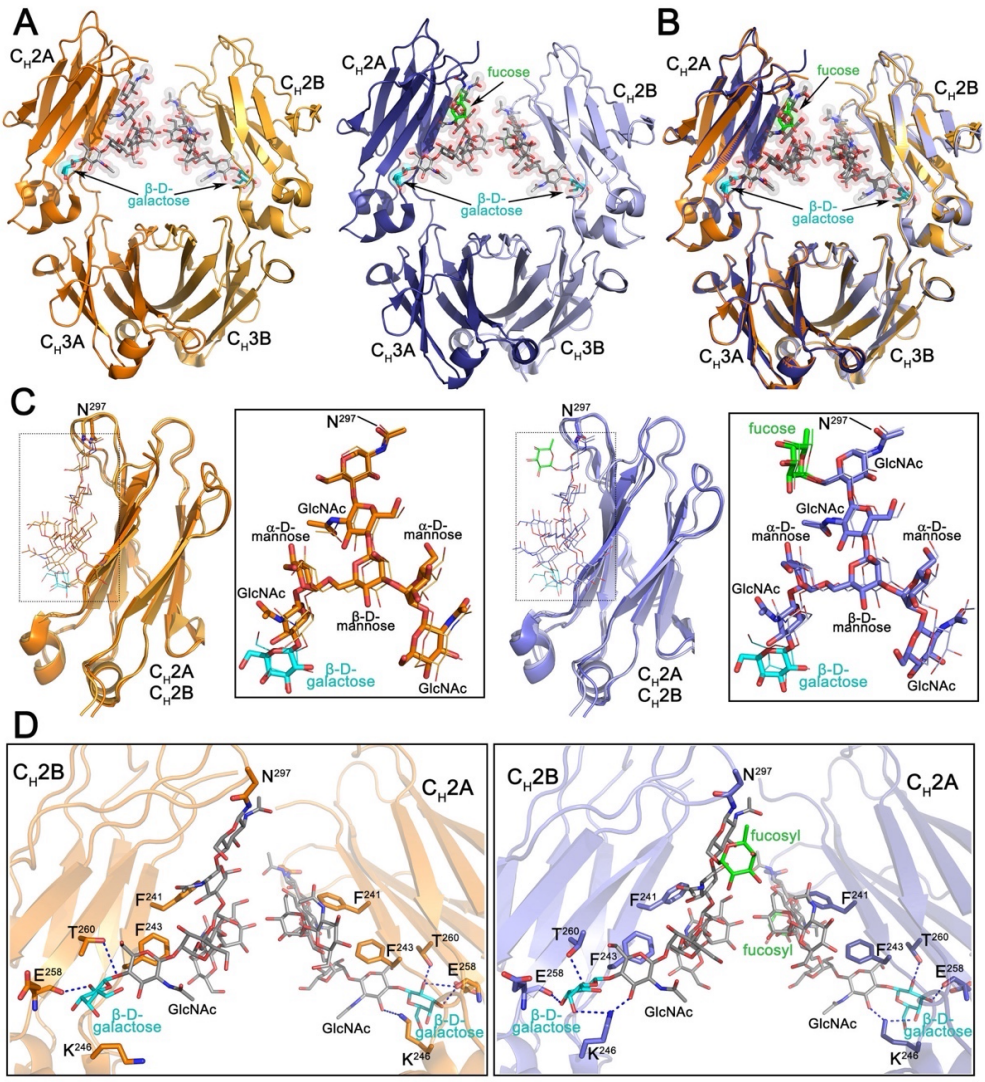

Figure 5.6. Structural characterization of the Fc regions of *N. benthamiana*-produced PGT121

(A) Crystal structures of afucosylated (right) and fucosylated (left) Fc. The overall structure is shown in a ribbon diagram with the two heavy chains (C_H2-C_H3 domains) in lighter (chain B) and darker (chain A) shades of orange and blue for afucosyated and fucosylated variant, respectively. The sugars attached to asparagine 297 are shown as sticks and spheres colored by atom type (gray for carbon, red for oxygen and blue for nitrogen). The fucose in the fucosylated Fc is colored green and the terminal galactose visible on the α6 arm of the glycan in both structures cyan. **(B)** Superposition of the afucosylated and fucosylated C_H2-C_H3 dimer (Fc domain) colored as in **(A)**. **(C)** Superposition of the C_H2 domains from the afucosylated (left) and fucosylated (right) Fc dimer. Blow up views to the right show the superposition of the glycan only with chain A shown as sticks and chain B as lines. Atom types are colored as in **(A)**. **(D)** Details of the glycan-glycan and glycan-protein contacts in the afucosyated (left) and fucosylated (right) Fc dimers. The glycan and interacting residues are shown as sticks and the protein backbone as a ribbon. Hydrogen bonds are shown with dashed lines. Atom types are colored as in **(A)**.

Table 5.2. Data collection and refinement statistics for fucosylated and afucosylated human Fc from *N. benthamiana*

	fucosylated human Fc	afucosylated human Fc
Data collection		
Wavelength, Å	0.920	0.979
Space group	$P2_12_12_1$	$P2_12_12_1$
Cell parameters		
a, b, c, Å	49.9, 79.9, 138.5	49.7, 80.3, 137.0
	90, 90, 90	90, 90, 90
α, β, γ, °	1	1
Fcs/a.u.	50-2.1 (2.21-2.1)	50-2.6 (2.74-2.6)
Resolution, (Å)		
	106,578	54,596
# of reflections	32,561	15,294
Total	9.7 (77.5)	8.3 (90.2)
Unique	6.1 (47.9)	4.7 (49.7)
R_{merge}[a], %	0.99 (0.50)	0.99 (0.68)
R_{pim}[b], %	5.4 (1.0)	8.3 (1.8)
$CC_{1/2}$[c]	98.7 (99.3)	88.0 (90.2)
I/σ	3.3 (3.4)	3.6 (3.6)
Completeness, %		
Redundancy		
Refinement Statistics		
Resolution, Å		
R[d] %	50.0 – 2.1	50.0 – 2.6
R_{free}[e], %	20.8	22.1
# of atoms	25.0	27.6
Protein		
Water	3,359	3,335
Ligand/glycan	189	20
Overall B value (Å)^2	236	200
Protein		
Water		
Ligand/Ion	59	81
RMSD[f]	48	46
Bond lengths, Å	80	102
Bond angles, °		
Ramachandran[g]	0.010	0.014
favored, %	1.1	1.6
allowed, %		
outliers, %	96.6	90.3
PDB ID	2.9	5.8
	0.5	3.9
	6VSL	6VSZ

Values in parentheses are for highest-resolution shell
[a]Rmerge = $\sum \left| I - \langle I \rangle \right| / \sum I$, where I is the observed intensity and <I> is the average intensity obtained from multiple observations of symmetry-related reflections after rejections
[b]Rpim = as defined in (Weiss 2001)

[c]CC1/2 = as defined by Karplus and Diederichs (Karplus and Diederichs 2012)
[d]$R = \sum \| Fo | - | Fc \| / \sum | Fo |$, where Fo and Fc are the observed and calculated structure factors, respectively
[e]Rfree = as defined by Brünger (Brunger 1997)
[f]RMSD = Root mean square deviation
[g]Calculated with MolProbity

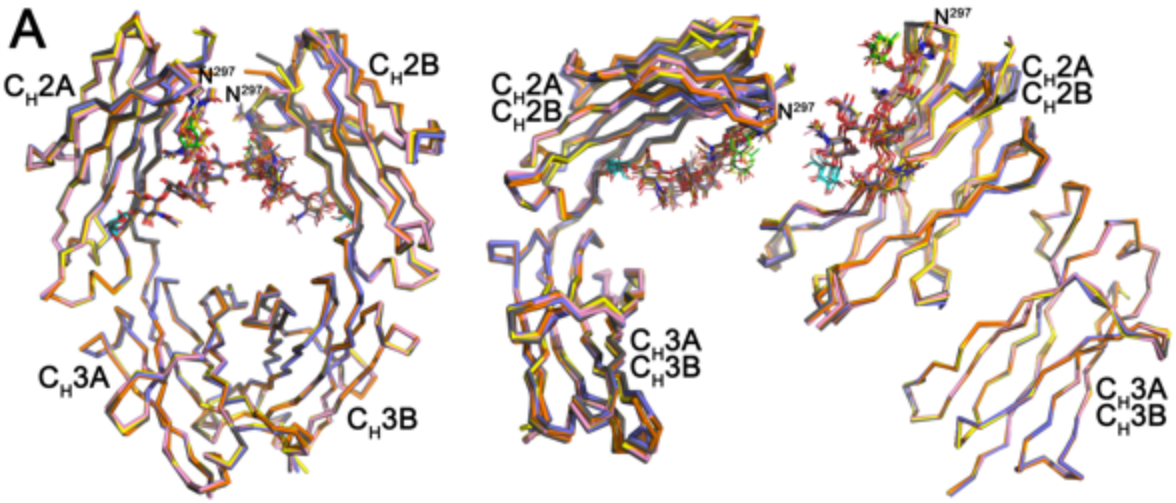

B

C_H2 domain

C_H3 domain	3AVE	2DTS	5VGP	afucosyl.	fucosyl.	C_H2 domain
3AVE	3AVE	1.09	1.23	1.37	1.17	
2DTS	0.87	2DTS	1.28	1.43	1.30	
5VGP	0.87	0.90	5VGP	1.45	1.16	
afucosyl.	0.85	0.99	0.93	afucosyl.	1.33	
fucosyl.	0.75	0.93	0.82	0.78	fucosyl.	

C_H3 domain

C_H2-C_H3 dimer (Fc domain)

C_H2-C_H3 monomer	3AVE	2DTS	5VGP	afucosyl.	fucosyl.	C_H2-C_H3 dimer (Fc domain)
3AVE	3AVE	0.41	0.53	0.63	0.56	
2DTS	0.65	2DTS	0.67	0.69	0.67	
5VGP	0.84	0.87	5VGP	0.63	0.39	
afucosyl.	0.84	0.82	0.91	afucosyl.	0.59	
fucosyl.	0.85	0.86	0.84	0.87	fucosyl.	

C_H2-C_H3 monomer

Figure 5.7. Comparison of the overall structures of *N. benthamiana* expressed and mammalian expressed human Fc domains

(A) Structural alignment of C_H2-C_H3 dimers (Fc), C_H2-C_H3 monomers, C_H2 domains, and C_H3 domains of *N. benthamiana* and mammalian expressed human Fcs including: a human fucosylated Fc lacking the terminal galactose (PDB ID 3AVE, yellow), an afucosylated Fc (2DTS, pink), and a fucosylated Fc containing a terminal galactose (5VGP, gray). *N. benthamiana* expressed Fcs are colored as in Figure 6 with fucose colored green and galactose cyan. **(B)** The average RMSD for main chain atom pairwise comparisons of C_H2 domains, C_H3 domains, C_H2-C_H3 monomers, and C_H2-C_H3 dimers (Fc domain) shown in tabular format color coded with smaller RMSD values green and larger RMSD values red.

5.6 Discussion

The results presented in this study suggest that *N. benthamiana* can be used as a reliable platform to produce bNAbs targeting HIV-1. No overall differences in viral neutralization and binding of Env but enhanced FcγRIIIa engagement and ADCC against infected cells were observed with some of the plant-derived PGT121 mAbs when compared to the 293F-produced PGT121. Importantly, Fc structures were found to be nearly identical whether the mAbs were produced in plants or in mammalian cell lines. The safety of plant-produced biological therapeutics and the value of having a rapid and adaptable system for mAb production was demonstrated during the 2014-2016 Ebolavirus (EBOV) outbreak in West Africa (66). ZMapp, a cocktail of mAbs targeting the EBOV envelope glycoprotein, was produced in *N. benthamiana* bearing predominantly G0 glycans and was used as a therapeutic treatment for EBOV disease (67). No major safety concerns were observed, while individuals receiving the ZMapp had reduced mortality as well as significantly shorter stays in treatment units (66).

Another advantage of using the *N. benthamiana* system is the ability to engineer the N-linked glycan composition of mAbs present on the Fc region of antibodies, which critically affects their affinity to FcγRs. Furthermore, using the KDFX transgenic *N. benthamiana* system, Fc regions of IgG proteins are systematically glycosylated with the G0 glycoform, without any core fucose or terminal galactose moieties (18, 68). The role of core fucosylation has been shown to be a strong determinant in the Fc affinity for FcγRIIIa and the removal of the fucose from the IgG Fc increases its affinity to FcγRIIIa (60, 69). Consequently, afucosylated mAbs can mediate significantly stronger ADCC responses (28, 69). Our results of improved FcγRIIIa interaction and ADCC activities of afucosylated PGT121 against SHIV or HIV-1 infected cells as well as endogenously HIV-1-infected cells cumulatively suggests that the mAb glycosylation profile can dictate its Fc-mediated effector functionality.

The presence of galactose has also been shown to enhance FcγRIIIa binding (70). However, there exists conflicting evidence on the role of galactosylation on antibody functionality. Some studies have found only modest differences between the presence or absence of galactose on Ab *in vivo* activities (71, 72). When considering the galactosylation status of PGT121 (G0 or

G2), we observed a slight enhancement of ADCC mediated by galactosylated PGT121 against CEM.NKr cells infected with HIV-1_{JRCSF}. However, no significant differences were seen in a more physiologically relevant context, *i.e.*, against primary CD4+ T cells. We believe these differences could be due to the lower cell-surface level of Env present on CEM.NKr cells, which could impact ADCC responses (73). Furthermore, as the observation by recent studies that the absence of fucose is more predominant than the presence of galactose on the ADCC activity of therapeutic mAbs (74), our results also strongly suggest that N-linked galactosylation is not required for the improved functionality of afucosylated PGT121. Lastly, to translationally utilize the *N. benthamiana* system to produce bNAbs targeting HIV-1, it is important to ensure high N-glycan homogeneity (51).

PGT121 was recently used in combination with a TLR7 agonist as an attempt to eliminate the cellular reservoir in SHIV-infected macaques (75, 76). PGT121 is also currently being tested in combination with other bNAbs for HIV-1 prophylaxis and therapy in clinical trials (NCT03721510). Two recent studies showed that the neutralization capacity of PGT121 is sufficient to protect NHP from SHIV challenges (42, 43). In these studies, Fc-impaired versions of PGT121 provided similar levels of protection as their wild-type counterparts. However, these studies were performed with primarily fucosylated PGT121 and did not comprehensively explore the capacity of PGT121 to clear the cellular reservoir. Passive administration of other potent bNAbs have been shown to decrease the number of infected cells and suppress viremia in animal models and infected individuals (2, 9, 12), with important contributions from their Fc-mediated effector functions (45). Our results suggest that afucosylated PGT121 could boost its Fc-mediated effector capacity and thus, its antiviral activity when used with a focus of controlling existing infection and decreasing disease progression.

Acknowledgments

We thank the CRCHUM Flow Cytometry and Biosafety Level 3 Laboratory Platforms and Mario Legault for cohort coordination and clinical samples. This study was supported by a National Research Council (Canada) Industrial Research Assistance Program (NRC-IRAP) grant to M.D.M. and A.F., by CIHR foundation grant 352417 to A.F., and by NIH grants R01 AI129 AI129769 to M.P. and A.F., R01 AI116274 to M.P., P01 AI120756 to Georgia Tomaras, R01 AI121135 and R37 AI095098 to D.T.E., and R01 AI148379 to A.F. and D.T.E. A.F. is the recipient of a Canada Research Chair on Retroviral Entry (grant RCHS0235 950-232424). L.H. was supported by NIH R01 AI136621-02 and NIH UM1 AI144462-01. D.R.B. was supported by NIH UM1 AI144462. Plant antibody production and analyses by PlantForm Corporation were supported in part by NRC-IRAP (catalog no. 778829 and 812182), and glycosylation analyses were performed by Warren Wakarchuk. S.P.A. and J.P. are supported by CIHR fellowships. This research used resources of the National Synchrotron Light Source II, a U.S. Department of Energy (DOE) Office of Science User Facility operated for the DOE Office of Science by the Brookhaven National Laboratory under contract DE-SC0012704. The Center for BioMolecular Structure (CBMS) is primarily supported by the National Institutes of Health, National Institute of General Medical Sciences (NIGMS), through a Center Core P30 grant (P30GM133893) and by the DOE Office of Biological and Environmental Research (KP1607011). The funders had no role in study design, data collection and analysis, the decision to publish, or preparation of the manuscript.

W.F.C., H.W., R.P., D.C., and M.D.M. are all employees of PlantForm Corporation.

The views expressed in this presentation are those of the authors and do not reflect the official policy or position of the Uniformed Services University, the U.S. Army, the Department of Defense, or the U.S. Government.

5.7 References

1. Barouch DH, Whitney JB, Moldt B, Klein F, Oliveira TY, Liu J, Stephenson KE, Chang HW, Shekhar K, Gupta S, Nkolola JP, Seaman MS, Smith KM, Borducchi EN, Cabral C, Smith JY, Blackmore S, Sanisetty S, Perry JR, Beck M, Lewis MG, Rinaldi W, Chakraborty AK, Poignard P, Nussenzweig MC, Burton DR. 2013. Therapeutic efficacy of potent neutralizing HIV-1-specific monoclonal antibodies in SHIV-infected rhesus monkeys. Nature 503:224-8.
2. Bournazos S, Klein F, Pietzsch J, Seaman MS, Nussenzweig MC, Ravetch JV. 2014. Broadly neutralizing anti-HIV-1 antibodies require Fc effector functions for in vivo activity. Cell 158:1243-1253.
3. Horwitz JA, Halper-Stromberg A, Mouquet H, Gitlin AD, Tretiakova A, Eisenreich TR, Malbec M, Gravemann S, Billerbeck E, Dorner M, Buning H, Schwartz O, Knops E, Kaiser R, Seaman MS, Wilson JM, Rice CM, Ploss A, Bjorkman PJ, Klein F, Nussenzweig MC. 2013. HIV-1 suppression and durable control by combining single broadly neutralizing antibodies and antiretroviral drugs in humanized mice. Proc Natl Acad Sci U S A 110:16538-43.
4. Klein F, Halper-Stromberg A, Horwitz JA, Gruell H, Scheid JF, Bournazos S, Mouquet H, Spatz LA, Diskin R, Abadir A, Zang T, Dorner M, Billerbeck E, Labitt RN, Gaebler C, Marcovecchio P, Incesu RB, Eisenreich TR, Bieniasz PD, Seaman MS, Bjorkman PJ, Ravetch JV, Ploss A, Nussenzweig MC. 2012. HIV therapy by a combination of broadly neutralizing antibodies in humanized mice. Nature 492:118-22.
5. Hessell AJ, Poignard P, Hunter M, Hangartner L, Tehrani DM, Bleeker WK, Parren PW, Marx PA, Burton DR. 2009. Effective, low-titer antibody protection against low-dose repeated mucosal SHIV challenge in macaques. Nat Med 15:951-4.
6. Hessell AJ, Rakasz EG, Poignard P, Hangartner L, Landucci G, Forthal DN, Koff WC, Watkins DI, Burton DR. 2009. Broadly neutralizing human anti-HIV antibody 2G12 is effective in protection against mucosal SHIV challenge even at low serum neutralizing titers. PLoS Pathog 5:e1000433.
7. Hessell AJ, Rakasz EG, Tehrani DM, Huber M, Weisgrau KL, Landucci G, Forthal DN, Koff WC, Poignard P, Watkins DI, Burton DR. 2010. Broadly neutralizing monoclonal antibodies 2F5 and 4E10 directed against the human immunodeficiency virus type 1 gp41 membrane-proximal external region protect against mucosal challenge by simian-human immunodeficiency virus SHIVBa-L. J Virol 84:1302-13.
8. Caskey M, Klein F, Lorenzi JC, Seaman MS, West AP, Jr., Buckley N, Kremer G, Nogueira L, Braunschweig M, Scheid JF, Horwitz JA, Shimeliovich I, Ben-Avraham S, Witmer-Pack M, Platten M, Lehmann C, Burke LA, Hawthorne T, Gorelick RJ, Walker BD, Keler T, Gulick RM, Fatkenheuer G, Schlesinger SJ, Nussenzweig MC. 2015. Viraemia suppressed in HIV-1-infected humans by broadly neutralizing antibody 3BNC117. Nature 522:487-91.
9. Caskey M, Schoofs T, Gruell H, Settler A, Karagounis T, Kreider EF, Murrell B, Pfeifer N, Nogueira L, Oliveira TY, Learn GH, Cohen YZ, Lehmann C, Gillor D, Shimeliovich I, Unson-O'Brien C, Weiland D, Robles A, Kummerle T, Wyen C, Levin R, Witmer-Pack M, Eren K, Ignacio C, Kiss S, West AP, Jr., Mouquet H,

Zingman BS, Gulick RM, Keler T, Bjorkman PJ, Seaman MS, Hahn BH, Fatkenheuer G, Schlesinger SJ, Nussenzweig MC, Klein F. 2017. Antibody 10-1074 suppresses viremia in HIV-1-infected individuals. Nat Med 23:185-191.
10. Lynch RM, Boritz E, Coates EE, DeZure A, Madden P, Costner P, Enama ME, Plummer S, Holman L, Hendel CS, Gordon I, Casazza J, Conan-Cibotti M, Migueles SA, Tressler R, Bailer RT, McDermott A, Narpala S, O'Dell S, Wolf G, Lifson JD, Freemire BA, Gorelick RJ, Pandey JP, Mohan S, Chomont N, Fromentin R, Chun TW, Fauci AS, Schwartz RM, Koup RA, Douek DC, Hu Z, Capparelli E, Graham BS, Mascola JR, Ledgerwood JE, Team VRCS. 2015. Virologic effects of broadly neutralizing antibody VRC01 administration during chronic HIV-1 infection. Sci Transl Med 7:319ra206.
11. Gautam R, Nishimura Y, Pegu A, Nason MC, Klein F, Gazumyan A, Golijanin J, Buckler-White A, Sadjadpour R, Wang K, Mankoff Z, Schmidt SD, Lifson JD, Mascola JR, Nussenzweig MC, Martin MA. 2016. A single injection of anti-HIV-1 antibodies protects against repeated SHIV challenges. Nature 533:105-109.
12. Mendoza P, Gruell H, Nogueira L, Pai JA, Butler AL, Millard K, Lehmann C, Suarez I, Oliveira TY, Lorenzi JCC, Cohen YZ, Wyen C, Kummerle T, Karagounis T, Lu CL, Handl L, Unson-O'Brien C, Patel R, Ruping C, Schlotz M, Witmer-Pack M, Shimeliovich I, Kremer G, Thomas E, Seaton KE, Horowitz J, West AP, Jr., Bjorkman PJ, Tomaras GD, Gulick RM, Pfeifer N, Fatkenheuer G, Seaman MS, Klein F, Caskey M, Nussenzweig MC. 2018. Combination therapy with anti-HIV-1 antibodies maintains viral suppression. Nature 561:479-484.
13. Ecker DM, Jones SD, Levine HL. 2015. The therapeutic monoclonal antibody market. MAbs 7:9-14.
14. Nandi S, Kwong AT, Holtz BR, Erwin RL, Marcel S, McDonald KA. 2016. Techno-economic analysis of a transient plant-based platform for monoclonal antibody production. MAbs 8:1456-1466.
15. Robinson MP, Ke N, Lobstein J, Peterson C, Szkodny A, Mansell TJ, Tuckey C, Riggs PD, Colussi PA, Noren CJ, Taron CH, DeLisa MP, Berkmen M. 2015. Efficient expression of full-length antibodies in the cytoplasm of engineered bacteria. Nat Commun 6:8072.
16. Potgieter TI, Cukan M, Drummond JE, Houston-Cummings NR, Jiang Y, Li F, Lynaugh H, Mallem M, McKelvey TW, Mitchell T, Nylen A, Rittenhour A, Stadheim TA, Zha D, d'Anjou M. 2009. Production of monoclonal antibodies by glycoengineered Pichia pastoris. J Biotechnol 139:318-25.
17. Ma JK, Drossard J, Lewis D, Altmann F, Boyle J, Christou P, Cole T, Dale P, van Dolleweerd CJ, Isitt V, Katinger D, Lobedan M, Mertens H, Paul MJ, Rademacher T, Sack M, Hundleby PA, Stiegler G, Stoger E, Twyman RM, Vcelar B, Fischer R. 2015. Regulatory approval and a first-in-human phase I clinical trial of a monoclonal antibody produced in transgenic tobacco plants. Plant Biotechnol J 13:1106-20.
18. McLean MD. 2017. Trastuzumab Made in Plants Using vivoXPRESS® Platform Technology. J Drug Des Res 4:1052.
19. Tschofen M, Knopp D, Hood E, Stoger E. 2016. Plant Molecular Farming: Much More than Medicines. Annu Rev Anal Chem (Palo Alto Calif) 9:271-94.

20. Tuse D, Tu T, McDonald KA. 2014. Manufacturing economics of plant-made biologics: case studies in therapeutic and industrial enzymes. Biomed Res Int 2014:256135.
21. Park JG, Ye C, Piepenbrink MS, Nogales A, Wang H, Shuen M, Meyers AJ, Martinez-Sobrido L, Kobie JJ. 2020. A Broad and Potent H1-Specific Human Monoclonal Antibody Produced in Plants Prevents Influenza Virus Infection and Transmission in Guinea Pigs. Viruses 12.
22. Garabagi F, Gilbert E, Loos A, McLean MD, Hall JC. 2012. Utility of the P19 suppressor of gene-silencing protein for production of therapeutic antibodies in Nicotiana expression hosts. Plant Biotechnol J 10:1118-28.
23. Strasser R, Altmann F, Steinkellner H. 2014. Controlled glycosylation of plant-produced recombinant proteins. Curr Opin Biotechnol 30:95-100.
24. Diamos AG, Hunter JGL, Pardhe MD, Rosenthal SH, Sun H, Foster BC, DiPalma MP, Chen Q, Mason HS. 2019. High Level Production of Monoclonal Antibodies Using an Optimized Plant Expression System. Front Bioeng Biotechnol 7:472.
25. Dent M, Hurtado J, Paul AM, Sun H, Lai H, Yang M, Esqueda A, Bai F, Steinkellner H, Chen Q. 2016. Plant-produced anti-dengue virus monoclonal antibodies exhibit reduced antibody-dependent enhancement of infection activity. J Gen Virol 97:3280-3290.
26. van Dolleweerd CJ, Teh AY, Banyard AC, Both L, Lotter-Stark HC, Tsekoa T, Phahladira B, Shumba W, Chakauya E, Sabeta CT, Gruber C, Fooks AR, Chikwamba RK, Ma JK. 2014. Engineering, expression in transgenic plants and characterisation of E559, a rabies virus-neutralising monoclonal antibody. J Infect Dis 210:200-8.
27. He J, Lai H, Engle M, Gorlatov S, Gruber C, Steinkellner H, Diamond MS, Chen Q. 2014. Generation and analysis of novel plant-derived antibody-based therapeutic molecules against West Nile virus. PLoS One 9:e93541.
28. Shields RL, Lai J, Keck R, O'Connell LY, Hong K, Meng YG, Weikert SH, Presta LG. 2002. Lack of fucose on human IgG1 N-linked oligosaccharide improves binding to human Fcgamma RIII and antibody-dependent cellular toxicity. J Biol Chem 277:26733-40.
29. Shields RL, Namenuk AK, Hong K, Meng YG, Rae J, Briggs J, Xie D, Lai J, Stadlen A, Li B, Fox JA, Presta LG. 2001. High resolution mapping of the binding site on human IgG1 for Fc gamma RI, Fc gamma RII, Fc gamma RIII, and FcRn and design of IgG1 variants with improved binding to the Fc gamma R. J Biol Chem 276:6591-604.
30. Jefferis R. 2009. Recombinant antibody therapeutics: the impact of glycosylation on mechanisms of action. Trends Pharmacol Sci 30:356-62.
31. Tao MH, Morrison SL. 1989. Studies of aglycosylated chimeric mouse-human IgG. Role of carbohydrate in the structure and effector functions mediated by the human IgG constant region. J Immunol 143:2595-601.
32. Teh AY, Maresch D, Klein K, Ma JK. 2014. Characterization of VRC01, a potent and broadly neutralizing anti-HIV mAb, produced in transiently and stably transformed tobacco. Plant Biotechnol J 12:300-11.
33. Loos A, Gach JS, Hackl T, Maresch D, Henkel T, Porodko A, Bui-Minh D, Sommeregger W, Wozniak-Knopp G, Forthal DN, Altmann F, Steinkellner H, Mach

L. 2015. Glycan modulation and sulfoengineering of anti-HIV-1 monoclonal antibody PG9 in plants. Proc Natl Acad Sci U S A 112:12675-80.
34. Singh AA, Pooe O, Kwezi L, Lotter-Stark T, Stoychev SH, Alexandra K, Gerber I, Bhiman JN, Vorster J, Pauly M, Zeitlin L, Whaley K, Mach L, Steinkellner H, Morris L, Tsekoa TL, Chikwamba R. 2020. Plant-based production of highly potent anti-HIV antibodies with engineered posttranslational modifications. Sci Rep 10:6201.
35. Forthal DN, Gach JS, Landucci G, Jez J, Strasser R, Kunert R, Steinkellner H. 2010. Fc-glycosylation influences Fcgamma receptor binding and cell-mediated anti-HIV activity of monoclonal antibody 2G12. J Immunol 185:6876-82.
36. Julien JP, Cupo A, Sok D, Stanfield RL, Lyumkis D, Deller MC, Klasse PJ, Burton DR, Sanders RW, Moore JP, Ward AB, Wilson IA. 2013. Crystal structure of a soluble cleaved HIV-1 envelope trimer. Science 342:1477-83.
37. Julien JP, Sok D, Khayat R, Lee JH, Doores KJ, Walker LM, Ramos A, Diwanji DC, Pejchal R, Cupo A, Katpally U, Depetris RS, Stanfield RL, McBride R, Marozsan AJ, Paulson JC, Sanders RW, Moore JP, Burton DR, Poignard P, Ward AB, Wilson IA. 2013. Broadly neutralizing antibody PGT121 allosterically modulates CD4 binding via recognition of the HIV-1 gp120 V3 base and multiple surrounding glycans. PLoS Pathog 9:e1003342.
38. Kong L, Lee JH, Doores KJ, Murin CD, Julien JP, McBride R, Liu Y, Marozsan A, Cupo A, Klasse PJ, Hoffenberg S, Caulfield M, King CR, Hua Y, Le KM, Khayat R, Deller MC, Clayton T, Tien H, Feizi T, Sanders RW, Paulson JC, Moore JP, Stanfield RL, Burton DR, Ward AB, Wilson IA. 2013. Supersite of immune vulnerability on the glycosylated face of HIV-1 envelope glycoprotein gp120. Nat Struct Mol Biol 20:796-803.
39. Pejchal R, Doores KJ, Walker LM, Khayat R, Huang PS, Wang SK, Stanfield RL, Julien JP, Ramos A, Crispin M, Depetris R, Katpally U, Marozsan A, Cupo A, Maloveste S, Liu Y, McBride R, Ito Y, Sanders RW, Ogohara C, Paulson JC, Feizi T, Scanlan CN, Wong CH, Moore JP, Olson WC, Ward AB, Poignard P, Schief WR, Burton DR, Wilson IA. 2011. A potent and broad neutralizing antibody recognizes and penetrates the HIV glycan shield. Science 334:1097-103.
40. Walker LM, Huber M, Doores KJ, Falkowska E, Pejchal R, Julien JP, Wang SK, Ramos A, Chan-Hui PY, Moyle M, Mitcham JL, Hammond PW, Olsen OA, Phung P, Fling S, Wong CH, Phogat S, Wrin T, Simek MD, Protocol GPI, Koff WC, Wilson IA, Burton DR, Poignard P. 2011. Broad neutralization coverage of HIV by multiple highly potent antibodies. Nature 477:466-70.
41. Moldt B, Rakasz EG, Schultz N, Chan-Hui PY, Swiderek K, Weisgrau KL, Piaskowski SM, Bergman Z, Watkins DI, Poignard P, Burton DR. 2012. Highly potent HIV-specific antibody neutralization in vitro translates into effective protection against mucosal SHIV challenge in vivo. Proc Natl Acad Sci U S A 109:18921-5.
42. Hangartner L, Beauparlant D, Rakasz E, Nedellec R, Hoze N, McKenney K, Martins MA, Seabright GE, Allen JD, Weiler AM, Friedrich TC, Regoes RR, Crispin M, Burton DR. 2021. Effector function does not contribute to protection from virus challenge by a highly potent HIV broadly neutralizing antibody in nonhuman primates. Sci Transl Med 13.

43. Parsons MS, Lee WS, Kristensen AB, Amarasena T, Khoury G, Wheatley AK, Reynaldi A, Wines BD, Hogarth PM, Davenport MP, Kent SJ. 2019. Fc-dependent functions are redundant to efficacy of anti-HIV antibody PGT121 in macaques. J Clin Invest 129:182-191.
44. Pauthner MG, Nkolola JP, Havenar-Daughton C, Murrell B, Reiss SM, Bastidas R, Prevost J, Nedellec R, von Bredow B, Abbink P, Cottrell CA, Kulp DW, Tokatlian T, Nogal B, Bianchi M, Li H, Lee JH, Butera ST, Evans DT, Hangartner L, Finzi A, Wilson IA, Wyatt RT, Irvine DJ, Schief WR, Ward AB, Sanders RW, Crotty S, Shaw GM, Barouch DH, Burton DR. 2019. Vaccine-Induced Protection from Homologous Tier 2 SHIV Challenge in Nonhuman Primates Depends on Serum-Neutralizing Antibody Titers. Immunity 50:241-252 e6.
45. Wang P, Gajjar MR, Yu J, Padte NN, Gettie A, Blanchard JL, Russell-Lodrigue K, Liao LE, Perelson AS, Huang Y, Ho DD. 2020. Quantifying the contribution of Fc-mediated effector functions to the antiviral activity of anti-HIV-1 IgG1 antibodies in vivo. Proc Natl Acad Sci U S A 117:18002-18009.
46. Hessell AJ, Hangartner L, Hunter M, Havenith CE, Beurskens FJ, Bakker JM, Lanigan CM, Landucci G, Forthal DN, Parren PW, Marx PA, Burton DR. 2007. Fc receptor but not complement binding is important in antibody protection against HIV. Nature 449:101-4.
47. Lu CL, Murakowski DK, Bournazos S, Schoofs T, Sarkar D, Halper-Stromberg A, Horwitz JA, Nogueira L, Golijanin J, Gazumyan A, Ravetch JV, Caskey M, Chakraborty AK, Nussenzweig MC. 2016. Enhanced clearance of HIV-1-infected cells by broadly neutralizing antibodies against HIV-1 in vivo. Science 352:1001-4.
48. Pietzsch J, Gruell H, Bournazos S, Donovan BM, Klein F, Diskin R, Seaman MS, Bjorkman PJ, Ravetch JV, Ploss A, Nussenzweig MC. 2012. A mouse model for HIV-1 entry. Proc Natl Acad Sci U S A 109:15859-64.
49. Forthal D, Finzi A. 2019. Blocking HIV-1 replication: are Fc-Fcgamma receptor interactions required? J Clin Invest 129:53-54.
50. Ma B, Guan X, Li Y, Shang S, Li J, Tan Z. 2020. Protein Glycoengineering: An Approach for Improving Protein Properties. Front Chem 8:622.
51. Montero-Morales L, Steinkellner H. 2018. Advanced Plant-Based Glycan Engineering. Front Bioeng Biotechnol 6:81.
52. Princiotto AM, Vrbanac VD, Melillo B, Park J, Tager AM, Smith AB, 3rd, Sodroski J, Madani N. 2018. A Small-Molecule CD4-Mimetic Compound Protects Bone Marrow-Liver-Thymus Humanized Mice From HIV-1 Infection. J Infect Dis 218:471-475.
53. Nishimura Y, Gautam R, Chun TW, Sadjadpour R, Foulds KE, Shingai M, Klein F, Gazumyan A, Golijanin J, Donaldson M, Donau OK, Plishka RJ, Buckler-White A, Seaman MS, Lifson JD, Koup RA, Fauci AS, Nussenzweig MC, Martin MA. 2017. Early antibody therapy can induce long-lasting immunity to SHIV. Nature 543:559-563.
54. Vogel CL, Cobleigh MA, Tripathy D, Gutheil JC, Harris LN, Fehrenbacher L, Slamon DJ, Murphy M, Novotny WF, Burchmore M, Shak S, Stewart SJ, Press M. 2002. Efficacy and safety of trastuzumab as a single agent in first-line treatment of HER2-overexpressing metastatic breast cancer. J Clin Oncol 20:719-26.

55. Richard J, Prevost J, Baxter AE, von Bredow B, Ding S, Medjahed H, Delgado GG, Brassard N, Sturzel CM, Kirchhoff F, Hahn BH, Parsons MS, Kaufmann DE, Evans DT, Finzi A. 2018. Uninfected Bystander Cells Impact the Measurement of HIV-Specific Antibody-Dependent Cellular Cytotoxicity Responses. MBio 9.
56. Veillette M, Desormeaux A, Medjahed H, Gharsallah NE, Coutu M, Baalwa J, Guan Y, Lewis G, Ferrari G, Hahn BH, Haynes BF, Robinson JE, Kaufmann DE, Bonsignori M, Sodroski J, Finzi A. 2014. Interaction with cellular CD4 exposes HIV-1 envelope epitopes targeted by antibody-dependent cell-mediated cytotoxicity. J Virol 88:2633-44.
57. Alpert MD, Heyer LN, Williams DE, Harvey JD, Greenough T, Allhorn M, Evans DT. 2012. A novel assay for antibody-dependent cell-mediated cytotoxicity against HIV-1- or SIV-infected cells reveals incomplete overlap with antibodies measured by neutralization and binding assays. J Virol 86:12039-52.
58. von Bredow B, Arias JF, Heyer LN, Moldt B, Le K, Robinson JE, Zolla-Pazner S, Burton DR, Evans DT. 2016. Comparison of Antibody-Dependent Cell-Mediated Cytotoxicity and Virus Neutralization by HIV-1 Env-Specific Monoclonal Antibodies. J Virol 90:6127-6139.
59. Arias JF, Heyer LN, von Bredow B, Weisgrau KL, Moldt B, Burton DR, Rakasz EG, Evans DT. 2014. Tetherin antagonism by Vpu protects HIV-infected cells from antibody-dependent cell-mediated cytotoxicity. Proc Natl Acad Sci U S A 111:6425-30.
60. Ferrara C, Grau S, Jager C, Sondermann P, Brunker P, Waldhauer I, Hennig M, Ruf A, Rufer AC, Stihle M, Umana P, Benz J. 2011. Unique carbohydrate-carbohydrate interactions are required for high affinity binding between FcgammaRIII and antibodies lacking core fucose. Proc Natl Acad Sci U S A 108:12669-74.
61. Wines BD, Vanderven HA, Esparon SE, Kristensen AB, Kent SJ, Hogarth PM. 2016. Dimeric FcgammaR Ectodomains as Probes of the Fc Receptor Function of Anti-Influenza Virus IgG. J Immunol 197:1507-16.
62. McLean MR, Madhavi V, Wines BD, Hogarth PM, Chung AW, Kent SJ. 2017. Dimeric Fcgamma Receptor Enzyme-Linked Immunosorbent Assay To Study HIV-Specific Antibodies: A New Look into Breadth of Fcgamma Receptor Antibodies Induced by the RV144 Vaccine Trial. J Immunol 199:816-826.
63. Anand SP, Prevost J, Baril S, Richard J, Medjahed H, Chapleau JP, Tolbert WD, Kirk S, Smith AB, 3rd, Wines BD, Kent SJ, Hogarth PM, Parsons MS, Pazgier M, Finzi A. 2019. Two Families of Env Antibodies Efficiently Engage Fc-Gamma Receptors and Eliminate HIV-1-Infected Cells. J Virol 93.
64. Borrok MJ, Jung ST, Kang TH, Monzingo AF, Georgiou G. 2012. Revisiting the role of glycosylation in the structure of human IgG Fc. ACS Chem Biol 7:1596-602.
65. Krapp S, Mimura Y, Jefferis R, Huber R, Sondermann P. 2003. Structural analysis of human IgG-Fc glycoforms reveals a correlation between glycosylation and structural integrity. J Mol Biol 325:979-89.
66. Group PIW, Multi-National PIIST, Davey RT, Jr., Dodd L, Proschan MA, Neaton J, Neuhaus Nordwall J, Koopmeiners JS, Beigel J, Tierney J, Lane HC, Fauci AS, Massaquoi MBF, Sahr F, Malvy D. 2016. A Randomized, Controlled Trial of ZMapp for Ebola Virus Infection. N Engl J Med 375:1448-1456.

67. Chen Q, Davis KR. 2016. The potential of plants as a system for the development and production of human biologics. F1000Res 5.
68. Strasser R, Stadlmann J, Schahs M, Stiegler G, Quendler H, Mach L, Glossl J, Weterings K, Pabst M, Steinkellner H. 2008. Generation of glyco-engineered Nicotiana benthamiana for the production of monoclonal antibodies with a homogeneous human-like N-glycan structure. Plant Biotechnol J 6:392-402.
69. Shinkawa T, Nakamura K, Yamane N, Shoji-Hosaka E, Kanda Y, Sakurada M, Uchida K, Anazawa H, Satoh M, Yamasaki M, Hanai N, Shitara K. 2003. The absence of fucose but not the presence of galactose or bisecting N-acetylglucosamine of human IgG1 complex-type oligosaccharides shows the critical role of enhancing antibody-dependent cellular cytotoxicity. J Biol Chem 278:3466-73.
70. Houde D, Peng Y, Berkowitz SA, Engen JR. 2010. Post-translational modifications differentially affect IgG1 conformation and receptor binding. Mol Cell Proteomics 9:1716-28.
71. Nimmerjahn F, Anthony RM, Ravetch JV. 2007. Agalactosylated IgG antibodies depend on cellular Fc receptors for in vivo activity. Proc Natl Acad Sci U S A 104:8433-7.
72. Peschke B, Keller CW, Weber P, Quast I, Lunemann JD. 2017. Fc-Galactosylation of Human Immunoglobulin Gamma Isotypes Improves C1q Binding and Enhances Complement-Dependent Cytotoxicity. Front Immunol 8:646.
73. Richard J, Veillette M, Brassard N, Iyer SS, Roger M, Martin L, Pazgier M, Schon A, Freire E, Routy JP, Smith AB, 3rd, Park J, Jones DM, Courter JR, Melillo BN, Kaufmann DE, Hahn BH, Permar SR, Haynes BF, Madani N, Sodroski JG, Finzi A. 2015. CD4 mimetics sensitize HIV-1-infected cells to ADCC. Proc Natl Acad Sci U S A 112:E2687-94.
74. Thomann M, Reckermann K, Reusch D, Prasser J, Tejada ML. 2016. Fc-galactosylation modulates antibody-dependent cellular cytotoxicity of therapeutic antibodies. Mol Immunol 73:69-75.
75. Borducchi EN, Liu J, Nkolola JP, Cadena AM, Yu WH, Fischinger S, Broge T, Abbink P, Mercado NB, Chandrashekar A, Jetton D, Peter L, McMahan K, Moseley ET, Bekerman E, Hesselgesser J, Li W, Lewis MG, Alter G, Geleziunas R, Barouch DH. 2018. Antibody and TLR7 agonist delay viral rebound in SHIV-infected monkeys. Nature 563:360-364.
76. Hsu DC, Schuetz A, Imerbsin R, Silsorn D, Pegu A, Inthawong D, Sopanaporn J, Visudhiphan P, Chuenarom W, Keawboon B, Shi W, Robb ML, Mascola JR, Geleziunas R, Koup RA, Barouch DH, Michael NL, Vasan S. 2021. TLR7 agonist, N6-LS and PGT121 delayed viral rebound in SHIV-infected macaques after antiretroviral therapy interruption. PLoS Pathog 17:e1009339.
77. Fontaine J, Coutlee F, Tremblay C, Routy JP, Poudrier J, Roger M, Montreal Primary HIVI, Long-Term Nonprogressor Study G. 2009. HIV infection affects blood myeloid dendritic cells after successful therapy and despite nonprogressing clinical disease. J Infect Dis 199:1007-18.
78. Fontaine J, Chagnon-Choquet J, Valcke HS, Poudrier J, Roger M, Montreal Primary HIVI, Long-Term Non-Progressor Study G. 2011. High expression levels of B

lymphocyte stimulator (BLyS) by dendritic cells correlate with HIV-related B-cell disease progression in humans. Blood 117:145-55.
79. Garabagi F, McLean MD, Hall JC. 2012. Transient and stable expression of antibodies in Nicotiana species. Methods Mol Biol 907:389-408.
80. Grohs BM, Niu Y, Veldhuis LJ, Trabelsi S, Garabagi F, Hassell JA, McLean MD, Hall JC. 2010. Plant-produced trastuzumab inhibits the growth of HER2 positive cancer cells. J Agric Food Chem 58:10056-63.
81. Timmermans MC, Maliga P, Vieira J, Messing J. 1990. The pFF plasmids: cassettes utilising CaMV sequences for expression of foreign genes in plants. J Biotechnol 14:333-44.
82. Castilho A, Beihammer G, Pfeiffer C, Goritzer K, Montero-Morales L, Vavra U, Maresch D, Grunwald-Gruber C, Altmann F, Steinkellner H, Strasser R. 2018. An oligosaccharyltransferase from Leishmania major increases the N-glycan occupancy on recombinant glycoproteins produced in Nicotiana benthamiana. Plant Biotechnol J 16:1700-1709.
83. An YQ, McDowell JM, Huang S, McKinney EC, Chambliss S, Meagher RB. 1996. Strong, constitutive expression of the Arabidopsis ACT2/ACT8 actin subclass in vegetative tissues. Plant J 10:107-21.
84. Strasser R, Castilho A, Stadlmann J, Kunert R, Quendler H, Gattinger P, Jez J, Rademacher T, Altmann F, Mach L, Steinkellner H. 2009. Improved virus neutralization by plant-produced anti-HIV antibodies with a homogeneous beta1,4-galactosylated N-glycan profile. J Biol Chem 284:20479-85.
85. Almquist KC, McLean MD, Niu Y, Byrne G, Olea-Popelka FC, Murrant C, Barclay J, Hall JC. 2006. Expression of an anti-botulinum toxin A neutralizing single-chain Fv recombinant antibody in transgenic tobacco. Vaccine 24:2079-86.
86. Olea-Popelka F, McLean MD, Horsman J, Almquist K, Brandle JE, Hall JC. 2005. Increasing expression of an anti-picloram single-chain variable fragment (ScFv) antibody and resistance to picloram in transgenic tobacco (Nicotiana tabacum). J Agric Food Chem 53:6683-90.
87. Li H, Wang S, Kong R, Ding W, Lee FH, Parker Z, Kim E, Learn GH, Hahn P, Policicchio B, Brocca-Cofano E, Deleage C, Hao X, Chuang GY, Gorman J, Gardner M, Lewis MG, Hatziioannou T, Santra S, Apetrei C, Pandrea I, Alam SM, Liao HX, Shen X, Tomaras GD, Farzan M, Chertova E, Keele BF, Estes JD, Lifson JD, Doms RW, Montefiori DC, Haynes BF, Sodroski JG, Kwong PD, Hahn BH, Shaw GM. 2016. Envelope residue 375 substitutions in simian-human immunodeficiency viruses enhance CD4 binding and replication in rhesus macaques. Proc Natl Acad Sci U S A 113:E3413-22.
88. Veillette M, Coutu M, Richard J, Batraville LA, Dagher O, Bernard N, Tremblay C, Kaufmann DE, Roger M, Finzi A. 2015. The HIV-1 gp120 CD4-bound conformation is preferentially targeted by antibody-dependent cellular cytotoxicity-mediating antibodies in sera from HIV-1-infected individuals. J Virol 89:545-51.
89. Richard J, Veillette M, Ding S, Zoubchenok D, Alsahafi N, Coutu M, Brassard N, Park J, Courter JR, Melillo B, Smith AB, 3rd, Shaw GM, Hahn BH, Sodroski J, Kaufmann DE, Finzi A. 2016. Small CD4 Mimetics Prevent HIV-1 Uninfected

Bystander CD4 + T Cell Killing Mediated by Antibody-dependent Cell-mediated Cytotoxicity. EBioMedicine 3:122-134.

CHAPTER VI

General Discussion

This chapter provides an overall discussion of the research results presented in this thesis. Section 6.1 discusses the summary of the main findings and contribution of the work to the current knowledge in the HIV research field. In Section 6.2, some outstanding questions and future work to address them are presented. The applicability of this research towards the development of a potential HIV cure is discussed in Section 6.3. Finally, the concluding remarks of this thesis are stated in section 6.4.

6.1 Summary of main findings

The studies presented in this thesis provide new insights into different factors modulating the efficacy of Fc-mediated effector responses (**Figure 6.1**). This work makes important contributions to the field of humoral immune responses against HIV-1-infected cells and broadly, to the field of HIV cure and eradication.

The 'open' CD4-bound conformation of Env is targeted by ADCC-mediating antibodies commonly present in HIV+ sera. Our work highlights the importance that the Fc regions of two families of nNAbs, anti-CoRBS and anti-Cluster A, have for the clearance of HIV-1-infected CD4+ T cells. This was demonstrated by using a biotin-tagged dimeric rsFcγRIIIa probe and with a functional *in vitro* FACS-based ADCC assay.

Furthermore, we describe a novel observation that the binding of certain bNAbs to the HIV-1 Env, decreases Env expression from the surface of HIV-1-infected CD4+ T cells. This was demonstrated by flow cytometry and confocal microscopy. We show that bNAb-mediated Env internalization is dynamin dependent, and a dynamin inhibitor was shown to enhance the ADCC activity of bNAbs using an *in vitro* FACS-based ADCC assay. Internalized bNAb-Env complexes were shown to accumulate in early endosome compartments and were excluded from intercellular lysosomal compartments. Interestingly, the binding of nNAbs also decreases Env expression from the surface of HIV-1-infected CD4+ T cells, but only upon the selective opening of Env, using sCD4 or CD4mc. To characterize the driving factors by which these immune complexes are internalized, we attempted to identify if the localization of Env on the plasma membrane could contribute to this phenotype. Consequently, we observed that bNAb-Env and nNAb(+CD4mc)-Env complexes are detected in DRMs by membrane fractionation using a sucrose gradient. Thus, an association of antibody-bound, functionally cleaved Env with certain lipid microdomains could influence its accelerated internalization.

Since certain bNAb-Env complexes are rapidly endocytosed, we sought to determine other ways, than endocytosis inhibition, to take advantage of the limited time frame that these immune complexes were formed and remained on the cell surface – exposed to the immune

system. We reasoned that enhancing the affinity of the Fc portion of bNAbs for respective FcRs could perhaps supersede the transient presence of Env-bNAb complexes at the cell surface. We therefore modified Fc N-linked glycans of PGT121, a potent bNAb, that we used here as a model for future bNAb design prototype. As expected, the different glycovariants of PGT121 produced in *N. benthamiana* did not affect their ability to recognize infected cells or neutralize viral particles. Interestingly, augmented FcγRIIIa interaction and ADCC against HIV-1-infected $CD4^+$ T cells were observed by using an afucosylated PGT121 both *in vitro* and *ex vivo* and the overall galactosylation profile of PGT121 did not enhance or diminish Fc functionality. These results could be important in a therapeutic context to accelerate infected cell clearance and slow disease progression and future studies to evaluate the potential of plant-produced afucosylated PGT121 in controlling HIV-1 replication *in vivo* are warranted.

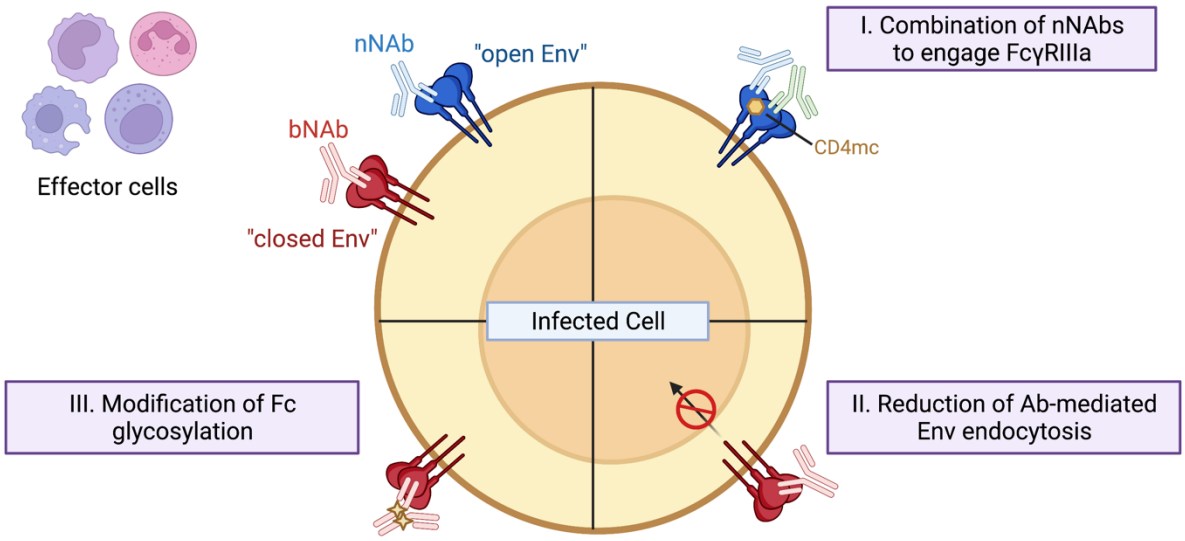

Figure 6.1 Overview of three different mechanisms described in this thesis to harness Fc-mediated immune responses against HIV-1-infected cells. The use of antibodies targeting non-overlapping epitopes that can cooperatively engage FcγRIIIa, reducing antibody-mediated Env endocytosis that limits immune complex stability, and modifying the Fc-glycosylation profile of antibodies. Diagram created with BioRender.com

6.1.1 Contribution to current knowledge

The work presented throughout this thesis focuses primarily on Fc-mediated effector responses of Env-specific antibodies, which have been shown to play a role in disease progression in humans (308, 388, 389) and vaccinal protection in the RV144 trail (260).

In chapter 2, we observe a synergy in the engagement of effector cells between two antibodies targeting highly conserved and non-overlapping epitopes. This data contributed to the development of a new cocktail (anti-CoRBS mAb/anti-cluster A mAb/CD4mc) that can stabilize a new Env conformation (State 2A) (233) and that can reduce the size of HIV-1 reservoir *in vivo* (279). Combination of monoclonal antibodies (mAbs) that target two or more non-overlapping antigenic epitopes have been used to enhance innate anti-tumour effector immune responses (390-392). Current antiviral strategies also include incorporating monoclonal antibodies that either target highly conserved epitopes (393) or combinations of two or more mAbs targeting various epitopes (394), such as cocktails SYN023 and CL184 against rabies virus variants (395, 396). For the ongoing coronavirus disease (COVID-19) pandemic caused by the severe acute respiratory syndrome coronavirus 2 (SARS-CoV-2), the Regeneron (REGN-COV2) cocktail has been authorized for emergency use authorization (EUA). REGN-COV2 is composed of two potent neutralizing mAbs, casirivimab and imdevimab, that target non-overlapping sites on the receptor binding domain of the SARS-CoV-2 Spike protein and its use in hospitalized patients resulted in a reduction of viral load and diminished the incidence and severity of lung disease in patients whose immune response had not been initiated (397). In addition to neutralization, neutralizing antibodies against SARS-CoV-2 also require Fc effector functions for optimal therapeutic protection (398, 399).

For HIV-1, recent therapeutic passive immunization clinical studies are utilizing combinations of bNAbs, such as CD4bs targeting 3BNC117 and V3 targeting 10-1074, during ART interruption to suppress viral rebound (400). This treatment strategy using bNAb infusion also affected the size of the HIV reservoir, with a decreased replication-competent reservoir detected in some individuals. While direct neutralization of virions is one major function of the bNAbs, additional Fc-mediated functions play a role in targeting already infected cells and

thus, can likely contribute to controlling viral loads (292, 309, 401-404). A recent study by Wang et al. to tease out the relative contribution of neutralization to prevent infection versus elimination of infected cells by Fc-mediated effector functions *in vivo* in HIV-1-infected humanized mice and SHIV-infected rhesus macaques, determined that Fc-mediated effector functions contribute to approximately 25% to 45% of the total antiviral activity (305). Therefore, combinations of bNAbs could possibly aid in clearance of infected cells via antibody-mediated effector functions. These studies also demonstrate that combination antibody therapies could be a useful addition to ART to suppress viremia. The passive transfer of antibodies is dependent on the half-life of antibodies and thus, it is important that they are provided at sufficiently high concentrations to achieve their intended biological functions. When working with RNA viruses, they also should harbour breadth to prevent the emergence of antibody-resistant variants. Thus, new technologies to improve their half-life *in vivo* (405), expand their distribution, enhance FcR engagement and administer as cocktails are currently being explored.

The epitopes recognized by CD4i Abs are hidden in the 'closed' Env and require its opening to have effective activities in infected cell clearance. Thus, using chimeric constructs that already link the CoRBS or cluster A IgG molecules to sCD4 (also called Ab-CD4 hybrid proteins), have shown to efficiently bind infected cells and eliminate them via ADCC *in vitro* and *ex-vivo.* These chimeras also shed light on the neutralizing ability of nNAbs, provided they can bind their cognate epitope (406). Furthermore, bi- and tri-specific antibodies, that are molecules combining two or more antigen-binding variable fragments to recognize separate epitopes on Env, have also been demonstrated to increase the potency and breadth of bNAbs (407), for example the combination of PGT121 and VRC07 (408). Bispecific proteins that are fusions of the CD4 receptor, co-receptor, and IgG Fc regions (such as CD4-Ig and eCD4-Ig) are also valuable strategies that have demonstrated enhanced neutralization activities than certain bNAbs alone (409, 410). Additionally, a naturally occurring dimeric form of the bNAb 2G12, containing four Fabs and two Fc regions, was shown to be more potent at mediating ADCC than its monomeric counterpart (411). Altogether, these studies suggest that multiple

antibodies can not only prevent viral escape but also enhance the clustering and cross-linking of FcγRs to activate effector cells and thus, have beneficial outputs (412).

HIV-1 have evolved diverse strategies to evade the action of Env-specific antibodies, including conformational and carbohydrate shield masking of critical epitopes and by simply reducing the amount of Env accessible for antibody binding. In chapter 3, we describe a novel strategy wherein antibody-bound Env glycoproteins are internalized in a conformation-specific manner and in chapter 4, we observe that this could be dependent on the localization of Env at the cell surface. These observations contribute to the field's current understanding of Env trafficking upon its production and cell-surface expression. An association of antibody-bound functionally cleaved Env with lipid microdomains and uncleaved Env with DSMs supports a recently published study describing trafficking of cleaved Env trimers via the conventional secretory pathway through the TGN and uncleaved Env trimers that are transported via an unconventional Golgi bypass pathway (163). The Env trimers that traffic via the Golgi are transported to regions on the cell surface, from where they are potentially incorporated into virions. Furthermore, our observations of rapid antibody-induced internalization of Env present in microdomains and their possible accumulation in early endosomes that could be trafficked to recycling endosomes support the field's understanding of Env internalization, recycling, and its targeted trafficking prior to virion incorporation (200). Additionally, the accelerated internalization of functionally cleaved Env trimers present in lipid microdomains upon antibody binding could possibly be an immune evasion strategy in place to reduce the overall surface levels of Env that do not get incorporated into virions. Since lipid microdomains have been described to be enriched in cholesterol and sphingolipids, studies measuring antibody-induced internalization upon cholesterol depletion or Env mutants with decreased cholesterol interactivity, would be of interest to confirm the phenotype of localization dictating this phenotype. Additionally, since evidence in the field points towards the interaction between the cytoplasmic tail of Env and Matrix (108), and the recruitment of Env to lipid microdomains for virion incorporation, membrane fractionation assays using either cells co-expressing Env and Gag or infected cells, could further clarify the role of Env localization in the context of infection for antibody-mediated Env internalization.

Our results from chapter 5 demonstrated the potential of glycoengineering PGT121 to augment its Fc-effector functionality via afucosylation without affecting its neutralization capacities. PGT121 is currently being tested in combination with the long-lasting bNAb VRC07-523LS (targets the CD4bs) and PGDM1400 (targets V1/V2 glycans) in both uninfected and infected adults for HIV-1 prevention and therapy in an ongoing clinical trial (NCT03721510). Thus, incorporating afucsoylated PGT121 in ongoing or future combination therapy trials could be a useful therapeutic option. We also observed that the overall galactosylation profile of PGT121 does not enhance or diminish Fc functionality and was dependent mainly on the presence or absence of fucose. These results are akin to recent studies demonstrating that effector functionality modulated by Fc galactosylation or sialylation are only dependent on the status of core fucosylation, with the absence of fucose leading to enhanced FcγRIIIa affinities (362, 413). However, future *in vivo* animal studies to understand the impact of Fc-glycosylation against infected cells are warranted, since a NHP study using a non-fucosylated b12 did not show enhanced protection from SHIV challenges (414). However, this study did not explore the capacity of b12 to clear out infection and the potent neutralizing activities of bNAbs alone could be highly effective in preventing infection. Boosting the Fc-effector functionalities of bNAbs could be beneficial when thinking of cure strategies, since the passive administration of bNAbs has been shown to decrease the number of infected cells and suppress viremia in infected individuals (296, 297, 301, 400).

6.2 Outstanding questions and future work

The research herein has resulted in the identification of (i) an interplay between two families of nNAbs that crosslink FcγRIIIa and eliminate HIV-1-infected cells in the presence of CD4mc, (ii) a new Fc effector evasion strategy in place to limit the cell surface expression of antibody-Env complexes, and (iii) an enhancement of FcγRIIIa engagement by modulating the glycosylation profile of bNAbs targeting the closed conformation. The results presented in this thesis warrant additional research to address some outstanding questions that could improve strategies to eliminate HIV-1-infected cells:

Are there other classes of anti-Env antibodies that collaborate in a polyclonal antibody response?

In chapter 2, we defined a collaboration between two classes of antibodies targeting highly conserved CD4i epitopes within the Env trimer; these antibodies are frequently elicited in HIV-1-infected individuals and can mediate potent ADCC upon epitope recognition. It is important to note that neutralizing antibodies targeting the native conformation of Env also harbour potent Fc effector and ADCC-mediating capacities (415). Nevertheless, during HIV-1 infection, the majority of elicited antibodies target CD4i epitopes that are occluded in the unliganded Env trimer present at the surface of infected cells or infectious viral particles (378). Thus, to understand what antibody specificities can synergize together to form a polyclonal antibody response, future studies need to dissect the contribution of other classes of antibodies targeting CD4i epitopes in the gp120 subunit, such as anti-V3 (*e.g.* 19b (416)) and anti-V2 (*e.g.* CH58 (417)) antibodies, and in the gp41 subunit, such as cluster I (*e.g.* 246D (418)) and cluster II (*e.g.* 98-6 (419)) antibodies. Likewise, determining a cocktail of neutralizing antibodies that target multiple specificities and harbour potent Fc-mediated effector activities, could potentially prevent viral escape and aid in long-term infection control. These results would lead to an understanding of the overall contribution of each class of antibody required to efficiently engage and crosslink FcγRs and subsequently, activate effector cells. This information would be useful in designing possible treatment options related to administering CD4mc that allows for the binding of CD4i antibodies. If a subset of patients does not naturally elicit a desired class of antibodies, these could be passively administered to boost effector cell responses. Likewise, these experiments could aid in the design of potential immunogens that elicit the desired antibodies targeting the epitopes of interest not naturally elicited in some patients (420, 421). The nNAbs from the anti-CoRBS mAb/anti-cluster A mAb/CD4mc cocktail target highly conserved epitopes and are easy to elicit by immunization, when compared to bNAbs.

Are there additional Fc-mediated effector mechanisms that are modulated by the three mechanistic processes highlighted in this thesis?

Since the studies presented herein describe different mechanisms by which ADCC is modulated, the question remains if other Fc-effector functionalities, such as ADCP, are also modulated by antibody cooperativity, antibody-mediated Env internalization, and Fc-glycan modifications.

We have started preliminary experiments to study the engagement of the dimeric rsFcγRIIa proteins (339) (H131 and R131 polymorphic variants) by anti-CoRBS and anti-cluster A antibodies. FcγRIIa/CD32a is expressed on the surface of monocytes, macrophages, neutrophils, and dendritic cells. Upon using either LALA mutated N12i2 or N5i5, we observe striking decreases in FcγRIIa binding, when compared to the binding observed with unmutated antibodies in our ELISA-based assay (**Figure 6.2**). Thus, only the combination of Fc-competent anti-cluster A and anti-CoRBS Abs engaged rsFcγRIIa, akin the results seen in chapter 2 with rsFcγRIIIa. Moreover, we observe similar trends with both the FcγRIIa H131 and R131 variants. Future experiments to evaluate this cooperativity in a functional ADCP assay with infected and effector cells are needed. An assay that measures the phagocytosis of infected primary CD4+ T cells by autologous monocytes and/or macrophages in the presence of antibodies would be desirable.

Other Fc-mediated functionalities could possibly include the induction of a 'vaccine effect' in infected individuals. The passive administration of bNAbs has been shown to increase HIV-1-specific T cell immunity, and a suggested mechanism for this phenotype was enhanced antigen presentation by activated dendritic cells that uptake bNAb-HIV-1 immune complexes (422).

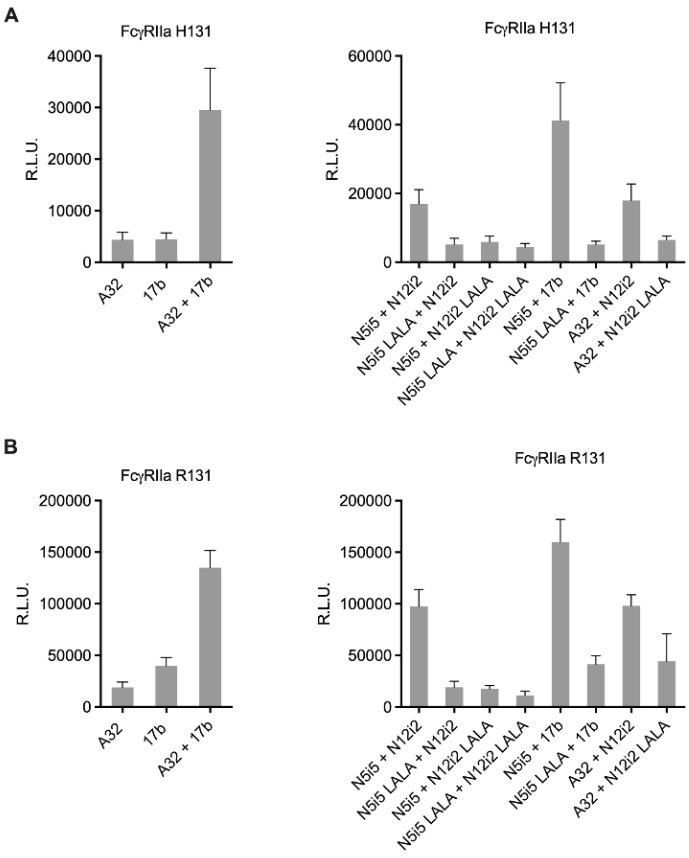

Figure 6.2 Introduction of LALA mutations in the Fc portion of both CoRBS and anti-cluster A antibodies decreases engagement of dimeric FcγRIIa.
(**A and B**) Indirect ELISA using recombinant YU2 ΔV1V2V3V5 gp120 protein (0.25 µg/ml) with a total concentration of 1 µg/ml of primary antibodies. Antibody binding to gp120 was detected using either (**A**) biotin-tagged dimeric rsFcγRIIa H131 (0.1 µg/ml) or (**B**) biotin-tagged dimeric rsFcγRIIa R131 (0.1 µg/ml) followed by the addition of HRP-conjugated streptavidin. Error bars indicate means ± the SEM.

What is the mode of antibody-mediated Env endocytosis?

Studies in chapter 3 demonstrated the involvement of the GTPase dynamin in antibody-mediated Env internalization. Since dynamin is recruited to both clathrin-coated pits and caveolae, the endocytic route involved remains to be determined; future studies will require the use of either chemical or genetic approaches to answer this question. The chemical approach involves pre-treating infected cells with amantadine, an inhibitory compound against clathrin (423), and nystatin, a sterol-binding agent which disrupts caveolae (424), before measuring surface levels of antibody-Env complexes. The genetic approach would utilize RNA interference to silence caveolin-1 expression, and proteins involved in clathrin-coated pit formation, such as the clathrin light chain B, using a methodology established by our group to electroporate siRNA in primary CD4+ T cells (425). Knowing which endocytic pathway is utilized by antibody-Env complexes would aid in selecting clinically approved endocytic inhibitors for further testing, for example prochlorperazine that targets clathrin-dependent endocytosis (426).

More importantly, a direct link between antibody binding and Env endocytosis induction remains to be determined. Studies in chapters 3 and 4 measured decreases in surface levels of Env upon antibody addition and did not measure constitutive Env endocytosis. It remains to be determined if the phenotypes we report are intrinsic features of Env, or if they are uniquely antibody induced. It would be interesting to understand whether antibodies act only as a ligand/probe for internalization of different Env conformational states present in microdomains or if endocytic signalling cascades are initiated upon antibody binding to allow for internalization of immune complexes. Our results with slower internalization using antibody Fab fragments, perhaps due to a lack of Env crosslinking in chapter 3 help support the hypothesis of antibody-mediated internalization in this context. However, future experiments should include turnover assays by labelling cell-surface Env with dyes or other probes, such as biotin, to measure constitutive endocytosis versus antibody-induced internalization. Future experiments using single-cell RNA-sequencing will also be performed to measure any transcriptomic changes that may occur upon antibody binding and to concur putative signalling cascades. Results generated from these transcriptional assessments could

be beneficial in the design of targeted strategies, such as the use of signalling inhibitors or using siRNAs to target genes involved in endocytic pathways specifically within infected cells to enhance the overall surface levels of Env.

Would plant-produced PGT121 glycovariants have an impact *in vivo*?

Plant-produced monoclonal antibodies are being explored due to the easy of production, scalability, and low cost. Several plant-produced antibodies have been tested *in vivo* with animal models and in humans, with no adverse effects, such as the ZMapp cocktail produced in *N. benthamiana* for EBOV disease (427). However, it remains to be determined what would be the effect *in vivo* of using an afucosylated PGT121 in terms of decreasing the viral reservoir. PGT121 monotherapy was recently used in a phase 1 clinical trial and a single dose transiently inhibited RNA replication in viremic, infected individuals with sensitive viruses, and significantly decreased viral loads in these individuals. However, eventual resistance and rebound occurred when PGT121 serum levels were below the limit of detection (299). Testing the ability of afucosylated PGT121 to maintain viral suppression in the context of ART interruption, particularly with other glycoengineered bNAbs that can harness effector cells more effectively, would be of interest.

6.3 Towards an HIV-1 Cure

One appealing idea in the toolbox of the HIV cure and eradication field is the 'shock and kill' approach. As mentioned, this relies on the reactivation of viral gene replication in latently infected cells, followed by an immune-mediated clearing of these cells. All the studies presented in this thesis are presented with a broader objective of harnessing the humoral immune and effector cell response to eliminate infected cells. In other words, the work presented in this thesis aims to bring us one step closer towards a functional HIV-1 cure. The findings from chapter 2 were informative in designing a recently published *in vivo* study using the cocktail of CD4mc with anti-cluster A and anti-CoRBS Abs to decrease the established HIV-1 reservoir in humanized mice (279). This treatment significantly delayed viral rebound upon ART interruption and was shown to be dependent on Fc-effector functionalities, since the use of Fc-competent antibodies was significantly associated with lower CD4+ T cell-associated proviral DNA. Treatment strategies exploiting the use of nNAbs to clear latently infected cells will require the administration of CD4mc to 'open-up' the Env and expose their epitopes. In this regard, ongoing studies are evaluating this strategy in NHPs. Furthermore, advantages of the anti-CoRBS mAb/anti-cluster A mAb/CD4mc cocktail include the targeting of highly conserved epitopes within Env, mediation of potent ADCC, and viral neutralization.

Recent studies showed that treatment of acutely HIV-infected humanized mice with ART plus a mixture of bNAbs and LRAs led to a reduced frequency or a delay in viral rebound after all interventions were removed (428). Additionally, current ongoing clinical trials include the combination of bNAbs with LRAs to reactivate latently infected cells, induce viral replication, allow for the cell-surface expression of Env, and consequently recognition by antibodies (NCT03041012, NCT03803605).

However, the shock and kill strategy for a possible functional cure still faces several obstacles since strategies that require effector functionality of antibodies also depend on the availability and functionality of the effector cells within HIV-1-infected individuals. HIV infection and high viral loads are associated with an expansion of dysfunctional NK cell populations that lack most NK cell effector functions, including impaired cytotoxicity and poor ADCC

responses (429-431). Similarly, there is a dysregulation of monocyte subsets, with higher viral loads being associated with less phagocytic monocytes (432). Although, some studies have reported a recovery of functional NK cells among people living with ART (431). Moreover, no LRA to date has successfully perturbed the reservoir in human clinical trials. Some LRAs can also interfere with 'kill' strategies since they can affect NK cell functionality (433). Thus, alternate LRA approaches that not only reactivate viral replication, but also harbour immunomodulatory activities to boost innate immune activities, such as TLR7 and 9 agonists (NCT03837756) or IL-15 that is a potent enhancer of NK cells' cyotoxic functionality (434, 435), are currently being explored (436). Additionally, LRAs could be combined with other cytokines, such as IFN-α and IL-21, that can rescue or activate the effector functions of NK cells (437, 438). Type 1 IFN and IL-27 also enhances the level of cell surface Env available for ADCC responses in a BST-2 dependent manner (379, 439).

Findings from chapters 3 and 4 could be informative in the design of antibody-drug conjugates, where antibodies are engineered to be conjugated to cytotoxic 'payloads' that utilize receptor/antigen internalization for intracellular delivery. The cancer immunotherapy field is currently leading the way for this technology with clinically approved antibody-drug conjugates for various cancers (440). BNAbs that can recognize and bind a broad range of Env and induce faster rates of Env internalization could be useful in the design of these drug conjugates for targeted delivery within HIV-1-infected cells. HIV-specific antibody-drug conjugates already studied in the field to reduce the reservoir size utilized toxins from bacteria, siRNAs, and small molecule drugs (441). However, the use of these conjugates could be challenging in terms of eliminating HIV-1-infected cells, since they require antigen binding and internalization and thus, latent cells first need to be reactivated to express Env at the cell surface. Thus, using antibody-drug conjugates with LRA administration or upon ART interruption could clear reactivated cells, potentiating a 'kill'. Moreover, it would also be important to accurately map the trafficking pathways and fate of internalized immune complexes since most antibody-drug conjugates require a lysosomal cleavage to deliver the payload. However, in chapter 3, we observed that internalized bNAb-Env complexes

accumulated in intracellular compartments that were negative for the lysosomal marker Lamp1.

6.4 Concluding remarks

Through the work presented in this thesis we gain a new understanding of some overlooked factors that affect Fc-effector functions of Env-specific antibodies. We demonstrate the requirement of two or more antibody specificities to effectively engage with FcγRIIIa and activate effector cells. Furthermore, we show that antibody-induced Env internalization could potentially impede effector cell engagement. However, this could possibly be circumvented by modifying the Fc N-linked glycans of antibodies that induce Env internalization. Thus, we emphasize the benefits of afucosylated antibodies to enhance the engagement of FcγRIIIa and thus, ADCC against HIV-1-infected cells. We also demonstrate the benefits of using plant-based platforms for protein production and bNAb glycoengineering, mainly due to its low-cost and high-yield.

To summarize, modulating antibody functionality could be beneficial for therapeutic strategies against HIV and it is likely that a regimen involving the combination of ART, LRAs, and immunotherapies would be required to reduce the size of the viral reservoir. Taken together, findings from this thesis focused on understanding underlying factors that could modulate Fc-effector functionalities and optimizing them to potentially boost the 'kill' strategies. The application of the research presented here could be useful towards the development of a possible functional HIV-1 cure to hopefully improve the lives of more than 37 million HIV-infected individuals around the world.

REFERENCES

1. Antiretroviral Therapy Cohort C. 2008. Life expectancy of individuals on combination antiretroviral therapy in high-income countries: a collaborative analysis of 14 cohort studies. Lancet 372:293-9.
2. Baeten JM, Donnell D, Ndase P, Mugo NR, Campbell JD, Wangisi J, Tappero JW, Bukusi EA, Cohen CR, Katabira E, Ronald A, Tumwesigye E, Were E, Fife KH, Kiarie J, Farquhar C, John-Stewart G, Kakia A, Odoyo J, Mucunguzi A, Nakku-Joloba E, Twesigye R, Ngure K, Apaka C, Tamooh H, Gabona F, Mujugira A, Panteleeff D, Thomas KK, Kidoguchi L, Krows M, Revall J, Morrison S, Haugen H, Emmanuel-Ogier M, Ondrejcek L, Coombs RW, Frenkel L, Hendrix C, Bumpus NN, Bangsberg D, Haberer JE, Stevens WS, Lingappa JR, Celum C, Partners Pr EPST. 2012. Antiretroviral prophylaxis for HIV prevention in heterosexual men and women. N Engl J Med 367:399-410.
3. Weller S, Davis K. 2002. Condom effectiveness in reducing heterosexual HIV transmission. Cochrane Database Syst Rev doi:10.1002/14651858.CD003255:CD003255.
4. Lederman MM, Funderburg NT, Sekaly RP, Klatt NR, Hunt PW. 2013. Residual immune dysregulation syndrome in treated HIV infection. Adv Immunol 119:51-83.
5. Masur H, Michelis MA, Greene JB, Onorato I, Stouwe RA, Holzman RS, Wormser G, Brettman L, Lange M, Murray HW, Cunningham-Rundles S. 1981. An outbreak of community-acquired Pneumocystis carinii pneumonia: initial manifestation of cellular immune dysfunction. N Engl J Med 305:1431-8.
6. Gottlieb MS, Schroff R, Schanker HM, Weisman JD, Fan PT, Wolf RA, Saxon A. 1981. Pneumocystis carinii pneumonia and mucosal candidiasis in previously healthy homosexual men: evidence of a new acquired cellular immunodeficiency. N Engl J Med 305:1425-31.
7. Centers for Disease C. 1982. Acquired immune deficiency syndrome (AIDS): precautions for clinical and laboratory staffs. MMWR Morb Mortal Wkly Rep 31:577-80.
8. Barre-Sinoussi F, Chermann JC, Rey F, Nugeyre MT, Chamaret S, Gruest J, Dauguet C, Axler-Blin C, Vezinet-Brun F, Rouzioux C, Rozenbaum W, Montagnier L. 1983. Isolation of a T-lymphotropic retrovirus from a patient at risk for acquired immune deficiency syndrome (AIDS). Science 220:868-71.
9. Gallo RC, Sarin PS, Gelmann EP, Robert-Guroff M, Richardson E, Kalyanaraman VS, Mann D, Sidhu GD, Stahl RE, Zolla-Pazner S, Leibowitch J, Popovic M. 1983. Isolation of human T-cell leukemia virus in acquired immune deficiency syndrome (AIDS). Science 220:865-7.
10. Popovic M, Sarngadharan MG, Read E, Gallo RC. 1984. Detection, isolation, and continuous production of cytopathic retroviruses (HTLV-III) from patients with AIDS and pre-AIDS. Science 224:497-500.
11. Coffin J, Haase A, Levy JA, Montagnier L, Oroszlan S, Teich N, Temin H, Toyoshima K, Varmus H, Vogt P, et al. 1986. Human immunodeficiency viruses. Science 232:697.
12. Case K. 1986. Nomenclature: human immunodeficiency virus. Ann Intern Med 105:133.
13. Clavel F, Guetard D, Brun-Vezinet F, Chamaret S, Rey MA, Santos-Ferreira MO, Laurent AG, Dauguet C, Katlama C, Rouzioux C, et al. 1986. Isolation of a new human retrovirus from West African patients with AIDS. Science 233:343-6.
14. Sharp PM, Bailes E, Robertson DL, Gao F, Hahn BH. 1999. Origins and evolution of AIDS viruses. Biol Bull 196:338-42.

15. Campbell-Yesufu OT, Gandhi RT. 2011. Update on human immunodeficiency virus (HIV)-2 infection. Clin Infect Dis 52:780-7.
16. Baltimore D. 1970. RNA-dependent DNA polymerase in virions of RNA tumour viruses. Nature 226:1209-11.
17. Temin HM, Mizutani S. 1970. RNA-dependent DNA polymerase in virions of Rous sarcoma virus. Nature 226:1211-3.
18. Roques P, Robertson DL, Souquiere S, Apetrei C, Nerrienet E, Barre-Sinoussi F, Muller-Trutwin M, Simon F. 2004. Phylogenetic characteristics of three new HIV-1 N strains and implications for the origin of group N. AIDS 18:1371-81.
19. Simon F, Mauclere P, Roques P, Loussert-Ajaka I, Muller-Trutwin MC, Saragosti S, Georges-Courbot MC, Barre-Sinoussi F, Brun-Vezinet F. 1998. Identification of a new human immunodeficiency virus type 1 distinct from group M and group O. Nat Med 4:1032-7.
20. Vallari A, Holzmayer V, Harris B, Yamaguchi J, Ngansop C, Makamche F, Mbanya D, Kaptue L, Ndembi N, Gurtler L, Devare S, Brennan CA. 2011. Confirmation of putative HIV-1 group P in Cameroon. J Virol 85:1403-7.
21. McCutchan FE. 2000. Understanding the genetic diversity of HIV-1. AIDS 14 Suppl 3:S31-44.
22. Robertson DL, Anderson JP, Bradac JA, Carr JK, Foley B, Funkhouser RK, Gao F, Hahn BH, Kalish ML, Kuiken C, Learn GH, Leitner T, McCutchan F, Osmanov S, Peeters M, Pieniazek D, Salminen M, Sharp PM, Wolinsky S, Korber B. 2000. HIV-1 nomenclature proposal. Science 288:55-6.
23. McCutchan FE, Salminen MO, Carr JK, Burke DS. 1996. HIV-1 genetic diversity. AIDS 10 Suppl 3:S13-20.
24. Korber B, Gaschen B, Yusim K, Thakallapally R, Kesmir C, Detours V. 2001. Evolutionary and immunological implications of contemporary HIV-1 variation. Br Med Bull 58:19-42.
25. Taylor BS, Hammer SM. 2008. The challenge of HIV-1 subtype diversity. N Engl J Med 359:1965-6.
26. Keele BF, Van Heuverswyn F, Li Y, Bailes E, Takehisa J, Santiago ML, Bibollet-Ruche F, Chen Y, Wain LV, Liegeois F, Loul S, Ngole EM, Bienvenue Y, Delaporte E, Brookfield JF, Sharp PM, Shaw GM, Peeters M, Hahn BH. 2006. Chimpanzee reservoirs of pandemic and nonpandemic HIV-1. Science 313:523-6.
27. D'Arc M, Ayouba A, Esteban A, Learn GH, Boue V, Liegeois F, Etienne L, Tagg N, Leendertz FH, Boesch C, Madinda NF, Robbins MM, Gray M, Cournil A, Ooms M, Letko M, Simon VA, Sharp PM, Hahn BH, Delaporte E, Mpoudi Ngole E, Peeters M. 2015. Origin of the HIV-1 group O epidemic in western lowland gorillas. Proc Natl Acad Sci U S A 112:E1343-52.
28. Hirsch VM, Olmsted RA, Murphey-Corb M, Purcell RH, Johnson PR. 1989. An African primate lentivirus (SIVsm) closely related to HIV-2. Nature 339:389-92.
29. Chakrabarti L, Guyader M, Alizon M, Daniel MD, Desrosiers RC, Tiollais P, Sonigo P. 1987. Sequence of simian immunodeficiency virus from macaque and its relationship to other human and simian retroviruses. Nature 328:543-7.
30. Briggs JA, Wilk T, Welker R, Krausslich HG, Fuller SD. 2003. Structural organization of authentic, mature HIV-1 virions and cores. EMBO J 22:1707-15.

31. Zhu P, Chertova E, Bess J, Jr., Lifson JD, Arthur LO, Liu J, Taylor KA, Roux KH. 2003. Electron tomography analysis of envelope glycoprotein trimers on HIV and simian immunodeficiency virus virions. Proc Natl Acad Sci U S A 100:15812-7.
32. Alfadhli A, Barklis RL, Barklis E. 2009. HIV-1 matrix organizes as a hexamer of trimers on membranes containing phosphatidylinositol-(4,5)-bisphosphate. Virology 387:466-72.
33. Li S, Hill CP, Sundquist WI, Finch JT. 2000. Image reconstructions of helical assemblies of the HIV-1 CA protein. Nature 407:409-13.
34. Zhao G, Perilla JR, Yufenyuy EL, Meng X, Chen B, Ning J, Ahn J, Gronenborn AM, Schulten K, Aiken C, Zhang P. 2013. Mature HIV-1 capsid structure by cryo-electron microscopy and all-atom molecular dynamics. Nature 497:643-6.
35. Fouchier RA, Simon JH, Jaffe AB, Malim MH. 1996. Human immunodeficiency virus type 1 Vif does not influence expression or virion incorporation of gag-, pol-, and env-encoded proteins. J Virol 70:8263-9.
36. Paxton W, Connor RI, Landau NR. 1993. Incorporation of Vpr into human immunodeficiency virus type 1 virions: requirement for the p6 region of gag and mutational analysis. J Virol 67:7229-37.
37. Welker R, Harris M, Cardel B, Krausslich HG. 1998. Virion incorporation of human immunodeficiency virus type 1 Nef is mediated by a bipartite membrane-targeting signal: analysis of its role in enhancement of viral infectivity. J Virol 72:8833-40.
38. Summers MF, Karn J. 2011. Special issue: Structural and molecular biology of HIV. J Mol Biol 410:489-90.
39. Pereyra F, Jia X, McLaren PJ, Telenti A, de Bakker PI, Walker BD, Ripke S, Brumme CJ, Pulit SL, Carrington M, Kadie CM, Carlson JM, Heckerman D, Graham RR, Plenge RM, Deeks SG, Gianniny L, Crawford G, Sullivan J, Gonzalez E, Davies L, Camargo A, Moore JM, Beattie N, Gupta S, Crenshaw A, Burtt NP, Guiducci C, Gupta N, Gao X, Qi Y, Yuki Y, Piechocka-Trocha A, Cutrell E, Rosenberg R, Moss KL, Lemay P, O'Leary J, Schaefer T, Verma P, Toth I, Block B, Baker B, Rothchild A, Lian J, Proudfoot J, Alvino DM, Vine S, Addo MM, Allen TM, et al. 2010. The major genetic determinants of HIV-1 control affect HLA class I peptide presentation. Science 330:1551-7.
40. Reicin AS, Kalpana G, Paik S, Marmon S, Goff S. 1995. Sequences in the human immunodeficiency virus type 1 U3 region required for in vivo and in vitro integration. J Virol 69:5904-7.
41. Frankel AD, Young JA. 1998. HIV-1: fifteen proteins and an RNA. Annu Rev Biochem 67:1-25.
42. Freed EO. 1998. HIV-1 gag proteins: diverse functions in the virus life cycle. Virology 251:1-15.
43. Krausslich HG, Facke M, Heuser AM, Konvalinka J, Zentgraf H. 1995. The spacer peptide between human immunodeficiency virus capsid and nucleocapsid proteins is essential for ordered assembly and viral infectivity. J Virol 69:3407-19.
44. Decroly E, Vandenbranden M, Ruysschaert JM, Cogniaux J, Jacob GS, Howard SC, Marshall G, Kompelli A, Basak A, Jean F, et al. 1994. The convertases furin and PC1 can both cleave the human immunodeficiency virus (HIV)-1 envelope glycoprotein gp160 into gp120 (HIV-1 SU) and gp41 (HIV-I TM). J Biol Chem 269:12240-7.
45. Dalgleish AG, Beverley PC, Clapham PR, Crawford DH, Greaves MF, Weiss RA. 1984. The CD4 (T4) antigen is an essential component of the receptor for the AIDS retrovirus. Nature 312:763-7.

46. Klatzmann D, Champagne E, Chamaret S, Gruest J, Guetard D, Hercend T, Gluckman JC, Montagnier L. 1984. T-lymphocyte T4 molecule behaves as the receptor for human retrovirus LAV. Nature 312:767-8.
47. Feng Y, Broder CC, Kennedy PE, Berger EA. 1996. HIV-1 entry cofactor: functional cDNA cloning of a seven-transmembrane, G protein-coupled receptor. Science 272:872-7.
48. Alkhatib G, Combadiere C, Broder CC, Feng Y, Kennedy PE, Murphy PM, Berger EA. 1996. CC CKR5: a RANTES, MIP-1alpha, MIP-1beta receptor as a fusion cofactor for macrophage-tropic HIV-1. Science 272:1955-8.
49. Deng H, Liu R, Ellmeier W, Choe S, Unutmaz D, Burkhart M, Di Marzio P, Marmon S, Sutton RE, Hill CM, Davis CB, Peiper SC, Schall TJ, Littman DR, Landau NR. 1996. Identification of a major co-receptor for primary isolates of HIV-1. Nature 381:661-6.
50. Choe H, Farzan M, Sun Y, Sullivan N, Rollins B, Ponath PD, Wu L, Mackay CR, LaRosa G, Newman W, Gerard N, Gerard C, Sodroski J. 1996. The beta-chemokine receptors CCR3 and CCR5 facilitate infection by primary HIV-1 isolates. Cell 85:1135-48.
51. Doranz BJ, Rucker J, Yi Y, Smyth RJ, Samson M, Peiper SC, Parmentier M, Collman RG, Doms RW. 1996. A dual-tropic primary HIV-1 isolate that uses fusin and the beta-chemokine receptors CKR-5, CKR-3, and CKR-2b as fusion cofactors. Cell 85:1149-58.
52. Ugolini S, Mondor I, Sattentau QJ. 1999. HIV-1 attachment: another look. Trends Microbiol 7:144-9.
53. Sattentau QJ, Moore JP, Vignaux F, Traincard F, Poignard P. 1993. Conformational changes induced in the envelope glycoproteins of the human and simian immunodeficiency viruses by soluble receptor binding. J Virol 67:7383-93.
54. Thali M, Moore JP, Furman C, Charles M, Ho DD, Robinson J, Sodroski J. 1993. Characterization of conserved human immunodeficiency virus type 1 gp120 neutralization epitopes exposed upon gp120-CD4 binding. J Virol 67:3978-88.
55. Hwang SS, Boyle TJ, Lyerly HK, Cullen BR. 1992. Identification of envelope V3 loop as the major determinant of CD4 neutralization sensitivity of HIV-1. Science 257:535-7.
56. Furuta RA, Wild CT, Weng Y, Weiss CD. 1998. Capture of an early fusion-active conformation of HIV-1 gp41. Nat Struct Biol 5:276-9.
57. He Y, Vassell R, Zaitseva M, Nguyen N, Yang Z, Weng Y, Weiss CD. 2003. Peptides trap the human immunodeficiency virus type 1 envelope glycoprotein fusion intermediate at two sites. J Virol 77:1666-71.
58. Chan DC, Fass D, Berger JM, Kim PS. 1997. Core structure of gp41 from the HIV envelope glycoprotein. Cell 89:263-73.
59. Lu M, Blacklow SC, Kim PS. 1995. A trimeric structural domain of the HIV-1 transmembrane glycoprotein. Nat Struct Biol 2:1075-82.
60. Weissenhorn W, Dessen A, Harrison SC, Skehel JJ, Wiley DC. 1997. Atomic structure of the ectodomain from HIV-1 gp41. Nature 387:426-30.
61. Sarafianos SG, Marchand B, Das K, Himmel DM, Parniak MA, Hughes SH, Arnold E. 2009. Structure and function of HIV-1 reverse transcriptase: molecular mechanisms of polymerization and inhibition. J Mol Biol 385:693-713.
62. Jiang M, Mak J, Ladha A, Cohen E, Klein M, Rovinski B, Kleiman L. 1993. Identification of tRNAs incorporated into wild-type and mutant human immunodeficiency virus type 1. J Virol 67:3246-53.
63. Panganiban AT, Fiore D. 1988. Ordered interstrand and intrastrand DNA transfer during reverse transcription. Science 241:1064-9.

64. Hu WS, Temin HM. 1990. Genetic consequences of packaging two RNA genomes in one retroviral particle: pseudodiploidy and high rate of genetic recombination. Proc Natl Acad Sci U S A 87:1556-60.
65. Charneau P, Alizon M, Clavel F. 1992. A second origin of DNA plus-strand synthesis is required for optimal human immunodeficiency virus replication. J Virol 66:2814-20.
66. Charneau P, Mirambeau G, Roux P, Paulous S, Buc H, Clavel F. 1994. HIV-1 reverse transcription. A termination step at the center of the genome. J Mol Biol 241:651-62.
67. Zennou V, Petit C, Guetard D, Nerhbass U, Montagnier L, Charneau P. 2000. HIV-1 genome nuclear import is mediated by a central DNA flap. Cell 101:173-85.
68. Bukrinsky M. 2004. A hard way to the nucleus. Mol Med 10:1-5.
69. von Schwedler U, Kornbluth RS, Trono D. 1994. The nuclear localization signal of the matrix protein of human immunodeficiency virus type 1 allows the establishment of infection in macrophages and quiescent T lymphocytes. Proc Natl Acad Sci U S A 91:6992-6.
70. Heinzinger NK, Bukrinsky MI, Haggerty SA, Ragland AM, Kewalramani V, Lee MA, Gendelman HE, Ratner L, Stevenson M, Emerman M. 1994. The Vpr protein of human immunodeficiency virus type 1 influences nuclear localization of viral nucleic acids in nondividing host cells. Proc Natl Acad Sci U S A 91:7311-5.
71. Campbell EM, Hope TJ. 2015. HIV-1 capsid: the multifaceted key player in HIV-1 infection. Nat Rev Microbiol 13:471-83.
72. Mamede JI, Cianci GC, Anderson MR, Hope TJ. 2017. Early cytoplasmic uncoating is associated with infectivity of HIV-1. Proc Natl Acad Sci U S A 114:E7169-E7178.
73. Arhel NJ, Souquere-Besse S, Munier S, Souque P, Guadagnini S, Rutherford S, Prevost MC, Allen TD, Charneau P. 2007. HIV-1 DNA Flap formation promotes uncoating of the pre-integration complex at the nuclear pore. EMBO J 26:3025-37.
74. Selyutina A, Persaud M, Lee K, KewalRamani V, Diaz-Griffero F. 2020. Nuclear Import of the HIV-1 Core Precedes Reverse Transcription and Uncoating. Cell Rep 32:108201.
75. Burdick RC, Li C, Munshi M, Rawson JMO, Nagashima K, Hu WS, Pathak VK. 2020. HIV-1 uncoats in the nucleus near sites of integration. Proc Natl Acad Sci U S A 117:5486-5493.
76. Diaz-Griffero F, Kar A, Lee M, Stremlau M, Poeschla E, Sodroski J. 2007. Comparative requirements for the restriction of retrovirus infection by TRIM5alpha and TRIMCyp. Virology 369:400-10.
77. Dharan A, Bachmann N, Talley S, Zwikelmaier V, Campbell EM. 2020. Nuclear pore blockade reveals that HIV-1 completes reverse transcription and uncoating in the nucleus. Nat Microbiol 5:1088-1095.
78. Craigie R, Bushman FD. 2012. HIV DNA integration. Cold Spring Harb Perspect Med 2:a006890.
79. Delelis O, Carayon K, Saib A, Deprez E, Mouscadet JF. 2008. Integrase and integration: biochemical activities of HIV-1 integrase. Retrovirology 5:114.
80. Cherepanov P, Maertens G, Proost P, Devreese B, Van Beeumen J, Engelborghs Y, De Clercq E, Debyser Z. 2003. HIV-1 integrase forms stable tetramers and associates with LEDGF/p75 protein in human cells. J Biol Chem 278:372-81.
81. Brown PO, Bowerman B, Varmus HE, Bishop JM. 1989. Retroviral integration: structure of the initial covalent product and its precursor, and a role for the viral IN protein. Proc Natl Acad Sci U S A 86:2525-9.

82. Schroder AR, Shinn P, Chen H, Berry C, Ecker JR, Bushman F. 2002. HIV-1 integration in the human genome favors active genes and local hotspots. Cell 110:521-9.
83. Berkhout B, Jeang KT. 1992. Functional roles for the TATA promoter and enhancers in basal and Tat-induced expression of the human immunodeficiency virus type 1 long terminal repeat. J Virol 66:139-49.
84. Patarca R, Heath C, Goldenberg GJ, Rosen CA, Sodroski JG, Haseltine WA, Hansen UM. 1987. Transcription directed by the HIV long terminal repeat in vitro. AIDS Res Hum Retroviruses 3:41-55.
85. Li Y, Flanagan PM, Tschochner H, Kornberg RD. 1994. RNA polymerase II initiation factor interactions and transcription start site selection. Science 263:805-7.
86. Kim SY, Byrn R, Groopman J, Baltimore D. 1989. Temporal aspects of DNA and RNA synthesis during human immunodeficiency virus infection: evidence for differential gene expression. J Virol 63:3708-13.
87. Purcell DF, Martin MA. 1993. Alternative splicing of human immunodeficiency virus type 1 mRNA modulates viral protein expression, replication, and infectivity. J Virol 67:6365-78.
88. Selby MJ, Bain ES, Luciw PA, Peterlin BM. 1989. Structure, sequence, and position of the stem-loop in tar determine transcriptional elongation by tat through the HIV-1 long terminal repeat. Genes Dev 3:547-58.
89. Sodroski J, Patarca R, Rosen C, Wong-Staal F, Haseltine W. 1985. Location of the trans-activating region on the genome of human T-cell lymphotropic virus type III. Science 229:74-7.
90. Meredith LW, Sivakumaran H, Major L, Suhrbier A, Harrich D. 2009. Potent inhibition of HIV-1 replication by a Tat mutant. PLoS One 4:e7769.
91. Wei P, Garber ME, Fang SM, Fischer WH, Jones KA. 1998. A novel CDK9-associated C-type cyclin interacts directly with HIV-1 Tat and mediates its high-affinity, loop-specific binding to TAR RNA. Cell 92:451-62.
92. Rausch JW, Le Grice SF. 2015. HIV Rev Assembly on the Rev Response Element (RRE): A Structural Perspective. Viruses 7:3053-75.
93. Malim MH, Cullen BR. 1991. HIV-1 structural gene expression requires the binding of multiple Rev monomers to the viral RRE: implications for HIV-1 latency. Cell 65:241-8.
94. Neville M, Stutz F, Lee L, Davis LI, Rosbash M. 1997. The importin-beta family member Crm1p bridges the interaction between Rev and the nuclear pore complex during nuclear export. Curr Biol 7:767-75.
95. Doyon L, Payant C, Brakier-Gingras L, Lamarre D. 1998. Novel Gag-Pol frameshift site in human immunodeficiency virus type 1 variants resistant to protease inhibitors. J Virol 72:6146-50.
96. Ono A, Ablan SD, Lockett SJ, Nagashima K, Freed EO. 2004. Phosphatidylinositol (4,5) bisphosphate regulates HIV-1 Gag targeting to the plasma membrane. Proc Natl Acad Sci U S A 101:14889-94.
97. Resh MD. 2005. Intracellular trafficking of HIV-1 Gag: how Gag interacts with cell membranes and makes viral particles. AIDS Rev 7:84-91.
98. Aloia RC, Tian H, Jensen FC. 1993. Lipid composition and fluidity of the human immunodeficiency virus envelope and host cell plasma membranes. Proc Natl Acad Sci U S A 90:5181-5.

99. Brugger B, Glass B, Haberkant P, Leibrecht I, Wieland FT, Krausslich HG. 2006. The HIV lipidome: a raft with an unusual composition. Proc Natl Acad Sci U S A 103:2641-6.
100. Ono A, Freed EO. 2001. Plasma membrane rafts play a critical role in HIV-1 assembly and release. Proc Natl Acad Sci U S A 98:13925-30.
101. Brown DA, London E. 2000. Structure and function of sphingolipid- and cholesterol-rich membrane rafts. J Biol Chem 275:17221-4.
102. Brown DA, Rose JK. 1992. Sorting of GPI-anchored proteins to glycolipid-enriched membrane subdomains during transport to the apical cell surface. Cell 68:533-44.
103. Ono A, Freed EO. 2005. Role of lipid rafts in virus replication. Adv Virus Res 64:311-58.
104. Favard C, Chojnacki J, Merida P, Yandrapalli N, Mak J, Eggeling C, Muriaux D. 2019. HIV-1 Gag specifically restricts PI(4,5)P2 and cholesterol mobility in living cells creating a nanodomain platform for virus assembly. Sci Adv 5:eaaw8651.
105. De Guzman RN, Wu ZR, Stalling CC, Pappalardo L, Borer PN, Summers MF. 1998. Structure of the HIV-1 nucleocapsid protein bound to the SL3 psi-RNA recognition element. Science 279:384-8.
106. Freed EO. 2015. HIV-1 assembly, release and maturation. Nat Rev Microbiol 13:484-96.
107. Murakami T, Freed EO. 2000. The long cytoplasmic tail of gp41 is required in a cell type-dependent manner for HIV-1 envelope glycoprotein incorporation into virions. Proc Natl Acad Sci U S A 97:343-8.
108. Alfadhli A, Staubus AO, Tedbury PR, Novikova M, Freed EO, Barklis E. 2019. Analysis of HIV-1 Matrix-Envelope Cytoplasmic Tail Interactions. J Virol 93.
109. Pezeshkian N, Groves NS, van Engelenburg SB. 2019. Single-molecule imaging of HIV-1 envelope glycoprotein dynamics and Gag lattice association exposes determinants responsible for virus incorporation. Proc Natl Acad Sci U S A 116:25269-25277.
110. Bhattacharya J, Repik A, Clapham PR. 2006. Gag regulates association of human immunodeficiency virus type 1 envelope with detergent-resistant membranes. J Virol 80:5292-300.
111. Wilk T, Pfeiffer T, Bosch V. 1992. Retained in vitro infectivity and cytopathogenicity of HIV-1 despite truncation of the C-terminal tail of the env gene product. Virology 189:167-77.
112. von Schwedler UK, Stuchell M, Muller B, Ward DM, Chung HY, Morita E, Wang HE, Davis T, He GP, Cimbora DM, Scott A, Krausslich HG, Kaplan J, Morham SG, Sundquist WI. 2003. The protein network of HIV budding. Cell 114:701-13.
113. Pettit SC, Everitt LE, Choudhury S, Dunn BM, Kaplan AH. 2004. Initial cleavage of the human immunodeficiency virus type 1 GagPol precursor by its activated protease occurs by an intramolecular mechanism. J Virol 78:8477-85.
114. Konvalinka J, Krausslich HG, Muller B. 2015. Retroviral proteases and their roles in virion maturation. Virology 479-480:403-17.
115. Kirchhoff F, Greenough TC, Brettler DB, Sullivan JL, Desrosiers RC. 1995. Brief report: absence of intact nef sequences in a long-term survivor with nonprogressive HIV-1 infection. N Engl J Med 332:228-32.
116. Kestler HW, 3rd, Ringler DJ, Mori K, Panicali DL, Sehgal PK, Daniel MD, Desrosiers RC. 1991. Importance of the nef gene for maintenance of high virus loads and for development of AIDS. Cell 65:651-62.
117. Kirchhoff F, Schindler M, Specht A, Arhel N, Munch J. 2008. Role of Nef in primate lentiviral immunopathogenesis. Cell Mol Life Sci 65:2621-36.

118. Quaranta MG, Mattioli B, Giordani L, Viora M. 2009. Immunoregulatory effects of HIV-1 Nef protein. Biofactors 35:169-74.
119. Schwartz O, Dautry-Varsat A, Goud B, Marechal V, Subtil A, Heard JM, Danos O. 1995. Human immunodeficiency virus type 1 Nef induces accumulation of CD4 in early endosomes. J Virol 69:528-33.
120. Aiken C, Konner J, Landau NR, Lenburg ME, Trono D. 1994. Nef induces CD4 endocytosis: requirement for a critical dileucine motif in the membrane-proximal CD4 cytoplasmic domain. Cell 76:853-64.
121. daSilva LL, Sougrat R, Burgos PV, Janvier K, Mattera R, Bonifacino JS. 2009. Human immunodeficiency virus type 1 Nef protein targets CD4 to the multivesicular body pathway. J Virol 83:6578-90.
122. Schaefer MR, Wonderlich ER, Roeth JF, Leonard JA, Collins KL. 2008. HIV-1 Nef targets MHC-I and CD4 for degradation via a final common beta-COP-dependent pathway in T cells. PLoS Pathog 4:e1000131.
123. Raulet DH. 2003. Roles of the NKG2D immunoreceptor and its ligands. Nat Rev Immunol 3:781-90.
124. Cerboni C, Neri F, Casartelli N, Zingoni A, Cosman D, Rossi P, Santoni A, Doria M. 2007. Human immunodeficiency virus 1 Nef protein downmodulates the ligands of the activating receptor NKG2D and inhibits natural killer cell-mediated cytotoxicity. J Gen Virol 88:242-50.
125. Parsons MS, Richard J, Lee WS, Vanderven H, Grant MD, Finzi A, Kent SJ. 2016. NKG2D Acts as a Co-Receptor for Natural Killer Cell-Mediated Anti-HIV-1 Antibody-Dependent Cellular Cytotoxicity. AIDS Res Hum Retroviruses 32:1089-1096.
126. Usami Y, Wu Y, Gottlinger HG. 2015. SERINC3 and SERINC5 restrict HIV-1 infectivity and are counteracted by Nef. Nature 526:218-23.
127. Cullen BR. 2006. Role and mechanism of action of the APOBEC3 family of antiretroviral resistance factors. J Virol 80:1067-76.
128. Sheehy AM, Gaddis NC, Choi JD, Malim MH. 2002. Isolation of a human gene that inhibits HIV-1 infection and is suppressed by the viral Vif protein. Nature 418:646-50.
129. Suspene R, Sommer P, Henry M, Ferris S, Guetard D, Pochet S, Chester A, Navaratnam N, Wain-Hobson S, Vartanian JP. 2004. APOBEC3G is a single-stranded DNA cytidine deaminase and functions independently of HIV reverse transcriptase. Nucleic Acids Res 32:2421-9.
130. Stopak K, de Noronha C, Yonemoto W, Greene WC. 2003. HIV-1 Vif blocks the antiviral activity of APOBEC3G by impairing both its translation and intracellular stability. Mol Cell 12:591-601.
131. Yu X, Yu Y, Liu B, Luo K, Kong W, Mao P, Yu XF. 2003. Induction of APOBEC3G ubiquitination and degradation by an HIV-1 Vif-Cul5-SCF complex. Science 302:1056-60.
132. Borel S, Robert-Hebmann V, Alfaisal J, Jain A, Faure M, Espert L, Chaloin L, Paillart JC, Johansen T, Biard-Piechaczyk M. 2015. HIV-1 viral infectivity factor interacts with microtubule-associated protein light chain 3 and inhibits autophagy. AIDS 29:275-86.
133. Okumura A, Alce T, Lubyova B, Ezelle H, Strebel K, Pitha PM. 2008. HIV-1 accessory proteins VPR and Vif modulate antiviral response by targeting IRF-3 for degradation. Virology 373:85-97.

134. Yuan X, Matsuda Z, Matsuda M, Essex M, Lee TH. 1990. Human immunodeficiency virus vpr gene encodes a virion-associated protein. AIDS Res Hum Retroviruses 6:1265-71.
135. Bachand F, Yao XJ, Hrimech M, Rougeau N, Cohen EA. 1999. Incorporation of Vpr into human immunodeficiency virus type 1 requires a direct interaction with the p6 domain of the p55 gag precursor. J Biol Chem 274:9083-91.
136. Jenkins Y, McEntee M, Weis K, Greene WC. 1998. Characterization of HIV-1 vpr nuclear import: analysis of signals and pathways. J Cell Biol 143:875-85.
137. He J, Choe S, Walker R, Di Marzio P, Morgan DO, Landau NR. 1995. Human immunodeficiency virus type 1 viral protein R (Vpr) arrests cells in the G2 phase of the cell cycle by inhibiting p34cdc2 activity. J Virol 69:6705-11.
138. Yao XJ, Mouland AJ, Subbramanian RA, Forget J, Rougeau N, Bergeron D, Cohen EA. 1998. Vpr stimulates viral expression and induces cell killing in human immunodeficiency virus type 1-infected dividing Jurkat T cells. J Virol 72:4686-93.
139. Conti L, Rainaldi G, Matarrese P, Varano B, Rivabene R, Columba S, Sato A, Belardelli F, Malorni W, Gessani S. 1998. The HIV-1 vpr protein acts as a negative regulator of apoptosis in a human lymphoblastoid T cell line: possible implications for the pathogenesis of AIDS. J Exp Med 187:403-13.
140. Wang L, Mukherjee S, Jia F, Narayan O, Zhao LJ. 1995. Interaction of virion protein Vpr of human immunodeficiency virus type 1 with cellular transcription factor Sp1 and trans-activation of viral long terminal repeat. J Biol Chem 270:25564-9.
141. Ayyavoo V, Mahboubi A, Mahalingam S, Ramalingam R, Kudchodkar S, Williams WV, Green DR, Weiner DB. 1997. HIV-1 Vpr suppresses immune activation and apoptosis through regulation of nuclear factor kappa B. Nat Med 3:1117-23.
142. Richard J, Sindhu S, Pham TN, Belzile JP, Cohen EA. 2010. HIV-1 Vpr up-regulates expression of ligands for the activating NKG2D receptor and promotes NK cell-mediated killing. Blood 115:1354-63.
143. Miller CM, Akiyama H, Agosto LM, Emery A, Ettinger CR, Swanstrom RI, Henderson AJ, Gummuluru S. 2017. Virion-Associated Vpr Alleviates a Postintegration Block to HIV-1 Infection of Dendritic Cells. J Virol 91.
144. Nodder SB, Gummuluru S. 2019. Illuminating the Role of Vpr in HIV Infection of Myeloid Cells. Front Immunol 10:1606.
145. Maldarelli F, Chen MY, Willey RL, Strebel K. 1993. Human immunodeficiency virus type 1 Vpu protein is an oligomeric type I integral membrane protein. J Virol 67:5056-61.
146. Wray V, Federau T, Henklein P, Klabunde S, Kunert O, Schomburg D, Schubert U. 1995. Solution structure of the hydrophilic region of HIV-1 encoded virus protein U (Vpu) by CD and 1H NMR spectroscopy. Int J Pept Protein Res 45:35-43.
147. Strebel K, Klimkait T, Martin MA. 1988. A novel gene of HIV-1, vpu, and its 16-kilodalton product. Science 241:1221-3.
148. Schubert U, Henklein P, Boldyreff B, Wingender E, Strebel K, Porstmann T. 1994. The human immunodeficiency virus type 1 encoded Vpu protein is phosphorylated by casein kinase-2 (CK-2) at positions Ser52 and Ser56 within a predicted alpha-helix-turn-alpha-helix-motif. J Mol Biol 236:16-25.
149. Magadan JG, Perez-Victoria FJ, Sougrat R, Ye Y, Strebel K, Bonifacino JS. 2010. Multilayered mechanism of CD4 downregulation by HIV-1 Vpu involving distinct ER retention and ERAD targeting steps. PLoS Pathog 6:e1000869.

150. Neil SJ, Zang T, Bieniasz PD. 2008. Tetherin inhibits retrovirus release and is antagonized by HIV-1 Vpu. Nature 451:425-30.
151. Schubert U, Anton LC, Bacik I, Cox JH, Bour S, Bennink JR, Orlowski M, Strebel K, Yewdell JW. 1998. CD4 glycoprotein degradation induced by human immunodeficiency virus type 1 Vpu protein requires the function of proteasomes and the ubiquitin-conjugating pathway. J Virol 72:2280-8.
152. Van Damme N, Goff D, Katsura C, Jorgenson RL, Mitchell R, Johnson MC, Stephens EB, Guatelli J. 2008. The interferon-induced protein BST-2 restricts HIV-1 release and is downregulated from the cell surface by the viral Vpu protein. Cell Host Microbe 3:245-52.
153. Dube M, Paquay C, Roy BB, Bego MG, Mercier J, Cohen EA. 2011. HIV-1 Vpu antagonizes BST-2 by interfering mainly with the trafficking of newly synthesized BST-2 to the cell surface. Traffic 12:1714-29.
154. Mangeat B, Gers-Huber G, Lehmann M, Zufferey M, Luban J, Piguet V. 2009. HIV-1 Vpu neutralizes the antiviral factor Tetherin/BST-2 by binding it and directing its beta-TrCP2-dependent degradation. PLoS Pathog 5:e1000574.
155. Schmidt S, Fritz JV, Bitzegeio J, Fackler OT, Keppler OT. 2011. HIV-1 Vpu blocks recycling and biosynthetic transport of the intrinsic immunity factor CD317/tetherin to overcome the virion release restriction. mBio 2:e00036-11.
156. Weinelt J, Neil SJ. 2014. Differential sensitivities of tetherin isoforms to counteraction by primate lentiviruses. J Virol 88:5845-58.
157. Galao RP, Le Tortorec A, Pickering S, Kueck T, Neil SJ. 2012. Innate sensing of HIV-1 assembly by Tetherin induces NFkappaB-dependent proinflammatory responses. Cell Host Microbe 12:633-44.
158. Matusali G, Potesta M, Santoni A, Cerboni C, Doria M. 2012. The human immunodeficiency virus type 1 Nef and Vpu proteins downregulate the natural killer cell-activating ligand PVR. J Virol 86:4496-504.
159. Shah AH, Sowrirajan B, Davis ZB, Ward JP, Campbell EM, Planelles V, Barker E. 2010. Degranulation of natural killer cells following interaction with HIV-1-infected cells is hindered by downmodulation of NTB-A by Vpu. Cell Host Microbe 8:397-409.
160. Checkley MA, Luttge BG, Freed EO. 2011. HIV-1 envelope glycoprotein biosynthesis, trafficking, and incorporation. J Mol Biol 410:582-608.
161. Li Y, Luo L, Thomas DY, Kang CY. 1994. Control of expression, glycosylation, and secretion of HIV-1 gp120 by homologous and heterologous signal sequences. Virology 204:266-78.
162. McCune JM, Rabin LB, Feinberg MB, Lieberman M, Kosek JC, Reyes GR, Weissman IL. 1988. Endoproteolytic cleavage of gp160 is required for the activation of human immunodeficiency virus. Cell 53:55-67.
163. Zhang S, Nguyen HT, Ding H, Wang J, Zou S, Liu L, Guha D, Gabuzda D, Ho DD, Kappes JC, Sodroski J. 2021. Dual Pathways of Human Immunodeficiency Virus Type 1 Envelope Glycoprotein Trafficking Modulate the Selective Exclusion of Uncleaved Oligomers from Virions. J Virol 95.
164. Helseth E, Olshevsky U, Furman C, Sodroski J. 1991. Human immunodeficiency virus type 1 gp120 envelope glycoprotein regions important for association with the gp41 transmembrane glycoprotein. J Virol 65:2119-23.

165. Yang X, Mahony E, Holm GH, Kassa A, Sodroski J. 2003. Role of the gp120 inner domain beta-sandwich in the interaction between the human immunodeficiency virus envelope glycoprotein subunits. Virology 313:117-25.
166. Kwong PD, Doyle ML, Casper DJ, Cicala C, Leavitt SA, Majeed S, Steenbeke TD, Venturi M, Chaiken I, Fung M, Katinger H, Parren PW, Robinson J, Van Ryk D, Wang L, Burton DR, Freire E, Wyatt R, Sodroski J, Hendrickson WA, Arthos J. 2002. HIV-1 evades antibody-mediated neutralization through conformational masking of receptor-binding sites. Nature 420:678-82.
167. Burton DR, Mascola JR. 2015. Antibody responses to envelope glycoproteins in HIV-1 infection. Nat Immunol 16:571-6.
168. Kwong PD, Mascola JR. 2018. HIV-1 Vaccines Based on Antibody Identification, B Cell Ontogeny, and Epitope Structure. Immunity 48:855-871.
169. Steckbeck JD, Kuhlmann AS, Montelaro RC. 2013. C-terminal tail of human immunodeficiency virus gp41: functionally rich and structurally enigmatic. J Gen Virol 94:1-19.
170. Sanders RW, Derking R, Cupo A, Julien JP, Yasmeen A, de Val N, Kim HJ, Blattner C, de la Pena AT, Korzun J, Golabek M, de Los Reyes K, Ketas TJ, van Gils MJ, King CR, Wilson IA, Ward AB, Klasse PJ, Moore JP. 2013. A next-generation cleaved, soluble HIV-1 Env Trimer, BG505 SOSIP.664 gp140, expresses multiple epitopes for broadly neutralizing but not non-neutralizing antibodies. PLoS Pathog 9:e1003618.
171. Julien JP, Cupo A, Sok D, Stanfield RL, Lyumkis D, Deller MC, Klasse PJ, Burton DR, Sanders RW, Moore JP, Ward AB, Wilson IA. 2013. Crystal structure of a soluble cleaved HIV-1 envelope trimer. Science 342:1477-83.
172. Alsahafi N, Anand SP, Castillo-Menendez L, Verly MM, Medjahed H, Prévost J, Herschhorn A, Richard J, Schön A, Melillo B. 2018. SOSIP changes affect human immunodeficiency virus type 1 envelope glycoprotein conformation and CD4 engagement. Journal of virology 92:e01080-18.
173. Alsahafi N, Debbeche O, Sodroski J, Finzi A. 2015. Effects of the I559P gp41 change on the conformation and function of the human immunodeficiency virus (HIV-1) membrane envelope glycoprotein trimer. PLoS One 10:e0122111.
174. Lu M, Ma X, Castillo-Menendez LR, Gorman J, Alsahafi N, Ermel U, Terry DS, Chambers M, Peng D, Zhang B, Zhou T, Reichard N, Wang K, Grover JR, Carman BP, Gardner MR, Nikic-Spiegel I, Sugawara A, Arthos J, Lemke EA, Smith AB, 3rd, Farzan M, Abrams C, Munro JB, McDermott AB, Finzi A, Kwong PD, Blanchard SC, Sodroski JG, Mothes W. 2019. Associating HIV-1 envelope glycoprotein structures with states on the virus observed by smFRET. Nature 568:415-419.
175. Torrents de la Pena A, de Taeye SW, Sliepen K, LaBranche CC, Burger JA, Schermer EE, Montefiori DC, Moore JP, Klasse PJ, Sanders RW. 2018. Immunogenicity in Rabbits of HIV-1 SOSIP Trimers from Clades A, B, and C, Given Individually, Sequentially, or in Combination. J Virol 92.
176. Finzi A, Xiang SH, Pacheco B, Wang L, Haight J, Kassa A, Danek B, Pancera M, Kwong PD, Sodroski J. 2010. Topological layers in the HIV-1 gp120 inner domain regulate gp41 interaction and CD4-triggered conformational transitions. Mol Cell 37:656-67.
177. Santosuosso M, Righi E, Lindstrom V, Leblanc PR, Poznansky MC. 2009. HIV-1 envelope protein gp120 is present at high concentrations in secondary lymphoid organs of individuals with chronic HIV-1 infection. J Infect Dis 200:1050-3.

178. Oh SK, Cruikshank WW, Raina J, Blanchard GC, Adler WH, Walker J, Kornfeld H. 1992. Identification of HIV-1 envelope glycoprotein in the serum of AIDS and ARC patients. J Acquir Immune Defic Syndr 5:251-6.
179. Rychert J, Strick D, Bazner S, Robinson J, Rosenberg E. 2010. Detection of HIV gp120 in plasma during early HIV infection is associated with increased proinflammatory and immunoregulatory cytokines. AIDS Res Hum Retroviruses 26:1139-45.
180. Richard J, Veillette M, Ding S, Zoubchenok D, Alsahafi N, Coutu M, Brassard N, Park J, Courter JR, Melillo B, Smith AB, 3rd, Shaw GM, Hahn BH, Sodroski J, Kaufmann DE, Finzi A. 2016. Small CD4 Mimetics Prevent HIV-1 Uninfected Bystander CD4 + T Cell Killing Mediated by Antibody-dependent Cell-mediated Cytotoxicity. EBioMedicine 3:122-34.
181. Willey RL, Rutledge RA, Dias S, Folks T, Theodore T, Buckler CE, Martin MA. 1986. Identification of conserved and divergent domains within the envelope gene of the acquired immunodeficiency syndrome retrovirus. Proc Natl Acad Sci U S A 83:5038-42.
182. Bernstein HB, Tucker SP, Hunter E, Schutzbach JS, Compans RW. 1994. Human immunodeficiency virus type 1 envelope glycoprotein is modified by O-linked oligosaccharides. J Virol 68:463-8.
183. Montefiori DC, Robinson WE, Jr., Mitchell WM. 1988. Role of protein N-glycosylation in pathogenesis of human immunodeficiency virus type 1. Proc Natl Acad Sci U S A 85:9248-52.
184. Kwong PD, Wyatt R, Robinson J, Sweet RW, Sodroski J, Hendrickson WA. 1998. Structure of an HIV gp120 envelope glycoprotein in complex with the CD4 receptor and a neutralizing human antibody. Nature 393:648-59.
185. Wang WK, Dudek T, Essex M, Lee TH. 1999. Hypervariable region 3 residues of HIV type 1 gp120 involved in CCR5 coreceptor utilization: therapeutic and prophylactic implications. Proc Natl Acad Sci U S A 96:4558-62.
186. Carrillo A, Ratner L. 1996. Human immunodeficiency virus type 1 tropism for T-lymphoid cell lines: role of the V3 loop and C4 envelope determinants. J Virol 70:1301-9.
187. Olshevsky U, Helseth E, Furman C, Li J, Haseltine W, Sodroski J. 1990. Identification of individual human immunodeficiency virus type 1 gp120 amino acids important for CD4 receptor binding. J Virol 64:5701-7.
188. Freed EO, Myers DJ, Risser R. 1990. Characterization of the fusion domain of the human immunodeficiency virus type 1 envelope glycoprotein gp41. Proc Natl Acad Sci U S A 87:4650-4.
189. Salzwedel K, West JT, Hunter E. 1999. A conserved tryptophan-rich motif in the membrane-proximal region of the human immunodeficiency virus type 1 gp41 ectodomain is important for Env-mediated fusion and virus infectivity. J Virol 73:2469-80.
190. Zwick MB, Labrijn AF, Wang M, Spenlehauer C, Saphire EO, Binley JM, Moore JP, Stiegler G, Katinger H, Burton DR, Parren PW. 2001. Broadly neutralizing antibodies targeted to the membrane-proximal external region of human immunodeficiency virus type 1 glycoprotein gp41. J Virol 75:10892-905.
191. Gabuzda D, Olshevsky U, Bertani P, Haseltine WA, Sodroski J. 1991. Identification of membrane anchorage domains of the HIV-1 gp160 envelope glycoprotein precursor. J Acquir Immune Defic Syndr 4:34-40.

192. Lee SJ, Hu W, Fisher AG, Looney DJ, Kao VF, Mitsuya H, Ratner L, Wong-Staal F. 1989. Role of the carboxy-terminal portion of the HIV-1 transmembrane protein in viral transmission and cytopathogenicity. AIDS Res Hum Retroviruses 5:441-9.
193. Gabuzda DH, Lever A, Terwilliger E, Sodroski J. 1992. Effects of deletions in the cytoplasmic domain on biological functions of human immunodeficiency virus type 1 envelope glycoproteins. J Virol 66:3306-15.
194. Venable RM, Pastor RW, Brooks BR, Carson FW. 1989. Theoretically determined three-dimensional structures for amphipathic segments of the HIV-1 gp41 envelope protein. AIDS Res Hum Retroviruses 5:7-22.
195. Lee SF, Ko CY, Wang CT, Chen SS. 2002. Effect of point mutations in the N terminus of the lentivirus lytic peptide-1 sequence of human immunodeficiency virus type 1 transmembrane protein gp41 on Env stability. J Biol Chem 277:15363-75.
196. Bultmann A, Muranyi W, Seed B, Haas J. 2001. Identification of two sequences in the cytoplasmic tail of the human immunodeficiency virus type 1 envelope glycoprotein that inhibit cell surface expression. J Virol 75:5263-76.
197. Vincent N, Genin C, Malvoisin E. 2002. Identification of a conserved domain of the HIV-1 transmembrane protein gp41 which interacts with cholesteryl groups. Biochim Biophys Acta 1567:157-64.
198. Rowell JF, Stanhope PE, Siliciano RF. 1995. Endocytosis of endogenously synthesized HIV-1 envelope protein. Mechanism and role in processing for association with class II MHC. J Immunol 155:473-88.
199. Sauter MM, Pelchen-Matthews A, Bron R, Marsh M, LaBranche CC, Vance PJ, Romano J, Haggarty BS, Hart TK, Lee WM, Hoxie JA. 1996. An internalization signal in the simian immunodeficiency virus transmembrane protein cytoplasmic domain modulates expression of envelope glycoproteins on the cell surface. J Cell Biol 132:795-811.
200. Kirschman J, Qi M, Ding L, Hammonds J, Dienger-Stambaugh K, Wang JJ, Lapierre LA, Goldenring JR, Spearman P. 2018. HIV-1 Envelope Glycoprotein Trafficking through the Endosomal Recycling Compartment Is Required for Particle Incorporation. J Virol 92.
201. Groppelli E, Len AC, Granger LA, Jolly C. 2014. Retromer regulates HIV-1 envelope glycoprotein trafficking and incorporation into virions. PLoS Pathog 10:e1004518.
202. Boge M, Wyss S, Bonifacino JS, Thali M. 1998. A membrane-proximal tyrosine-based signal mediates internalization of the HIV-1 envelope glycoprotein via interaction with the AP-2 clathrin adaptor. J Biol Chem 273:15773-8.
203. Byland R, Vance PJ, Hoxie JA, Marsh M. 2007. A conserved dileucine motif mediates clathrin and AP-2-dependent endocytosis of the HIV-1 envelope protein. Mol Biol Cell 18:414-25.
204. Ohno H, Aguilar RC, Fournier MC, Hennecke S, Cosson P, Bonifacino JS. 1997. Interaction of endocytic signals from the HIV-1 envelope glycoprotein complex with members of the adaptor medium chain family. Virology 238:305-15.
205. Bhakta SJ, Shang L, Prince JL, Claiborne DT, Hunter E. 2011. Mutagenesis of tyrosine and di-leucine motifs in the HIV-1 envelope cytoplasmic domain results in a loss of Env-mediated fusion and infectivity. Retrovirology 8:37.
206. LaBranche CC, Sauter MM, Haggarty BS, Vance PJ, Romano J, Hart TK, Bugelski PJ, Marsh M, Hoxie JA. 1995. A single amino acid change in the cytoplasmic domain of the simian immunodeficiency virus transmembrane molecule increases envelope glycoprotein expression on infected cells. J Virol 69:5217-27.

207. von Bredow B, Arias JF, Heyer LN, Gardner MR, Farzan M, Rakasz EG, Evans DT. 2015. Envelope Glycoprotein Internalization Protects Human and Simian Immunodeficiency Virus-Infected Cells from Antibody-Dependent Cell-Mediated Cytotoxicity. J Virol 89:10648-55.
208. Praefcke GJ, McMahon HT. 2004. The dynamin superfamily: universal membrane tubulation and fission molecules? Nat Rev Mol Cell Biol 5:133-47.
209. Ferguson SM, De Camilli P. 2012. Dynamin, a membrane-remodelling GTPase. Nat Rev Mol Cell Biol 13:75-88.
210. Daumke O, Roux A, Haucke V. 2014. BAR domain scaffolds in dynamin-mediated membrane fission. Cell 156:882-92.
211. Pandey KN. 2009. Functional roles of short sequence motifs in the endocytosis of membrane receptors. Front Biosci (Landmark Ed) 14:5339-60.
212. Epand RM, Sayer BG, Epand RF. 2005. Caveolin scaffolding region and cholesterol-rich domains in membranes. J Mol Biol 345:339-50.
213. Subtil A, Gaidarov I, Kobylarz K, Lampson MA, Keen JH, McGraw TE. 1999. Acute cholesterol depletion inhibits clathrin-coated pit budding. Proc Natl Acad Sci U S A 96:6775-80.
214. Munro JB, Gorman J, Ma X, Zhou Z, Arthos J, Burton DR, Koff WC, Courter JR, Smith AB, 3rd, Kwong PD, Blanchard SC, Mothes W. 2014. Conformational dynamics of single HIV-1 envelope trimers on the surface of native virions. Science 346:759-63.
215. Herschhorn A, Ma X, Gu C, Ventura JD, Castillo-Menendez L, Melillo B, Terry DS, Smith AB, 3rd, Blanchard SC, Munro JB, Mothes W, Finzi A, Sodroski J. 2016. Release of gp120 Restraints Leads to an Entry-Competent Intermediate State of the HIV-1 Envelope Glycoproteins. MBio 7:doi:10.1128/mBio.01598-16.
216. Ma X, Lu M, Gorman J, Terry DS, Hong X, Zhou Z, Zhao H, Altman RB, Arthos J, Blanchard SC, Kwong PD, Munro JB, Mothes W. 2018. HIV-1 Env trimer opens through an asymmetric intermediate in which individual protomers adopt distinct conformations. Elife 7.
217. Kwon YD, Finzi A, Wu X, Dogo-Isonagie C, Lee LK, Moore LR, Schmidt SD, Stuckey J, Yang Y, Zhou T, Zhu J, Vicic DA, Debnath AK, Shapiro L, Bewley CA, Mascola JR, Sodroski JG, Kwong PD. 2012. Unliganded HIV-1 gp120 core structures assume the CD4-bound conformation with regulation by quaternary interactions and variable loops. Proc Natl Acad Sci U S A 109:5663-8.
218. Madani N, Schon A, Princiotto AM, Lalonde JM, Courter JR, Soeta T, Ng D, Wang L, Brower ET, Xiang SH, Do Kwon Y, Huang CC, Wyatt R, Kwong PD, Freire E, Smith AB, 3rd, Sodroski J. 2008. Small-molecule CD4 mimics interact with a highly conserved pocket on HIV-1 gp120. Structure 16:1689-701.
219. Xiang SH, Kwong PD, Gupta R, Rizzuto CD, Casper DJ, Wyatt R, Wang L, Hendrickson WA, Doyle ML, Sodroski J. 2002. Mutagenic stabilization and/or disruption of a CD4-bound state reveals distinct conformations of the human immunodeficiency virus type 1 gp120 envelope glycoprotein. J Virol 76:9888-99.
220. Prevost J, Zoubchenok D, Richard J, Veillette M, Pacheco B, Coutu M, Brassard N, Parsons MS, Ruxrungtham K, Bunupuradah T, Tovanabutra S, Hwang KK, Moody MA, Haynes BF, Bonsignori M, Sodroski J, Kaufmann DE, Shaw GM, Chenine AL, Finzi A. 2017. Influence of the Envelope gp120 Phe 43 Cavity on HIV-1 Sensitivity to Antibody-Dependent Cell-Mediated Cytotoxicity Responses. J Virol 91:e02452-16.

221. Schader SM, Colby-Germinario SP, Quashie PK, Oliveira M, Ibanescu RI, Moisi D, Mesplede T, Wainberg MA. 2012. HIV gp120 H375 is unique to HIV-1 subtype CRF01_AE and confers strong resistance to the entry inhibitor BMS-599793, a candidate microbicide drug. Antimicrob Agents Chemother 56:4257-67.
222. Edwards TG, Wyss S, Reeves JD, Zolla-Pazner S, Hoxie JA, Doms RW, Baribaud F. 2002. Truncation of the cytoplasmic domain induces exposure of conserved regions in the ectodomain of human immunodeficiency virus type 1 envelope protein. J Virol 76:2683-91.
223. Chen J, Kovacs JM, Peng H, Rits-Volloch S, Lu J, Park D, Zablowsky E, Seaman MS, Chen B. 2015. HIV-1 ENVELOPE. Effect of the cytoplasmic domain on antigenic characteristics of HIV-1 envelope glycoprotein. Science 349:191-5.
224. Campbell SM, Crowe SM, Mak J. 2002. Virion-associated cholesterol is critical for the maintenance of HIV-1 structure and infectivity. AIDS 16:2253-61.
225. Salimi H, Johnson J, Flores MG, Zhang MS, O'Malley Y, Houtman JC, Schlievert PM, Haim H. 2020. The lipid membrane of HIV-1 stabilizes the viral envelope glycoproteins and modulates their sensitivity to antibody neutralization. J Biol Chem 295:348-362.
226. Ablan S, Rawat SS, Viard M, Wang JM, Puri A, Blumenthal R. 2006. The role of cholesterol and sphingolipids in chemokine receptor function and HIV-1 envelope glycoprotein-mediated fusion. Virol J 3:104.
227. Graham DR, Chertova E, Hilburn JM, Arthur LO, Hildreth JE. 2003. Cholesterol depletion of human immunodeficiency virus type 1 and simian immunodeficiency virus with beta-cyclodextrin inactivates and permeabilizes the virions: evidence for virion-associated lipid rafts. J Virol 77:8237-48.
228. Melillo B, Liang S, Park J, Schon A, Courter JR, LaLonde JM, Wendler DJ, Princiotto AM, Seaman MS, Freire E, Sodroski J, Madani N, Hendrickson WA, Smith AB, 3rd. 2016. Small-Molecule CD4-Mimics: Structure-Based Optimization of HIV-1 Entry Inhibition. ACS Med Chem Lett 7:330-4.
229. Laumaea A, Smith AB, 3rd, Sodroski J, Finzi A. 2020. Opening the HIV envelope: potential of CD4 mimics as multifunctional HIV entry inhibitors. Curr Opin HIV AIDS 15:300-308.
230. Madani N, Princiotto AM, Zhao C, Jahanbakhshsefidi F, Mertens M, Herschhorn A, Melillo B, Smith AB, 3rd, Sodroski J. 2017. Activation and Inactivation of Primary Human Immunodeficiency Virus Envelope Glycoprotein Trimers by CD4-Mimetic Compounds. J Virol 91.
231. Madani N, Princiotto AM, Easterhoff D, Bradley T, Luo K, Williams WB, Liao HX, Moody MA, Phad GE, Vazquez Bernat N, Melillo B, Santra S, Smith AB, 3rd, Karlsson Hedestam GB, Haynes B, Sodroski J. 2016. Antibodies Elicited by Multiple Envelope Glycoprotein Immunogens in Primates Neutralize Primary Human Immunodeficiency Viruses (HIV-1) Sensitized by CD4-Mimetic Compounds. J Virol 90:5031-46.
232. Richard J, Veillette M, Brassard N, Iyer SS, Roger M, Martin L, Pazgier M, Schon A, Freire E, Routy JP, Smith AB, 3rd, Park J, Jones DM, Courter JR, Melillo BN, Kaufmann DE, Hahn BH, Permar SR, Haynes BF, Madani N, Sodroski JG, Finzi A. 2015. CD4 mimetics sensitize HIV-1-infected cells to ADCC. Proc Natl Acad Sci U S A 112:E2687-94.
233. Alsahafi N, Bakouche N, Kazemi M, Richard J, Ding S, Bhattacharyya S, Das D, Anand SP, Prévost J, Tolbert WD, Lu H, Medjahed H, Gendron-Lepage G, Ortega Delgado GG,

Kirk S, Melillo B, Mothes W, Sodroski J, Smith AB, 3rd, Kaufmann DE, Wu X, Pazgier M, Rouiller I, Finzi A, Munro JB. 2019. An Asymmetric Opening of HIV-1 Envelope Mediates Antibody-Dependent Cellular Cytotoxicity. Cell Host Microbe 25:578-587.e5.
234. Shaw GM, Hunter E. 2012. HIV transmission. Cold Spring Harb Perspect Med 2.
235. Joseph SB, Swanstrom R, Kashuba AD, Cohen MS. 2015. Bottlenecks in HIV-1 transmission: insights from the study of founder viruses. Nat Rev Microbiol 13:414-25.
236. Keele BF, Giorgi EE, Salazar-Gonzalez JF, Decker JM, Pham KT, Salazar MG, Sun C, Grayson T, Wang S, Li H, Wei X, Jiang C, Kirchherr JL, Gao F, Anderson JA, Ping LH, Swanstrom R, Tomaras GD, Blattner WA, Goepfert PA, Kilby JM, Saag MS, Delwart EL, Busch MP, Cohen MS, Montefiori DC, Haynes BF, Gaschen B, Athreya GS, Lee HY, Wood N, Seoighe C, Perelson AS, Bhattacharya T, Korber BT, Hahn BH, Shaw GM. 2008. Identification and characterization of transmitted and early founder virus envelopes in primary HIV-1 infection. Proc Natl Acad Sci U S A 105:7552-7.
237. Fenton-May AE, Dibben O, Emmerich T, Ding H, Pfafferott K, Aasa-Chapman MM, Pellegrino P, Williams I, Cohen MS, Gao F, Shaw GM, Hahn BH, Ochsenbauer C, Kappes JC, Borrow P. 2013. Relative resistance of HIV-1 founder viruses to control by interferon-alpha. Retrovirology 10:146.
238. Parrish NF, Gao F, Li H, Giorgi EE, Barbian HJ, Parrish EH, Zajic L, Iyer SS, Decker JM, Kumar A, Hora B, Berg A, Cai F, Hopper J, Denny TN, Ding H, Ochsenbauer C, Kappes JC, Galimidi RP, West AP, Jr., Bjorkman PJ, Wilen CB, Doms RW, O'Brien M, Bhardwaj N, Borrow P, Haynes BF, Muldoon M, Theiler JP, Korber B, Shaw GM, Hahn BH. 2013. Phenotypic properties of transmitted founder HIV-1. Proc Natl Acad Sci U S A 110:6626-33.
239. Cooper DA, Gold J, Maclean P, Donovan B, Finlayson R, Barnes TG, Michelmore HM, Brooke P, Penny R. 1985. Acute AIDS retrovirus infection. Definition of a clinical illness associated with seroconversion. Lancet 1:537-40.
240. Daar ES, Moudgil T, Meyer RD, Ho DD. 1991. Transient high levels of viremia in patients with primary human immunodeficiency virus type 1 infection. N Engl J Med 324:961-4.
241. Brenchley JM, Schacker TW, Ruff LE, Price DA, Taylor JH, Beilman GJ, Nguyen PL, Khoruts A, Larson M, Haase AT, Douek DC. 2004. CD4+ T cell depletion during all stages of HIV disease occurs predominantly in the gastrointestinal tract. J Exp Med 200:749-59.
242. Finzi D, Hermankova M, Pierson T, Carruth LM, Buck C, Chaisson RE, Quinn TC, Chadwick K, Margolick J, Brookmeyer R, Gallant J, Markowitz M, Ho DD, Richman DD, Siliciano RF. 1997. Identification of a reservoir for HIV-1 in patients on highly active antiretroviral therapy. Science 278:1295-300.
243. Chomont N, El-Far M, Ancuta P, Trautmann L, Procopio FA, Yassine-Diab B, Boucher G, Boulassel MR, Ghattas G, Brenchley JM, Schacker TW, Hill BJ, Douek DC, Routy JP, Haddad EK, Sekaly RP. 2009. HIV reservoir size and persistence are driven by T cell survival and homeostatic proliferation. Nat Med 15:893-900.
244. Ho DD, Neumann AU, Perelson AS, Chen W, Leonard JM, Markowitz M. 1995. Rapid turnover of plasma virions and CD4 lymphocytes in HIV-1 infection. Nature 373:123-6.
245. McDonald RA, Mayers DL, Chung RC, Wagner KF, Ratto-Kim S, Birx DL, Michael NL. 1997. Evolution of human immunodeficiency virus type 1 env sequence variation in patients with diverse rates of disease progression and T-cell function. J Virol 71:1871-9.
246. Grossman Z, Meier-Schellersheim M, Paul WE, Picker LJ. 2006. Pathogenesis of HIV infection: what the virus spares is as important as what it destroys. Nat Med 12:289-95.

247. Doitsh G, Greene WC. 2016. Dissecting How CD4 T Cells Are Lost During HIV Infection. Cell Host Microbe 19:280-91.
248. Cummins NW, Badley AD. 2010. Mechanisms of HIV-associated lymphocyte apoptosis: 2010. Cell Death Dis 1:e99.
249. Koup RA, Safrit JT, Cao Y, Andrews CA, McLeod G, Borkowsky W, Farthing C, Ho DD. 1994. Temporal association of cellular immune responses with the initial control of viremia in primary human immunodeficiency virus type 1 syndrome. J Virol 68:4650-5.
250. Li CJ, Friedman DJ, Wang C, Metelev V, Pardee AB. 1995. Induction of apoptosis in uninfected lymphocytes by HIV-1 Tat protein. Science 268:429-31.
251. Westendorp MO, Frank R, Ochsenbauer C, Stricker K, Dhein J, Walczak H, Debatin KM, Krammer PH. 1995. Sensitization of T cells to CD95-mediated apoptosis by HIV-1 Tat and gp120. Nature 375:497-500.
252. Anonymous. 1992. 1993 revised classification system for HIV infection and expanded surveillance case definition for AIDS among adolescents and adults. MMWR Recomm Rep 41:1-19.
253. Okulicz JF, Marconi VC, Landrum ML, Wegner S, Weintrob A, Ganesan A, Hale B, Crum-Cianflone N, Delmar J, Barthel V, Quinnan G, Agan BK, Dolan MJ, Infectious Disease Clinical Research Program HIVWG. 2009. Clinical outcomes of elite controllers, viremic controllers, and long-term nonprogressors in the US Department of Defense HIV natural history study. J Infect Dis 200:1714-23.
254. Deeks SG, Walker BD. 2007. Human immunodeficiency virus controllers: mechanisms of durable virus control in the absence of antiretroviral therapy. Immunity 27:406-16.
255. Fischl MA, Richman DD, Grieco MH, Gottlieb MS, Volberding PA, Laskin OL, Leedom JM, Groopman JE, Mildvan D, Schooley RT, et al. 1987. The efficacy of azidothymidine (AZT) in the treatment of patients with AIDS and AIDS-related complex. A double-blind, placebo-controlled trial. N Engl J Med 317:185-91.
256. Larder BA, Kemp SD. 1989. Multiple mutations in HIV-1 reverse transcriptase confer high-level resistance to zidovudine (AZT). Science 246:1155-8.
257. Pau AK, George JM. 2014. Antiretroviral therapy: current drugs. Infect Dis Clin North Am 28:371-402.
258. Martin AR, Siliciano RF. 2016. Progress Toward HIV Eradication: Case Reports, Current Efforts, and the Challenges Associated with Cure. Annu Rev Med 67:215-28.
259. Harrigan PR, Whaley M, Montaner JS. 1999. Rate of HIV-1 RNA rebound upon stopping antiretroviral therapy. AIDS 13:F59-62.
260. Haynes BF, Gilbert PB, McElrath MJ, Zolla-Pazner S, Tomaras GD, Alam SM, Evans DT, Montefiori DC, Karnasuta C, Sutthent R, Liao HX, DeVico AL, Lewis GK, Williams C, Pinter A, Fong Y, Janes H, DeCamp A, Huang Y, Rao M, Billings E, Karasavvas N, Robb ML, Ngauy V, de Souza MS, Paris R, Ferrari G, Bailer RT, Soderberg KA, Andrews C, Berman PW, Frahm N, De Rosa SC, Alpert MD, Yates NL, Shen X, Koup RA, Pitisuttithum P, Kaewkungwal J, Nitayaphan S, Rerks-Ngarm S, Michael NL, Kim JH. 2012. Immune-correlates analysis of an HIV-1 vaccine efficacy trial. N Engl J Med 366:1275-86.
261. Karnasuta C, Akapirat S, Madnote S, Savadsuk H, Puangkaew J, Rittiroongrad S, Rerks-Ngarm S, Nitayaphan S, Pitisuttithum P, Kaewkungwal J, Tartaglia J, Sinangil F, Francis DP, Robb ML, de Souza MS, Michael NL, Excler JL, Kim JH, O'Connell RJ, Karasavvas

N. 2017. Comparison of Antibody Responses Induced by RV144, VAX003, and VAX004 Vaccination Regimens. AIDS Res Hum Retroviruses 33:410-423.
262. McElrath MJ, De Rosa SC, Moodie Z, Dubey S, Kierstead L, Janes H, Defawe OD, Carter DK, Hural J, Akondy R, Buchbinder SP, Robertson MN, Mehrotra DV, Self SG, Corey L, Shiver JW, Casimiro DR, Step Study Protocol T. 2008. HIV-1 vaccine-induced immunity in the test-of-concept Step Study: a case-cohort analysis. Lancet 372:1894-1905.
263. Gray GE, Allen M, Moodie Z, Churchyard G, Bekker LG, Nchabeleng M, Mlisana K, Metch B, de Bruyn G, Latka MH, Roux S, Mathebula M, Naicker N, Ducar C, Carter DK, Puren A, Eaton N, McElrath MJ, Robertson M, Corey L, Kublin JG, team HPs. 2011. Safety and efficacy of the HVTN 503/Phambili study of a clade-B-based HIV-1 vaccine in South Africa: a double-blind, randomised, placebo-controlled test-of-concept phase 2b study. Lancet Infect Dis 11:507-15.
264. de Souza MS, Ratto-Kim S, Chuenarom W, Schuetz A, Chantakulkij S, Nuntapinit B, Valencia-Micolta A, Thelian D, Nitayaphan S, Pitisuttithum P, Paris RM, Kaewkungwal J, Michael NL, Rerks-Ngarm S, Mathieson B, Marovich M, Currier JR, Kim JH, Ministry of Public Health-Thai AVEGC. 2012. The Thai phase III trial (RV144) vaccine regimen induces T cell responses that preferentially target epitopes within the V2 region of HIV-1 envelope. J Immunol 188:5166-76.
265. Hammer SM, Sobieszczyk ME, Janes H, Karuna ST, Mulligan MJ, Grove D, Koblin BA, Buchbinder SP, Keefer MC, Tomaras GD, Frahm N, Hural J, Anude C, Graham BS, Enama ME, Adams E, DeJesus E, Novak RM, Frank I, Bentley C, Ramirez S, Fu R, Koup RA, Mascola JR, Nabel GJ, Montefiori DC, Kublin J, McElrath MJ, Corey L, Gilbert PB, Team HS. 2013. Efficacy trial of a DNA/rAd5 HIV-1 preventive vaccine. N Engl J Med 369:2083-92.
266. Adepoju P. 2020. Moving on from the failed HIV vaccine clinical trial. Lancet HIV 7:e161.
267. Dahabieh MS, Battivelli E, Verdin E. 2015. Understanding HIV latency: the road to an HIV cure. Annu Rev Med 66:407-21.
268. Gupta RK, Abdul-Jawad S, McCoy LE, Mok HP, Peppa D, Salgado M, Martinez-Picado J, Nijhuis M, Wensing AMJ, Lee H, Grant P, Nastouli E, Lambert J, Pace M, Salasc F, Monit C, Innes AJ, Muir L, Waters L, Frater J, Lever AML, Edwards SG, Gabriel IH, Olavarria E. 2019. HIV-1 remission following CCR5Delta32/Delta32 haematopoietic stem-cell transplantation. Nature 568:244-248.
269. Hutter G, Nowak D, Mossner M, Ganepola S, Mussig A, Allers K, Schneider T, Hofmann J, Kucherer C, Blau O, Blau IW, Hofmann WK, Thiel E. 2009. Long-term control of HIV by CCR5 Delta32/Delta32 stem-cell transplantation. N Engl J Med 360:692-8.
270. Verheyen J, Thielen A, Lubke N, Dirks M, Widera M, Dittmer U, Kordelas L, Daumer M, de Jong DCM, Wensing AMJ, Kaiser R, Nijhuis M, Esser S. 2019. Rapid Rebound of a Preexisting CXCR4-tropic Human Immunodeficiency Virus Variant After Allogeneic Transplantation With CCR5 Delta32 Homozygous Stem Cells. Clin Infect Dis 68:684-687.
271. Gutierrez C, Serrano-Villar S, Madrid-Elena N, Perez-Elias MJ, Martin ME, Barbas C, Ruiperez J, Munoz E, Munoz-Fernandez MA, Castor T, Moreno S. 2016. Bryostatin-1 for latent virus reactivation in HIV-infected patients on antiretroviral therapy. AIDS 30:1385-92.
272. Rasmussen TA, Tolstrup M, Brinkmann CR, Olesen R, Erikstrup C, Solomon A, Winckelmann A, Palmer S, Dinarello C, Buzon M, Lichterfeld M, Lewin SR, Ostergaard L, Sogaard OS. 2014. Panobinostat, a histone deacetylase inhibitor, for latent-virus

reactivation in HIV-infected patients on suppressive antiretroviral therapy: a phase 1/2, single group, clinical trial. Lancet HIV 1:e13-21.
273. Kessing CF, Nixon CC, Li C, Tsai P, Takata H, Mousseau G, Ho PT, Honeycutt JB, Fallahi M, Trautmann L, Garcia JV, Valente ST. 2017. In Vivo Suppression of HIV Rebound by Didehydro-Cortistatin A, a "Block-and-Lock" Strategy for HIV-1 Treatment. Cell Rep 21:600-611.
274. Vargas B, Giacobbi NS, Sanyal A, Venkatachari NJ, Han F, Gupta P, Sluis-Cremer N. 2019. Inhibitors of Signaling Pathways That Block Reversal of HIV-1 Latency. Antimicrob Agents Chemother 63.
275. Saez-Cirion A, Bacchus C, Hocqueloux L, Avettand-Fenoel V, Girault I, Lecuroux C, Potard V, Versmisse P, Melard A, Prazuck T, Descours B, Guergnon J, Viard JP, Boufassa F, Lambotte O, Goujard C, Meyer L, Costagliola D, Venet A, Pancino G, Autran B, Rouzioux C, Group AVS. 2013. Post-treatment HIV-1 controllers with a long-term virological remission after the interruption of early initiated antiretroviral therapy ANRS VISCONTI Study. PLoS Pathog 9:e1003211.
276. Luzuriaga K, Gay H, Ziemniak C, Sanborn KB, Somasundaran M, Rainwater-Lovett K, Mellors JW, Rosenbloom D, Persaud D. 2015. Viremic relapse after HIV-1 remission in a perinatally infected child. N Engl J Med 372:786-8.
277. Madani N, Princiotto AM, Mach L, Ding S, Prevost J, Richard J, Hora B, Sutherland L, Zhao CA, Conn BP, Bradley T, Moody MA, Melillo B, Finzi A, Haynes BF, Smith Iii AB, Santra S, Sodroski J. 2018. A CD4-mimetic compound enhances vaccine efficacy against stringent immunodeficiency virus challenge. Nat Commun 9:2363.
278. Hatziioannou T, Evans DT. 2012. Animal models for HIV/AIDS research. Nat Rev Microbiol 10:852-67.
279. Rajashekar JK, Richard J, Beloor J, Prevost J, Anand SP, Beaudoin-Bussieres G, Shan L, Herndler-Brandstetter D, Gendron-Lepage G, Medjahed H, Bourassa C, Gaudette F, Ullah I, Symmes K, Peric A, Lindemuth E, Bibollet-Ruche F, Park J, Chen HC, Kaufmann DE, Hahn BH, Sodroski J, Pazgier M, Flavell RA, Smith AB, 3rd, Finzi A, Kumar P. 2021. Modulating HIV-1 envelope glycoprotein conformation to decrease the HIV-1 reservoir. Cell Host Microbe 29:904-916 e6.
280. Tomaras GD, Yates NL, Liu P, Qin L, Fouda GG, Chavez LL, Decamp AC, Parks RJ, Ashley VC, Lucas JT, Cohen M, Eron J, Hicks CB, Liao HX, Self SG, Landucci G, Forthal DN, Weinhold KJ, Keele BF, Hahn BH, Greenberg ML, Morris L, Karim SS, Blattner WA, Montefiori DC, Shaw GM, Perelson AS, Haynes BF. 2008. Initial B-cell responses to transmitted human immunodeficiency virus type 1: virion-binding immunoglobulin M (IgM) and IgG antibodies followed by plasma anti-gp41 antibodies with ineffective control of initial viremia. J Virol 82:12449-63.
281. Davis KL, Gray ES, Moore PL, Decker JM, Salomon A, Montefiori DC, Graham BS, Keefer MC, Pinter A, Morris L, Hahn BH, Shaw GM. 2009. High titer HIV-1 V3-specific antibodies with broad reactivity but low neutralizing potency in acute infection and following vaccination. Virology 387:414-26.
282. Wei X, Decker JM, Wang S, Hui H, Kappes JC, Wu X, Salazar-Gonzalez JF, Salazar MG, Kilby JM, Saag MS, Komarova NL, Nowak MA, Hahn BH, Kwong PD, Shaw GM. 2003. Antibody neutralization and escape by HIV-1. Nature 422:307-12.
283. Gray ES, Madiga MC, Hermanus T, Moore PL, Wibmer CK, Tumba NL, Werner L, Mlisana K, Sibeko S, Williamson C, Abdool Karim SS, Morris L. 2011. The neutralization

breadth of HIV-1 develops incrementally over four years and is associated with CD4+ T cell decline and high viral load during acute infection. J Virol 85:4828-40.
284. Schroeder HW, Jr., Cavacini L. 2010. Structure and function of immunoglobulins. J Allergy Clin Immunol 125:S41-52.
285. Ugolini S, Mondor I, Parren PW, Burton DR, Tilley SA, Klasse PJ, Sattentau QJ. 1997. Inhibition of virus attachment to CD4+ target cells is a major mechanism of T cell line-adapted HIV-1 neutralization. J Exp Med 186:1287-98.
286. Frey G, Peng H, Rits-Volloch S, Morelli M, Cheng Y, Chen B. 2008. A fusion-intermediate state of HIV-1 gp41 targeted by broadly neutralizing antibodies. Proc Natl Acad Sci U S A 105:3739-44.
287. Sok D, Burton DR. 2018. Recent progress in broadly neutralizing antibodies to HIV. Nat Immunol 19:1179-1188.
288. Seabright GE, Doores KJ, Burton DR, Crispin M. 2019. Protein and Glycan Mimicry in HIV Vaccine Design. J Mol Biol 431:2223-2247.
289. Hraber P, Seaman MS, Bailer RT, Mascola JR, Montefiori DC, Korber BT. 2014. Prevalence of broadly neutralizing antibody responses during chronic HIV-1 infection. AIDS 28:163-9.
290. Gruell H, Klein F. 2014. Opening Fronts in HIV Vaccine Development: Tracking the development of broadly neutralizing antibodies. Nat Med 20:478-9.
291. Barouch DH, Whitney JB, Moldt B, Klein F, Oliveira TY, Liu J, Stephenson KE, Chang HW, Shekhar K, Gupta S, Nkolola JP, Seaman MS, Smith KM, Borducchi EN, Cabral C, Smith JY, Blackmore S, Sanisetty S, Perry JR, Beck M, Lewis MG, Rinaldi W, Chakraborty AK, Poignard P, Nussenzweig MC, Burton DR. 2013. Therapeutic efficacy of potent neutralizing HIV-1-specific monoclonal antibodies in SHIV-infected rhesus monkeys. Nature 503:224-8.
292. Bournazos S, Klein F, Pietzsch J, Seaman MS, Nussenzweig MC, Ravetch JV. 2014. Broadly neutralizing anti-HIV-1 antibodies require Fc effector functions for in vivo activity. Cell 158:1243-1253.
293. Shingai M, Nishimura Y, Klein F, Mouquet H, Donau OK, Plishka R, Buckler-White A, Seaman M, Piatak M, Jr., Lifson JD, Dimitrov DS, Nussenzweig MC, Martin MA. 2013. Antibody-mediated immunotherapy of macaques chronically infected with SHIV suppresses viraemia. Nature 503:277-80.
294. Horwitz JA, Halper-Stromberg A, Mouquet H, Gitlin AD, Tretiakova A, Eisenreich TR, Malbec M, Gravemann S, Billerbeck E, Dorner M, Buning H, Schwartz O, Knops E, Kaiser R, Seaman MS, Wilson JM, Rice CM, Ploss A, Bjorkman PJ, Klein F, Nussenzweig MC. 2013. HIV-1 suppression and durable control by combining single broadly neutralizing antibodies and antiretroviral drugs in humanized mice. Proc Natl Acad Sci U S A 110:16538-43.
295. Ledgerwood JE, Coates EE, Yamshchikov G, Saunders JG, Holman L, Enama ME, DeZure A, Lynch RM, Gordon I, Plummer S, Hendel CS, Pegu A, Conan-Cibotti M, Sitar S, Bailer RT, Narpala S, McDermott A, Louder M, O'Dell S, Mohan S, Pandey JP, Schwartz RM, Hu Z, Koup RA, Capparelli E, Mascola JR, Graham BS, Team VRCS. 2015. Safety, pharmacokinetics and neutralization of the broadly neutralizing HIV-1 human monoclonal antibody VRC01 in healthy adults. Clin Exp Immunol 182:289-301.
296. Caskey M, Klein F, Lorenzi JC, Seaman MS, West AP, Jr., Buckley N, Kremer G, Nogueira L, Braunschweig M, Scheid JF, Horwitz JA, Shimeliovich I, Ben-Avraham S,

Witmer-Pack M, Platten M, Lehmann C, Burke LA, Hawthorne T, Gorelick RJ, Walker BD, Keler T, Gulick RM, Fatkenheuer G, Schlesinger SJ, Nussenzweig MC. 2015. Viraemia suppressed in HIV-1-infected humans by broadly neutralizing antibody 3BNC117. Nature 522:487-91.

297. Caskey M, Schoofs T, Gruell H, Settler A, Karagounis T, Kreider EF, Murrell B, Pfeifer N, Nogueira L, Oliveira TY, Learn GH, Cohen YZ, Lehmann C, Gillor D, Shimeliovich I, Unson-O'Brien C, Weiland D, Robles A, Kummerle T, Wyen C, Levin R, Witmer-Pack M, Eren K, Ignacio C, Kiss S, West AP, Jr., Mouquet H, Zingman BS, Gulick RM, Keler T, Bjorkman PJ, Seaman MS, Hahn BH, Fatkenheuer G, Schlesinger SJ, Nussenzweig MC, Klein F. 2017. Antibody 10-1074 suppresses viremia in HIV-1-infected individuals. Nat Med 23:185-191.
298. Gaudinski MR, Houser KV, Doria-Rose NA, Chen GL, Rothwell RSS, Berkowitz N, Costner P, Holman LA, Gordon IJ, Hendel CS, Kaltovich F, Conan-Cibotti M, Gomez Lorenzo M, Carter C, Sitar S, Carlton K, Gall J, Laurencot C, Lin BC, Bailer RT, McDermott AB, Ko SY, Pegu A, Kwon YD, Kwong PD, Namboodiri AM, Pandey JP, Schwartz R, Arnold F, Hu Z, Zhang L, Huang Y, Koup RA, Capparelli EV, Graham BS, Mascola JR, Ledgerwood JE, team VRCs. 2019. Safety and pharmacokinetics of broadly neutralising human monoclonal antibody VRC07-523LS in healthy adults: a phase 1 dose-escalation clinical trial. Lancet HIV 6:e667-e679.
299. Stephenson KE, Julg B, Tan CS, Zash R, Walsh SR, Rolle CP, Monczor AN, Lupo S, Gelderblom HC, Ansel JL, Kanjilal DG, Maxfield LF, Nkolola J, Borducchi EN, Abbink P, Liu J, Peter L, Chandrashekar A, Nityanandam R, Lin Z, Setaro A, Sapiente J, Chen Z, Sunner L, Cassidy T, Bennett C, Sato A, Mayer B, Perelson AS, deCamp A, Priddy FH, Wagh K, Giorgi EE, Yates NL, Arduino RC, DeJesus E, Tomaras GD, Seaman MS, Korber B, Barouch DH. 2021. Safety, pharmacokinetics and antiviral activity of PGT121, a broadly neutralizing monoclonal antibody against HIV-1: a randomized, placebo-controlled, phase 1 clinical trial. Nat Med doi:10.1038/s41591-021-01509-0.
300. Klein F, Halper-Stromberg A, Horwitz JA, Gruell H, Scheid JF, Bournazos S, Mouquet H, Spatz LA, Diskin R, Abadir A, Zang T, Dorner M, Billerbeck E, Labitt RN, Gaebler C, Marcovecchio PM, Incesu RB, Eisenreich TR, Bieniasz PD, Seaman MS, Bjorkman PJ, Ravetch JV, Ploss A, Nussenzweig MC. 2012. HIV therapy by a combination of broadly neutralizing antibodies in humanized mice. Nature 492:118-22.
301. Bar-On Y, Gruell H, Schoofs T, Pai JA, Nogueira L, Butler AL, Millard K, Lehmann C, Suarez I, Oliveira TY, Karagounis T, Cohen YZ, Wyen C, Scholten S, Handl L, Belblidia S, Dizon JP, Vehreschild JJ, Witmer-Pack M, Shimeliovich I, Jain K, Fiddike K, Seaton KE, Yates NL, Horowitz J, Gulick RM, Pfeifer N, Tomaras GD, Seaman MS, Fatkenheuer G, Caskey M, Klein F, Nussenzweig MC. 2018. Safety and antiviral activity of combination HIV-1 broadly neutralizing antibodies in viremic individuals. Nat Med 24:1701-1707.
302. Corey L, Gilbert PB, Juraska M, Montefiori DC, Morris L, Karuna ST, Edupuganti S, Mgodi NM, deCamp AC, Rudnicki E, Huang Y, Gonzales P, Cabello R, Orrell C, Lama JR, Laher F, Lazarus EM, Sanchez J, Frank I, Hinojosa J, Sobieszczyk ME, Marshall KE, Mukwekwerere PG, Makhema J, Baden LR, Mullins JI, Williamson C, Hural J, McElrath MJ, Bentley C, Takuva S, Gomez Lorenzo MM, Burns DN, Espy N, Randhawa AK, Kochar N, Piwowar-Manning E, Donnell DJ, Sista N, Andrew P, Kublin JG, Gray G, Ledgerwood JE, Mascola JR, Cohen MS, Hvtn H, Teams HHS. 2021. Two Randomized

Trials of Neutralizing Antibodies to Prevent HIV-1 Acquisition. N Engl J Med 384:1003-1014.
303. Haim H, Salas I, McGee K, Eichelberger N, Winter E, Pacheco B, Sodroski J. 2013. Modeling virus- and antibody-specific factors to predict human immunodeficiency virus neutralization efficiency. Cell Host Microbe 14:547-58.
304. Burton DR, Desrosiers RC, Doms RW, Koff WC, Kwong PD, Moore JP, Nabel GJ, Sodroski J, Wilson IA, Wyatt RT. 2004. HIV vaccine design and the neutralizing antibody problem. Nat Immunol 5:233-6.
305. Wang P, Gajjar MR, Yu J, Padte NN, Gettie A, Blanchard JL, Russell-Lodrigue K, Liao LE, Perelson AS, Huang Y, Ho DD. 2020. Quantifying the contribution of Fc-mediated effector functions to the antiviral activity of anti-HIV-1 IgG1 antibodies in vivo. Proc Natl Acad Sci U S A 117:18002-18009.
306. Richard J, Prevost J, Alsahafi N, Ding S, Finzi A. 2018. Impact of HIV-1 Envelope Conformation on ADCC Responses. Trends Microbiol 26:253-265.
307. Hessell AJ, Hangartner L, Hunter M, Havenith CE, Beurskens FJ, Bakker JM, Lanigan CM, Landucci G, Forthal DN, Parren PW, Marx PA, Burton DR. 2007. Fc receptor but not complement binding is important in antibody protection against HIV. Nature 449:101-4.
308. Baum LL, Cassutt KJ, Knigge K, Khattri R, Margolick J, Rinaldo C, Kleeberger CA, Nishanian P, Henrard DR, Phair J. 1996. HIV-1 gp120-specific antibody-dependent cell-mediated cytotoxicity correlates with rate of disease progression. J Immunol 157:2168-73.
309. Lu CL, Murakowski DK, Bournazos S, Schoofs T, Sarkar D, Halper-Stromberg A, Horwitz JA, Nogueira L, Golijanin J, Gazumyan A, Ravetch JV, Caskey M, Chakraborty AK, Nussenzweig MC. 2016. Enhanced clearance of HIV-1-infected cells by broadly neutralizing antibodies against HIV-1 in vivo. Science 352:1001-4.
310. Milligan C, Richardson BA, John-Stewart G, Nduati R, Overbaugh J. 2015. Passively acquired antibody-dependent cellular cytotoxicity (ADCC) activity in HIV-infected infants is associated with reduced mortality. Cell Host Microbe 17:500-6.
311. Thomas AS, Moreau Y, Jiang W, Isaac JE, Ewing A, White LF, Kourtis AP, Sagar M. 2021. Pre-existing infant antibody-dependent cellular cytotoxicity associates with reduced HIV-1 acquisition and lower morbidity. Cell Reports Medicine 2:100412.
312. Forthal DN, Landucci G, Haubrich R, Keenan B, Kuppermann BD, Tilles JG, Kaplan J. 1999. Antibody-dependent cellular cytotoxicity independently predicts survival in severely immunocompromised human immunodeficiency virus-infected patients. J Infect Dis 180:1338-41.
313. Ferrari G, Pollara J, Kozink D, Harms T, Drinker M, Freel S, Moody MA, Alam SM, Tomaras GD, Ochsenbauer C, Kappes JC, Shaw GM, Hoxie JA, Robinson JE, Haynes BF. 2011. An HIV-1 gp120 envelope human monoclonal antibody that recognizes a C1 conformational epitope mediates potent antibody-dependent cellular cytotoxicity (ADCC) activity and defines a common ADCC epitope in human HIV-1 serum. J Virol 85:7029-36.
314. Acharya P, Tolbert WD, Gohain N, Wu X, Yu L, Liu T, Huang W, Huang CC, Kwon YD, Louder RK, Luongo TS, McLellan JS, Pancera M, Yang Y, Zhang B, Flinko R, Foulke JS, Jr., Sajadi MM, Kamin-Lewis R, Robinson JE, Martin L, Kwong PD, Guan Y, DeVico AL, Lewis GK, Pazgier M. 2014. Structural definition of an antibody-dependent cellular cytotoxicity response implicated in reduced risk for HIV-1 infection. J Virol 88:12895-906.

315. Veillette M, Desormeaux A, Medjahed H, Gharsallah NE, Coutu M, Baalwa J, Guan Y, Lewis G, Ferrari G, Hahn BH, Haynes BF, Robinson JE, Kaufmann DE, Bonsignori M, Sodroski J, Finzi A. 2014. Interaction with cellular CD4 exposes HIV-1 envelope epitopes targeted by antibody-dependent cell-mediated cytotoxicity. J Virol 88:2633-44.
316. Bruhns P, Jonsson F. 2015. Mouse and human FcR effector functions. Immunol Rev 268:25-51.
317. Nimmerjahn F, Ravetch JV. 2008. Fcgamma receptors as regulators of immune responses. Nat Rev Immunol 8:34-47.
318. Bournazos S, DiLillo DJ, Ravetch JV. 2015. The role of Fc-FcgammaR interactions in IgG-mediated microbial neutralization. J Exp Med 212:1361-9.
319. Nimmerjahn F, Ravetch JV. 2005. Divergent immunoglobulin g subclass activity through selective Fc receptor binding. Science 310:1510-2.
320. Pyzik M, Sand KMK, Hubbard JJ, Andersen JT, Sandlie I, Blumberg RS. 2019. The Neonatal Fc Receptor (FcRn): A Misnomer? Front Immunol 10:1540.
321. Ravetch JV, Bolland S. 2001. IgG Fc receptors. Annu Rev Immunol 19:275-90.
322. Fauriat C, Long EO, Ljunggren HG, Bryceson YT. 2010. Regulation of human NK-cell cytokine and chemokine production by target cell recognition. Blood 115:2167-76.
323. Lanier LL. 2008. Up on the tightrope: natural killer cell activation and inhibition. Nat Immunol 9:495-502.
324. Oliva A, Kinter AL, Vaccarezza M, Rubbert A, Catanzaro A, Moir S, Monaco J, Ehler L, Mizell S, Jackson R, Li Y, Romano JW, Fauci AS. 1998. Natural killer cells from human immunodeficiency virus (HIV)-infected individuals are an important source of CC-chemokines and suppress HIV-1 entry and replication in vitro. J Clin Invest 102:223-31.
325. Alter G, Malenfant JM, Altfeld M. 2004. CD107a as a functional marker for the identification of natural killer cell activity. J Immunol Methods 294:15-22.
326. de Saint Basile G, Menasche G, Fischer A. 2010. Molecular mechanisms of biogenesis and exocytosis of cytotoxic granules. Nat Rev Immunol 10:568-79.
327. Bots M, Medema JP. 2006. Granzymes at a glance. J Cell Sci 119:5011-4.
328. Hogarth PM, Pietersz GA. 2012. Fc receptor-targeted therapies for the treatment of inflammation, cancer and beyond. Nat Rev Drug Discov 11:311-31.
329. Helmy KY, Katschke KJ, Jr., Gorgani NN, Kljavin NM, Elliott JM, Diehl L, Scales SJ, Ghilardi N, van Lookeren Campagne M. 2006. CRIg: a macrophage complement receptor required for phagocytosis of circulating pathogens. Cell 124:915-27.
330. van Egmond M, Vidarsson G, Bakema JE. 2015. Cross-talk between pathogen recognizing Toll-like receptors and immunoglobulin Fc receptors in immunity. Immunol Rev 268:311-27.
331. Sorman A, Zhang L, Ding Z, Heyman B. 2014. How antibodies use complement to regulate antibody responses. Mol Immunol 61:79-88.
332. Lee CH, Romain G, Yan W, Watanabe M, Charab W, Todorova B, Lee J, Triplett K, Donkor M, Lungu OI, Lux A, Marshall N, Lindorfer MA, Goff OR, Balbino B, Kang TH, Tanno H, Delidakis G, Alford C, Taylor RP, Nimmerjahn F, Varadarajan N, Bruhns P, Zhang YJ, Georgiou G. 2017. IgG Fc domains that bind C1q but not effector Fcgamma receptors delineate the importance of complement-mediated effector functions. Nat Immunol 18:889-898.
333. Lux A, Yu X, Scanlan CN, Nimmerjahn F. 2013. Impact of immune complex size and glycosylation on IgG binding to human FcgammaRs. J Immunol 190:4315-23.

334. Taborda CP, Rivera J, Zaragoza O, Casadevall A. 2003. More is not necessarily better: prozone-like effects in passive immunization with IgG. J Immunol 170:3621-30.
335. Ding S, Veillette M, Coutu M, Prevost J, Scharf L, Bjorkman PJ, Ferrari G, Robinson JE, Sturzel C, Hahn BH, Sauter D, Kirchhoff F, Lewis GK, Pazgier M, Finzi A. 2015. A Highly Conserved Residue of the HIV-1 gp120 Inner Domain Is Important for Antibody-Dependent Cellular Cytotoxicity Responses Mediated by Anti-cluster A Antibodies. J Virol 90:2127-34.
336. Richard J, Pacheco B, Gohain N, Veillette M, Ding S, Alsahafi N, Tolbert WD, Prevost J, Chapleau JP, Coutu M, Jia M, Brassard N, Park J, Courter JR, Melillo B, Martin L, Tremblay C, Hahn BH, Kaufmann DE, Wu X, Smith AB, 3rd, Sodroski J, Pazgier M, Finzi A. 2016. Co-receptor Binding Site Antibodies Enable CD4-Mimetics to Expose Conserved Anti-cluster A ADCC Epitopes on HIV-1 Envelope Glycoproteins. EBioMedicine 12:208-218.
337. Anand SP, Prévost J, Baril S, Richard J, Medjahed H, Chapleau J-P, Tolbert WD, Kirk S, Smith AB, Wines BD. 2018. Two families of Env antibodies efficiently engage Fc-gamma receptors and eliminate HIV-1-infected cells. Journal of Virology:JVI. 01823-18.
338. Strohmeier GR, Brunkhorst BA, Seetoo KF, Bernardo J, Weil GJ, Simons ER. 1995. Neutrophil functional responses depend on immune complex valency. J Leukoc Biol 58:403-14.
339. Wines BD, Billings H, McLean MR, Kent SJ, Hogarth PM. 2017. Antibody Functional Assays as Measures of Fc Receptor-Mediated Immunity to HIV - New Technologies and their Impact on the HIV Vaccine Field. Curr HIV Res 15:202-215.
340. Tolbert WD, Sherburn R, Gohain N, Ding S, Flinko R, Orlandi C, Ray K, Finzi A, Lewis GK, Pazgier M. 2020. Defining rules governing recognition and Fc-mediated effector functions to the HIV-1 co-receptor binding site. BMC Biol 18:91.
341. Ahmed AA, Keremane SR, Vielmetter J, Bjorkman PJ. 2016. Structural characterization of GASDALIE Fc bound to the activating Fc receptor FcgammaRIIIa. J Struct Biol 194:78-89.
342. Saunders KO. 2019. Conceptual Approaches to Modulating Antibody Effector Functions and Circulation Half-Life. Front Immunol 10:1296.
343. Keeler SP, Fox JM. 2021. Requirement of Fc-Fc Gamma Receptor Interaction for Antibody-Based Protection against Emerging Virus Infections. Viruses 13.
344. Zalevsky J, Chamberlain AK, Horton HM, Karki S, Leung IW, Sproule TJ, Lazar GA, Roopenian DC, Desjarlais JR. 2010. Enhanced antibody half-life improves in vivo activity. Nat Biotechnol 28:157-9.
345. Dall'Acqua WF, Woods RM, Ward ES, Palaszynski SR, Patel NK, Brewah YA, Wu H, Kiener PA, Langermann S. 2002. Increasing the affinity of a human IgG1 for the neonatal Fc receptor: biological consequences. J Immunol 169:5171-80.
346. Forthal DN, Landucci G, Bream J, Jacobson LP, Phan TB, Montoya B. 2007. FcgammaRIIa genotype predicts progression of HIV infection. J Immunol 179:7916-23.
347. French MA, Tanaskovic S, Law MG, Lim A, Fernandez S, Ward LD, Kelleher AD, Emery S. 2010. Vaccine-induced IgG2 anti-HIV p24 is associated with control of HIV in patients with a 'high-affinity' FcgammaRIIa genotype. AIDS 24:1983-90.
348. Spiro RG. 2002. Protein glycosylation: nature, distribution, enzymatic formation, and disease implications of glycopeptide bonds. Glycobiology 12:43R-56R.

349. Arnold JN, Wormald MR, Sim RB, Rudd PM, Dwek RA. 2007. The impact of glycosylation on the biological function and structure of human immunoglobulins. Annu Rev Immunol 25:21-50.
350. Jefferis R. 2009. Glycosylation of antibody therapeutics: optimisation for purpose. Methods Mol Biol 483:223-38.
351. Anonymous. 2015. *In* rd, Varki A, Cummings RD, Esko JD, Stanley P, Hart GW, Aebi M, Darvill AG, Kinoshita T, Packer NH, Prestegard JH, Schnaar RL, Seeberger PH (ed), Essentials of Glycobiology, Cold Spring Harbor (NY).
352. Irvine EB, Alter G. 2020. Understanding the role of antibody glycosylation through the lens of severe viral and bacterial diseases. Glycobiology 30:241-253.
353. Jennewein MF, Alter G. 2017. The Immunoregulatory Roles of Antibody Glycosylation. Trends Immunol 38:358-372.
354. Ferrara C, Grau S, Jager C, Sondermann P, Brunker P, Waldhauer I, Hennig M, Ruf A, Rufer AC, Stihle M, Umana P, Benz J. 2011. Unique carbohydrate-carbohydrate interactions are required for high affinity binding between FcgammaRIII and antibodies lacking core fucose. Proc Natl Acad Sci U S A 108:12669-74.
355. Ferrara C, Stuart F, Sondermann P, Brunker P, Umana P. 2006. The carbohydrate at FcgammaRIIIa Asn-162. An element required for high affinity binding to non-fucosylated IgG glycoforms. J Biol Chem 281:5032-6.
356. Shields RL, Lai J, Keck R, O'Connell LY, Hong K, Meng YG, Weikert SH, Presta LG. 2002. Lack of fucose on human IgG1 N-linked oligosaccharide improves binding to human Fcgamma RIII and antibody-dependent cellular toxicity. J Biol Chem 277:26733-40.
357. Shinkawa T, Nakamura K, Yamane N, Shoji-Hosaka E, Kanda Y, Sakurada M, Uchida K, Anazawa H, Satoh M, Yamasaki M, Hanai N, Shitara K. 2003. The absence of fucose but not the presence of galactose or bisecting N-acetylglucosamine of human IgG1 complex-type oligosaccharides shows the critical role of enhancing antibody-dependent cellular cytotoxicity. J Biol Chem 278:3466-73.
358. Mizushima T, Yagi H, Takemoto E, Shibata-Koyama M, Isoda Y, Iida S, Masuda K, Satoh M, Kato K. 2011. Structural basis for improved efficacy of therapeutic antibodies on defucosylation of their Fc glycans. Genes Cells 16:1071-80.
359. Yamane-Ohnuki N, Kinoshita S, Inoue-Urakubo M, Kusunoki M, Iida S, Nakano R, Wakitani M, Niwa R, Sakurada M, Uchida K, Shitara K, Satoh M. 2004. Establishment of FUT8 knockout Chinese hamster ovary cells: an ideal host cell line for producing completely defucosylated antibodies with enhanced antibody-dependent cellular cytotoxicity. Biotechnol Bioeng 87:614-22.
360. Davies J, Jiang L, Pan LZ, LaBarre MJ, Anderson D, Reff M. 2001. Expression of GnTIII in a recombinant anti-CD20 CHO production cell line: Expression of antibodies with altered glycoforms leads to an increase in ADCC through higher affinity for FC gamma RIII. Biotechnol Bioeng 74:288-94.
361. Heyl KA, Karsten CM, Slevogt H. 2016. Galectin-3 binds highly galactosylated IgG1 and is crucial for the IgG1 complex mediated inhibition of C5aReceptor induced immune responses. Biochem Biophys Res Commun 479:86-90.
362. Thomann M, Reckermann K, Reusch D, Prasser J, Tejada ML. 2016. Fc-galactosylation modulates antibody-dependent cellular cytotoxicity of therapeutic antibodies. Mol Immunol 73:69-75.

363. Chung AW, Crispin M, Pritchard L, Robinson H, Gorny MK, Yu X, Bailey-Kellogg C, Ackerman ME, Scanlan C, Zolla-Pazner S, Alter G. 2014. Identification of antibody glycosylation structures that predict monoclonal antibody Fc-effector function. AIDS 28:2523-30.
364. Kaneko Y, Nimmerjahn F, Ravetch JV. 2006. Anti-inflammatory activity of immunoglobulin G resulting from Fc sialylation. Science 313:670-3.
365. Anthony RM, Ravetch JV. 2010. A novel role for the IgG Fc glycan: the anti-inflammatory activity of sialylated IgG Fcs. J Clin Immunol 30 Suppl 1:S9-14.
366. Scallon BJ, Tam SH, McCarthy SG, Cai AN, Raju TS. 2007. Higher levels of sialylated Fc glycans in immunoglobulin G molecules can adversely impact functionality. Mol Immunol 44:1524-34.
367. Moore JS, Wu X, Kulhavy R, Tomana M, Novak J, Moldoveanu Z, Brown R, Goepfert PA, Mestecky J. 2005. Increased levels of galactose-deficient IgG in sera of HIV-1-infected individuals. AIDS 19:381-9.
368. Vadrevu SK, Trbojevic-Akmacic I, Kossenkov AV, Colomb F, Giron LB, Anzurez A, Lynn K, Mounzer K, Landay AL, Kaplan RC, Papasavvas E, Montaner LJ, Lauc G, Abdel-Mohsen M. 2018. Frontline Science: Plasma and immunoglobulin G galactosylation associate with HIV persistence during antiretroviral therapy. J Leukoc Biol 104:461-471.
369. Ackerman ME, Crispin M, Yu X, Baruah K, Boesch AW, Harvey DJ, Dugast AS, Heizen EL, Ercan A, Choi I, Streeck H, Nigrovic PA, Bailey-Kellogg C, Scanlan C, Alter G. 2013. Natural variation in Fc glycosylation of HIV-specific antibodies impacts antiviral activity. J Clin Invest 123:2183-92.
370. Mir-Artigues P, Twyman RM, Alvarez D, Cerda Bennasser P, Balcells M, Christou P, Capell T. 2019. A simplified techno-economic model for the molecular pharming of antibodies. Biotechnol Bioeng 116:2526-2539.
371. Strasser R, Stadlmann J, Schahs M, Stiegler G, Quendler H, Mach L, Glossl J, Weterings K, Pabst M, Steinkellner H. 2008. Generation of glyco-engineered Nicotiana benthamiana for the production of monoclonal antibodies with a homogeneous human-like N-glycan structure. Plant Biotechnol J 6:392-402.
372. Bardor M, Faveeuw C, Fitchette AC, Gilbert D, Galas L, Trottein F, Faye L, Lerouge P. 2003. Immunoreactivity in mammals of two typical plant glyco-epitopes, core alpha(1,3)-fucose and core xylose. Glycobiology 13:427-34.
373. Jansing J, Sack M, Augustine SM, Fischer R, Bortesi L. 2019. CRISPR/Cas9-mediated knockout of six glycosyltransferase genes in Nicotiana benthamiana for the production of recombinant proteins lacking beta-1,2-xylose and core alpha-1,3-fucose. Plant Biotechnol J 17:350-361.
374. Castilho A, Steinkellner H. 2016. Transient Expression of Mammalian Genes in N. benthamiana to Modulate N-Glycosylation. Methods Mol Biol 1385:99-113.
375. Forthal DN, Gach JS, Landucci G, Jez J, Strasser R, Kunert R, Steinkellner H. 2010. Fc-glycosylation influences Fcgamma receptor binding and cell-mediated anti-HIV activity of monoclonal antibody 2G12. J Immunol 185:6876-82.
376. Stelter S, Paul MJ, Teh AY, Grandits M, Altmann F, Vanier J, Bardor M, Castilho A, Allen RL, Ma JK. 2019. Engineering the interactions between a plant-produced HIV antibody and human Fc receptors. Plant Biotechnol J doi:10.1111/pbi.13207.
377. Loos A, Gach JS, Hackl T, Maresch D, Henkel T, Porodko A, Bui-Minh D, Sommeregger W, Wozniak-Knopp G, Forthal DN, Altmann F, Steinkellner H, Mach L. 2015. Glycan

modulation and sulfoengineering of anti-HIV-1 monoclonal antibody PG9 in plants. Proc Natl Acad Sci U S A 112:12675-80.
378. Veillette M, Coutu M, Richard J, Batraville LA, Dagher O, Bernard N, Tremblay C, Kaufmann DE, Roger M, Finzi A. 2015. The HIV-1 gp120 CD4-bound conformation is preferentially targeted by antibody-dependent cellular cytotoxicity-mediating antibodies in sera from HIV-1-infected individuals. J Virol 89:545-51.
379. Arias JF, Heyer LN, von Bredow B, Weisgrau KL, Moldt B, Burton DR, Rakasz EG, Evans DT. 2014. Tetherin antagonism by Vpu protects HIV-infected cells from antibody-dependent cell-mediated cytotoxicity. Proc Natl Acad Sci U S A 111:6425-30.
380. Alsahafi N, Richard J, Prevost J, Coutu M, Brassard N, Parsons MS, Kaufmann DE, Brockman M, Finzi A. 2017. Impaired Downregulation of NKG2D Ligands by Nef Proteins from Elite Controllers Sensitizes HIV-1-Infected Cells to Antibody-Dependent Cellular Cytotoxicity. J Virol 91:e00109-17.
381. Veillette M, Richard J, Pazgier M, Lewis GK, Parsons MS, Finzi A. 2016. Role of HIV-1 Envelope Glycoproteins Conformation and Accessory Proteins on ADCC Responses. Curr HIV Res 14:9-23.
382. Lyerly HK, Matthews TJ, Langlois AJ, Bolognesi DP, Weinhold KJ. 1987. Human T-cell lymphotropic virus IIIB glycoprotein (gp120) bound to CD4 determinants on normal lymphocytes and expressed by infected cells serves as target for immune attack. Proc Natl Acad Sci U S A 84:4601-5.
383. Leemans A, De Schryver M, Van der Gucht W, Heykers A, Pintelon I, Hotard AL, Moore ML, Melero JA, McLellan JS, Graham BS, Broadbent L, Power UF, Caljon G, Cos P, Maes L, Delputte P. 2017. Antibody-Induced Internalization of the Human Respiratory Syncytial Virus Fusion Protein. J Virol 91.
384. Guan Y, Pazgier M, Sajadi MM, Kamin-Lewis R, Al-Darmarki S, Flinko R, Lovo E, Wu X, Robinson JE, Seaman MS, Fouts TR, Gallo RC, DeVico AL, Lewis GK. 2013. Diverse specificity and effector function among human antibodies to HIV-1 envelope glycoprotein epitopes exposed by CD4 binding. Proc Natl Acad Sci U S A 110:E69-78.
385. Dewerchin HL, Cornelissen E, Nauwynck HJ. 2006. Feline infectious peritonitis virus-infected monocytes internalize viral membrane-bound proteins upon antibody addition. J Gen Virol 87:1685-90.
386. Parsons MS, Lee WS, Kristensen AB, Amarasena T, Khoury G, Wheatley AK, Reynaldi A, Wines BD, Hogarth PM, Davenport MP, Kent SJ. 2019. Fc-dependent functions are redundant to efficacy of anti-HIV antibody PGT121 in macaques. J Clin Invest 129:182-191.
387. Hangartner L, Beauparlant D, Rakasz E, Nedellec R, Hoze N, McKenney K, Martins MA, Seabright GE, Allen JD, Weiler AM, Friedrich TC, Regoes RR, Crispin M, Burton DR. 2021. Effector function does not contribute to protection from virus challenge by a highly potent HIV broadly neutralizing antibody in nonhuman primates. Sci Transl Med 13.
388. Lambotte O, Ferrari G, Moog C, Yates NL, Liao HX, Parks RJ, Hicks CB, Owzar K, Tomaras GD, Montefiori DC, Haynes BF, Delfraissy JF. 2009. Heterogeneous neutralizing antibody and antibody-dependent cell cytotoxicity responses in HIV-1 elite controllers. AIDS 23:897-906.
389. Ackerman ME, Mikhailova A, Brown EP, Dowell KG, Walker BD, Bailey-Kellogg C, Suscovich TJ, Alter G. 2016. Polyfunctional HIV-Specific Antibody Responses Are Associated with Spontaneous HIV Control. PLoS Pathog 12:e1005315.

390. Chester C, Marabelle A, Houot R, Kohrt HE. 2015. Dual antibody therapy to harness the innate anti-tumor immune response to enhance antibody targeting of tumors. Curr Opin Immunol 33:1-8.
391. Jacobsen HJ, Poulsen TT, Dahlman A, Kjaer I, Koefoed K, Sen JW, Weilguny D, Bjerregaard B, Andersen CR, Horak ID, Pedersen MW, Kragh M, Lantto J. 2015. Pan-HER, an Antibody Mixture Simultaneously Targeting EGFR, HER2, and HER3, Effectively Overcomes Tumor Heterogeneity and Plasticity. Clin Cancer Res 21:4110-22.
392. Chao MP, Alizadeh AA, Tang C, Myklebust JH, Varghese B, Gill S, Jan M, Cha AC, Chan CK, Tan BT, Park CY, Zhao F, Kohrt HE, Malumbres R, Briones J, Gascoyne RD, Lossos IS, Levy R, Weissman IL, Majeti R. 2010. Anti-CD47 antibody synergizes with rituximab to promote phagocytosis and eradicate non-Hodgkin lymphoma. Cell 142:699-713.
393. Gilchuk P, Kuzmina N, Ilinykh PA, Huang K, Gunn BM, Bryan A, Davidson E, Doranz BJ, Turner HL, Fusco ML, Bramble MS, Hoff NA, Binshtein E, Kose N, Flyak AI, Flinko R, Orlandi C, Carnahan R, Parrish EH, Sevy AM, Bombardi RG, Singh PK, Mukadi P, Muyembe-Tamfum JJ, Ohi MD, Saphire EO, Lewis GK, Alter G, Ward AB, Rimoin AW, Bukreyev A, Crowe JE, Jr. 2018. Multifunctional Pan-ebolavirus Antibody Recognizes a Site of Broad Vulnerability on the Ebolavirus Glycoprotein. Immunity 49:363-374 e10.
394. Keeffe JR, Van Rompay KKA, Olsen PC, Wang Q, Gazumyan A, Azzopardi SA, Schaefer-Babajew D, Lee YE, Stuart JB, Singapuri A, Watanabe J, Usachenko J, Ardeshir A, Saeed M, Agudelo M, Eisenreich T, Bournazos S, Oliveira TY, Rice CM, Coffey LL, MacDonald MR, Bjorkman PJ, Nussenzweig MC, Robbiani DF. 2018. A Combination of Two Human Monoclonal Antibodies Prevents Zika Virus Escape Mutations in Non-human Primates. Cell Rep 25:1385-1394 e7.
395. Chao TY, Ren S, Shen E, Moore S, Zhang SF, Chen L, Rupprecht CE, Tsao E. 2017. SYN023, a novel humanized monoclonal antibody cocktail, for post-exposure prophylaxis of rabies. PLoS Negl Trop Dis 11:e0006133.
396. Franka R, Carson WC, Ellison JA, Taylor ST, Smith TG, Kuzmina NA, Kuzmin IV, Marissen WE, Rupprecht CE. 2017. In Vivo Efficacy of a Cocktail of Human Monoclonal Antibodies (CL184) Against Diverse North American Bat Rabies Virus Variants. Trop Med Infect Dis 2.
397. Weinreich DM, Sivapalasingam S, Norton T, Ali S, Gao H, Bhore R, Musser BJ, Soo Y, Rofail D, Im J, Perry C, Pan C, Hosain R, Mahmood A, Davis JD, Turner KC, Hooper AT, Hamilton JD, Baum A, Kyratsous CA, Kim Y, Cook A, Kampman W, Kohli A, Sachdeva Y, Graber X, Kowal B, DiCioccio T, Stahl N, Lipsich L, Braunstein N, Herman G, Yancopoulos GD, Trial I. 2021. REGN-COV2, a Neutralizing Antibody Cocktail, in Outpatients with Covid-19. N Engl J Med 384:238-251.
398. Ullah I, Prevost J, Ladinsky MS, Stone H, Lu M, Anand SP, Beaudoin-Bussieres G, Symmes K, Benlarbi M, Ding S, Gasser R, Fink C, Chen Y, Tauzin A, Goyette G, Bourassa C, Medjahed H, Mack M, Chung K, Wilen CB, Dekaban GA, Dikeakos JD, Bruce EA, Kaufmann DE, Stamatatos L, McGuire AT, Richard J, Pazgier M, Bjorkman PJ, Mothes W, Finzi A, Kumar P, Uchil PD. 2021. Live imaging of SARS-CoV-2 infection in mice reveals that neutralizing antibodies require Fc function for optimal efficacy. Immunity 54:2143-2158 e15.
399. Winkler ES, Gilchuk P, Yu J, Bailey AL, Chen RE, Chong Z, Zost SJ, Jang H, Huang Y, Allen JD, Case JB, Sutton RE, Carnahan RH, Darling TL, Boon ACM, Mack M, Head RD, Ross TM, Crowe JE, Jr., Diamond MS. 2021. Human neutralizing antibodies against

SARS-CoV-2 require intact Fc effector functions for optimal therapeutic protection. Cell 184:1804-1820 e16.
400. Mendoza P, Gruell H, Nogueira L, Pai JA, Butler AL, Millard K, Lehmann C, Suarez I, Oliveira TY, Lorenzi JCC, Cohen YZ, Wyen C, Kummerle T, Karagounis T, Lu CL, Handl L, Unson-O'Brien C, Patel R, Ruping C, Schlotz M, Witmer-Pack M, Shimeliovich I, Kremer G, Thomas E, Seaton KE, Horowitz J, West AP, Jr., Bjorkman PJ, Tomaras GD, Gulick RM, Pfeifer N, Fatkenheuer G, Seaman MS, Klein F, Caskey M, Nussenzweig MC. 2018. Combination therapy with anti-HIV-1 antibodies maintains viral suppression. Nature 561:479-484.
401. Asokan M, Dias J, Liu C, Maximova A, Ernste K, Pegu A, McKee K, Shi W, Chen X, Almasri C, Promsote W, Ambrozak DR, Gama L, Hu J, Douek DC, Todd JP, Lifson JD, Fourati S, Sekaly RP, Crowley AR, Ackerman ME, Ko SH, Kilam D, Boritz EA, Liao LE, Best K, Perelson AS, Mascola JR, Koup RA. 2020. Fc-mediated effector function contributes to the in vivo antiviral effect of an HIV neutralizing antibody. Proc Natl Acad Sci U S A 117:18754-18763.
402. Moog C, Dereuddre-Bosquet N, Teillaud JL, Biedma ME, Holl V, Van Ham G, Heyndrickx L, Van Dorsselaer A, Katinger D, Vcelar B, Zolla-Pazner S, Mangeot I, Kelly C, Shattock RJ, Le Grand R. 2014. Protective effect of vaginal application of neutralizing and nonneutralizing inhibitory antibodies against vaginal SHIV challenge in macaques. Mucosal Immunol 7:46-56.
403. Sun Y, Asmal M, Lane S, Permar SR, Schmidt SD, Mascola JR, Letvin NL. 2011. Antibody-dependent cell-mediated cytotoxicity in simian immunodeficiency virus-infected rhesus monkeys. J Virol 85:6906-12.
404. Liu J, Ghneim K, Sok D, Bosche WJ, Li Y, Chipriano E, Berkemeier B, Oswald K, Borducchi E, Cabral C, Peter L, Brinkman A, Shetty M, Jimenez J, Mondesir J, Lee B, Giglio P, Chandrashekar A, Abbink P, Colantonio A, Gittens C, Baker C, Wagner W, Lewis MG, Li W, Sekaly RP, Lifson JD, Burton DR, Barouch DH. 2016. Antibody-mediated protection against SHIV challenge includes systemic clearance of distal virus. Science 353:1045-1049.
405. Johnson PR, Schnepp BC, Zhang J, Connell MJ, Greene SM, Yuste E, Desrosiers RC, Clark KR. 2009. Vector-mediated gene transfer engenders long-lived neutralizing activity and protection against SIV infection in monkeys. Nat Med 15:901-6.
406. Richard J, Nguyen DN, Tolbert WD, Gasser R, Ding S, Vezina D, Yu Gong S, Prevost J, Gendron-Lepage G, Medjahed H, Gottumukkala S, Finzi A, Pazgier M. 2021. Across Functional Boundaries: Making Nonneutralizing Antibodies To Neutralize HIV-1 and Mediate Fc-Mediated Effector Killing of Infected Cells. mBio 12:e0140521.
407. Xu L, Pegu A, Rao E, Doria-Rose N, Beninga J, McKee K, Lord DM, Wei RR, Deng G, Louder M, Schmidt SD, Mankoff Z, Wu L, Asokan M, Beil C, Lange C, Leuschner WD, Kruip J, Sendak R, Kwon YD, Zhou T, Chen X, Bailer RT, Wang K, Choe M, Tartaglia LJ, Barouch DH, O'Dell S, Todd JP, Burton DR, Roederer M, Connors M, Koup RA, Kwong PD, Yang ZY, Mascola JR, Nabel GJ. 2017. Trispecific broadly neutralizing HIV antibodies mediate potent SHIV protection in macaques. Science 358:85-90.
408. Asokan M, Rudicell RS, Louder M, McKee K, O'Dell S, Stewart-Jones G, Wang K, Xu L, Chen X, Choe M, Chuang G, Georgiev IS, Joyce MG, Kirys T, Ko S, Pegu A, Shi W, Todd JP, Yang Z, Bailer RT, Rao S, Kwong PD, Nabel GJ, Mascola JR. 2015. Bispecific

Antibodies Targeting Different Epitopes on the HIV-1 Envelope Exhibit Broad and Potent Neutralization. J Virol 89:12501-12.
409. Fellinger CH, Gardner MR, Weber JA, Alfant B, Zhou AS, Farzan M. 2019. eCD4-Ig Limits HIV-1 Escape More Effectively than CD4-Ig or a Broadly Neutralizing Antibody. J Virol 93.
410. Gardner MR, Kattenhorn LM, Kondur HR, von Schaewen M, Dorfman T, Chiang JJ, Haworth KG, Decker JM, Alpert MD, Bailey CC, Neale ES, Jr., Fellinger CH, Joshi VR, Fuchs SP, Martinez-Navio JM, Quinlan BD, Yao AY, Mouquet H, Gorman J, Zhang B, Poignard P, Nussenzweig MC, Burton DR, Kwong PD, Piatak M, Jr., Lifson JD, Gao G, Desrosiers RC, Evans DT, Hahn BH, Ploss A, Cannon PM, Seaman MS, Farzan M. 2015. AAV-expressed eCD4-Ig provides durable protection from multiple SHIV challenges. Nature 519:87-91.
411. Klein JS, Webster A, Gnanapragasam PN, Galimidi RP, Bjorkman PJ. 2010. A dimeric form of the HIV-1 antibody 2G12 elicits potent antibody-dependent cellular cytotoxicity. AIDS 24:1633-40.
412. Koenderman L. 2019. Inside-Out Control of Fc-Receptors. Front Immunol 10:544.
413. Li T, DiLillo DJ, Bournazos S, Giddens JP, Ravetch JV, Wang LX. 2017. Modulating IgG effector function by Fc glycan engineering. Proc Natl Acad Sci U S A 114:3485-3490.
414. Moldt B, Shibata-Koyama M, Rakasz EG, Schultz N, Kanda Y, Dunlop DC, Finstad SL, Jin C, Landucci G, Alpert MD, Dugast AS, Parren PW, Nimmerjahn F, Evans DT, Alter G, Forthal DN, Schmitz JE, Iida S, Poignard P, Watkins DI, Hessell AJ, Burton DR. 2012. A nonfucosylated variant of the anti-HIV-1 monoclonal antibody b12 has enhanced FcgammaRIIIa-mediated antiviral activity in vitro but does not improve protection against mucosal SHIV challenge in macaques. J Virol 86:6189-96.
415. Bruel T, Guivel-Benhassine F, Amraoui S, Malbec M, Richard L, Bourdic K, Donahue DA, Lorin V, Casartelli N, Noel N, Lambotte O, Mouquet H, Schwartz O. 2016. Elimination of HIV-1-infected cells by broadly neutralizing antibodies. Nat Commun 7:10844.
416. Moore JP, Trkola A, Korber B, Boots LJ, Kessler JA, 2nd, McCutchan FE, Mascola J, Ho DD, Robinson J, Conley AJ. 1995. A human monoclonal antibody to a complex epitope in the V3 region of gp120 of human immunodeficiency virus type 1 has broad reactivity within and outside clade B. J Virol 69:122-30.
417. Nicely NI, Wiehe K, Kepler TB, Jaeger FH, Dennison SM, Rerks-Ngarm S, Nitayaphan S, Pitisuttithum P, Kaewkungwal J, Robb ML, O'Connell RJ, Michael NL, Kim JH, Liao HX, Munir Alam S, Hwang KK, Bonsignori M, Haynes BF. 2015. Structural analysis of the unmutated ancestor of the HIV-1 envelope V2 region antibody CH58 isolated from an RV144 vaccine efficacy trial vaccinee. EBioMedicine 2:713-22.
418. Tyler DS, Stanley SD, Zolla-Pazner S, Gorny MK, Shadduck PP, Langlois AJ, Matthews TJ, Bolognesi DP, Palker TJ, Weinhold KJ. 1990. Identification of sites within gp41 that serve as targets for antibody-dependent cellular cytotoxicity by using human monoclonal antibodies. J Immunol 145:3276-82.
419. Taniguchi Y, Zolla-Pazner S, Xu Y, Zhang X, Takeda S, Hattori T. 2000. Human monoclonal antibody 98-6 reacts with the fusogenic form of gp41. Virology 273:333-40.
420. Beaudoin-Bussieres G, Prevost J, Gendron-Lepage G, Melillo B, Chen J, Smith Iii AB, Pazgier M, Finzi A. 2020. Elicitation of Cluster A and Co-Receptor Binding Site Antibodies are Required to Eliminate HIV-1 Infected Cells. Microorganisms 8.

421. Sherburn R, Tolbert WD, Gottumukkala S, Beaudoin-Bussieres G, Finzi A, Pazgier M. 2020. Effects of gp120 Inner Domain (ID2) Immunogen Doses on Elicitation of Anti-HIV-1 Functional Fc-Effector Response to C1/C2 (Cluster A) Epitopes in Mice. Microorganisms 8.
422. Niessl J, Baxter AE, Mendoza P, Jankovic M, Cohen YZ, Butler AL, Lu CL, Dube M, Shimeliovich I, Gruell H, Klein F, Caskey M, Nussenzweig MC, Kaufmann DE. 2020. Combination anti-HIV-1 antibody therapy is associated with increased virus-specific T cell immunity. Nat Med 26:222-227.
423. Eckels PC, Banerjee A, Moore EE, McLaughlin NJ, Gries LM, Kelher MR, England KM, Gamboni-Robertson F, Khan SY, Silliman CC. 2009. Amantadine inhibits platelet-activating factor induced clathrin-mediated endocytosis in human neutrophils. Am J Physiol Cell Physiol 297:C886-97.
424. Rothberg KG, Heuser JE, Donzell WC, Ying YS, Glenney JR, Anderson RG. 1992. Caveolin, a protein component of caveolae membrane coats. Cell 68:673-82.
425. Prevost J, Pickering S, Mumby MJ, Medjahed H, Gendron-Lepage G, Delgado GG, Dirk BS, Dikeakos JD, Sturzel CM, Sauter D, Kirchhoff F, Bibollet-Ruche F, Hahn BH, Dube M, Kaufmann DE, Neil SJD, Finzi A, Richard J. 2019. Upregulation of BST-2 by Type I Interferons Reduces the Capacity of Vpu To Protect HIV-1-Infected Cells from NK Cell Responses. mBio 10.
426. Simanjuntak Y, Liang JJ, Lee YL, Lin YL. 2015. Repurposing of prochlorperazine for use against dengue virus infection. J Infect Dis 211:394-404.
427. Group PIW, Multi-National PIIST, Davey RT, Jr., Dodd L, Proschan MA, Neaton J, Neuhaus Nordwall J, Koopmeiners JS, Beigel J, Tierney J, Lane HC, Fauci AS, Massaquoi MBF, Sahr F, Malvy D. 2016. A Randomized, Controlled Trial of ZMapp for Ebola Virus Infection. N Engl J Med 375:1448-1456.
428. Halper-Stromberg A, Lu CL, Klein F, Horwitz JA, Bournazos S, Nogueira L, Eisenreich TR, Liu C, Gazumyan A, Schaefer U, Furze RC, Seaman MS, Prinjha R, Tarakhovsky A, Ravetch JV, Nussenzweig MC. 2014. Broadly neutralizing antibodies and viral inducers decrease rebound from HIV-1 latent reservoirs in humanized mice. Cell 158:989-999.
429. Milush JM, Lopez-Verges S, York VA, Deeks SG, Martin JN, Hecht FM, Lanier LL, Nixon DF. 2013. CD56negCD16(+) NK cells are activated mature NK cells with impaired effector function during HIV-1 infection. Retrovirology 10:158.
430. Mavilio D, Lombardo G, Benjamin J, Kim D, Follman D, Marcenaro E, O'Shea MA, Kinter A, Kovacs C, Moretta A, Fauci AS. 2005. Characterization of CD56-/CD16+ natural killer (NK) cells: a highly dysfunctional NK subset expanded in HIV-infected viremic individuals. Proc Natl Acad Sci U S A 102:2886-91.
431. Mavilio D, Benjamin J, Daucher M, Lombardo G, Kottilil S, Planta MA, Marcenaro E, Bottino C, Moretta L, Moretta A, Fauci AS. 2003. Natural killer cells in HIV-1 infection: dichotomous effects of viremia on inhibitory and activating receptors and their functional correlates. Proc Natl Acad Sci U S A 100:15011-6.
432. Kedzierska K, Azzam R, Ellery P, Mak J, Jaworowski A, Crowe SM. 2003. Defective phagocytosis by human monocyte/macrophages following HIV-1 infection: underlying mechanisms and modulation by adjunctive cytokine therapy. J Clin Virol 26:247-63.
433. Desimio MG, Giuliani E, Ferraro AS, Adorno G, Doria M. 2018. In Vitro Exposure to Prostratin but Not Bryostatin-1 Improves Natural Killer Cell Functions Including Killing

of CD4(+) T Cells Harboring Reactivated Human Immunodeficiency Virus. Front Immunol 9:1514.
434. Carson WE, Giri JG, Lindemann MJ, Linett ML, Ahdieh M, Paxton R, Anderson D, Eisenmann J, Grabstein K, Caligiuri MA. 1994. Interleukin (IL) 15 is a novel cytokine that activates human natural killer cells via components of the IL-2 receptor. J Exp Med 180:1395-403.
435. Seay K, Church C, Zheng JH, Deneroff K, Ochsenbauer C, Kappes JC, Liu B, Jeng EK, Wong HC, Goldstein H. 2015. In Vivo Activation of Human NK Cells by Treatment with an Interleukin-15 Superagonist Potently Inhibits Acute In Vivo HIV-1 Infection in Humanized Mice. J Virol 89:6264-74.
436. McBrien JB, Mavigner M, Franchitti L, Smith SA, White E, Tharp GK, Walum H, Busman-Sahay K, Aguilera-Sandoval CR, Thayer WO, Spagnuolo RA, Kovarova M, Wahl A, Cervasi B, Margolis DM, Vanderford TH, Carnathan DG, Paiardini M, Lifson JD, Lee JH, Safrit JT, Bosinger SE, Estes JD, Derdeyn CA, Garcia JV, Kulpa DA, Chahroudi A, Silvestri G. 2020. Robust and persistent reactivation of SIV and HIV by N-803 and depletion of CD8(+) cells. Nature 578:154-159.
437. Harper J, Huot N, Micci L, Tharp G, King C, Rascle P, Shenvi N, Wang H, Galardi C, Upadhyay AA, Villinger F, Lifson J, Silvestri G, Easley K, Jacquelin B, Bosinger S, Muller-Trutwin M, Paiardini M. 2021. IL-21 and IFNalpha therapy rescues terminally differentiated NK cells and limits SIV reservoir in ART-treated macaques. Nat Commun 12:2866.
438. Tomescu C, Tebas P, Montaner LJ. 2017. IFN-alpha augments natural killer-mediated antibody-dependent cellular cytotoxicity of HIV-1-infected autologous CD4+ T cells regardless of major histocompatibility complex class 1 downregulation. AIDS 31:613-622.
439. Richard J, Prevost J, von Bredow B, Ding S, Brassard N, Medjahed H, Coutu M, Melillo B, Bibollet-Ruche F, Hahn BH, Kaufmann DE, Smith AB, 3rd, Sodroski J, Sauter D, Kirchhoff F, Gee K, Neil SJ, Evans DT, Finzi A. 2017. BST-2 Expression Modulates Small CD4-Mimetic Sensitization of HIV-1-Infected Cells to Antibody-Dependent Cellular Cytotoxicity. J Virol 91:e00219-17.
440. Hafeez U, Parakh S, Gan HK, Scott AM. 2020. Antibody-Drug Conjugates for Cancer Therapy. Molecules 25.
441. Umotoy JC, de Taeye SW. 2021. Antibody Conjugates for Targeted Therapy Against HIV-1 as an Emerging Tool for HIV-1 Cure. Front Immunol 12:708806.

APPENDIX

Permissions to use copyright material

Chapter I (Introduction) and Chapter VI (Discussion): Anand, S.P. and Finzi, A., **2019**. Understudied factors influencing Fc-mediated immune responses against viral infections. *Vaccines*, 7(3), p.103; DOI: 10.3390/vaccines7030103

For all articles published in MDPI journals, copyright is retained by the authors. Thus, as an author of this article, we retain the right to include it in a thesis or dissertation, provided it is not published commercially. This is an open access article distributed under the Creative Commons Attribution License which permits unrestricted use, distribution, and reproduction in any medium, provided the original work is properly cited. All co-authors agreed to the inclusion of parts of this manuscript to the present thesis.

Chapter II: Anand, S.P., Prévost, J., Baril, S., Richard, J., Medjahed, H., Chapleau, J.P., Tolbert, W.D., Kirk, S., Smith III, A.B., Wines, B.D., Kent, S.J., Hogarth, P.M., Parsons, M.S., Pazgier, M., & Finzi, A. **2019.** Two families of Env antibodies efficiently engage Fc-gamma receptors and eliminate HIV-1-infected cells. *Journal of Virology*, 93(3), pp.e01823-18; DOI: 10.1128/JVI.01823-18.

ASM grants the author the right to republish discrete portions of his/her article in any other publication (including print, CD-ROM, and other electronic formats) of which he or she is author or editor, provided that proper credit is given to the original ASM publication. An ASM author also retains the right to reuse the full article in his/her dissertation or thesis. All co-authors agreed to the inclusion of parts of this manuscript to the present thesis.

Chapter III: Anand, S.P., Grover, J.R., Tolbert, W.D., Prévost, J., Richard, J., Ding, S., Baril, S., Medjahed, H., Evans, D.T., Pazgier, M. and Mothes, W., & Finzi, A. **2019**. Antibody-induced internalization of HIV-1 Env proteins limits surface expression of the closed conformation of Env. *Journal of Virology*, 93(11), pp.e00293-19l; DOI: 10.1128/JVI.00293-19.

ASM grants the author the right to republish discrete portions of his/her article in any other publication (including print, CD-ROM, and other electronic formats) of which he or she is author or editor, provided that proper credit is given to the original ASM publication. An ASM author also retains the right to reuse the full article in his/her dissertation or thesis. All co-authors agreed to the inclusion of parts of this manuscript to the present thesis.

Chapter IV: Anand, S.P., Prévost, J., Descôteaux-Dinelle, J., Richard, J., Nguyen, D.N., Medjahed, H., Chen, H.C., Smith, A.B., Pazgier, M. & Finzi, A., **2021.** HIV-1 Envelope Glycoprotein Cell Surface Localization Is Associated with Antibody-Induced Internalization. *Viruses*, 13(10), p.1953; DOI: 10.3390/v13101953

For all articles published in MDPI journals, copyright is retained by the authors. Thus, as an author of this article, we retain the right to include it in a thesis or dissertation, provided it is not published commercially. This is an open access article distributed under the Creative Commons Attribution License which permits unrestricted use, distribution, and reproduction in any medium, provided the original work is properly cited. All co-authors agreed to the inclusion of parts of this manuscript to the present thesis.

Chapter V: Anand, S.P., Ding, S., Tolbert, W.D., Prévost, J., Richard, J., Gil, H.M., Gendron-Lepage, G., Cheung, W.F., Wang, H., Pastora, R. and Saxena, H., Wakarchuk, W., Medjahed, H., Wines, B.D., Hogarth, P.M., Shaw, G.M., Martin, M.M., Burton, D.R., Hangartner, L., Evans, D.T., Pazgier, M., Cossar, D., McLean, M.D., & Finzi, A. **2021**. Enhanced Ability of Plant-Derived PGT121 Glycovariants to Eliminate HIV-1-Infected Cells. *Journal of Virology*, 95(18), pp.e00796-21; DOI: 10.1128/JVI.00796-21

ASM grants the author the right to republish discrete portions of his/her article in any other publication (including print, CD-ROM, and other electronic formats) of which he or she is author or editor, provided that proper credit is given to the original ASM publication. An ASM author also retains the right to reuse the full article in his/her dissertation or thesis. All co-authors agreed to the inclusion of parts of this manuscript to the present thesis.

Figure 1.5 Envelope glycoprotein composition. From Steckbeck JD, Kuhlmann AS, Montelaro RC. 2013. C-terminal tail of human immunodeficiency virus gp41: functionally rich and structurally enigmatic. *J Gen Virol* 94:1-19.

Figure 1.6 Stages of HIV-1 infection. From Grossman Z, Meier-Schellersheim M, Paul WE, Picker LJ. 2006. Pathogenesis of HIV infection: what the virus spares is as important as what it destroys. *Nat Med* 12:289-95.

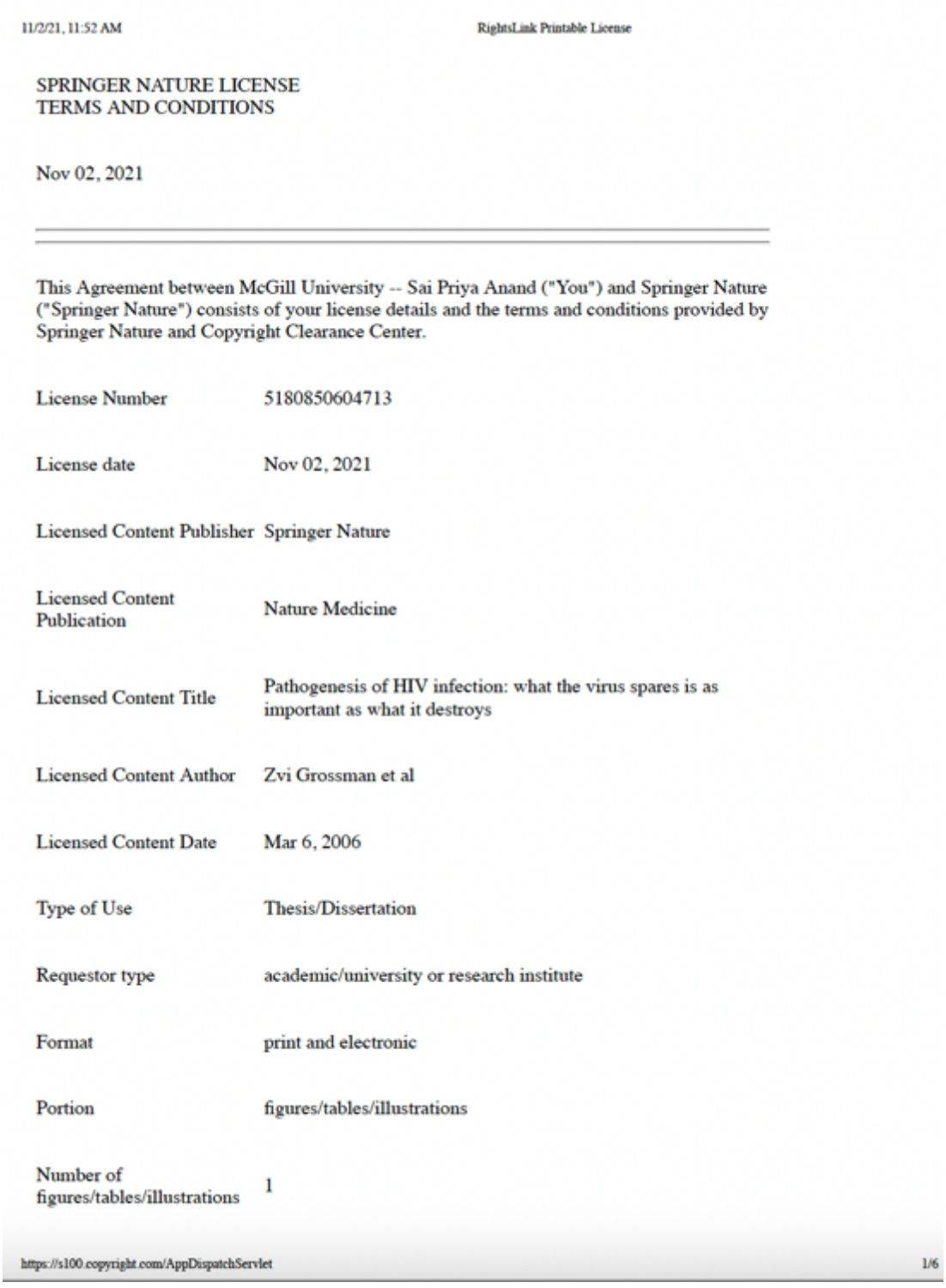

11/2/21, 11:52 AM RightsLink Printable License

SPRINGER NATURE LICENSE
TERMS AND CONDITIONS

Nov 02, 2021

This Agreement between McGill University -- Sai Priya Anand ("You") and Springer Nature ("Springer Nature") consists of your license details and the terms and conditions provided by Springer Nature and Copyright Clearance Center.

License Number	5180850604713
License date	Nov 02, 2021
Licensed Content Publisher	Springer Nature
Licensed Content Publication	Nature Medicine
Licensed Content Title	Pathogenesis of HIV infection: what the virus spares is as important as what it destroys
Licensed Content Author	Zvi Grossman et al
Licensed Content Date	Mar 6, 2006
Type of Use	Thesis/Dissertation
Requestor type	academic/university or research institute
Format	print and electronic
Portion	figures/tables/illustrations
Number of figures/tables/illustrations	1

https://s100.copyright.com/AppDispatchServlet 1/6

High-res required	no
Will you be translating?	no
Circulation/distribution	1 - 29
Author of this Springer Nature content	no
Title	Harnessing antibody-dependant cellular cytotoxicity against HIV-1-infected cells
Institution name	McGill University
Expected presentation date	Apr 2022
Portions	Figure 3 from the article will be used for Figure 1.6 in the thesis
Requestor Location	McGill University 3775 Rue University Room 511 Montreal, QC H3A 2B4 Canada Attn: McGill University
Total	0.00 USD

Figure 1.9. Env conformations recognized by bNAbs and nNAbs. From Richard J, Prevost J, Alsahafi N, Ding S, Finzi A. 2018. Impact of HIV-1 Envelope Conformation on ADCC Responses. *Trends Microbiol* 26:253-265.

Type of Use	reuse in a thesis/dissertation
Portion	figures/tables/illustrations
Number of figures/tables/illustrations	1
Format	both print and electronic
Are you the author of this Elsevier article?	No
Will you be translating?	No
Title	Harnessing antibody-dependant cellular cytotoxicity against HIV-1-infected cells
Institution name	McGill University
Expected presentation date	Apr 2022
Portions	Figure 3 from the article will be used in Figure 1.8 of the thesis.
Requestor Location	McGill University 3775 Rue University Room 511 Montreal, QC H3A 2B4 Canada Attn: McGill University
Publisher Tax ID	GB 494 6272 12
Total	0.00 CAD

Figure 1.13. Sequential Processing of the Fc Glycan. From Jennewein, M and Alter, G. 2017. The Immunoregulatory Roles of Antibody Glycosylation. *Trends Immunol.* 38(5):358-372.

Portion	figures/tables/illustrations
Number of figures/tables/illustrations	1
Format	both print and electronic
Are you the author of this Elsevier article?	No
Will you be translating?	No
Title	Harnessing antibody-dependant cellular cytotoxicity against HIV-1-infected cells
Institution name	McGill University
Expected presentation date	Apr 2022
Portions	Figure I in Box 2 will be used as Figure 1.13 of the thesis
Requestor Location	McGill University 3775 Rue University Room 511 Montreal, QC H3A 2B4 Canada Attn: McGill University
Publisher Tax ID	GB 494 6272 12
Total	0.00 CAD

Terms and Conditions